Genetic Engineering of *Saccharomyces cerevisiae* for Improved Cytosolic Isobutanol Biosynthesis

Dissertation

zur Erlangung des Doktorgrades

der Naturwissenschaften

vorgelegt beim Fachbereich Biowissenschaften

der Johann Wolfgang Goethe-Universität

in Frankfurt am Main

von

Martin Brinek

aus Seligenstadt am Main

Frankfurt am Main, 2021

(D 30)

Vom Fachbereich Biowissenschaften
der Johann Wolfgang Goethe-Universität
als Dissertation angenommen.

Dekan: Prof. Dr. Sven Klimpel

Gutachter: Prof. Dr. Eckhard Boles
Prof. Dr. Jörg Soppa

Datum der Disputation: 17.02.2022

Table of Content

1. SUMMARY 1

2. INTRODUCTION 3

2.1. BIOECONOMY: BIO-BASED PRODUCTS FROM RENEWABLE BIOMASS 3

2.2. METABOLIC ENGINEERING IN BIOTECHNOLOGY AND BIOECONOMY 3

2.3. *S. CEREVISIAE* IN RESEARCH AND BIOECONOMY 5

2.4. ROLE OF BIOFUELS IN BIOECONOMY 6

2.5. NATIVE AND METABOLICALLY ENGINEERED BRANCHED CHAIN ALCOHOL PRODUCTION IN *S. CEREVISIAE* 7

2.5.1. *De novo* Synthesis of Branched Chain Amino Acid in *S. cerevisiae* 8

2.5.1.1. Ilv2 - Acetolactate Synthase 9

2.5.1.2. Ilv5 - Ketol-Acid Reductoisomerase 10

2.5.1.3. Ilv3 - Dihydroxyacid Dehydratase 12

2.5.2. BCAA-Catabolism *via* Ehrlich Pathways in *S. cerevisiae* 14

2.5.2.1. Transamination as nitrogen source 14

2.5.2.2. Decarboxylation 15

2.5.2.3. Reduction/Oxidation 16

2.6. METABOLIC ENGINEERING STRATEGIES FOR ISOBUTANOL PRODUCTION IN PROKARYOTES 17

2.7. METABOLIC ENGINEERING STRATEGIES FOR ISOBUTANOL PRODUCTION IN *S. CEREVISIAE* 18

2.8. IRON-SULPHUR-CLUSTER ENZYMES AND THEIR BIOGENESIS IN *S. CEREVISIAE* 23

2.9. OBJECTIVES OF THIS WORK 26

3. MATERIAL AND METHODS 27

3.1. MEDIA, MICROORGANISMS, CULTIVATION AND STORAGE 27

3.1.1. Media 27

3.1.2. Microorganisms, Cultivation and Storage 28

3.2. PLASMIDS 30

3.3. SYNTHETIC DNA 34

3.4. CHEMICALS, ENZYMES, AND KITS 34

3.5. EQUIPMENT AND OTHER MATERIALS 35

3.6. MOLECULAR BIOLOGICAL METHODS 36

3.6.1. Isolation of Plasmid DNA from *E. coli* 36

3.6.2. Isolation of Plasmid and Genomic DNA from *S. cerevisiae* 36
3.6.3. Preparation of Genomic DNA from *S. cerevisiae* for PCR Amplification 37
3.6.4. Polymerase Chain Reaction..... 37
3.6.4.1. Polymerase Chain Reaction using Phusion High-Fidelity DNA Polymerase..... 38
3.6.4.2. Polymerase Chain Reaction using Q5 High-Fidelity DNA Polymerase..... 38
3.6.4.3. Polymerase Chain Reaction using DreamTaq DNA Polymerase 39
3.6.5. Agarose Gel Electrophoresis for DNA Separation 39
3.6.5.1. DNA-Purification and DNA-Extraction from Agarose Gels..... 40
3.6.6. Plasmid Assembly..... 40
3.6.6.1. Plasmid Construction by Homologous Recombination in S. cerevisiae 40
3.6.6.2. Plasmid Construction by Gibson Isothermal Assembly..... 41
3.6.6.3. Plasmid Construction by Ligation..... 42
3.6.7. Measurement of Nucleic Acid Concentration 43
3.6.8. Transformation of *E. coli* 43
3.6.9. Transformation of *S. cerevisiae* 44
3.6.10. Gene Deletion by CRISPR/Cas9 45
3.7. METHODS FOR CELL CULTIVATION AND FERMENTATION..... 45
3.7.1. Determination of Cell Density..... 45
3.7.2. Online Cell Growth Monitoring by Cell Growth Quantifier (CGQ)..... 46
3.7.3. Serial Dilution Spot Assay..... 46
3.7.4. Replica Plating 46
3.7.5. Aerobic High OD Isobutanol Biosynthesis 47
3.7.6. Evolutionary Engineering 47
3.7.7. Metabolite Analysis by HPLC..... 47
3.8. BIOINFORMATIC METHODS 48
3.8.1. Codon Optimisation of Genes..... 48
3.8.2. DNA Sequencing 48
3.8.3. Genome Sequencing 48

4. RESULTS 49

4.1. LIMITATIONS IN CYTOSOLIC ISOBUTANOL BIOSYNTHESIS CAUSED BY EXPRESSION OF ILV-ENZYMES IN *S. CEREVISIAE* 49

4.1.1. Cytosolic Expression of Acetolactate Synthase.....49

4.1.1.1. Heterologous Expression of *ilvB* and Small Regulatory Subunit *ilvN* from *C. glutamicum* 53

4.1.1.2. Cytosolic Isobutanol Production in Medium Supplemented With and Without Valine by Expression of Ilv2Δ54 and Ilv6 Variants 56

4.1.2. Cytosolic Expression of Ketol-Acid Reductoisomerase 59

4.1.2.1. Expression of Ilv5Δ48 or *ilvC*^{6E6} with cyt-ILV and EP-Enzymes . 60

4.1.3. Cytosolic Expression of Dihydroxyacid Dehydratase 61

4.1.3.1. Altering the C-terminus of DHAD to Increase Affinity towards the Adapter Complex of the Cytosolic Iron-Sulphur Assembling Machinery . 62

4.1.3.2. Establishing of a Cytosolic CIA Independent ISC Assembly Mechanism by Expression of Grx Proteins 66

4.1.3.3. Improved Cytosolic X-S Availability by Deletion of Protease Pim1 ……...67

4.1.3.4. Improved Cytosolic Iron Availability by Deletion of the Regulatory Protein Fra2 69

4.2. EVOLUTIONARY ENGINEERING OF *S. CEREVISIAE* TO INCREASE VALINE PRODUCTION BY APPLYING SELECTION PRESSURE WITH NORVALINE.....70

4.2.1. Reverse Engineering of Evolved and Isolated MBY36, MBY39 and MBY42 78

4.3. RATIONAL ENGINEERING OF *S. CEREVISIAE* TO AVOID INTERMEDIATE LEAKAGE INTO COMPETING PATHWAYS DURING ISOBUTANOL PRODUCTION 80

4.3.1. Additional Expression of Each Enzyme Involved in Isobutanol Production to Identify Existing Bottlenecks.....83

4.4. PRODUCTION OF ISOBUTYRIC ACID IN *S. CEREVISIAE* 86

4.5. CONFIRMATION OF BENEFICIAL APPROACHES FOR ISOBUTANOL PRODUCTION USING THE BEST ISOBUTANOL PRODUCER AT TIME 90

5. DISCUSSION 93

5.1. OPTIMISATION OF THE CYTOSOLIC ISOBUTANOL BIOSYNTHESIS METABOLIC PATHWAY IN *S. CEREVISIAE* 93

5.1.1. Cytosolic Expression of Acetolactate Synthases and Their Impact on Cell Growth and medium composition 93

5.1.2. Approaches to Overcome the Co-Factor and Redox Imbalances of the Isobutanol Pathway 98

5.1.3. Approaches to harmonise Iron-Sulphur-Cluster Biogenesis and DHAD activity in the Cytosol of *S. cerevisiae* 101

5.1.4. Combination of Approaches for Improves Cytosolic Isobutanol Biosynthesis in *S. cerevisiae* 104

5.2. OPTIMISATION OF *S. CEREVISIAE* FOR EFFICIENT ISOBUTANOL PRODUCTION .. 105

5.3. PRODUCTION OF ISOBUTYRIC ACID IN *S. CEREVISIAE* 109

6. ZUSAMMENFASSUNG 111

7. REFERENCES 119

APPENDIX 135

I. ABBREVIATION 135

II. OLIGONUCLEOTIDES / PRIMERS 139

III. SYNTHETIC GENES 151

IV. ZUSAMMENFASSUNG (KURZ) 155

1. SUMMARY

The finite nature of fossil resources and the environmental problems caused by their excessive usage requires alternative approaches. The transformation from a fossil-based economy to one based on renewable biomass is called a “bioeconomy”. To substitute fossil resources, various microorganisms have already been modified for the biosynthesis of valuable chemicals from biomass. However, the development of such efficient microorganisms at an industrial scale, remains a major challenge. The most prominent and robust microorganism for industrial production is the yeast *Saccharomyces cerevisiae*, which is known to produce ethanol that is used as renewable biofuel. However, *S. cerevisiae* is also naturally able to produce isobutanol in small amounts. Isobutanol is favoured as a biofuel compared to ethanol due to its higher octane-number and lower hygroscopicity, which makes it more suitable for application in conventional combustion engines. In *S. cerevisiae,* the biosynthesis of isobutanol is permitted by the combination of mitochondrial valine synthesis (catalysed by Ilv2, Ilv5 and Ilv3) and its cytosolic degradation (catalysed by Aro10 and Adh2). The different compartmentalisation of the two pathways limit isobutanol biosynthesis. Thus, Brat *et al.* (2012) were able to increase the isobutanol yield up to 15 mg/g_{Glc} by cytosolic re-localisation of the enzymes Ilv2Δ54, Ilv5Δ48 and Ilv3Δ19 (cyt-ILV), with simultaneous deletion of *ilv2*. This corresponds to approximately 3.7% of the theoretical yield of 410 mg/g_{Glc}, implying existing limitations in isobutanol biosynthesis, which have been investigated in this work.

For yet unknown reasons, isobutanol was only produced by *S. cerevisiae* in a valine-free medium, according to Brat *et al.* (2012). This work shows that this can be attributed to the catalytic activity of Ilv2Δ54, which acted as growth inhibitor to *S. cerevisiae*. By this logic, a negative selection on the *ILV2Δ54* gene was exerted, which made the *ilv2* deletion and simultaneous valine exclusion necessary to maintain the functional expression of toxic *ILV2Δ54*. Furthermore, it was shown that valine exclusion is not mandatory due to the feedback regulation of Ilv2, permitted by Ilv6. Rather, increased isobutanol yield was observed when cytosolic Ilv6Δ61 was expressed in the valine-free medium, which is explained by the enhanced regulation of Ilv2Δ54 by Ilv6Δ61 when BCAA are absent. Isobutanol biosynthesis is neither redox- nor NAD(P)H co-factor balanced. It was seen that co-factor imbalance could be mitigated by the expression of an NADH-oxidase (NOX), but not by expression of the NADH dependent $ilvC^{6E6}$, since the latter showed low *in vivo* activity.

Furthermore, it was seen that NAD(H) imbalance did already limit isobutanol biosynthesis, but the NADP(H) imbalance did not. Another limitation of cytosolic isobutanol biosynthesis is the secretion of the intermediate 2-dihydroxyisovalerate, which then no longer is taken up by *S. cerevisiae,* causing a reduced isobutanol yield. This is attributed to insufficient Ilv3Δ19 activity, due to poor iron-sulphur-cluster apo-protein maturation. Therefore, it was aimed to replace Ilv3Δ19 by heterologous dihydroxyacid dehydratases. Even though some of the enzymes were functionally expressed, none showed better *in vivo* activity than Ilv3Δ19. Therefore, the Ilv3Δ19 apo-protein maturation was improved. This was achieved by the genomic deletion of *fra2* or *pim1* as well as by the cytosolic expression of Grx5Δ29.

In addition to the isobutanol pathway, *S. cerevisiae* was optimised for isobutanol biosynthesis by rational and evolutionary engineering. For this purpose, the genes which are necessary for isobutanol production were integrated into the *ilv2* locus, and the resulting strain was evolved in a medium containing the toxic amino acid analogue norvaline. Evolved single colonies were isolated, which presented improved growth and increased isobutanol yields (0.59 mg/g_{Glc}) in a valine-free medium, as compared to the initial strain. This is explained by a gene dosage effect which occurred during the evolutionary engineering experiment. In collaboration with Dr. Wess, the genes *ilv2, bdh1/2, leu4/9, ecm31, ilv1, adh1, gpd1/2* and *ald6* were cumulatively deleted in CEN.PK113-7D to block competing metabolic pathways. The resulting strain JWY23 achieved isobutanol yields up to 67.3 mg/g_{Glc}, when expressing the cyt-ILV enzymes from a multi-copy vector. The most promising approaches of this work, namely the deletion of *fra2* and the expression of Grx5Δ29, Ilv6Δ61, and NOX, were confirmed in this JWY23 strain. The highest isobutanol yield from this work was observed at 72 mg/g_{Glc} for Ilv6Δ61 and cyt-ILV enzymes expressing JWY23, which corresponds to 17.6% of the theoretical isobutanol yield.

Isobutyric acid (IBA) is a by-product of isobutanol biosynthesis, but it is also considered a valuable platform chemical. Therefore, the approaches that improved isobutanol biosynthesis were applied to the biosynthesis of IBA in *S. cerevisiae*. The highest IBA yield of 9.8 mg/g_{Glc} was observed in a valine-free medium by expression of cyt-ILV enzymes, NOX and Ald6 in JWY04 (CEN.PK113-7D *Δilv2; Δbdh1; Δbdh2; Δleu4; Δleu9; Δecm31; Δilv1*). This corresponded to an 8.9-fold increase compared with the control and is, to our best knowledge, the highest IBA yield reported to date for *S. cerevisiae*.

2. INTRODUCTION

2.1. BIOECONOMY: BIO-BASED PRODUCTS FROM RENEWABLE BIOMASS

The finite nature of fossil resources combined with the environmental issues caused by their excessive usage, has dramatically increased the interest in replacing fossil-based chemicals by chemicals derived from renewable biomass. This transition from a fossil-based economy towards a bio-based one is referred to as “bioeconomy”. Today, bio-based products are mainly produced from primary biomass. For the industrial large-scale production of bio-based chemicals, the spectrum of carbon sources must be expanded beyond the usage of primary biomass such as sugarcane, corn starch, and vegetable oil. This is especially important in order to avoid competition with agricultural food production, thereby helping the concept of bioeconomy gain broader acceptance in policymaking, population, and industries. Therefore, much research has been conducted to expand the utilisation of primary biomasses to include lignocellulosic biomass as a carbon source. Moreover, lignocellulosic biomass like crop waste, forestry residues and municipal solid waste, offer a high potential as feedstock for bio-based products, as they are the most abundant sustainable raw material worldwide, and additionally occur as by-products, without any competing use. However, not only providing an abundant feedstock with no competition to food production but also the development of microorganisms that produce valuable compounds is of outstanding interest. Thus, researchers have applied different technologies to modify organisms to produce bio-based chemicals that meet the market’s needs (Lee *et al.* 2012a; Guo and Song 2019).

2.2. METABOLIC ENGINEERING IN BIOTECHNOLOGY AND BIOECONOMY

For the demanding replacement of fossil-based compounds in the industry, systems- and synthetic biology, evolutionary engineering, random mutagenesis, and metabolic engineering can be considered as key technologies. Systems biology studies organisms in all their complexities by combining genomic and proteomic data with the organisms’ physiologies. Synthetic biology aims to develop enzymes, signalling pathways and organisms with novel functioning. Evolutionary engineering simulates microbial evolution in the laboratory by exerting a selection pressure on an organism to choose for desired properties. Random mutagenesis is the artificial mutagenesis of genes by applying mutagen agents or radiation; the mutated genes are then selected for beneficial properties. Metabolic engineering is considered a combinatorial technology that uses data from evolutionary engineering, random

mutagenesis, and systems- and synthetic biology to establish microbial cell factories in order to produce valuable compounds. By this approach, fossil-based and chemically synthesised compounds can be substituted by microbially produced compounds, derived from renewable biomass. In addition, metabolic engineering enables industries to produce complex compounds that are difficult to synthesise chemically, such as hormones, antibiotics, or vitamins. However, microbes are often unable to produce the desired product in sufficient amounts naturally. For industrially worthwhile production, the researchers first have to solve a number of issues, including uptake and export of substrate and product, co-factor supply or redox balance. Redirection of the metabolic flux through the desired metabolic pathway or compartments without feedback-inhibition and improving the host's tolerance to toxic intermediates or products remains a challenge, too. For these reasons, many fast and efficient metabolic engineering techniques have been developed in the past years that allow an easy modification of microbes, to create highly efficient cell-factories for the production of valuable bio-based chemicals. Consequently, metabolic engineering tools, such as gene cloning, bioinformatics algorithms, gene sequencing and DNA synthesis technologies, are becoming cheaper and more efficient. Many genes from different organisms have been identified and intensively studied for heterologous expression, in order to overcome existing limitations in microbial biosynthesis of valuable compounds (Chae *et al.* 2017; Choi *et al.* 2019).

Some promising and well-known organisms for metabolic engineering are, for instance, bacteria such as *Escherichia coli*, *Corynebacterium glutamicum*, *Pseudomonas putida,* or the yeast *Saccharomyces cerevisiae*. These organisms have been modified to produce many different compounds. For example, *E. coli* has been modified to produce various compounds such as insulin (Baeshen *et al.* 2014), 1,4-butanediol (Yim *et al.* 2011), salicylic acid (Noda *et al.* 2016) or caffeic acid (Furuya *et al.* 2012). *P. putida* is known to produce *cis-cis*-muconic acid (Johnson *et al.* 2016) and p-hydroxystyrene (Kallscheuer *et al.* 2016), while *C. glutamicum* has been modified for pinosylvin (Verhoef *et al.* 2009) production, and *S. cerevisiae* for ethanol (Mohd Azhar *et al.* 2017), mandelic acid (Reifenrath and Boles 2018) or resveratrol (Li *et al.* 2015) production, among others.

2.3. *S. CEREVISIAE* IN RESEARCH AND BIOECONOMY

S. cerevisiae and other yeasts have been used by humans for thousands of years for microbial bread, beer and wine production. In fact, centuries ago, humans domesticated and isolated yeasts from nature to use them for industrial processes. Today, *S. cerevisiae* is recognised by the FDA as a “generally recognised as safe” (GRAS) organism and can be used for food and drug production processes without further approval. *S. cerevisiae* is robust against processing conditions with high sugar concentration, high osmotic pressure, or low pH. Furthermore, it can be cultivated under anaerobic conditions and is resistant to many toxic products or inhibitors from renewable biomass hydrolysates. Due to the early interest in *S. cerevisiae*, and its robust properties during fermentation, *S. cerevisiae* has become a well-studied eukaryotic model organism. Because of this, many techniques for genetic engineering of *S. cerevisiae* are available to solve numerous challenges in metabolic engineering. New recombinant DNA techniques, such as Golden-Gate Cloning (Agmon *et al.* 2015) or CRISPR-Cas (Generoso *et al.* 2016), make DNA modification convenient and highly efficient. Furthermore, different compartmentalisation strategies to avoid diffusion or toxic effects of intermediates are already available (Choi *et al.* 2019; Hammer and Avalos 2017), and scaffold-complexes for efficient substrate uptake or redirecting the metabolic flux through desired metabolic pathways have also been established (Thomik *et al.* 2017). These, and many other metabolic tools, make pathway engineering in *S. cerevisiae* less demanding and faster than other, less well-studied organisms. Thus, several industrial processes to produce valuable compounds with *S. cerevisiae* have already been realised.

Following are some examples of industrially produced compounds using *S. cerevisiae*. GlaxoSmithKline (GSK) produces many vaccines, for instance, against Hepatitis A and B (Twinrix). Farnesene, an insect repellent, is produced by Amyris, while resveratrol, a dietary supplement, is produced by Evolva (Srivastava 2018). In addition to recombinant proteins and fine chemicals, bulk chemicals such as lactic and succinic acids are industrially produced using *S. cerevisiae*. Lactic acid, a precursor to polylactic acid (PLA) thermoplastic, is produced by Natureworks LLC. Succinic acid, a food additive and also a polymer precursor, is produced by BioAmber (Borodina and Nielsen 2014). Other bulk chemicals such as fatty acids and bio-based fuels are also industrially produced using *S. cerevisiae*, discussed in the next chapter.

2.4. Role of Biofuels in Bioeconomy

The bioeconomy combined with the power of metabolic engineering, can contribute to a sustainable industry, and will play a key role in climate protection. The agreement to limit global warming to 2 C urges governments to reduce greenhouse gas emission of the energy sector. In 2015, more than 95% of fossil carbon sources were used to generate energy for industry, housing, and transportation, of which about 300 million tons of fossil carbon sources were used in the chemical industry (Kircher 2015). In 2019, a total of 38 billion tons of fossil CO_2 was produced worldwide, while power industry, housing, and transportation remained the significant CO_2 drivers (Crippa *et al.* 2020). Thus, there is a strong socioeconomic and political interest in replacing fossil-based fuels with bio-based fuels (biofuels).

First-generation bioethanol produced from primary feedstock was the first biofuel blend to be commercially used as a gasoline substitute. In recent years, the question of primary feedstock utilisation, which competes with food and feed production, has been successfully solved by the metabolic engineering of *S. cerevisiae*. Today, some companies are already producing second-generation bioethanol from lignocellulotic feedstock (Jansen *et al.* 2017). However, various properties of bioethanol, such as low energy density and high hygroscopicity, lead to storage and transportation issues when used as a fuel blend. For this reason, in the United States, almost 90% of the energy consumed for transportation is still derived from fossil-based fuels. These fuels, like gasoline, diesel and jet fuel, have a high carbon content between C4 and C20. This makes them more suitable for internal combustion engines than ethanol, due to their higher energy density and lower hygroscopicity. In addition, parameters such as viscosity, freezing point, octane or cetane number, vapour pressure, flash point, and toxicity are properties that must be considered when selecting alternatives for fossil-based fuels (MacLean and Lave 2003).

In general, biofuels are divided into short-chain (C4-C8), medium-chain (C9-C14) and long-chain (C15–C20) fuels and then further divided into straight-chain (e.g., alcohols, fatty acids) or branched-chain (e.g., isoprenoids, alcohols) biofuels. Branched short-chain alcohols have higher octane values than their linear-chain counterparts. Branched long-chain fuels offer improved properties compared to their straight-chain counterparts, such as lower freezing point, better cold flow, and lower cloud point, which are essential for the practical use of biofuels at low temperatures and high altitudes, especially for jet fuels (Bai *et al.* 2019). Many well-studied

microorganisms are already capable of producing a broad variety of compounds found in fossil fuels from primary and/or secondary feedstock. For example, alcohols, isoprenoids, and fatty acids can be produced by microorganisms as biofuels or precursors. The production of non-ethanol alternatives from renewable lignocellulosic biomass is often challenging and usually requires metabolic engineering of microorganisms, prior to industrial biofuel production.

S. cerevisiae has been modified to produce many biofuels that can be classified into the abovementioned categories; for example, the branched-chain isoprenoid farnesene (Meadows *et al.* 2016) but also long- and medium-chain fatty acids and alcohols (Runguphan and Keasling 2014) as well as short-chain fatty-alcohols (Henritzi *et al.* 2018). For a more detailed review of additional biofuels and the recent advances towards commercialisation, see Meadows *et al.* (2018).

Alcohols play a predominant role as biofuel since *S. cerevisiae* is an alcohol producer by nature. Great efforts have been made to improve the titers of higher alcohols, such as n-butanol (Schadeweg and Boles 2016; Si *et al.* 2014) and the branched chain alcohol isobutanol (Matsuda *et al.* 2013; Suga *et al.* 2013; Brat *et al.* 2012). The metabolic pathway of *S. cerevisiae* for branched-chain alcohol production is explained in detail below.

2.5. Native and Metabolically Engineered Branched Chain Alcohol Production in *S. cerevisiae*

S. cerevisiae is naturally able to produce branched-chain alcohols by degradation of the branched-chain amino acids (BCAAs) valine, leucine, and isoleucine *via* the Ehrlich pathway (Ehrlich 1907). In addition, *S. cerevisiae* is also able to *de novo* synthesise BCAAs from pyruvate. Pyruvate is derived from sugar utilisation during glycolysis. Thus, *S. cerevisiae* already natively contains all genetic information necessary to produce branched-chained alcohols, such as isobutanol. The catabolic enzymes of the Ehrlich pathway are expressed in the cytosol, while the anabolic enzymes necessary for the *de novo* synthesise of BCAA are functionally expressed in the mitochondria (Bussey and Umbarger 1969; Satyanarayana and Umbarger 1968).

2.5.1. *De novo* Synthesis of Branched Chain Amino Acid in *S. cerevisiae*

The BCAAs, isoleucine, leucine, and valine (ILV) are *de novo* synthesised by the enzymes of the ILV pathway, namely Ilv2, Ilv6, Ilv5, Ilv3 and Bat1. The BCAA anabolism is catalysed in the mitochondria, but the ribosomal synthesis of the enzymes takes places in the cytosol. After protein translation, the immature unfolded protein contains an amino-terminal mitochondrial targeting-sequence (MTS), which is recognised by various mitochondrial import machineries (for instance, energy dependent TOM-TIM import machinery). MTS typically consist of different lengths and amino acid compositions. In yeast, common MTS sequences consist of 15 to 55 amino acids, and usually contain basic and positively charged amino acids. After mitochondrial import of the unfolded protein, the MTS is usually cleaved off, resulting in the correctly folded protein (Heijne 1986; Roise *et al.* 1986). The mechanism of the mitochondrial import is not described in detail, as it has been satisfactorily reviewed by Kulawiak *et al.* (2013).

For the valine and leucine synthesis, two molecules of pyruvate are condensed by the acetolactate synthase (ALS) Ilv2 to 2-acetolactate (ALAC) while cleaving CO_2. Similarly, in isoleucine synthesis, one molecule of pyruvate is condensed with 2-oxobutanoate to 2-aceto-2-hydroxybutanoic acid (AHBA). Both ALAC and AHBA are further isomerised and reduced by ketol-acid reductoisomerase (KARI) Ilv5 to 2-dihydroxyisovalerate (DIV) and 2,3-dihydroxy-methylvalerate (DMV), respectively. Finally, DIV or DMV are dehydrated by the dihydroxyacid dehydratase (DHAD) Ilv3 to form 2-ketoisovalerat (KIV) or 2-keto-3-methylvalerate (KMV). For the synthesis of leucine, KIV is further processed by the enzymes Leu4 and Leu9. For valine and isoleucine synthesis, KIV or KMV is finally transaminated by Bat1, respectively (Satyanarayana and Umbarger 1968; Bussey and Umbarger 1969).

The intermediates KIV and KMV are important targets for biofuel production in *S. cerevisiae*, since both can be degraded *via* the catabolic Ehrlich pathway to isobutanol and 2-methyl-2-butanol, respectively. Hence, it is of outstanding interest for research and industry to increase KIV production by metabolic engineering of *S. cerevisiae,* to achieve high amounts of isobutanol. In the following sections, the ILV enzymes, as well as the state-of-the-art metabolic engineering to overcome limitations in isobutanol biosynthesis, are discussed in detail (Figure 1).

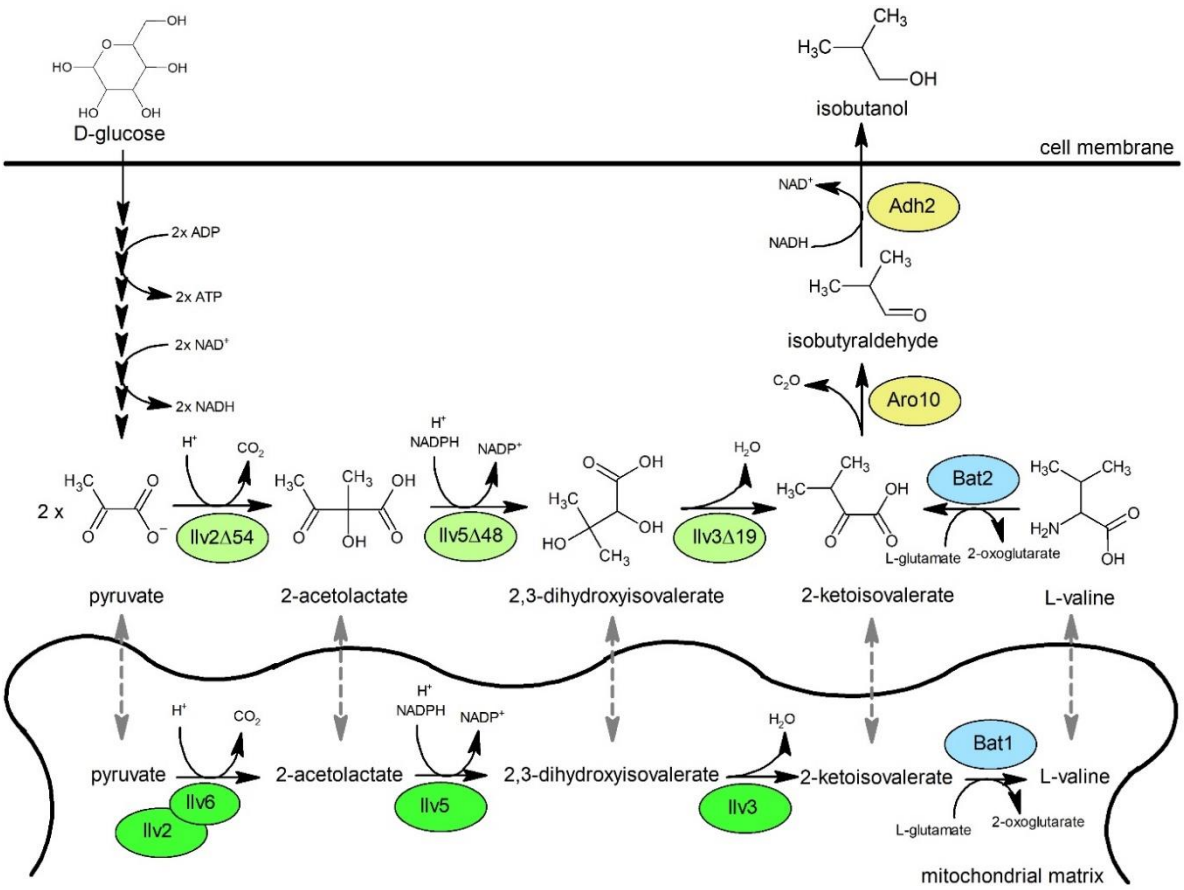

Figure 1 Overview of the native and genetic engineered (Brat *et al.* 2012) isobutanol biosynthetic pathway with co-factors, intermediates and enzymes in *S. cerevisiae*. Glucose is converted into two molecules of pyruvate by the multistage glycolysis, whereby two molecules of ATP are produced, and two molecules of NAD^+ are reduced to NADH. Pyruvate is then transported into the mitochondria and processed by the native ILV-enzymes Ilv2/Ilv6, Ilv5 and Ilv3 (green) to 2-acetolactate; 2,3-dihydroxyisovalerate and 2-ketoisovalerate, respectively. During these enzymatic reactions, CO_2 and water are cleaved off and one molecule of NADPH is oxidised to $NADP^+$ by Ilv5. The mitochondrial anabolic transaminase Bat1 (blue) finally synthesizes valine from 2-ketoisovalerate. Valine is then exported to the cytosol and degraded to 2-ketoisovalerate by the cytosolic and catabolic Bat2 enzyme (blue). Finally, the enzymes of the Ehrlich pathway e.g., Aro10 and Adh2 (yellow), use 2-ketoisovalerate to produce isobutyraldehyde and isobutanol, respectively. During isobutyraldehyde production one molecule of CO_2 is cleaved and one molecule of NADH is oxidised to NAD^+ during the reduction reaction of isobutyraldehyde to isobutanol. Brat *et al.* (2012) showed that all intermediates of the ILV pathway are able to diffuse between the cytosol and mitochondrial matrix (depicted by grey dotted arrows). However, for a more efficient isobutanol production, the ILV enzymes have been re-localised by an N-terminal truncation (light green) to localise the ILV enzymes and the Ehrlich pathway in the same compartment. Additionally, the native ILV2 gene was deleted to inhibit initial *de novo* synthesis of valine (not indicated in the figure).

2.5.1.1. ILV2 - ACETOLACTATE SYNTHASE

Acetolactate synthase Ilv2 catalyses the first enzymatic reaction of the BCAA pathway in the mitochondria. It condenses two molecules of pyruvate to ALAC or one pyruvate and 2-oxobutanoate to AHBA for the synthesis of leucine, valine, or isoleucine. Ilv2 is a thiamine pyrophosphate (TPP) dependent enzyme that requires magnesium, or other divalent cations, and flavin adenine dinucleotide (FAD) as co-factors. The latter is not necessary for catalytic activity and is, therefore, intended to be a structural stabilising co-factor (Pang *et al.* 2002). Biochemical analyses of the Ilv2 enzymes showed that the ILV pathway is regulated by isoleucine, leucine, and

valine. Gene expression is regulated by the concentration of these amino acids using the Gcn4-dependent general amino acid control (GAAC); this mechanism increases basal gene expression in case of amino acid deficiency (Kakar and Wagner 1964; Xiao and Rank 1988). While Ilv2 is responsible for catalytic activity, *S. cerevisiae* possesses an additional protein Ilv6, which regulates the activity of Ilv2; therefore, Ilv6 is considered a regulatory subunit. Ilv6 is also translated as an unfolded protein, with N-terminal MTS in the cytosol, then imported into the mitochondrion and further processed to matured Ilv6. The combination of Ilv6 with Ilv2 in the mitochondrion increases both the activity of Ilv2 and sensitivity to valine inhibition (Cullin *et al.* 1996; Duggleby 1997; Pang and Duggleby 1999). Feedback insensitive Ilv6 variants have been developed, which no longer regulate the catalytic activity of Ilv2 in the presence of valine (Takpho *et al.* 2018).

It is known that the cytosolic Ilv2 activity during the beer brewing process causes an unwanted buttery flavour. This results from increased diacetyl content, which is caused by an increased ALAC concentration, since the cytosolic pyruvate is easily accessible to cytosolic Ilv2 (Dasari and Kölling 2011). However, during isobutanol biosynthesis in *S. cerevisiae,* a high ALAC is necessary for isobutanol biosynthesis. Brat *et al.* (2012) created a cytosolic and catalytically active isoform of the enzyme through deletion of the first 54 N-terminal amino acids (hereafter referred to as Ilv2Δ54). With the re-localisation and constitutive expression of Ilv2Δ54 together with the deletion of native *ilv2*, Brat *et al.* (2012) were able to increase isobutanol production in *S. cerevisiae*. Furthermore, bacterial ALS isoforms, for instance, from *C. glutamicum* or *L. plantarum,* have already been expressed in *S. cerevisiae* for isobutanol production (Milne *et al.* 2016; Ishii *et al.* 2018).

2.5.1.2. ILV5 - KETOL-ACID REDUCTOISOMERASE

The second step of the BCAA pathway is catalysed by the mitochondrial enzyme ketol-acid reductoisomerase Ilv5. The substrates ALAC or AHBA are isomerised, and subsequently reduced by Ilv5 to DIV or DMV, respectively. First, the substrate is isomerised by the mechanism of alkylmigration using Mg^{2+}-ions. Then, the isomerised intermediate is reduced by the transfer of a hydride ion from the co-factor NADPH to it. During the multistage reaction, the intermediate is permanently bound to the enzyme and thus not released from the enzyme, until the end of the catalytic reaction (Arfin *et al.* 1969; Chunduru *et al.* 1989).

In addition to its catalytic activity, Ilv5 also stabilises the mitochondrial DNA (mtDNA) and contributes to the distribution of mtDNA-nucleoids. Deletion of Ilv5 leads to BCAA auxotrophy and, in addition, an accumulation of mutants with disturbed mitochondrial activity (Zelenaya-Troitskaya *et al.* 1995). Because of the mtDNA stabilising function of Ilv5, Brat *et al.* (2012) established a combined isobutanol pathway with a constitutive expression of a cytosolic isoform Ilv5Δ48, with the native Ilv5 still being present in the yeast's genome. This ensured efficient cytosolic catalytic activity without disturbing the mtDNA stabilising effect of native Ilv5.

Furthermore, metabolic engineering for the KARI enzyme has been performed in order to change the co-factor utilisation from NADPH to NADH. During glycolysis, two NADH are produced per glucose. However, in the isobutanol pathway only one NAD^+ is recovered by the Adh2 reduction reaction in the Ehrlich pathway. Ilv5 on the contrary uses NADPH for the reduction reaction. Therefore, isobutanol production from glucose is neither NAD(H) nor NADP(H) co-factor balanced. As a result, it is not possible to establish the isobutanol pathway as main fermentative pathway in *S. cerevisiae,* without metabolic engineering. Suga *et al.* (2013) constructed a transhydrogenase-like shunt for the conversion of NADH to NADPH by the enzymes Pyc2, Mdh2, and a cytosolic version of Mae1. In this futile cycle, pyruvate is converted to oxaloacetate (by pyruvate carboxylase Pyc2), then to malate (by malate dehydrogenase Mdh2) and finally back to pyruvate (by cytosolic mutant of the malic enzyme sMae1). Excess NADH from the glycolysis is recovered, and excess NADPH is produced, which is then used by the Ilv5 (Figure 2). With this co-factor exchange strategy and additional disruption of the pyruvate dehydrogenase complex by deletion of *lpd1,* a isobutanol yield of 16 mg/g_{Glc} was achieved in *S. cerevisiae* (Matsuda *et al.* 2013; Suga *et al.* 2013).

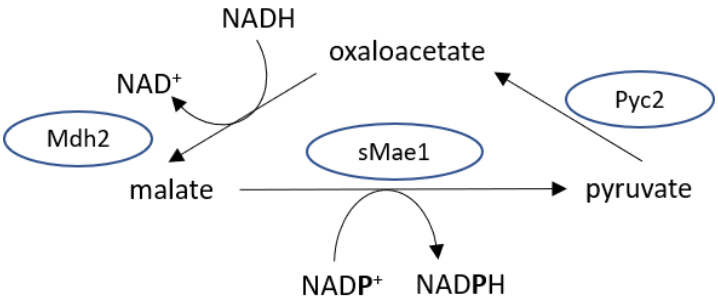

Figure 2 Schematic overview of the futile shunt to oxidise excess NADH by producing NADPH (Suga *et al.* 2013). In this cycle, pyruvate is converted to oxaloacetate (by Pyc2), then to malate (by Mdh2) and finally back to pyruvate (by cytosolic sMae1); Mdh2 oxidises NADH, while sMae1 reduces $NADP^+$.

A different approach was employed by Bastian *et al.* (2011) for isobutanol production in *E. coli*. Here, the bacterial KARI (*ilvC*) enzyme was modified in order to convert a NADPH dependent *ilvC* into a NADH dependent mutant (hereafter referred to as $ilvC^{6E6}$). This was achieved by site-directed mutagenesis of A71S, R76D, S78D, and G110V in *ilvC*, by which the K_m for NADH decreased from 1080 µM to 30 µM, while the K_m for NADPH increased from 40 µM to 650 µM. By this approach, Bastian *et al.* (2011) achieved 100% of the theoretical isobutanol yield in *E. coli*. Furthermore, $ilvC^{6E6}$ has already been shown to be actively expressed in *S. cerevisiae,* and has been successfully used for isobutanol production (Generoso *et al.* 2017). Today, more NADH dependent KARIs have already been developed by using the mutagenesis approach, as described by Brinkmann-Chen *et al.* (2013).

2.5.1.3. ILV3 - DIHYDROXYACID DEHYDRATASE

The enzyme dihydroxyacid dehydratase Ilv3 catalyses the dehydration and tautomerisation of DIV or DMV to its corresponding keto-acids KIV or KMV, respectively (Pirrung *et al.* 1991; Wixom *et al.* 1960). KIV is used for the synthesis of valine or leucine, while the Ehrlich pathway uses KIV as precursor to produce isobutanol. In contrast, the keto-acid KMV serves as a precursor of isoleucine and the corresponding alcohol 2-methyl-1-butanol. For the catalytic activity of Ilv3, a Mg^{2+}-ion and an iron-sulphur-cluster (ISC) are required as co-factor. Like the other ILV-enzymes, Ilv3 is translated as an unfolded protein with an N-terminal MTS. After mitochondrial import, the N-terminal truncated apo-enzyme is activated by incorporation of an ISC. Brat *et al.* (2012) constructed a N-terminal truncated and catalytically active Ilv3 isoform (hereafter referred to as Ilv3Δ19) for cytosolic isobutanol production. However, it is still unknown whether Ilv3 contains [2Fe-2S] ISC or [4Fe-4S] ISC in its active holo-state. Studies with *S. cerevisiae* mutants, lacking a functional late acting [4Fe-4S] ISC assembly machinery, did not show any decrease in Ilv3 enzyme activity. These results suggest that Ilv3 contains [2Fe-2S] ISC (Mühlenhoff *et al.* 2010). If Ilv3 contains [2Fe-2S] ISC, this might cause an issue when establishing an entirely cytosolic BCAA-pathway, as the [2Fe-2S] ISC maturation occurs exclusively in the mitochondria (Lill *et al.* 2015; Lill 2020). Since it is known that expression of bacterial ISC enzymes in *S. cerevisiae* remain challenging, it would also be challenging to substitute cytosolic Ilv3Δ19 by a heterologous [4Fe-4S] DHAD (Benisch and Boles 2014).

Benisch and Boles (2014), for example, failed to implement the Entner–Doudoroff pathway (EDP) in *S. cerevisiae*. For implementation of the bacterial EDP heterologous expression of only two enzymes, 6-phospho-D-gluconatedehydratase (PGDH) and a 2-dehydro-3-deoxy-D-gluconate-6-phosphate (KDPG) aldolase are necessary. First, the 6-phospho-D-gluconate is converted by PGDH to KDPG, which is then cleaved by a KDPG aldolase into D-glyceraldehyde-3-phosphate (GAP) and pyruvate. By implementing the EDP in *S. cerevisiae,* it would be possible to catabolise glycose by only producing one ATP, NADH and NADPH, each. Glycolysis, in contrast, produces two ATP and NADH per glucose. Therefore, the EDP would be also of interest for isobutanol biosynthesis, as the isobutanol pathway could be co-factor balanced when employing the EDP for glucose utilisation. As a result, isobutanol biosynthesis could be established as the main fermentative pathway in *S. cerevisiae*. However, the implementation of the EDP failed due to low PGDH activity. The authors have suggested that activity remained low as PGDH contains [4Fe-4S] ISC, and cytosolic apo-protein maturation of PGDH was insufficient due to poor compatibility with the cytosolic ISC assembly (CIA) machinery of *S. cerevisiae*. Another example of non-functional bacterial ISC enzyme expression in *S. cerevisiae* is the replacement of the endogenous mevalonate pathway of *S. cerevisiae* by the bacterial 2-C-methyl-d-erythritol-4-phosphate pathway. It is composed of the enzymes 1-hydroxy-2-methyl-2-(E)-butenyl-4-phosphate synthase (*ispG*) and 1-hydroxy-2-methyl-2-(E)-butenyl-4-phosphate reductase (*ispH*), which require [4Fe-4S] ISC to be catalytically active (Carlsen *et al.* 2013; Partow *et al.* 2012).

Nevertheless, experiments in which heterologous ISC enzymes were expressed in *S. cerevisiae* are also described in the literature. Carlsen *et al.* (2013) also showed that bacterial *leuC* and *leuD*, encoding the heterodimeric [4Fe-4S] ISC enzyme isopropylmalate isomerase, could complement a *leu1* auxotrophy in *S. cerevisiae*. These results show that *S. cerevisiae* is able to functionally express bacterial ISC proteins e.g., DHADS, even though it remains challenging.

Furthermore, when expressing the cytosolic isoforms of the ILV enzymes high DIV secretion, the substrate of Ilv3Δ19, was observed. This is considered as a limitation during cytosolic isobutanol production (Generoso *et al.* 2017).

2.5.2. BCAA-CATABOLISM *VIA* EHRLICH PATHWAYS IN *S. CEREVISIAE*

S. cerevisiae can use BCAA and aromatic amino acids (AAA) as nitrogen sources *via* the Ehrlich pathway. The amino acids are transaminated by the transaminases Bat1 and Bat2 for BCAAs as well as by Aro8 and Aro9 for AAA to its corresponding α-ketoacids. These α-ketoacids are then used as substrate by decarboxylases Pdc1, Pdc5, Pdc6, and Aro10, resulting in the corresponding aldehyde. Finally, the aldehyde is reduced by alcohol dehydrogenases Adh1-5 to the corresponding fusel alcohol. The following sections describe the enzymatic steps of the BCAA degradation in general and of valine in particular.

2.5.2.1. TRANSAMINATION AS NITROGEN SOURCE

The first step of the catabolic BCAA pathway is catalysed by the transaminases Bat1 and Bat2. By transferring the amino-group from e.g., valine to α-ketoglutarate, KIV and glutamate are formed. The amino group of glutamate and the amide group of glutamine serve as nitrogen sources for biosynthesis of other macromolecules in *S. cerevisiae* (Miller and Magasanik 1990). The NAD^+ dependent glutamate dehydrogenase Gdh2 converts glutamate to 2-oxoglutarate and ammonium. However, *S. cerevisiae* also contains $NADP^+$ dependent glutamate dehydrogenase Gdh1 and its paralogue Gdh3, which catalyse the reverse reaction under fermentative or non-fermentative conditions, respectively (Moye *et al.* 1985; Avendaño *et al.* 1997). Through this coordinated regulation of Gdh1, Gdh2 and Gdh3, the glutamate biosynthesis as well as the α-ketoglutarate utilisation are balanced under fermentative and respiratory conditions (DeLuna *et al.* 2001).

Although, Bat1 and Bat2 show high similarity, Bat1 is localised in the mitochondria, while Bat2 is localised in the cytosol. Gene expression of Bat1 and Bat2 are regulated depending on the cell cycle – Bat1 is expressed during exponential cell growth, while Bat2 is highly expressed in a stationary phase (Eden *et al.* 1996). Although the enzymes can complement each other, mitochondrial Bat1 favours the valine synthesis, while the cytosolic Bat2 favours the valine degradation (Colón *et al.* 2011). Hence, expression of Bat2 results in an increase of isobutanol production, while expression of Bat1 does not. Accordingly, the deletion of Bat2 decreases isobutanol biosynthesis (Eden *et al.* 2001; Yoshimoto *et al.* 2002; Lilly *et al.* 2006).

2.5.2.2. DECARBOXYLATION

During the second step of the Ehrlich pathway, α-ketoacid is decarboxylated to its corresponding aldehyde. Five endogenous enzymes Pdc1, Pdc5, Pdc6, Aro10 and Thi3 are described to be related to the decarboxylation step of the Ehrlich pathway (Dickinson *et al.* 1998). Thi3 has not only been described as a catalytic enzyme but also as a regulatory protein (Dickinson *et al.* 1997). However, Thi3 is not involved in the valine catabolism, which is why it is not further discussed in this section. In valine catabolism, KIV is mainly converted to isobutyraldehyde by the endogenous TPP-dependent pyruvate decarboxylases Pdc1, Pdc5 and Pdc6. However, it has been shown that an isogenic pyruvate decarboxylase-negative strain also produces isobutyraldehyde. Therefore, KIV decarboxylation is not exclusively catalysed by the PDC isoenzymes (Schure *et al.* 1998). For an efficient isobutanol biosynthesis in *S. cerevisiae,* the competing ethanol fermentation must be reduced to a minimum. Therefore, decarboxylases with low activity towards pyruvate but high affinity towards KIV are of interest. In literature, three decarboxylases, endogenous Aro10 (Romagnoli *et al.* 2012; Brat *et al.* 2012), bacterial *kivD* (Plaza *et al.* 2004; Chae *et al.* 2017; Lee *et al.* 2012b; Atsumi *et al.* 2008) and *kdcA* (Milne *et al.* 2015) from *L. lactis* are controversially discussed as efficient KIV-decarboxylases, with lower activity towards pyruvate. Plaza et al. (2004) identified, purified, and characterised a α-ketoacid decarboxylase from *L. lactis* that showed high activity towards KIV (80.7 ± 5.7 U $mg_{protein}^{-1}$) but not for pyruvate (0.46 ± 0.0 U $mg_{protein}^{-1}$). These data were confirmed by *in vivo* expression in *S. cerevisiae,* and by an enzyme assay from a crude cell extraction (Lee *et al.* 2012b). Milne *et al.* (2015) describes three α-ketoacid decarboxylases, Aro10 from *S. cerevisisae*, *kivD* and *kdcA* from *L. lactis,* which were investigated with respect to their properties of isobutanol production in *S. cerevisiae.* In this study it was demonstrated, based on *in vitro* data, that *kdcA* showed the best KIV-decarboxylation activity. However, in an *in vivo* complementation and KIV bio-conversion experiment, no enzyme showed selective KIV decarboxylation. Aro10 is a α-ketoacid decarboxylase with broad substrate specificity, but primarily catalyses the decarboxylation of the aromatic substrate phenylpyruvate. When phenylalanine, leucin or methionine are used as sole nitrogen sources, *ARO10* is upregulated post-transcriptionally (Vuralhan *et al.* 2005). Furthermore, Aro10 has a high affinity towards branched-chain α-ketoacid, e.g., KIV, and is therefore an important enzyme in isobutanol biosynthesis (Romagnoli *et al.*

2012; Brat *et al.* 2012). Crude extracts of a *pdc* null strain, with Aro10 being constitutively expressed, almost completely substituted the missing decarboxylase activity of the Pdc enzymes (32.83 ± 8.72 mU $mg_{protein}^{-1}$), while not showing high ethanol formation. Crude extracts with expressed *kivD* from *L. lactis* only partially complemented the activity of the Pdc enzymes (19.61 ± 2.52 mU $mg_{protein}^{-1}$) (Brat *et al.* 2012).

2.5.2.3. REDUCTION/OXIDATION

The last step of the Ehrlich pathway is the reduction of the aldehyde to its alcohol by NAD(P)H dependent oxidoreductases. However, studies have shown that it strongly depends on the fermentation conditions, whether the aldehyde is reduced to the alcohol (by alcohol dehydrogenases) or oxidised to the corresponding acid (by aldehyde dehydrogenases). When *S. cerevisiae* grows under anaerobic- or high-glucose conditions, growth is mainly fermentative, and alcohols are predominately formed. Under aerobic but glucose-limited conditions, with amino acids as sole nitrogen sources, the amino acids are mainly converted into fusel acids instead of alcohols (Hazelwood *et al.* 2008; Vuralhan *et al.* 2005).

The reduction of, for instance, isobutyraldehyde derived from valine can be catalysed by any of the NADH dependent ethanol dehydrogenases Adh1 to Adh5 or by the formaldehyde dehydrogenase Sfa1. But even with several oxidoreductase deletions, leucine was still be converted to 3-methyl-1-butanol by as yet unknown oxidoreductases. This indicates so far unknown enzymes in *S. cerevisiae* with the ability to reduce branched-chain aldehydes (Dickinson *et al.* 2003). Furthermore, the NADPH dependent members of the cinnamyl alcohol dehydrogenase family, Adh6 and Adh7, can catalyse the reduction of isobutyraldehyde to isobutanol (Larroy *et al.* 2002; Kondo *et al.* 2012). In the studies by Brat *et al.* (2012), the Adh6 activity, with respect to isobutanol biosynthesis, was not confirmed *in vivo*, but Adh2 showed best *in vivo* activity. For acid production from aldehydes, *S. cerevisiae* encodes three cytosolic aldehyde dehydrogenases, Ald1, Ald2 and Ald6, as well as three mitochondrial dehydrogenases, Ald3 Ald4 and Ald5. The different Ald enzymes require NAD^+ or $NADP^+$ as co-factors: Ald1, Ald5 and Ald6 use $NADP^+$, Ald2 and Ald3 use NAD^+, while Ald4 can use both. Furthermore, it is known that only NADP dependent cytosolic Ald6 produces isobutyric acid from isobutyraldehyde (Lee *et al.* 2018; Ida *et al.* 2015; Park *et al.* 2014; Buijs *et al.* 2013) .

2.6. Metabolic Engineering Strategies for Isobutanol Production in Prokaryotes

As described above, isobutanol is produced by combining the valine *de novo* biosynthesis and the catabolic Ehrlich pathway. Only a few organisms, such as *L. lactis, S. cerevisiae* or *Candida sp.*, are natively capable of producing isobutanol in very small amounts, far from the theoretical maximum (Generoso *et al.* 2015). Therefore, various organisms have been modified by metabolic engineering to increase isobutanol biosynthesis. In the following section, strategies for isobutanol biosynthesis in prokaryotes are discussed.

Model organisms such as *E. coli* or *C. glutamicum* are known as BCAA (e.g., valine) producers and are, therefore, able to produce KIV. Valine is synthesised in *E. coli via* the ILV pathway encoded by acetohydroxy acid synthase complexes AHAS I ($ilvB^{ilvN}$), AHAS II ($ilvG^{ilvM}$) and AHAS III ($ilvI^{ilvH}$), which consist of a large catalytic unit and a small regulatory unit, each. AHAS I-III are regulated and feedback inhibited differently by the three BCAAs: isoleucine, leucine and valine. In contrast, *C. glutamicum* contains only one AHAS, which consist of a large catalytic unit *ilvB,* and a small regulatory unit, *ilvN*. An *ilvN* feedback-resistant mutant, $ilvN^{M13}$ has been developed by side-directed mutagenesis (Elisakova *et al.* 2005). Both organisms contain a NADP dependent ketol-acid reductoisomerase *ilvC* and an ISC containing dihydroxyacid dehydratase *ilvD* (Park and Lee 2010). However, *E. coli* and *C. glutamicum* naturally lack the ability to decarboxylate and reduce KIV to isobutanol; therefore, a heterologous expression of the Ehrlich pathway is necessary. Atsumi *et al.* (2008) created a non-fermentative isobutanol biosynthesis pathway in *E. coli,* by constitutive expression of the ILV and Ehrlich pathway (Adh2 from *S. cerevisiae* and *kivD* from *L. lactis*). Furthermore, they achieved a further increase of isobutanol yield by substituting AHAS III with an acetohydroxy-acid synthase *alsS* from *B. subtilis,* together with a deletion of *pflB* to reduce competition for pyruvate. For the *alsS* expressing *E. coli* strain, a 1.7-fold increase of isobutanol was observed, resulting in a theoretical yield of 86%. Later, the group showed that NADH dependent alcohol dehydrogenase *adhA* from *L. lactis* was even better for isobutanol biosynthesis in *E. coli*, because *adhA* showed higher activity towards isobutyraldehyde and lower activity towards acetaldehyde (Atsumi *et al.* 2010). Based on these results, a fermentative isobutanol pathway producing 100% of the theoretical yield was established by Bastian *et al.* (2011). This was achieved by the

expression of an engineered NADH dependent *ilvC* from *E. coli* (hereafter referred to as *ilvC*^{6E6}), and NADH dependent alcohol dehydrogenase *adhA* from *L. lactis* (hereafter referred to as *adhA*^{RE1}), which was modified to be highly active towards isobutyraldehyde. The K_m of *adhA*^{RE1} was decreased from 11.7 mM to 1.7 mM, k_{cat} quadrupled, and the catalytic efficiency of *adhA*^{RE1} towards isobutyraldehyde increased 40-fold compared to wild-type *adhA* (Bastian *et al.* 2011).

In another study, the ED pathway was combined with the isobutanol pathway to establish a fermentative isobutanol pathway in *E. coli* (Noda *et al.* 2019; Liang *et al.* 2018). As described above, the ED pathway produces one ATP, NADH and NADPH per glucose, which allows NADPH utilization by *ilvC* during isobutanol biosynthesis in *E. coli*. In the study of Noda *et al.* (2019) *alsS* from *B. subtilis*, *ilvC* and *ilvD* from *E. coli*, *kivD* and *adhA* from *L. lactis* were expressed. The combination of the ED pathway with the isobutanol biosynthesis pathway is an effective strategy to establish a co-factor balanced isobutanol biosynthesis in *E. coli*, reaching 90% of the theoretical yield.

2.7. Metabolic Engineering Strategies for Isobutanol Production in *S. cerevisiae*

Although, the engineered prokaryotes produced isobutanol yields up to theoretical maximum, these hosts have usually a low tolerance to e.g., high alcohol concentrations and low pH values, which is a major bottleneck in alcohol biosynthesis on an industrial scale. Consequently, *S. cerevisiae* is preferably used for industrial alcohol fermentation, due to its tolerance towards the harsh conditions that occur during industrial fermentation with lignocellulosic hydrolysates (Liu and Qureshi 2009; Weber *et al.* 2010).

In prokaryotes, the main challenge of isobutanol biosynthesis is to solve the co-factor balance and the heterologous expression of the Ehrlich pathway. Contrarily, *S. cerevisiae* already contains this pathway by nature. However, the issue of NAD(P)H co-factor imbalance during isobutanol biosynthesis also exists. Furthermore, additional bottlenecks such as compartmentation between glycolysis, valine anabolism and catabolism as well as ISC containing DHAD are additional challenges for isobutanol biosynthesis in *S. cerevisiae (Generoso et al. 2015).*

The first isobutanol biosynthesis using *S. cerevisiae*, which is described in literature, showed an improvement of isobutanol from 0.28 mg/g_{Glc} to 3.86 mg/g_{Glc},

by constitutive expressions of Ilv2, Ilv5, Ilv3 and Bat2. Additional expression of Ilv6 and supply of BCAA showed no further improvement for the engineered strain. However, isobutanol production increased in the reference strain when BCAA were added, indicating other existing bottlenecks as soon as the ILV pathway was constitutively expressed (Chen *et al.* 2011). The expression of *kivD* from *L. lactis,* together with the ILV enzymes, additionally increased isobutanol biosynthesis. However, the efficiency remained below 1% of the theoretical yield (Lee *et al.* 2012b). Kondo *et al.* (2012) increased the isobutanol yield to 6.6 mg/g_{Glc} *via* the additional expression of Adh6, and redirection of the metabolic flux from ethanol to isobutanol by *pdc1* deletion. A similar approach was performed by Park *et al.* (2014) with constitutive expression of Leu3Δ601 (a constitutively active form of Leu3), Ilv2, Ilv3, Ilv5, Aro10, and Adh2 in a *bat1* and *ald6* deletion strain, resulting in an isobutanol yield of 3.77 mg/g_{Glc}. In the same strain, isobutanol production was further improved by deletion of *lpd1,* and the constitutive expressions of Mpc1 and Mpc3. Lpd1 is a subunit of the pyruvate dehydrogenase, which competes with the isobutanol biosynthesis at the level of pyruvate. Mpc1 and Mpc3 are responsible for pyruvate transport from the cytoplasm into the mitochondrial matrix. However, the best results in this strain have been obtained by additional mitochondrial compartmentalisation of the enzymes of the Ehrlich pathway. Therefore, Aro10 and Adh2 have been tagged with a N-terminal MTS of Cox4 (Maarse *et al.* 1984; Avalos *et al.* 2013), which increased the isobutanol yield to 16.55 mg/g_{Glc} (Park *et al.* 2016).

This example shows that the different compartmentalisation of the ILV pathway (mitochondrial) and Ehrlich pathway (cytosolic) is a major limitation during isobutanol biosynthesis in *S. cerevisiae*. Therefore, two strategies that have been intensively studied are as follows: first, the expression of the Ehrlich pathway in mitochondria, and second, the expression of the ILV pathway in the cytosol. The expression of two different pathways in the mitochondria, or other cell compartments, is an interesting tool for metabolic engineering to increase production of valuable compounds. Compartmentalisation can prevent the loss of intermediate to competing pathways, and can mitigate transport limitations or toxic effects of intermediates. (Choi *et al.* 2019)

Avalos *et al.* (2013) for example achieved the best isobutanol titers in their studies when the ILV pathway was co-expressed with mitochondrial re-located Aro10 and $adhA^{RE1}$ from *L. lactis* – this strategy increased isobutanol yield up to 6.7 mg/g_{Glc}.

This mitochondrial strategy was then further optimised by Yuan and Ching (2015) who balanced the expression level of the five enzymes, using the genomic δ-integration system. The integration of ILV enzymes and mitochondrial versions of *ARO10* and *ADH7* was verified by a qRT-PCR, and found to be significantly higher than that of the parental strain. By this confirmation of chromosomal gene integration, they found that *ILV5* and *ADH7* had the highest mRNA expression level, which was due to multiple genomic integrations, leading to an isobutanol yield of 15 mg/g_{Glc}. However, the fermentation was performed in SC-mineral medium without valine, using galactose as a carbon source. This makes a comparison with the data of Avalos *et al.* (2013) difficult, because in the said study glucose was used as carbon source and valine was added to the fermentation medium.

Although the mitochondrial isobutanol biosynthesis strategy is very promising, it must be mentioned that mitochondria are mainly formed under aerobic growth conditions (Polakis *et al.* 1964; Lukins *et al.* 1966; Wallace *et al.* 1968). For cost reasons, industrial fermentations are predominantly performed anaerobically without oxygen supply. Therefore, a cytosolic isobutanol biosynthesis would be advantageous for industrial production. However, by the cytosolic approach, new issues such as the diffusion of intermediates, competing cytosolic pathways, toxic effects of intermediates, and the cytosolic activity of the ISC containing Ilv3, need to be solved. Some of these limitations have already been addressed in several studies, included in the following sections or in Table 1.

Brat *et al.* (2012) expressed cytosolic ILV isoforms Ilv2Δ54, Ilv5Δ48, and Ilv3Δ19 (cyt-ILV), together with Aro10 and Adh2 in an *ilv2* deletion strain, resulting in an isobutanol yield of 15 mg/g_{Glc}.

Another cytosolic strategy addressed the issues of co-factor imbalance by using a transhydrogenase like shunt (described in Section 2.5.1.2), and simultaneously blocking the pyruvate competition by *lpd1* deletion together with expression of cyt-ILV enzymes. This strategy resulted in an isobutanol yield of 16 mg/g_{Glc} (Matsuda *et al.* 2013).

The limitation of intermediate loss due to competing pathways was addressed by Ida *et al.* (2015). In this study, *ald6*, *ecm31* or *ilv1* were deleted in *S. cerevisiae* to block the competing production of isobutyric acid, pantothenate and isoleucine, respectively. The deletion of each individual gene increased isobutanol production,

with the *ilv1* deletion being most effective. The *ilv1* deletion, with additional expression of Ilv2, *kivD* and Adh6, combined with the transhydrogenase like shunt, resulted in an isobutanol yield of 12 mg/g_{Glc}. Wess *et al.* (2019) achieved a isobutanol yield of 59.6 mg/g_{Glc} by the expression of cyt-ILV enzymes in a *ilv2, bdh1, bdh2, leu4, leu9, ecm31, ilv1, adh1, gpd1, gpd2* and *ald6* deletion strain which was not able to produce various competing compounds.

Milne *et al.* (2016) established a full bacterial isobutanol pathway in *S. cerevisiae*, using the feedback resistant $ilvN^{M13}$ and *ilvB* from *C. glutamicum* (Elisakova *et al.* 2005), $ilvC^{6E6}$ from *E. coli* (Bastian *et al.* 2011), as well as *ilvD* (Urano *et al.* 2009) and *kdcA* from *L. lactis* (Milne *et al.* 2015). In the said study, the cytosolic isobutanol pathway was expressed in an *pdc* and *ilv2* deletion strain, with constitutive expression of *MTH1ΔT* (Oud *et al.* 2012). Significant secretion of by-products and intermediate was observed for this approach, with DIV being the most prominent. This finding was also confirmed when Ilv3Δ19 was used in a cytosolic approach as described by Generoso *et al.* (2017). These findings indicated that the cytosolic DHAD activity remains a major limitation during isobutanol production due to the insufficient apo-protein maturation with ISC (Generoso *et al.* 2017).

Table 1 Summary of metabolic engineering strategies in *S. cerevisiae* for isobutanol production.

Strategy	Gene Deletion	Gene Expression	Isobutanol Yield [mg/g_{Glc}]	Reference
Mitochondrial		*ILV2, ILV3 ILV5, BAT2*	3.9	Chen *et al.* 2011
Mitochondrial/ cytosolic		*ILV2, ILV3 ILV5, BAT2, kivD (L. Lactis)*	3.8	Lee *et al.* 2012b
Mitochondrial/ cytosolic	*pdc1*	*ILV2, ADH6, kivD (L. Lactis),*	6.6	Kondo *et al.* 2012
Mitochondrial/ cytosolic	*ald6, bat1*	*ILV2, ILV3 ILV5, LEU3Δ601, ARO10, ADH2*	3.8	Park *et al.* 2014
Mitochondrial	*ald6, bat1, lpd1*	*ILV2, ILV3 ILV5, LEU3Δ601, $_{MTS}$ARO10, $_{MTS}$ADH2, MPC1, MPC3*	16.6	Park *et al.* 2016
Mitochondrial		*ILV2, ILV3 ILV5, $_{MTS}$ARO10, $_{MTS}$adhA^{RE1} (L. lactis)*	6.7	Avalos *et al.* 2013
Mitochondrial		*ILV2, ILV3 ILV5, $_{MTS}$ARO10, $_{MTS}$adhA^{RE1}*	15.0	Yuan and Ching 2015
cytosolic	*ilv2*	*ILV2Δ54, ILV3Δ19, ILV5Δ48, ARO10, ADH2*	15.0	Brat *et al.* 2012
cytosolic	*lpd1*	*ILV2Δ54, ILV3Δ19 ILV5Δ48, ADH6, kivD (L. lactis), MAE1, MDH2, PYC2*	16.0	Matsuda *et al.* 2013
Mitochondrial/ cytosolic	*ilv1*	*ILV2, ADH6, kivD (L. lactis), sMAE1, MAE1, MDH2, PYC2*	12.0	Ida *et al.* 2015
cytosolic	*pdc1, pdc5, pdc6, ilv2*	*MTH1ΔT, ilvB, ilvN^{M13} (C. glutamicum), ilvC^{6E6}, ilvD (E. coli), kdcA (L. lactis)*	-	Milne *et al.* 2016
Mitochondrial/ cytosolic	*bat1, ilv1, ald6, leu1, adh1*	*ILV2, ILV3 ILV5, BAT2, kivD (L. lactis)*	6.7	Lee *et al.* 2018
Mitochondrial/ cytosolic	*pdc1, pdc5, pdc6, bat1*	*ILV2, ILV3 ILV5, ARO10, adhA^{RE1} (L. lactis)*	30.7 (batch), 53.5 (fed batch)	Zhao *et al.* 2018
Mitochondrial/ cytosolic	*ilv2, bdh1, bdh2, leu4, leu9, ecm31, ilv1, adh1, gpd1, gpd2, ald6*	*ILV2Δ54, ILV3Δ19 ILV5Δ48*	59.6	Wess *et al.* 2019

2.8. Iron-Sulphur-Cluster Enzymes and Their Biogenesis in *S. cerevisiae*

Enzymes containing an Iron Sulphur Cluster (ISC) are found in all kingdoms of life, and play a crucial role in the viability of cells. ISC can participate in electron transfer reactions, act as Lewis acid, supply enzymatic reactions with iron and sulphur or maintain the structure of protein. ISC enzymes have various physiological functions in the mitochondria, cytosol, endoplasmic reticulum and nucleus. In *S. cerevisiae,* the ISC proteins, for instance, contribute to energy conversion in the respiratory chain (complex I, II and III), and in the citrate cycle (Aco1). Furthermore, ISC proteins are not only responsible for genome maintenance (DNA-polymerase and helicases) and protein translation (ribosome modulator and tRNA modification enzymes) but also regulatory functions (e.g., iron regulation) or anti-viral responses (Viperin) (Braymer and Lill 2017). Finally, ISC enzymes contribute to the metabolism of *S. cerevisiae's,* e.g., biosynthesis of BCAA (Leu1, Ilv3), and are therefore also important for efficient isobutanol biosynthesis.

In *S. cerevisiae,* the biogenesis, trafficking, and insertion of [2Fe-2S] ISC or [4Fe-4S] ISC into its mitochondrial, cytosolic or nuclear apo-proteins is strictly regulated and achieved by a cascade of almost 30 proteins. Initially, 18 known ISC assembly proteins (known as the ISC machinery) are involved in mitochondrial ISC biogenesis, trafficking, and insertion. Then, 11 known cytosolic ISC assembly proteins (known as the CIA machinery) were found to be involved in the cytosolic ISC biogenesis and insertion (Lill *et al.* 2014; Lill *et al.* 2015). Both machineries are illustrated in Figure 3.

Mitochondrial ISC protein biogenesis starts with *de novo* synthesis of [2Fe-2S] ISC on a scaffold protein Isu1, which requires sulphide from the cysteine-desulphurase complex composed of Nfs1, Isd11, and Acp1 as well as electrons from the transfer chain composed of NADPH dependent Arh1, the ferredoxin Yah1 and the iron regulator Yfh1. The Isu1 bound [2Fe-2S] ISC is then released by the Hsp70 chaperones, Ssq1 and Jac1 to the monothiol glutaredoxin Grx5. Therefore, ADP and ATP are exchanged at Ssq1 by the factor Mge1, resulting in a [2Fe-2S] ISC, which is finally coordinated at a Grx5 dimer. The [2Fe-2S] ISC Grx5 dimer then either incorporates [2Fe-2S] ISC into an apo-protein, or transports the [2Fe-2S] ISC to the late-acting ISC machinery for mitochondrial [4Fe-4S] ISC biogenesis. For the cytosolic [4Fe-4S] ISC biogenesis by the CIA machinery, a yet unknown

sulphur-containing species (X-S) is synthesised and exported *via* Atm1. The mitochondrial transformation of the [2Fe-2S] ISC into a [4Fe-4S] ISC requires the late-acting ISC machinery consisting of the Isa1-Isa2-Iba57 complex. Trafficking and insertion of the synthesised [4Fe-4S] ISC is performed by apo-protein specific targeting factors, such as Nfu1, Ind1, Bol1/3 (Braymer and Lill 2017; Lill *et al.* 2015).

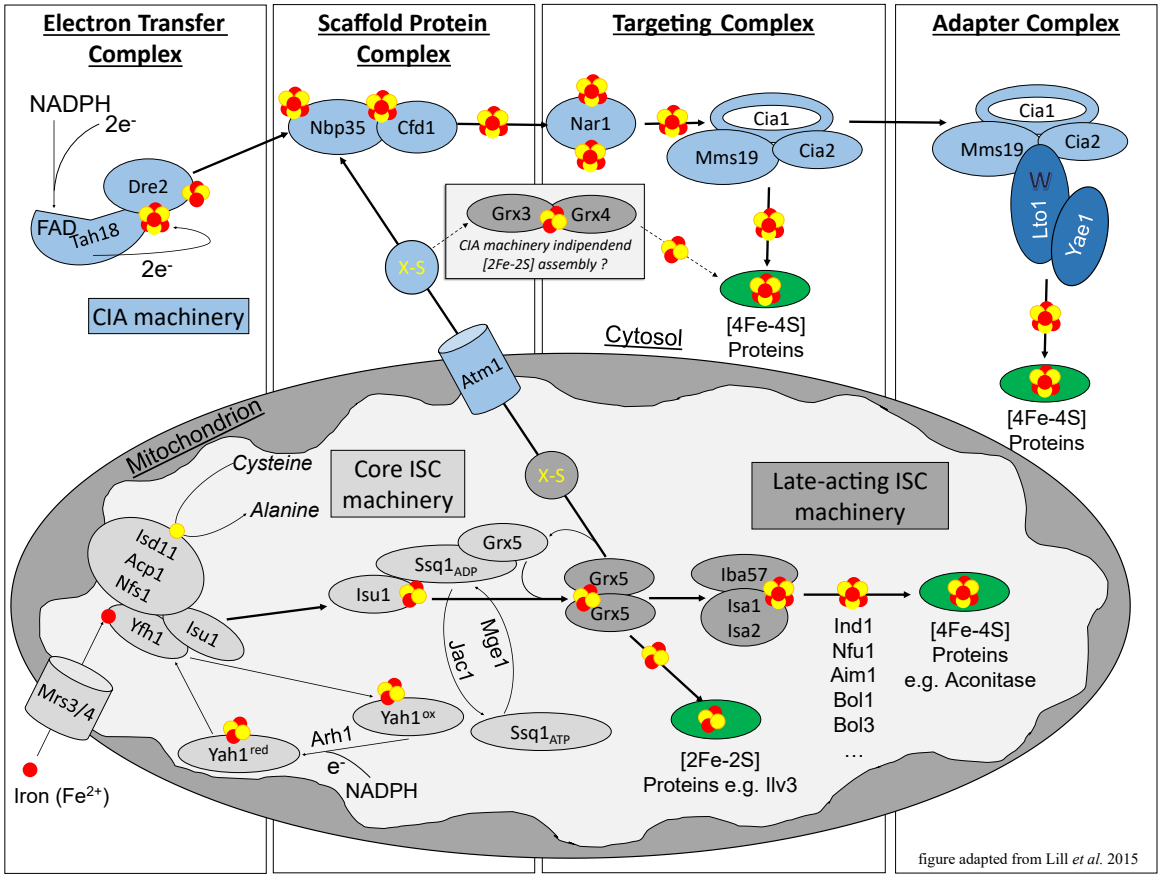

Figure 3 Schematic overview of mitochondrial and cytosolic ISC protein biogenesis in *S. cerevisiae*. The proteins of the [2Fe-2S] ISC machinery are depicted in light grey, and the proteins of the late acting [4Fe-4S] ISC assembling machinery are depicted in dark grey. Proteins of the cytosolic [4Fe-4S] ISC assembly (CIA) machinery are depicted in light blue. Maturated ISC proteins are highlighted in green. First iron (red cycle) is imported by mitochondrial carrier Mrs3/4, and is transferred to the regulator or iron donor Yfh1. Electrons for [2Fe-2S] ISC assembly are then transferred from NADPH-to Yfh1 by the transfer chain consisting of Arh1 and the ferredoxin Yah1. The *de novo* synthesis of [2Fe-2S] ISC starts at the scaffold protein Isu1, which requires sulphide (yellow cycle) from the cysteine-desulphurase complex composed of Nfs1, Isd11 and Acp1. The Isu1 bound [2Fe-2S] ISC is then released by the ATP dependent chaperon Ssq1 and Jac1 to a monothiol glutaredoxin Grx5-dimer. ATP is exchanged by the factor Mge1. The [2Fe-2S] ISC containing Grx5-dimer then either incorporates ISC into an apo-protein or transports the [2Fe-2S] ISC to the late-acting ISC machinery for [4Fe-4S] ISC biogenesis. For the cytosolic [4Fe-4S] ISC biogenesis, an yet unknown sulphur-containing species (X-S) is exported *via* Atm1. The mitochondrial transformation of the [2Fe-2S] ISC into a [4Fe-4S] ISC requires the late-acting ISC machinery consisting of the Isa1-Isa2-Iba57 complex, while insertion of the [4Fe-4S] ISC is performed by apo-protein specific targeting factors such as e.g., Nfu1, Ind1, Bol1, and Bol3. The cytosolic biosynthesis of [4Fe-4S] ISC requires the exported Atm1 substrate X-S, which is utilized by the CIA machinery. Some proteins of the CIA machinery itself require [4Fe-4S] ISC for functional [4Fe-4S] ISC biosynthesis. First, a bridging [4Fe-4S] ISC is assembled on the scaffold proteins Cfd1 and Nbp35. Then, two electrons from NADPH are supplied by the electron transfer complex, via the diflavin reductase Tah18, and the ISC enzyme Dre2. The synthesised [4Fe-4S] ISC is then transferred by the ISC protein Nar1 to the targeting complex composed of Cia1, Cia2, and Met18a, and subsequently incorporated into an apo protein. Some specific apo-proteins are recruited by an adapter complex composed of e.g., Lto1-Yae1 (highlighted in dark blue), which bind to the targeting complex via a conserved C-terminal tryptophan (W) of Lto1. After recruitment by this adapter complex, the [4Fe-4S] ISC is then incorporated into the apo-protein by the targeting complex. The cytosolic multidomain monothiol glutaredoxins Grx3 and Grx4, which contain an X-S derived [2Fe-2S] ISC, contribute in a, so far, unknown manner to cytosolic and nuclear ISC (not published hypothesis is indicated by dotted arrows). The figure was adapted from Lill *et al.* (2015).

The cytosolic biosynthesis of [4Fe-4S] ISC requires the exported Atm1 substrate X-S, which is utilised by the CIA machinery. Some proteins of the CIA machinery require [4Fe-4S] ISC for functional [4Fe-4S] ISC biosynthesis. First, a bridging [4Fe-4S] ISC is assembled on the scaffold proteins Cfd1 and ISC protein Nbp35. For the [4Fe-4S] ISC biosynthesis, two electrons from NADPH are supplied by the electron transfer complex *via* the diflavin reductase: Tah18 and the ISC enzyme Dre2. The synthesised [4Fe-4S] ISC is then transferred by the ISC protein Nar1 to the targeting complex composed of Cia1, Cia2, and Met18, and subsequently incorporated into an apo-protein. However, specific apo-proteins, like Rli1 or Viperin, are recruited by an adapter complex composed of e.g., Lto1-Yae1, which first binds to the targeting complex *via* a conserved C-terminal tryptophan of Lto1. After recruitment by this adapter complex, the [4Fe-4S] ISC is then incorporated into the apo-protein by the described targeting complex (Lill 2020; Lill *et al.* 2015; Lill *et al.* 2014).

The cytosolic multidomain monothiol glutaredoxins, Grx3 and Grx4, which contain an X-S derived [2Fe-2S] ISC, contribute in a previously unknown manner, to cytosolic and nuclear ISC biosynthesis. Furthermore, Grx3 or Grx4 together with Bol2 (formerly known as Fra2) form a complex to sense cytosolic iron *via* ISC concentration, and negatively regulate the nuclear transcription factors Aft1 and Aft2 (Li and Outten 2012; Courel *et al.* 2005; Kumánovics *et al.* 2008). These transcription factors, as well as the protein Yap5, regulate the iron uptake in *S. cerevisiae* (Li *et al.* 2008; Li *et al.* 2012). The role of ISC in yeasts for iron sensing by Aft1/2 and Yap5, as well as the relationship between iron homeostasis and thiol redox metabolism were reviewed by Outten and Albetel (2013) or Martínez-Pastor *et al.* (2017). For a more generalised overview of the iron acquisition and its transcriptional regulation in yeast, see Kaplan and Kaplan (2009).

2.9. OBJECTIVES OF THIS WORK

Although significant improvements in cytosolic isobutanol biosynthesis with *S. cerevisiae* were made through Brat *et al.*'s (2012) approach, the isobutanol yield did not exceed 3.7% of the theoretical maximum. The low isobutanol yield, which was obtained in *S. cerevisiae,* can mainly be attributed to limitations like the formation of competitive compounds (e.g., ethanol); high intermediate secretion (e.g., DIV) due to low Ilv3Δ19 activity, caused by insufficient apo-protein maturation with ISC; as well as NAD(P)H co-factor- and redox-imbalance of the isobutanol biosynthesis pathway. These and potentially other, so far, unknown limitations have been investigated in this work, to identify probable solutions that can contribute to an increased cytosolic isobutanol production in *S. cerevisiae.* However, not only the isobutanol pathway itself but also the *S. cerevisiae* shall be engineered at a laboratory scale by rational and evolutionary engineering, to identify beneficial approaches that could be applied to industrial isobutanol producer strains.

Beneficial approaches of isobutanol pathway and strain engineering will be combined to confirm the approaches in a strong and efficient isobutanol producer background. By this, the current limitations will be mitigated and cytosolic isobutanol biosynthesis will be improved.

Similar to isobutanol, isobutyric acid is considered a valuable platform chemical (Petrognani *et al.* 2020; Zhang *et al.* 2011). Both share the metabolic pathway from glucose to isobutyraldehyde. At this stage, either alcohol- or aldehyde-dehydrogenase's reaction determines whether isobutyraldehyde is reduced to isobutanol, or oxidised to isobutyric acid, respectively. However, to the best of our knowledge, only one approach is described in the literature to produce isobutyric acid in *S. cerevisiae* (Yu *et al.* 2016). Therefore, the beneficial approaches for isobutanol biosynthesis from this work, will be transferred to the isobutyric acid pathway of *S. cerevisiae* to improve isobutyric acid production.

3. MATERIAL AND METHODS

3.1. MEDIA, MICROORGANISMS, CULTIVATION AND STORAGE

3.1.1. MEDIA

The composition of media used for the cultivation of *E. coli* and *S. cerevisiae* are listed in Table 2. The media were autoclaved without carbon source and antibiotics; both were only added afterwards, when the media reached less than 60°C. The carbon source [glucose (D) or fructose (F)] was added to a final concentration of 20 g/l for the cultivation of *S. cerevisiae* on a liquid or solid medium. For isobutanol biosynthesis, according to Brat *et al.* (2012), 40 g/l of glucose was added to a valine-free SC-medium. For the preparation of solid media, 19 g/l agar-agar was added to the media, prior to autoclavation.

Table 2 Media used in this work.

Media	Components	Reference
Luria-Bertani (LB)	10 g/l tryptone, 5 g/l yeast extract, 5 g/l NaCl. pH 7.5 was adjusted with NaOH	Sambrook and Russell 2001
S.O.C. Outgrowth Medium	Commercially available	New England Biolabs (NEB), England
Synthetic complete (SC)	1.7 g/l yeast nitrogen base w/o amino acids and ammonium sulphate, 5 g/l ammonium sulphate $(NH_4)2SO_4$, 50 ml/l 20x Amino acid and nucleobase solution (Table 4) and drop-out solutions as needed. pH 6.3 was adjusted with KOH	Zimmermann 1975 modified as described by Bruder *et al.* 2016
Yeast extract peptone (YEP)	10 g/l yeast extract, 20 g/l bacteriological peptone	Zimmermann 1975

If plasmid selection was performed via antibiotic resistance, the antibiotics listed in Table 3 were added accordingly.

Table 3 Antibiotics used in this work.

	Substance	Concentration		Selection marker
		final [µg/ml]	1000x stock solution [mg/ml]	
antibacterial	Ampicillin	100	100 in H_2O	*ampR*
	Kanamycin	50	50 in H_2O	*kanR*
	Chloramphenicol	30	30 in EtOH	*ampR*
antifungal	Geneticin – G418 (K)	200	200 in H_2O	*kanMX*
	Hygromycin B (H)	200	200 in H_2O	*hphNT1*
	Nourseothricin – clonNAT (N)	100	100 in H_2O	*natMX*

The SC-medium was supplemented with a 20x amino acid and nucleobase solution and uracil, L-tryptophane, L-histidine and L-leucin, as needed, for drop-out

media. Only for isobutanol biosynthesis, according to Brat *et al.* (2012), the SC-medium was prepared without L-valine. The preparation of the solutions is described in Table 4.

Table 4 Amino acid and nucleobase solutions which were used to supplement the SC-medium, with drop out compounds L-histidine, L-leucine, L-tryptophan and uracil (Bruder *et al.* 2016). Stock solutions were sterilised and stored at 4°C.

Name	Substance	Concentration		
		stock solution [g/l]	stock solution [mM]	Final [mM]
20x amino acid and nucleobase solutions	Adenine	0.224	1.66	0.083
	L-tyrosine	0.288	1.59	0.079
	L-arginine	0.768	4.41	0.220
	L-methionine	0.768	5.15	0.257
	L-phenylalanine	0.960	5.81	0.291
	L-isoleucine	1.152	8.78	0.439
	L-lysine	1.152	7.88	0.351
	L-valine[a)]	1.152	9.83	0.492
	L-threonine	1.152	9.67	0.484
Uracil solution 62.5x[b)]	Uracil	1.2	10.71	0.171
L-tryptophan solution 125x	L-tryptophan	2.4	11.57	0.093
L-histidine solution 125x	L-histidine	2.4	15.47	0.124
L-leucine solution 62.5x	L-leucine	3.6	27.44	0.439

a) Omitted for isobutanol biosynthesis according to Brat *et al.* (2012)
b) Stored at room temperature

3.1.2. Microorganisms, Cultivation and Storage

The *E. coli* strains used in this work are listed in Table 5. *E. coli* was cultivated in an LB medium at 37°C, with respective antibiotics added (as described in Table 3), if required for plasmid selection. For permanent cultivation, the *E. coli*, culture was grown to a stationary phase and 500 µl of culture was mixed with 500 µl of sterile 50% (v/v) glycerol/water. This mixture was then stored at -80°C for cryopreservation.

Table 5 *E. coli* strains used in this work.

Strain	Genotype	Source
Escherichia coli DH10B	F– *mcrA* Δ(*mrr-hsdRMS-mcrBC*) φ80*lacZ*ΔM15 Δ*lacX74 recA1 endA1 araD139* Δ (*ara-leu*) 7697 *galU galK* λ– *rpsL*(Str^R) *nupG*	Thermo Fisher Scientific, USA
Escherichia coli NEB10	Δ*(ara-leu) 7697 araD139 fhuA* Δ*lacX74 galK16 galE15 e14-* ϕ*80*d*lacZ*Δ*M15 recA1 relA1 endA1 nupG rpsL* (Str^R) *rph spoT1* Δ*(mrr-hsdRMS-mcrBC)*	New England Biolabs (NEB), England

The *S. cerevisiae* strains used in this work are listed in Table 6, and Table 7. *S. cerevisiae* was cultivated in the YEP, SC or SM mediums, with the respective carbon source and antibiotics added (as described in Table 3), if required, for plasmid selection. For permanent cultivation, the *S. cerevisiae* culture was grown to a stationary phase and 500 µl of culture was mixed with 500 µl of sterile

50% (v/v) glycerol/water. This mixture was then stored at -80°C for cryopreservation. The *S. cerevisiae* strains were stored without any plasmid.

Table 6 *S. cerevisiae* strains used in this work.

Strain	Genotype	Source
CEN.PK113-7D	*MATa; MAL2-8c; SUC2*	Euroscarf, Germany
CEN.PK2-1C	*MATa; leu2-3,112; ura3-52; trp1-289; his3-Δ1; MAL2-8c; SUC2*	Euroscarf, Germany
JWY00	*MATa; MAL2-8c; SUC2; ilv2Δ::-*	Wess *et al.* 2019
JWY01	*MATa; MAL2-8c; SUC2; ilv2Δ::-; bdh1Δ::-; bdh2Δ::-*	Wess *et al.* 2019
JWY02	*MATa; MAL2-8c; SUC2; ilv2Δ::-; bdh1Δ::-; bdh2Δ::-; leu4Δ::-; leu9Δ::-;*	Wess *et al.* 2019
JWY03	*MATa; MAL2-8c; SUC2; ilv2Δ::-; bdh1Δ::-; bdh2Δ::-; leu4Δ::-; leu9Δ::-; ecm31Δ::-*	Wess *et al.* 2019
JWY04	*MATa; MAL2-8c; SUC2; ilv2Δ::-; bdh1Δ::-; bdh2Δ::-; leu4Δ::-; leu9Δ::-; ecm31Δ::-; ilv1Δ::-;*	Wess *et al.* 2019
JWY16	*MATa; MAL2-8c; SUC2; ilv2Δ::-; bdh1Δ::-; bdh2Δ::-; leu4Δ::-; leu9Δ::-; ecm31Δ::-; ilv1Δ::-; adh1Δ::-*	Wess *et al.* 2019
JWY18	*MATa; MAL2-8c; SUC2; ilv2Δ::-; bdh1Δ::-; bdh2Δ::-; leu4Δ::-; leu9Δ::-; ecm31Δ::-; ilv1Δ::-; adh1Δ::-; gpd2Δ::-*	Wess *et al.* 2019
JWY19	*MATa; MAL2-8c; SUC2; ilv2Δ::-; bdh1Δ::-; bdh2Δ::-; leu4Δ::-; leu9Δ::-; ecm31Δ::-; ilv1Δ::-; adh1Δ::-; gpd1Δ::-; gpd2Δ::-*	Wess *et al.* 2019
JWY23	*MATa; MAL2-8c; SUC2; ilv2Δ::-; bdh1Δ::-; bdh2Δ::-; leu4Δ::-; leu9Δ::-; ecm31Δ::-; ilv1Δ::-; adh1Δ::-; gpd1Δ::-; gpd2Δ::-; ald6Δ::-*	Wess *et al.* 2019
IsoY08	*MATa leu2-3,112; ura3-52; trp1-289; his3-Δ1; MAL2-8c SUC2; ilv2Δ::loxP*	Brat *et al.* 2012
IsoY10	*MATa leu2-3,112; ura3-52; trp1-289; his3-Δ1; MAL2-8c SUC2; ilv3Δ::loxP*	Brat *et al.* 2012
WGY21	*MATa; MAL2-8c; SUC2; ilv2::Δ1-1464*	Generoso *et al.* 2017
TAM	*MATa*; *pdc1(−6,−2)::loxP; pdc5(−6,−2)::loxP; pdc6(−6,−2)::loxP; ura3-52,* selected for C_2 independence in glucose-limited chemostats and glucose-tolerant growth in batch culture	van Maris *et al.* 2004

Table 7 *S. cerevisiae* strains constructed in this work.

Strain	Genotype
MBY19	*MATa; MAL2-8c; SUC2; ilv2Δ::-; pim1Δ::-*
MBY25	*MATa; MAL2-8c; SUC2; ilv2Δ::-*
MBY29[a)]	*MATa; MAL2-8c; SUC2;* ilv2Δ*::ILV3Δ19-ILV2Δ54-ilvC^{6E6}-ARO10-ADH2*[b)]
MBY32	*TAM: MAT*a; *pdc1(−6,−2)::loxP; pdc5(−6,−2)::loxP; pdc6(−6,−2)::loxP; ura3-52;* ilv2Δ*::ILV3Δ19-ILV2Δ54-ilvC^{6E6}-ARO10-ADH2*[b)]
MBY33 (MBY29.NVA-1)	*MATa; MAL2-8c; SUC2;* ilv2Δ*::ILV3Δ19-ILV2Δ54-ilvC^{6E6}-ARO10-ADH2*[b)], with $SCD_{norvaline}$ evolved culture 1 *selected for high valine biosynthesis*
MBY34 (MBY29.NVA-2)	*MATa; MAL2-8c; SUC2;* ilv2Δ*::ILV3Δ19-ILV2Δ54-ilvC^{6E6}-ARO10-ADH2*[b)], with $SCD_{norvaline}$ evolved culture 2 *selected for high valine biosynthesis*
MBY35 (MBY29.NVA-3)	*MATa; MAL2-8c; SUC2;* ilv2Δ*::ILV3Δ19-ILV2Δ54-ilvC^{6E6}-ARO10-ADH2*[b)], with $SCD_{norvaline}$ evolved culture 3 *selected for high valine biosynthesis*
MBY36[a)] (MBY29.NVA-1.1)	*MATa; MAL2-8c; SUC2;* ilv2Δ*::ILV3Δ19-ILV2Δ54-ilvC^{6E6}-ARO10-ADH2*[b)], isolated single colony 1 from MBY29.NVA-1
MBY37 (MBY29.NVA-1.2)	*MATa; MAL2-8c; SUC2;* ilv2Δ*::ILV3Δ19-ILV2Δ54-ilvC^{6E6}-ARO10-ADH2*[b)], isolated single colony 2 from MBY29.NVA-1
MBY38 (MBY29.NVA-1.3)	*MATa; MAL2-8c; SUC2;* ilv2Δ*::ILV3Δ19-ILV2Δ54-ilvC^{6E6}-ARO10-ADH2*[b)], isolated single colony 3 from MBY29.NVA-1
MBY39 [a)] (MBY29.NVA-2.1)	*MATa; MAL2-8c; SUC2;* ilv2Δ*::ILV3Δ19-ILV2Δ54-ilvC^{6E6}-ARO10-ADH2*[b)], isolated single colony 1 from MBY29.NVA-2
MBY40 (MBY29.NVA-2.2)	*MATa; MAL2-8c; SUC2;* ilv2Δ*::ILV3Δ19-ILV2Δ54-ilvC^{6E6}-ARO10-ADH2*[b)], isolated single colony 2 from MBY29.NVA-2
MBY41 (MBY29.NVA-2.3)	*MATa; MAL2-8c; SUC2;* ilv2Δ*::ILV3Δ19-ILV2Δ54-ilvC^{6E6}-ARO10-ADH2*[b)], isolated single colony 3 from MBY29.NVA-2
MBY42[a)] (MBY29.NVA-3.1)	*MATa; MAL2-8c; SUC2;* ilv2Δ*::ILV3Δ19-ILV2Δ54-ilvC^{6E6}-ARO10-ADH2*[b)], isolated single colony 1 from MBY29.NVA-3
MBY43 (MBY29.NVA-3.2)	*MATa; MAL2-8c; SUC2;* ilv2Δ*::ILV3Δ19-ILV2Δ54-ilvC^{6E6}-ARO10-ADH2*[b)], isolated single colony 2 from MBY29.NVA-3
MBY44 (MBY29.NVA-3.3)	*MATa; MAL2-8c; SUC2;* ilv2Δ*::ILV3Δ19-ILV2Δ54-ilvC^{6E6}-ARO10-ADH2*[b)], isolated single colony 3 from MBY29.NVA-3
MBY51	*MATa; MAL2-8c; SUC2; ilv2::Δ1-1464; Ilv6Δ::-*
MBY52	*MATa; MAL2-8c; SUC2; ilv2::Δ1-1464; fra2Δ::-*
MBY59	*MATa; MAL2-8c; SUC2; ilv2Δ::-; bdh1Δ::-; bdh2Δ::-; leu4Δ::-; leu9Δ::-; ecm31Δ::-; ilv1Δ::-; adh1Δ::-; gpd2Δ::-; pgi1Δ::-*
MBY60	*MATa; MAL2-8c; SUC2; ilv2Δ::-; bdh1Δ::-; bdh2Δ::-; leu4Δ::-; leu9Δ::-; Δecm31::-; ilv1Δ::-; adh1Δ::-; gpd1Δ::-; gpd2Δ::-; pgi1Δ::-*
MBY63	*MATa; MAL2-8c; SUC2; ilv2Δ::-; bdh1Δ::-; bdh2Δ::-; leu4Δ::-; leu9Δ::-; ecm31Δ::-; ilv1Δ::-; adh1Δ::-; gpd1Δ::-; gpd2Δ::-; ald6Δ::-; fra2Δ::-*

a) Selected for whole genome sequencing as described in 3.8.3
b) *ilv2*Δ integrative plasmid MBV57, encoding for *ILV3Δ19^{CO}-ILV2Δ54^{CO}-ilvC^{6E6-CO}-ARO10-ADH2* is further abbreviated as cyt-ILV_*ilvC*^{6E6}+EP. Codon optimised genes of this plasmid are not highlighted in the table.

3.2. PLASMIDS

The plasmids that were used in this work are provided in Table 8. The plasmids were constructed using the Gibson assembly (Section 3.6.6.2), homologous recombination in yeast (Section 3.6.6.1), or by ligation (Section 3.6.6.3). The vectors were derived from the plasmid series pRS41 for the single-copy and pRS42 for multi-copy plasmids, from Euroscarf (Germany).

Table 8 Plasmids used in this work.

Name	Description	Source
$pRS41_H$	CEN4/ARS1 plasmid for expression of genes under the control of the constitutive *HXT7-1,-392* promotor fragment (*HXT7*p) and *CYC1* terminator with *hphNT1* selection marker. *E. coli* ampicillin-marker and *pBR322*-origin.	Prof. Boles, Frankfurt
$pRS62_N$	*2µ* plasmid for expression of genes under the control of the constitutive *HXT7-1,-392* promotor fragment (*HXT7*p) and *CYC1* terminator with *natMX* selection marker. *E. coli* ampicillin-marker and *pBR322*-origin.	Prof. Boles, Frankfurt
$pRS62_H$	*2µ* plasmid for expression of genes under the control of the constitutive *HXT7-1,-392* promotor fragment (*HXT7*p) and *CYC1* terminator with *hphNT1* selection marker. *E. coli* ampicillin-marker and *pBR322*-origin.	Prof. Boles, Frankfurt
$pRS62_K$	*2µ* plasmid for expression of genes under the control of the constitutive *HXT7-1,-392* promotor fragment (*HXT7*p) and *CYC1* terminator with *kanMX* selection marker. *E. coli* ampicillin-marker and *pBR322*-origin.	Prof. Boles, Frankfurt
$IsoV100_K$	*2µ* plasmid for expression of $ILV3\Delta19^{CO}$, $ILV5\Delta48^{CO}$ and $ILV2\Delta54^{CO}$ with *kanMX* selection marker. *E. coli* ampicillin-marker and *pBR322*-origin.	Brat *et al.* 2012
$SBV85_H$	*2µ* plasmid for expression of codon optimized NADH-Oxidase from *Streptococcus pneuminiae* D39 under the control of the *TPI1*-Promotor and *PGK1*-Terminator with *hphNT1* selection marker. *E. coli* ampicillin-marker and *pBR322*-origin.	Prof. Boles, Frankfurt
$SBV89_H$	CEN4/ARS1 plasmid for expression of codon optimized NADH-Oxidase from *Streptococcus pneuminiae* D39 under the control of the *UBR2*-Promotor and *PGK1*-Terminator with *hphNT1* selection marker. E. coli ampicillin-marker and *pBR322*-origin.	Prof. Boles, Frankfurt
$pWG017_N$	$pRS62_N$ based plasmid for expression of $ILV3\Delta19^{CO}$ from *S. cerevisiae*	Prof. Boles, Frankfurt
$pWG044_N$	$pRS62_N$ based plasmid for the expression of *ilvD2* from *C. clutamicum*	Prof. Boles, Frankfurt
$pWG046_N$	$pRS62_N$ based plasmid for the expression of *ilvD2* from *N. crassa*	Prof. Boles, Frankfurt
$pWG087_N$	pRCCN based plasmid for the deletion of *ILV2*	Generoso *et al.* 2016
$pWG108_K$	CEN4/ARS1 plasmid for expression of genes $ILV2\Delta54^{CO}$; $ilvC^{6E6\text{-}CO}$; $ILV3\Delta19^{CO}$; *ARO10* and *ADH2* with *kanMX* selection marker. *E. coli* ampicillin-marker and *pBR322*-origin.	Generoso *et al.* 2017
$pWG136_K$	CEN4/ARS1 plasmid for expression of genes $ILV2\Delta54^{CO}$; $ilvC^{6E6\text{-}CO}$; $ILV3\Delta19^{CO}$; $ARO10^{CO}$ and *ADH2* with *kanMX* selection marker. *E. coli* ampicillin-marker and *pBR322*-origin.	Prof. Boles, Frankfurt
$pRCC_K_K$	*2µ* plasmid for expression of codon optimized Cas9 from *Streptococcus pyogenes* under control of *ROX3* promoter with *kanMX* selection marker.	Generoso *et al.* 2016
$pRCC_N_N$	*2µ* plasmid for expression of codon optimized Cas9 from *Streptococcus pyogenes* under control of *ROX3* promoter with *natMX* selection marker.	Generoso *et al.* 2016

Table 9 Plasmids constructed in this work

Name	Description	Source
MBV007$_N$	pRS62$_N$ based plasmid for the expression of *ilvD2* from *N. crassa,* fused with C-terminal tryptophane (W)	pWG046$_N$
MBV008$_N$	pRS62$_N$ based plasmid for the expression of *ilvD2* from *N. crassa,* fused with C-terminal KVHQDW	pWG046$_N$
MBV009$_N$	pRS62$_N$ based plasmid for the expression of *ilvD* from *C. clutamicum,* fused with C-terminal tryptophane (W)	pWG044$_N$
MBV010$_N$	pRS62$_N$ based plasmid for the expression of *ilvD* from *C. clutamicum,* fused with C-terminal KVHQDW	pWG044$_N$
MBV011$_N$	pRS62$_N$ based plasmid for the expression of *ILV3Δ19^{CO}* from *S. cerevisiae,* fused with C-terminal tryptophane (W)	pWG017$_N$
MBV012$_N$	pRS62$_N$ based plasmid for the expression of *ILV3Δ19^{CO}* from *S. cerevisiae,* fused with C-terminal KVHQDW	pWG017$_N$
MBV024$_N$	pRS62$_N$ based plasmid for the expression of *ilvD^{CO}* from *E. coli*	Synthetic gene from Table 35
MBV030$_N$	pRS62$_N$ based plasmid for the expression of *ilvD^{CO}* from *B. subtilis*	Synthetic gene from Table 35
MBV031$_N$	pRS62$_N$ based plasmid for the expression of *ilvD^{CO}* from *B. subtilis,* fused with C-terminal tryptophane (W)	Synthetic gene from Table 35
MBV032$_N$	pRS62$_N$ based plasmid for the expression of *ilvD^{CO}* from *B. subtilis,* fused with C-terminal KVHQDW	Synthetic gene from Table 35
MBV033$_N$	pRS62$_N$ based plasmid for the expression of *ilvD^{CO}* from *Citrobacter sp*	Synthetic gene from Table 35
MBV034$_N$	pRS62$_N$ based plasmid for the expression of *ilvD^{CO}* from *Citrobacter sp,* fused with C-terminal tryptophane (W)	Synthetic gene from Table 35
MBV035$_N$	pRS62$_N$ based plasmid for the expression of *ilvD^{CO}* from *Citrobacter sp,* fused with C-terminal KVHQDW	Synthetic gene from Table 35
MBV036$_N$	pRS62$_N$ based plasmid for the expression of *ilvD^{CO}* from *P. carotovorum*	Synthetic gene from Table 35
MBV037$_N$	pRS62$_N$ based plasmid for the expression of *ilvD^{CO}* from *P. carotovorum,* fused with C-terminal tryptophane (W)	Synthetic gene from Table 35
MBV038$_N$	pRS62$_N$ based plasmid for the expression of *ilvD^{CO}* from *P. carotovorum,* fused with C-terminal KVHQDW	Synthetic gene from Table 35
MBV039$_N$	pRS62$_N$ based plasmid for the expression of *ilvD^{CO}* from *X. nematophila*	Synthetic gene from Table 35
MBV040$_N$	pRS62$_N$ based plasmid for the expression of *ilvD^{CO}* from *X. nematophila,* fused with C-terminal tryptophane (W)	Synthetic gene from Table 35
MBV041$_N$	pRS62$_N$ based plasmid for the expression of *ilvD^{CO}* from *X. nematophila,* fused with C-terminal KVHQDW	Synthetic gene from Table 35
MBV042$_N$	pRS62$_N$ based plasmid for the expression of *ilvD^{CO}* from *E. coli,* fused with C-terminal tryptophane (W)	Synthetic gene from Table 35
MBV043$_N$	pRS62$_N$ based plasmid for the expression of *ilvD^{CO}* from *E. coli,* fused with C-terminal KVHQDW	Synthetic gene from Table 35
MBV044$_H$	pRS62$_H$ based plasmid for the expression of *GRX3*	CEN.PK113-7D
MBV045$_H$	pRS62$_H$ based plasmid for the expression of *GRX4*	CEN.PK113-7D
MBV046$_H$	pRS62$_H$ based plasmid for the expression of *GRX5*	CEN.PK113-7D
MBV048$_H$	pRS62$_H$ based plasmid for the expression of *GRX5*Δ29	CEN.PK113-7D
MBV053$_N$	pRCC_N$_N$ based plasmid for the deletion of *pim1*	pRCC_N$_N$
MBV057$_K$	*2µ* plasmid for expression of *ILV3Δ19^{CO}, ilvC^{6E6-CO}, ILV2Δ54^{CO}* and *ARO10* and *ADH2* with *kanMX* selection marker. *E. coli* ampicillin-marker and *pBR322*-origin. The plasmid is designed as destructive integrative vectors for *ILV2* after *PmeI* digestion.	IsoV100$_K$

Name	Description	Source
MBV058$_N$	pRS62$_N$ based plasmid for the expression of *ILV2Δ54^{CO}*	IsoV100$_K$
MBV059$_N$	pRS62$_N$ based plasmid for the expression of *ilvC^{6E6-CO}*	pWG108$_K$
MBV060$_N$	pRS62$_N$ based plasmid for the expression of *ILV3Δ19^{CO}*	IsoV100$_K$
MBV061$_N$	pRS62$_N$ based plasmid for the expression of *ARO10^{CO}*	pWG136$_K$
MBV062$_N$	pRS62$_N$ based plasmid for the expression of *ADH2*	pWG108$_K$
MBV063$_N$	pRS62$_N$ based plasmid for the expression of *ILV2*	CEN.PK113-7D
MBV064$_N$	pRS62$_N$ based plasmid for the expression of *ILV2^{E139A}*	CEN.PK113-7D
MBV065$_N$	pRS62$_N$ based plasmid for the expression of *ILV2Δ54^{E139A}*	IsoV100$_K$
MBV074$_N$	pRS62$_N$ based plasmid for the expression of *alsLP^{CO}* from *L. plantarum*	Synthetic gene from Table 35
MBV075$_H$	pRS62$_H$ based plasmid for the expression of *ILV6*	CEN.PK113-7D
MBV076$_H$	pRS62$_H$ based plasmid for the expression of *ILV6*Δ61	CEN.PK113-7D
MBV077$_H$	pRS62$_H$ based plasmid for the expression of *ILV6Δ61^{N86A}*	CEN.PK113-7D
MBV078$_H$	pRS62$_H$ based plasmid for the expression of *ILV6^{N86A}*	CEN.PK113-7D
MBV079$_K$	pRCC_K$_K$ based plasmid for the deletion of *ilv6*	pRCC_K$_K$
MBV080$_K$	pRCC_K$_K$ based plasmid for the deletion of fra2	pRCC_K$_K$
MBV083$_H$	pRS62$_H$ based plasmid for the expression of *ilvN^{CO}*	Synthetic gene from Table 35
MBV084$_H$	pRS62$_H$ based plasmid for the expression of *ilvN^{M13-CO}*	Synthetic gene from Table 35
MBV085$_H$	pRS41$_H$ based plasmid for the expression of *ARN1^{L25M}*	MBY36
MBV086$_H$	pRS41$_H$ based plasmid for the expression of *ATG34^{K20N}*	MBY36
MBV087$_H$	pRS41$_H$ based plasmid for the expression of *CIT1^{T432A}*	MBY36
MBV088$_H$	pRS41$_H$ based plasmid for the expression of *DAL80^{S194L}*	MBY36
MBV089$_H$	pRS41$_H$ based plasmid for the expression of *FRT1^{N185T}*	MBY36
MBV090$_H$	pRS41$_H$ based plasmid for the expression of *HIR2^{R752K}*	MBY36
MBV091$_H$	pRS41$_H$ based plasmid for the expression of *HSP104^{I338F}*	MBY36
MBV092$_H$	pRS41$_H$ based plasmid for the expression of *OSM1^{Frameshift}*	MBY36
MBV093$_H$	pRS41$_H$ based plasmid for the expression of *PGD1^{Frameshift}*	MBY36
MBV094$_H$	pRS41$_H$ based plasmid for the expression of *SNG1^{Y329S}*	MBY36
MBV095$_H$	pRS41$_H$ based plasmid for the expression of *TPS3^{R145I}*	MBY36
MBV096$_H$	pRS41$_H$ based plasmid for the expression of *WHI2^{Q24*}*	MBY36
MBV097$_N$	pRS62$_N$ based plasmid for the expression of *ilvB^{CO}* from *C. glutamicum*	Synthetic gene from Table 35
MBV098$_N$	pRCC_N$_N$ based plasmid for the deletion of *pgi1*	pRCC_N$_N$
MBV099$_K$	*2µ* plasmid for expression of *ILV3Δ19^{CO}, ILV5Δ48^{CO} and ilvB^{CO}* from *C. glutamicum* with *kanMX* selection marker. *E. coli* ampicillin-marker and *pBR322*-origin.	IsoV100$_K$/MBB097$_N$
MBV100$_K$	*2µ* plasmid for expression of *ILV3Δ19^{CO}, ILV5Δ48^{CO}, ILV2Δ54^{CO}* and *ARO10* and *ADH2* with *kanMX* selection marker. *E. coli* ampicillin-marker and *pBR322*-origin. The plasmid is designed as destructive integrative vectors for *ILV2* after *PmeI* digestion.	MBV57$_K$/IsoV100$_K$
MBV109$_N$	pRS62N based plasmid for the expression of *ALD6*	CEN.PK113-7D
MBV113$_K$	*2µ* plasmid for expression of *ILV3Δ19^{CO}, ilvC^{6E6}* and *ILV2Δ54^{CO}* with *kanMX* selection marker. *E. coli* ampicillin-marker and *pBR322*-origin.	pWG108$_K$
MBV114$_K$	*2µ* plasmid for expression of *ILV3Δ19^{CO}, ilvC$^{A1D2-P1-CO}$* and *ILV2Δ54^{CO}* with *kanMX* selection marker. *E. coli* ampicillin-marker and *pBR322*-origin.	pWG108$_K$

3.3. Synthetic DNA

Oligonucleotides and primers used in this work were synthesised by Biomers.net LLC., Germany or Microsynth Seqlab GmbH, Germany. The oligonucleotides and primers used in this work are listed in Table 33 and Table 34. The synthetic genes used in this work were ordered from GeneArt (Thermo Fisher Scientific, Germany), and synthesised by the strings DNA fragments method. Synthetic genes used in this work are listed in Table 35.

3.4. Chemicals, Enzymes, and Kits

Chemicals, enzymes and kits used in this work are listed in Table 10.

Table 10 Chemicals, enzymes, and kits used in this work.

Product	Producer
All chemicals except those listed in this table	Roth
Bacterial tryptone	Difco
Bacteriological peptone	Oxoid
ClonNAT (Nourseothricin)	WERNER BioAgents
DL-Norvaline	Merck
DNA loading dye	NEB, Fermentas
DreamTaq, incl. buffer	NEB
Geneticin (G418)	Calbiochem
Geneticin (G418)	Merck
β-Nicotinamide-adenine-dinucleotide hydrate (NAD^+)	Roche
Phusion DNA polymerase, incl. buffers, DNA loading dye, DNA Ladder, 10 mM dNTP mix	NEB
Q5 DNA polymerase, incl. buffers, DNA loading dye, DNA Ladder, 10 mM dNTP mix	NEB
Restriction enzymes, incl. buffer and DNA loading dye	NEB
Sheared salmon sperm DNA	Ambion
Sulphuric acid	Merck
T4 DNA ligase incl. buffer	NEB
T7 DNA ligase incl. buffer	NEB
Taq DNA ligase	NEB
UltraPure™ Agarose	life technologies
Uracil	Merck
Yeast extract	Difco
Yeast nitrogen base (YNB) w/o amino acids and w/o ammonium sulfate	Difco
Kits:	
GeneJET Plasmid Miniprep kit	Thermo Scientific
NucleoSpin Gel and PCR clean up	Macherey-Nagel

3.5. Equipment and Other Materials

Devices which are beyond the standard equipment, but used in this work, are listed in Table 11.

Table 11 Equipment and other materials used in this work.

Device	Producer
Agarose gel-electrophoresis chambers	Neolab
Cell electroporator, Gene Pulser	Bio-Rad
Cell growth quantifier	Aquila Biolabs
Centrifuge Avanti J-25 with rotors JA-10 and JA-25.50	Beckman
Centrifuges (5415D, 5415R, 5702, 5810R)	eppendorf, Germany
Durapore membrane filter (PVDF, hydrophilic, 0.22 µm, 47 mm)	Millipore
Incubator	Multitron Standard, Infors HT
Nanodrop 1000 spectrophotometer	Thermo Fisher Scientific
PCR Cycler, labcycler triple block	SensoQuest
PCR Cycler, Piko thermal cycler	Finnzymes
pH-meter 765 Calimatic	Knick
Pipette, 0.1–2.5 µl	Starlab/eppendorf
Pipette, 0.5–10 µl	Starlab/eppendorf
Pipette, 10–100 µl	Starlab/eppendorf
Pipette, 100–1000 µl	Starlab/eppendorf
Shaker	Infors HT
Spectrophotometer Ultrospec 2100 pro	Amersham Bioscience
Thermomixer comfort	eppendorf
UV-crosslinker, gel-documentation system	Vilber Lourmat
Vibrax VXR basic	IKA
HPLC system	
Ultimate3000:	
Autosampler	WPS300SL, Thermo Scientific
Column oven	TCC-300SD, Thermo Scientific
Pump system	ISO-3100SD, Thermo Scientific
Degasser	Ultimate3000, Thermo Scientific
RI-detector	RI-101, Shodex
Column	HyperREZ XP Carbohydrate H^+ 8 µm, Thermo Scientific
Software	Chromeleon™

3.6. Molecular Biological Methods

3.6.1. Isolation of Plasmid DNA from *E. coli*

For a small scale plasmid DNA preparation from stationary *E. coli* culture (5-15 ml), the GeneJET Plasmid Miniprep kit from Thermo Scientific was used. The procedure was performed according to the manufacturer's protocols.

3.6.2. Isolation of Plasmid and Genomic DNA from *S. cerevisiae*

For the isolation of genomic and plasmid DNA from stationary yeast culture (5-10 ml), the cells were harvested by centrifugation (2 min, 3000 x g). The supernatant was discarded, and the cell pellet was washed once in 1 ml sterile ddH_2O and centrifuged again. The washed pellet was then re-suspended in 400 µl of resuspension buffer 1 (Table 12) by vortexing. Then, the cell suspension was lysed by adding 400 µl of lysis buffer 2 (Table 13), and 1/3rd volume of glass beads (diameter 0.45 mm) were added to the tube. The tube was then shaken using a VXR basic Vibrax (IKA) at the maximum speed for 8–15 min at 4°C. Cell debris were then pelleted by centrifugation (30 sec, 16000 x g), and 650 µl of the supernatant was transferred into a fresh 1.5 ml test tube. Afterwards, 325 µl of cold precipitation buffer 3 (Table 14) was added and gently mixed, followed by 10 min of incubation on ice. To remove the precipitated proteins or other contaminants, the sample was centrifuged for at least 15 min at maximum speed at 4°C. Afterwards, 700 µl of the clear supernatant was transferred into a fresh 1.5 ml test tube and mixed vigorously with 700 µl isopropanol. The mixture was then incubated for 10 min at room temperature, then the precipitated DNA was pelleted by centrifugation for at least 15 min at maximum speed. The DNA pellet was washed with 500 µl of cold (-20°C) 70% (v/v) ethanol and centrifuged for 5 min at maximum speed. The washing step was repeated, and the DNA pellet was dried afterwards at room temperature until full evaporation of the washing solution. The dry DNA pellet was then dissolved in 15-30 µl sterile ddH_2O and incubated at room temperature for at least 30 min.

Table 12 Composition of resuspension buffer 1. The buffer was autoclaved and stored at 4°C.

Compound	Concentration
EDTA (Titriplex III)	10 mM
Tris-HCl, pH 8	25 mM
RNase A[a)]	100 ml^{-1}

a) RNase A was added after the buffer was autoclaved.

Table 13 Composition of lysis buffer 2. The buffer was autoclaved and stored at room temperature.

Compound	Concentration
NaOH	0.2 M
SDS	1 % (w/v)

Table 14 Composition of precipitation buffer 3. The buffer was autoclaved and stored at 4°C. The pH was adjusted to 5.5.

Compound	Concentration
Potassium acetate	3 M

3.6.3. Preparation of Genomic DNA from *S. cerevisiae* for PCR Amplification

For polymerase chain reaction (PCR) amplification from genomic DNA, a small amount of desired yeast cells was transferred to the PCR tube from the solid medium, using a sterile 2 µl pipet tip. The closed PCR tube was placed in the microwave, which was then turned to full power for 1-2 min. The respective PCR mix was pipetted to the tube (containing the desired genomic template) and mixed vigorously. Subsequently, the PCR programme was initiated as needed.

3.6.4. Polymerase Chain Reaction

To amplify the DNA from different sources, the PCR was performed. Depending on the purpose, different commercially available DNA-polymerases were chosen. For cloning or sequencing applications, the precise Phusion High-Fidelity DNA Polymerase (Section 3.6.4.1) and Q5 High-Fidelity DNA (Section 3.6.4.2) from New England Biolabs were used. These DNA polymerases contain a proofreading function that causes less amplification mistakes, compared to the Taq DNA polymerase. However, for some PCR applications, the amplification speed is more important because only fragment lengths, instead of high amplification precision, is of interest (e.g., confirmation of genomic gene deletion or integration). For these purposes, the DNA-polymerase DreamTaq DNA Polymerase (Section 3.6.4.3) from Thermo Fisher Scientific was used. Table 15 to Table 20 summarise the PCR conditions recommended by the manufacturer's protocols and were employed in this work. Annealing temperatures of primer pairs were calculated with the NEB Tm Calculator tool from New England Biolabs. All PCRs were performed in a labcycler (SensoQues) or Piko Thermo Cycler (Finnzymes), and were verified *via* agarose gel electrophoresis in a 1% agarose gel (Section 3.6.5).

3.6.4.1. Polymerase Chain Reaction using Phusion High-Fidelity DNA Polymerase

The reaction mix and PCR conditions for using Phusion High-Fidelity DNA Polymerase are summarised in the following tables (Table 15 and Table 16).

Table 15 Reaction mix for Phusion High-Fidelity DNA Polymerase. Volume was added up to 50 µl with ddH_2O.

Component	Stock solution	Concentration in mix	Volume used [µl]
Phusion HF buffer	5x	1x	10
dNTP Mix	10 mM of each	200 µM of each	1
Primer	10 µM of each	0.5 µM of each	2.5 of each
DMSO*	100%	3%	1.5
Phusion DNA polymerase	2000 U ml^{-1}	1 U	0.5
Template	-	20 ng	variable

*Only applied for GC rich sequences.

Table 16 PCR conditions for standard PCR protocol using Phusion High-Fidelity DNA Polymerase. The lid of the thermocycler was preheated to 96°C

Step	Temperature	Duration	Function
1	98°C	30 s	Denaturation of DNA
2 (35-40 cycles)	98°C	5-10 s	Denaturation of DNA
	45–72°C	10 s	Primer annealing
	72°C	15-30 s/kb	DNA extension
3	72°C	5 min	Final extension
4	10°C	Hold	Hold

3.6.4.2. Polymerase Chain Reaction using Q5 High-Fidelity DNA Polymerase

The reaction mix and PCR conditions for using Q5 high-fidelity DNA polymerase are summarised in the following tables (Table 17 and Table 18).

Table 17 Reaction mix for Q5 High-Fidelity DNA Polymerase. Volume was added up to 50 µl with ddH_2O.

Component	Stock solution	Concentration in mix	Volume used [µl]
Q5 Reaction Buffer	5x	1x	10
dNTP Mix	10 mM of each	200 µM of each	1
Primer	10 µM of each	0.5 µM of each	2.5 each
Q5 DNA Polymerase	2000 U ml^{-1}	1 U	0.5
Template	-	20 ng	variable

Table 18 PCR conditions for standard PCR protocol using Q5 High-Fidelity DNA Polymerase. The lid of the thermocycler was preheated to 96°C.

Step	Temperature	Duration	Function
1	98°C	30 s	Denaturation of DNA
2	98°C	5-10 s	Denaturation of DNA
	50-72°C	10-30 s	Primer annealing
	72°C	20-30 s/kb	DNA extension
3	72°C	2 min	Final extension
4	10°C	Hold	Hold

3.6.4.3. Polymerase Chain Reaction using DreamTaq DNA Polymerase

The reaction mix and PCR conditions for using DreamTaq DNA polymerase are summarised in the following tables (Table 19 and Table 20). Furthermore, the 10x DreamTag green buffer already contains a loading dye for later analysis *via* agarose gel electrophoresis in a 1% agarose gel, thereby making the addition of further loading dye unnecessary.

Table 19 Reaction mix for DreamTaq DNA Polymerase. Volume was added up to 12.5 µl with ddH_2O.

Component	Stock solution	Concentration in mix	Volume used [µl]
10X DreamTaq green buffer	10x	1x	1.25
dNTP Mix	2 mM of each	200 µM of each	1.25
Primer	10 µM of each	0.5 µM of each	0.625 each
DreamTag DNA Polymerase	5 U $µl^{-1}$	1.75 U	0.35
Template	-	variable	variable

Table 20 PCR conditions for standard PCR protocol using DreamTaq DNA Polymerase. The lid of the thermocycler was preheated to 96°C.

Step	Temperature	Duration	Function
1	98°C	1-3 min	Denaturation of DNA
2	98°C	30 s	Denaturation of DNA
	50-72°C	30 s	Primer annealing
	72°C	1 min up to 2kb*	DNA extension
3	72°C	2 min	Final extension
4	10°C	Hold	Hold

*For longer products, the extension time should be prolonged by 1 min/kb

3.6.5. Agarose Gel Electrophoresis for DNA Separation

Because of the negatively charged phosphate backbone of DNA, the fragment can be separated with an electric field, according to their size. Therefore, 1.0% (w/v) agarose gel was mixed with 1x TAE-buffer (Table 21) and heated until the agarose was completely dissolved. The liquid 1% (w/v) agarose was poured into a dedicated gel tray (Bio-Rad) and cooled at room temperature. The solid agarose gel was then

transferred to the 1x TAE-buffer. DNA of interest was mixed accordingly with purple gel loading dye (6x) from New England Biolabs. The gel was then applied to 6-10 V/cm for 30-60 minutes, depending on the expected DNA fragment sizes. The GeneRuler 1 kb DNA ladder (Fisher Scientific) was used as reference to estimate the size of the DNA fragments. The DNA was then visualised with UV-light (254 nm) after incubation of the gel in an ethidium bromide bath.

Table 21 Composition of 1xTAE-buffer. pH was adjusted to 8.3 with acetic acid.

Compound	Concentration
TRIS	40 mM
EDTA	1 mM

3.6.5.1. DNA-Purification and DNA-Extraction from Agarose Gels

For purification of DNA fragments (e.g., after PCR or restriction digestions) from agarose gels, the NucleoSpin Extract II-Kit (Macherey-Nagel) was used following the manufacturer's protocols.

3.6.6. Plasmid Assembly

Diverse methods have been developed for plasmid assembly of vectors that can be used in various organisms. In this work, the yeast homologous recombination cloning (Section 3.6.6.1), Gibson isothermal assembly (Section 3.6.6.2), and restriction-ligation cloning (Section 3.6.6.3) were used for plasmid assembly. First, the vector was linearised by site specific restriction, using endonucleases from New England Biolabs (NEB), according to the manufacturer's protocols (summarised in Table 22). Furthermore, restriction endonucleases were not only used for vector preparation but also for assembly confirmation.

Table 22 Typical reaction mixture for DNA digestion by restriction endonucleases. Volume was added up to 10 µl, and reaction mix was incubated at 37°C for at least 4 h. Variations in incubation temperature and time were possible, if needed, according to the manufacturer's protocol.

Compound	Concentration
DNA	500-1000 ng
Enzyme specific reaction buffer	1.0 µl
Restriction enzyme	0.5 µl

3.6.6.1. Plasmid Construction by Homologous Recombination in S. cerevisiae

Homologous recombination is known as the most prominent DNA repairing mechanism in *S. cerevisiae*. Thus, plasmids were constructed *in vivo* by using linearised vector(s) and insert(s), with the appropriate homologous overhangs (at least 30 bp). In case of multiple fragments, insertions into the vector of fragments

containing homologous overhangs to each other were done in the assembly order it was specified.

For plasmid assembly, the fragments were amplified by PCR using primers with corresponding homologous 5' ends, if needed. *S. cerevisiae* was then transformed with the respective linearised vectors and appropriate DNA fragments. The transformants were plated on solid SCD- or YEPD-mediums containing appropriate selection agents. Suitable amounts of yeast transformants were collected from the solid medium, and the plasmid DNA was isolated (Section 3.6.2), transformed into *E. coli* DH10b, and plated on a solid LB medium containing appropriate selection agents (Section 3.6.8). The plasmids were isolated from single *E. coli* transformants (Section 3.6.1), and the assembly was verified using endonuclease digestion and sequencing (Section 3.6.6 and Section 3.8.2). At least one *E. coli* transformant containing a correct and verified plasmid was prepared for permanent storage at -80°C (Section 3.1.2).

3.6.6.2. Plasmid Construction by Gibson Isothermal Assembly

Gibson isothermal assembly is an isothermal single-reaction method for assembling overlapping DNA molecules. Hereby, a 5′-exonuclease was used to generate DNA fragments with single-stranded homologous overhangs (20-50 nt), which were then specifically annealed and covalently joined by a DNA polymerase and ligase (Gibson *et al.* 2009).

For plasmid assembly, 50 ng backbone DNA (fragment containing the selection marker) was mixed with up with five DNA fragments, in a molar ratio of 1:3. Then, the 2x Gibson isothermal assembly master mix was added to the DNA mixture, together with the amount of ddH_2O needed (Table 24). The reaction mix was incubated at 50°C for 1 h and transformed into *E. coli* DH10b, and plated on a solid LB medium containing appropriate selection agents (Section 3.6.8). The plasmid was isolated from single *E. coli* transformants (Section 3.6.1), and the assembly was verified using endonuclease digestion and sequencing (Section 3.6.6 and Section 3.8.2). At least one *E. coli* transformant containing a correct and verified plasmid was prepared for permanent storage at -80°C (Section 3.1.2).

Table 23 Composition of 5x Isothermal reaction buffer. The buffer was stored at -20°C, which is needed to prepare the 2x Gibson isothermal assembly master mix (Table 24).

Compound	Concentration
PEG-8000	25%
Tris-HCl, pH 7.5	500 mM
$MgCl_2$	50 mM
DTT	50 mM
dNTP	1 mM
NAD^+	5 mM

Table 24 Composition of 2x Gibson isothermal assembly master mix. Master mix stored as 5 µl single use aliquots at 20°C.

Compound	Concentration
5x Isothermal reaction buffer (see Table 23)	1x
T5 exonuclease	10 U μl^{-1}
Taq DNA ligase	40 U μl^{-1}
Phusion DNA polymerase	2 U μl^{-1}

3.6.6.3. Plasmid Construction by Ligation

The DNA digested with suitable restriction endonucleases can be joined by a DNA ligase catalysed reaction. In this enzymatic reaction, two cohesive- or blunt-ended strands of DNA are joined between the 5´-phosphate and the 3´-hydroxyl groups of adjacent nucleotides.

For plasmid assembly, digested DNA fragments and vectors were gel purified, as described in Section 3.6.5.1. The digested and purified DNA fragments and vectors were then added to the ligation mix of T4- or T7-DNA-ligase, obtained from New England Biolabs, according to the manufacturer's protocols (summarised in Table 25). The reaction mix with assembled plasmids was then transformed into *E. coli* DH10b, and plated on a solid LB medium containing appropriate selection agents (Section 3.6.8). The plasmids were isolated from single *E. coli* transformants (Section 3.6.1), and the assembly was verified using endonuclease digestion and sequencing (Section 3.6.6 and Section 3.8.2). At least one *E. coli* transformant containing a correct and verified plasmid was prepared for permanent storage at -80°C (Section 3.1.2).

Table 25 Typical reaction mixture for ligation catalysed by T4- or T7-DNA ligase. Volume was added up to 10 µl and incubate at room temperature or 5°C overnight.

Compound	Concentration
DNA (each piece)	100-500 ng
Ligase buffer	1 µl
DNA ligase	0.5 µl

3.6.7. MEASUREMENT OF NUCLEIC ACID CONCENTRATION

Concentration and quality (A_{260}/A_{280} ratio) of plasmid DNA samples were measured using a NanoDrop 1000 spectrophotometer (Thermo Scientific), according to the manufacturer's protocols.

3.6.8. TRANSFORMATION OF *E. COLI*

For transformation of *E. coli*, commercially available NEB 10-beta or prepared DH10b were used. To prepare the electro competent DH10b, 5 ml of liquid LB medium was inoculated with a single DH10b colony grown on a solid LB medium. Then, the culture was incubated at 37°C and 180 rpm. Prewarmed 400 ml liquid LB medium was inoculated in a one litre baffled shake flask and incubated at 30°C until an optical density at 600 nm (OD_{600}) of 0.6-0.7 was obtained. The culture was then transferred to ice cold 50 ml-tubes and chilled on ice for 30 min. The cells were harvested by centrifugation at 4000 x g at 4°C for 15 min. The cell pellet was then washed in 25 ml ice cold ddH_2O, and two aliquots were pooled to one 50 ml tube, which was then centrifuged again at 4000 x g at 4°C for 15 min. The washing procedure was repeated until the whole culture could be pooled to one 50 ml tube. The final cell pellet was washed with 4 ml of sterile and ice cold 10% (w/v) glycerol and centrifuged at 4000 x g at 4°C for 15 min. The cells were resuspended in 4 ml of sterile and ice cold 10% (w/v) glycerol and aliquoted to 50 µl single use aliquots, which were frozen and stored at -80°C.

Electro competent *E. coli* cells were transformed by electroporation, in accordance to the protocols of Dower *et al.* (1988). Plasmid DNA (from *E. coli* [Section 3.6.1] or *S. cerevisiae* [Section 3.6.2]) was added to the frozen competent *E. coli* single-use aliquot in suitable amounts, and thawed on ice for about 10 min. The cell suspension was then transferred to an ice-cold electroporation cuvette, and an electric pulse was applied by using the Bio-Rad Gene Pulser. The pulse was applied at a voltage of 2.5 kV/cm, an electrical resistance of 200 Ω and a capacity of 25 µF. After the pulse, 1 ml of LB medium was added to the DH10b, or 1 ml of S.O.C medium to the NEB 10-beta cells. The cell suspension was then transferred from the cuvette to a 1.5 ml test tube and incubated at 37°C for 1 h. About 350 µl of the cell suspension was then plated on solid LB medium containing appropriate selection agent and incubated at 37°C overnight (Section 3.1.2).

3.6.9. TRANSFORMATION OF *S. CEREVISIAE*

The yeast transformations were performed by chemical competent *S cerevisiae,* in accordance to Gietz and Schiestl (2007). First, 50 ml of YEPD was inoculated to an OD_{600} of about 0.05 with the desired *S. cerevisiae* strain, and incubated at 30°C and 180 rpm in aerobic shake flasks. When the early exponential phase (OD_{600} of 0.6-1.5) was reached, the cells were harvested at 3000 x g for 3 min, washed with 25 ml ddH_2O, and centrifuged again. The washing step was repeated, and the supernatant was discarded. The pellet was re-suspended in 50 µl of FCC solution (Table 26) per 5 OD_{600} equivalents of cells, and divided into 50 µl single-use aliquots. These single-use aliquots were then either used directly or stored at -80°C for further use, where they could be used the following day to at least one year.

Table 26 Composition of frozen competent cell (FCC) solution.

Compound	Concentration
Glycerin	5% (v/v)
DMSO	10% (v/v)

For the transformation, the freshly prepared or thawed single-use aliquots were pelleted by centrifugation at 3000 x g for 30 s. The supernatant was discarded carefully, and 306 µl of prepared transformation mix was added to the pellet by pipetting the viscous solution carefully. Then, 54 µl DNA solution was added (Table 27). The mixture was thoroughly mixed until homogenous cell suspension was observed. The cells where then incubated at 42°C for 40-60 min. Afterwards, the solution was transferred to 5 ml YEPD, and the culture was incubated for 2-4 h (regeneration phase), at 30°C, if a dominant selection marker was used. If an auxotrophic selection marker was used, no regeneration phase was necessary. After the regeneration phase, the transformations were harvested by centrifugation at 3000 x g for 2 min, and plated on a solid medium containing the appropriate selection agent (Section 3.1.2).

Table 27 Composition of *S. cerevisiae* transformation- and DNA mix. Both, 306 µl of premixed transformation mix and 54 µl of premixed DNA mix were added to the cell pellet.

Premix	Compound	Stock concentration	Volume	Final concentration
Transformation mix	PEG 4000	50 % (w/v)	260 µl	36% (w/v)
	LiAcetat	1.0 M	36 µl	100 mM
	Salmon Sperm DNA	2 mg/ml	10 µl	56 µg/ml
	total added to the cell pellet:		**306 µl**	
DNA mix	DNA	500 ng of each	Fill up to **54 µl** with ddH_2O	1389 ng/ml each

3.6.10. Gene Deletion by CRISPR/Cas9

Genomic gene deletions or insertions were performed with the CRISPR/Cas9 approach, as described by Generoso *et al.* (2016). The identification of a suitable protospacer sequence was performed with the *CRISPR gRNA Design tool (ATUM)*. The protospacers consisted of a 20-nt sequence, with an NNG PAM sequence upstream. They were assembled downstream of the guide-RNA (gRNA) sequence in the pRCC-K or pRCC-N plasmids. These plasmids encode for $Cas9^{Co}$ from *S. pyogenesis,* controlled by a *ROX3* promoter. Assembly of pRCC-X was performed mainly by using not only the Gibson isothermal assembly (Section 3.6.6.2) but also homologous recombination (Section 3.6.6.1), together with donor DNA, if a simultaneous genomic modification of *S. cerevisiae* was possible. Otherwise, a previously assembled deletion plasmid was co-transformed with a donor into *S. cerevisiae* (Section 3.6.9). The donor was necessary to promote the deletion or insertion of the gene of interest. For deletion, 300 pmol of an 80-bp single-stranded donor, which contains 40-nt downstream and 40-nt upstream of the gene of interest, was co-transformed. For insertion of a fragment, about 20 µl of a PCR product, which bared 40-nt downstream and 40-nt upstream of the genomic region of interest, was co-transformed. The transformants were plated on solid media containing the appropriate selection agent, after the 2-4 h regeneration phase in YEPD. The transformants were then verified *via* colony-PCR with appropriate primers targeting the genomic region of interest (Section 3.6.3 and Section 3.6.4.3). Transformants with expected genomic regions were cured from the CRISPR/Cas9 plasmid by omitting the selection agent and were then stored as plasmid-free permanent culture (Section 3.1.2).

3.7. Methods for Cell Cultivation and Fermentation

3.7.1. Determination of Cell Density

Liquid cell cultures were quantified spectrophotometrically at OD_{600}. The cell culture of interest was measured directly or diluted with a blank diluent, if necessary. Therefore, the sample suspension was transferred to a polystyrene cuvette. The Blank and sample were analysed in an Ultrospec 2100 pro spectrophotometer from Amersham Bioscience. The cell suspension aimed to obtain OD_{600} value between 0.05-1.2. If the values were out of this range, the dilution was adjusted accordingly and re-measured.

3.7.2. Online Cell Growth Monitoring by Cell Growth Quantifier (CGQ)

The growth comparison of *S. cerevisiae* in liquid media was online monitored *via* the use of the CGQ system from Aquila Biolabs, according to the of the manufacturer's instruction; the approach is also described in Bruder *et al.* (2016). Data were evaluated with the CGQuant software from Aquila Biolabs.

3.7.3. Serial Dilution Spot Assay

For growth comparison of *S. cerevisiae* on solid media, a serial dilution spot assay was performed. Cells were pre-grown in liquid YEPD culture to the exponential phase, harvested by centrifugation at 3000 x g for 2 min, and washed twice with sterile ddH_2O. The washed cell pellet was then resuspended to an OD_{600} of 1.0 in sterile ddH_2O. From this initial cell suspension (10^0), a serial ten-fold dilution was prepared in sterile ddH_2O four times: 10^{-1}, 10^{-2} and 10^{-3}. From this serial dilution, 5 µl of each concentration was transferred to a solid media of interest and allowed to dry. All plates tested were treated equally and incubated at 30°C for several days.

3.7.4. Replica Plating

With the replica plating method, the same colony, derived from one cell, can be grown on one or more different solid media. Replica plating is especially useful for negative screening, meaning that cells can be screen for conditions in which they are unable to grow. With this method, it was, for example, possible to verify if a transformant was cured from a plasmid (e.g., no longer possesses an antibiotic resistant).

Therefore, an original plate in which the selection pressure to be tested had not been applied was inoculated with a cell culture, containing roughly 30-500 of the cells of interest. The original plate was then incubated appropriately (yeast 30°C, bacteria 37°C). Once the cells were grown to well-visible colonies, the original plate was reproduced by keeping the original pattern of colonies. This was ensured by marking the original plate and all solid media plates to be tested at the petri dish as an orientation. Then, a sterile velvet was fixed on a plastic block with the radius of a petri dish. The original plate was then applied to the velvet with appropriate pressure. Thereby, the colony pattern was transferred to the velvet. The solid media to be tested was then pressed to the velvet in the same orientation as the original plate, by which the cells were transferred from the velvet to the solid medium. The last medium to be tested was the same medium as the original plate, and served as control. All

plates were then incubated appropriately and compared, once the colonies of the control plate had grown to an appropriate colony size. If a colony did not grow on a medium to be tested, the corresponding colony could still be isolated from the control plate, since it was attributable to the same colony pattern across all plates tested.

3.7.5. Aerobic High OD Isobutanol Biosynthesis

Pre-precultures for aerobic isobutanol fermentations were grown in YEPD. Therefore, 100 ml of YEPD media containing appropriate selection agents were inoculated with the desired isobutanol producer, to an OD_{600} of 0.1. Pre-precultures were then incubated at 30°C and 180 rpm, until OD_{600} of 3-4 was reached. Afterward, the cells were harvested and washed with 50 ml of sterile ddH_2O by centrifugation at 3000 x g for 2 min. The cells were then transferred to 200 ml of SCD medium in duplicates, to reach an OD_{600} of 0.2, and incubated in shake flasks at 30°C and 180 rpm, until an OD_{600} of 3-6 was reached. All precultures (duplicates) were then harvested and washed with 100 ml of sterile ddH_2O, separately, by centrifugation at 5000 x g for 15 min, at 5°C. The washed precultures were then resuspended in 50 ml $SCD_{\text{-valine}}$ containing 40 g/l of glucose to a final OD_{600} of 8 each. The fermentation was carried out in 100 ml aerobic shake flasks at 30°C, containing a magnetic stirrer, and samples were collected periodically for HPLC analysis. Average value was calculated from the HPLC data, obtained from at least duplicates and reported. The values were reported with no decimal place when > 10.00 mg/g_{Glc}, with one decimal place when ≤ 10.00 mg/g_{Glc} but ≥ 0.10 mg/g_{Glc}, and two decimal place when < 0.10 mg/g_{Glc}. The results shown in Section 4.3 (Figure 23) were calculated from the data published in Wess *et al.* (2019).

3.7.6. Evolutionary Engineering

The norvaline evolutionary engineering was carried out in triplicates by sequential aerobic shake flask cultivation, as described in Section 4.2. At the end of the experiment, some clones were isolated, stored as permanent culture and analysed as described in Section 4.2.1.

3.7.7. Metabolite Analysis by HPLC

For metabolite analyses by high performance liquid chromatography (HPLC), 1 ml of cell broth was centrifuged at 16000 x g for 5 min. Afterward, 450 µl of cell-free supernatant was mixed with 50 µl 5-sulfosalicylic acid. An additional centrifugation step (16000 x *g* for 5 min) was conducted. Then 500 µl, of the supernatant were

transferred to a 2.0 ml HPLC autosampler vial. For HPLC analyses, 10 µl of cell-free sample solution was injected into the HPLC device. The HPLC was equipped with a HyperREZ XP Carbohydrate H^+ column (300 × 700 mm, 8 µm), coupled with a refractive index detector. The mobile phase consisted of 5 mM of H_2SO_4 at a constant flow rate of 0.6 ml/min. The column oven temperature was set to 65°C.

3.8. Bioinformatic methods

3.8.1. Codon Optimisation of Genes

The codon-optimisation of synthetic genes listed in Table 35 was performed according to the codon adaptation index, evaluated by the web-based Jcat tool (Grote *et al.* 2005).

3.8.2. DNA Sequencing

DNA samples were sequenced by GATC Biotech AG (Konstanz, Germany). The DNA samples were diluted, mixed with suitable primers, and test tubes were labelled accordingly. Prepared test tubes were sent to GATC Biotech, with sequencing data analysed by the Clone Manager software from Sci Ed software.

3.8.3. Genome Sequencing

Evolved strains MBY36, MBY39 and MBY42 were grown in 150 ml YEPD media, and the cells were harvested at a stationary phase after the centrifugation at 3000 x g for 3 min. The supernatant was discarded, and samples were prepared according to the “Next generation sequencing: Sample preparation and shipping guidelines” (GATC Biotech AG, September 2014). The prepared cell pellets were frozen and shipped on dry ice in 50 ml test tubes to the GATC Biotech AG (GATC Biotech, European Genome and Diagnostics Centre, Jakob-Stadler-Platz 7, 78467 Konstanz). The DNA was isolated, and a standard genomic library was constructed with Illumina sequencing by GATC Biotech AG. The resulting data was annotated against reference *S. cerevisiae* CEN.PK113-7D, accession number *PRJNA393501* (https://www.ncbi.nlm.nih.gov/bioproject/PRJNA393501/). For the correct annotation, the integrative isobutanol cassette, based on MBV057, which was integrated in the *ilv2* locus of MBY29, was considered as well (Table 7). All detected SNPs und InDels were annotated and attributed to the ORF of genes, if possible. The final data report was provided by GATC Biotech AG, and further evaluation was performed as described in Section 4.2.1.

4. RESULTS

The aim of this work was to improve the cytosolic isobutanol biosynthesis, as described by Brat *et al.* (2012). By the described cytosolic approach, a maximum isobutanol yield of 15 mg/g_{Glc} was achieved in *S. cerevisiae*, representing 3.7% of the theoretical maximum. To optimise the cytosolic isobutanol biosynthesis, various bottlenecks need to be solved. As already described, major challenges of cytosolic isobutanol biosynthesis remain the redox- and co-factor imbalance of the isobutanol pathway, feedback regulation of the *de novo* valine synthesis by regulatory subunit Ilv6, elimination of competing pathways, enzyme harmonisation to avoid intermediate accumulation (e.g., DIV secretion), growth defects of *ilv2* deletion strains, and cytosolic ISC apo-protein maturation of Ilv3Δ19. These and other yet unknown limitations have been addressed in this work.

4.1. Limitations in Cytosolic Isobutanol Biosynthesis Caused by Expression of ILV-Enzymes in *S. cerevisiae*

S. cerevisiae has evolved to naturally *de novo* synthesise valine in the mitochondria. Consequently, enzymes, intermediates and co-factors have evolved to adapt to the environmental conditions of the mitochondrial compartment. To efficiently produce isobutanol, cytosolic ILV enzymes Ilv2Δ54, Ilv5Δ48 and Ilv3Δ19 (referred to as cyt-ILV) are expressed together with the enzymes Aro10 and Adh2 of the Ehrlich pathway (referred to as EP-enzymes). The changed environmental conditions for cyt-ILV enzymes might lead to inappropriate enzyme activity, due to unknown reasons. In the following sections, limitations of the cyt-ILV enzymes have been investigated.

4.1.1. Cytosolic Expression of Acetolactate Synthase

The initial step of the *de novo* valine biosynthesis is the mitochondrial formation of 2-acetolactate (ALAC) from two molecules of pyruvate, which are catalysed by the acetolactate synthase Ilv2 (ALS). For cytosolic isobutanol biosynthesis, as described by Brat *et al.* (2012), this reaction was shifted to the cytosol by expression of the truncated isoform Ilv2Δ54, and simultaneous deletion of native *ilv2*. During complementation growth assays with Ilv2Δ54 in auxotrophic IsoY08 (CEN.PK2-1C *Δilv2*), heterogeneous growth was observed (Brat *et al.* 2012). The reason for the deficient growth phenotype remained unclear.

To assess whether expression of Ilv2Δ54 is the reason for this growth phenotype, prototrophic CEN.PK113-7D was transformed with a plasmid constitutively expressing Ilv2Δ54 ($MBV058_N$) and Ilv2 ($MBV063_N$) as control (in this work, the antibiotic selection marker of the respective plasmid is indicated as subscripted letters. Whereas, “N” indicates a ClonNAT resistance, “K” indicates a G418 resistance, and “H” indicates a hygromycin B resistance). The transformants were then incubated on solid YEPD medium at 30°C for two days (Figure 4).

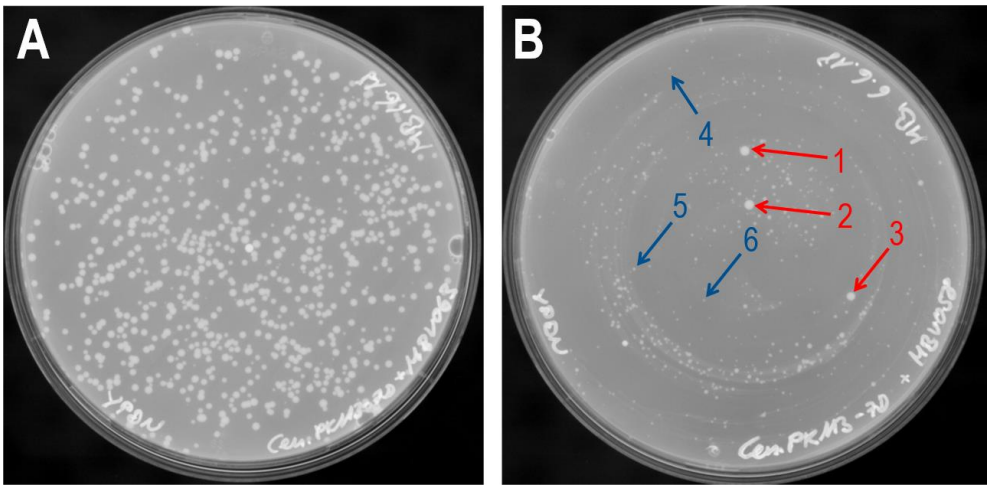

Figure 4 Growth test of CEN.PK113-7D constitutively expressing Ilv2 (A) and Ilv2Δ54 (B). Prototrophic CEN.PK113-7D was transformed with plasmids constitutively expressing Ilv2Δ54 ($MBV058_N$) and Ilv2 ($MBV063_N$). The transformants were then incubated on solid YEPD medium containing ClonNAT as selection marker. The images were recorded after two days of incubation at 30°C. Red (T^{1-3}) and blue (T^{4-6}) arrows highlight these transformants which were selected to assess growth defects in Ilv2Δ54 expressing CEN.PK113-7D. T^{1-3} show a growth phenotype comparable to that of Ilv2 control. T^{4-6} show a deficient growth phenotype compared to that of Ilv2 control.

CEN.PK113-7D transformants that constitutively expressed Ilv2, showed a homogeneous growth phenotype (Figure 4A). Expression of Ilv2Δ54 caused a heterogeneous and deficient growth phenotype on solid YEPD medium. However, some suppressor colonies were observed among the transformant expressing Ilv2Δ54. Three suppressor transformants (Figure 4B, red arrows, referred to as T^{1-3}), and three transformants with deficient growth phenotypes (Figure 4B, blue arrows, referred to as T^{4-6}) were isolated, re-grown on solid YEPD medium, and the plasmid DNA was extracted from T^{1-6}. The ORFs of the isolated plasmids from $T^{1,\ 3\text{-}4\ \text{and}\ 6}$ were verified by restriction and sequencing (plasmid DNA isolation was not successful for $T^{2\ \text{and}\ 5}$). Plasmids isolated from $T^{4\ \text{and}\ 6}$ showed the expected restriction patterns for $MBV058_N$. On the contrary, the restriction patterns of plasmids isolated from suppressors $T^{1\ \text{and}\ 3}$ indicated truncation in the restriction fragment that contained the ORF of *ILV2Δ54* (data not shown). To verify whether the truncation was in the *ILV2Δ54* ORF, the ORFs of the re-isolated plasmids $T^{1,\ 3\text{-}4\ \text{and}\ 6}$ was sequenced. The

results proved that ORFs of *ILV2Δ54* in the re-isolated plasmids of suppressors $T^{1 \text{ and } 3}$ were altered. No mutation was found in the ORFs of *ILV2Δ54* of re-isolated plasmids of $T^{4 \text{ and } 6}$ (data not shown).

To investigate if altered ORFs of *ILV2Δ54* from suppressors $T^{1 \text{ and } 3}$ were catalytically active, the re-isolated $MBV058_N$ plasmids were transformed into IsoY08 (CEN.PK2-1C Δ*ilv2*). Transformation of the original plasmid $MBV058_N$, as well as the re-isolated $MBV058_N$, from the deficient growth transformant T^4 served as control. Transformants were then incubated in YEPD liquid medium and grown at 30°C at 180 rpm. Subsequently, a spot-assay was performed on solid $SCD_{-valine}$, SCD and YEPD mediums (Figure 5).

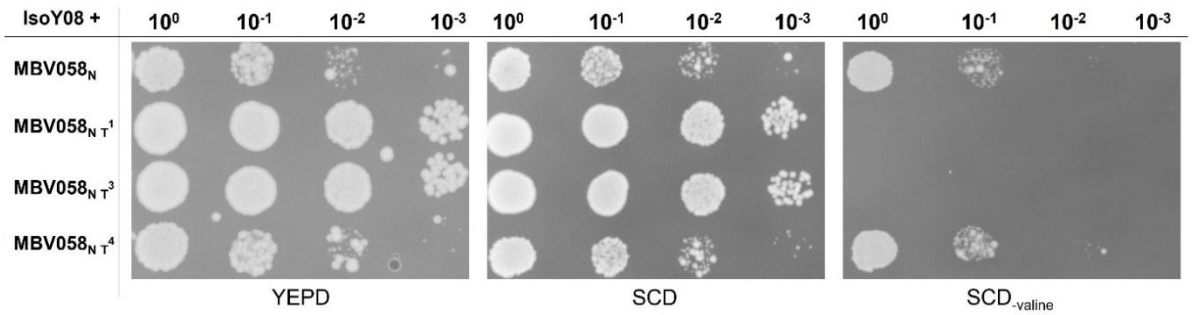

Figure 5 Growth assay to assess if valine auxotrophy of IsoY08 is complemented by isolated $MBV058_N$ variants. IsoY08 (CEN.PK2-1C Δ*ilv2*) was transformed with original plasmid $MBV058_N$ (constitutively expressing *ILV2Δ54*) and $MBV058_N$ re-isolated from suppressors $T^1$and T^3 as well as deficient growth transformant T^4. The transformants were plated on solid YEPD, SCD and $SCD_{-valine}$ mediums containing ClonNAT as the section marker. 10^0 represents OD_{600} of 1 and was used for further serial dilution to 10^{-1}, 10^{-2} and 10^{-3}. The image was recorded after two days of incubation at 30°C for YEPD and SCD as well as after five days for $SCD_{-valine}$.

Figure 5 shows that the expression of isolated plasmids $MBV058_{N\,T^1}$ and $MBV058_{N\,T^3}$ did not cause a growth phenotype in solid SCD and YEPD mediums, and neither did they complement the *ilv2*-deletion on the solid $SCD_{-valine}$ medium. On the contrary, transformants expressing the original $MBV058_N$ plasmid or deficient growth control $MBV058_{T^4}$ caused a deficient growth phenotype in the SCD and YEPD mediums, and complemented the *ilv2*-deletion of IsoY08 on the $SCD_{-valine}$ medium. By showing that $MBV058_{N\,T^1}$ and $MBV058_{N\,T^3}$ were not catalytically active (equals vector control), it can be assumed that deficient growth phenotypes in YEPD and SCD were not caused by the *ilv2*-deletion itself, but rather by constitutive expression of cytosolic *ILV2Δ54*. This is also supported by the results of Figure 4B that show deficient growth phenotype in a prototrophic CEN.PK113-7D background, when *ILV2Δ54* is constitutively expressed.

However, it was still unclear if the growth phenotype was caused by the cytosolic Ilv2Δ54 protein or the catalytical activity of Ilv2Δ54 (e.g., caused by toxic effects of the product or derived downstream molecules that might be produced in the cytosol, but may not occur in the mitochondria). Moreover, the deficient growth phenotype of *S. cerevisiae* constitutively expressing *ILV2Δ54* was only prominent on solid mediums, whereas it was barely evident in liquid cultures (data not shown). To investigate the root cause for the growth deficit in *ILV2Δ54* expressing *S. cerevisiae*, catalytic inactive mutants *ILV2*^{E139A} and *ILV2Δ54*^{E139A}, as described by Espinosa-Cantú *et al.* (2017), were cloned into the pRS62$_N$ vector for constitutive expression (MBV064$_N$ and MBV065$_N$, respectively). Additionally, a bacterial ALS from *L. plantarum* (referred to as *alsLP*) was cloned into the same vector (MBV074$_N$). *AlsLP* is reported to be catalytically active in *S. cerevisiae,* with no growth phenotype being described (Ishii *et al.* 2018). IsoY08 (CEN.PK2-1C Δ*ilv2)* was then transformed with MBV064$_N$, MBV065$_N$ and MBV074$_N$, respectively. Transformation of IsoY08 with vector, as well as plasmids for expression of Ilv2 (MBV063$_N$) or Ilv2Δ54 (MBV058$_N$), served as control. To investigate why deficient growth phenotype was prominent in solid medium but not in liquid, the transformants were pre-grown in liquid YEPD, and additionally prepared from the YEPD transformation plate directly for growth assay (Figure 6).

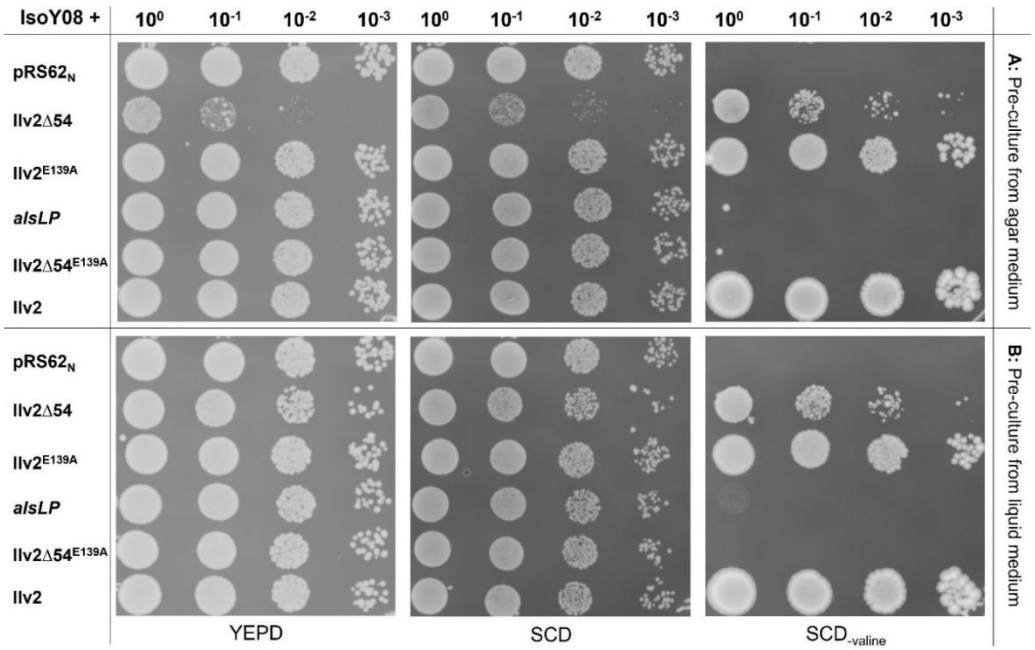

Figure 6 Growth assay to assess valine complementation in IsoY08 and growth phenotypes of (non-) catalytical ALS variants and *alsLP* from precultures grown on solid medium (A) or liquid medium (B). IsoY08 (CEN.PK2-1C Δ*ilv2*) was transformed with vector or Ilv2Δ54 (MBV058$_N$), Ilv2^{E139A} (MBV064$_N$), *alsLP* (MBV074$_N$), Ilv2Δ54^{E139A} (MBV065$_N$), and Ilv2 (MBV063$_N$) constitutively expressing plasmids, respectively. The transformants were plated on solid YEPD, SCD and SCD$_{-valine}$ mediums containing ClonNAT as section marker. 10^0 represents OD_{600} of 1 and was used for further serial dilution to 10^{-1}, 10^{-2} and 10^{-3}. The image was recorded after two days of incubation at 30°C for YEPD and SCD as well as after seven days for SCD$_{-valine}$.

As can be seen from the comparison between Figure 6A and Figure 6B (line 2), the deficient growth phenotype of the transformant expressing Ilv2Δ54 was only evident in solid SCD and YEPD mediums, when the pre-cultures were not grown in liquid YEPD. However, expression of Ilv2Δ54 complemented *ilv2*-deletion in $SCD_{-valine}$, regardless of whether the transformants were prepared from liquid medium or solid medium. No deficient growth phenotype was observed for other transformants tested on SCD and YEPD, independent of pre-treatment (line 1 and 3 to 6). Among the tested ALS variants, only Ilv2Δ54, Ilv2, and $Ilv2^{E139A}$ expressing transformants were able to complement *ilv2*-deletion in IsoY08 (Figure 6, lines 2, 3, and 6). Amino acid replacement of glutamic acid 139 to alanine (E139A) did not disturb catalytic activity for mitochondrial $Ilv2^{E139A}$, but did for cytosolic $Ilv2\Delta54^{E139A}$ (Figure 6, line 4). By comparing the growth of Ilv2Δ54 and $Ilv2\Delta54^{E139A}$ expressing transformants, it was shown that the deficient growth phenotype was eliminated with catalytic inactivity (Figure 6, lines 2 and 5). Heterologous expression of *alsLP* did not cause a deficient growth phenotype either, but could barely complement the *ilv2*-deletion of IsoY08 on solid $SCD_{-valine}$ medium (Figure 6, line 4). However, expression of ALS *ilvB* from *C. glutamicum* was assessed as alternative bacterial ALS for isobutanol synthesis in the following chapter.

From the results, it was concluded that catalytic activity of Ilv2Δ54, not the protein, caused the growth deficiency. Furthermore, it was shown that transformants, when released from selection pressure of valine production, recombine the *Δ54* ORF to obtain catalytically inactive Ilv2Δ54 mutants, in order to mitigate the deficient growth phenotype.

4.1.1.1. Heterologous Expression of *ilvB* and Small Regulatory Subunit *ilvN* from *C. glutamicum*

Because of the deficient growth phenotype observed in *S. cerevisiae,* by expression of Ilv2Δ54, the heterologous expression of the ALS *ilvB* from *C. glutamicum* was assessed regarding isobutanol production. The enzyme *ilvB* is described in the literature to be functionally expressible in *S. cerevisiae* (Milne *et al.* 2016; Cordes *et al.* 1992). Also, small regulatory subunits *ilvN* (Eggeling *et al.* 1987) and feedback insensitive $ilvN^{M13}$ have already been described in the literature. If the organism is lacking BCAA, ALS activity can be improved by the small regulatory subunit *ilvN* and, in reverse, it inhibits ALS activity when BCAA is available (Elisakova *et al.* 2005; Milne *et al.* 2016).

Codon optimised *ilvB*^{Co} was cloned into pRS62$_N$ (MBV097$_N$), and codon optimised *ilvN*^{Co} *and ilvN*$^{M13\text{-}Co}$ were cloned into pRS62$_H$ (MBV083$_H$ and MBV084$_H$) for constitutive expression. Subsequently, WGY21 (CEN.PK113-7D Δ*ilv2*) was transformed with the plasmids expressing *ilvB*^{Co} and combined with *ilvN*^{Co}, *ilvN*$^{M13\text{-}Co}$ or the vectors, respectively. As control, WGY21 was transformed with both vectors, as well as Ilv2 or Ilv2Δ54 together with the corresponding vector. The transformants were then incubated on solid YEPD and SCD$_{\text{-valine}}$ mediums containing ClonNAT and Hygromycin B as section markers for several days at 30°C (Figure 7).

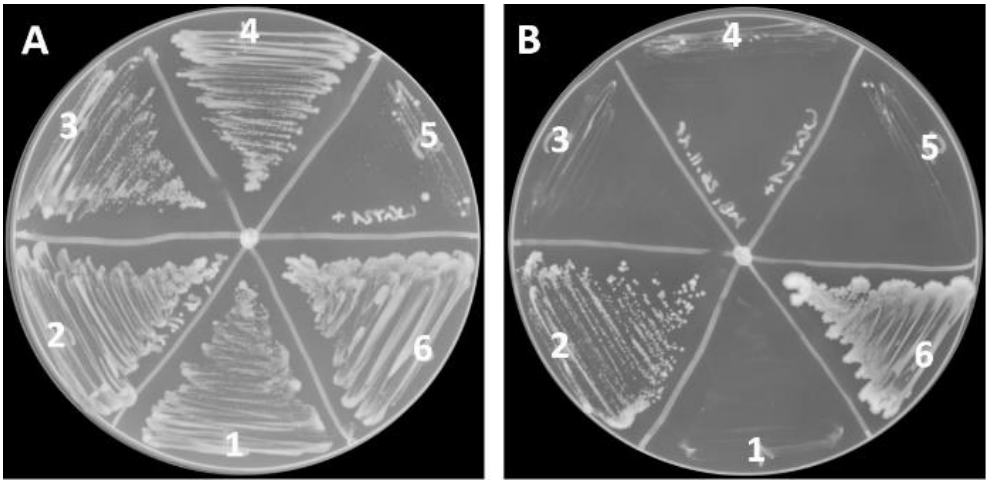

Figure 7 Growth assay to assess valine complementation in WGY21 constitutively expressing different ALS and corresponding regulatory subunits on solid YEPD (A) and SCD$_{\text{-valine}}$ (B) mediums. WGY21 was transformed with 1: pRS62$_N$ + pRS62$_H$, 2: *ilvB* (MBV097$_N$) + *ilvN* (MBV083$_H$), 3: *ilvB* + *ilvN*^{M13} (MBV084$_H$), 4: *ilvB* + pRS62$_H$, 5: Ilv2Δ54 (MBV058$_N$) + pRS62$_H$ and 6: Ilv2 (MBV063$_N$) + pRS62$_H$ expressing plasmids. The transformants were plated on solid YEPD, and SCD$_{\text{-valine}}$ mediums containing ClonNAT and Hygromycin B as section markers. The image was recorded after two days of incubation at 30°C in YEPD and after five days in SCD$_{\text{-valine}}$.

As shown in Figure 7A (No. 5), a deficient growth phenotype on solid YEPD medium was caused by the expression of Ilv2Δ54. Expression of *ilvB* together with small regulatory subunit variants or respective controls (No. 1-4 and 6), did not inhibit growth on solid YEPD medium. However, growth on SCD$_{\text{-valine}}$ was only mediated by expression of Ilv2 or *ilvB* + *ilvN* expressing transformants (Figure 7B, No. 6 and 2). Transformants expressing *ilvB* + *ilvN*^{M13} or vectors did not grow on solid SCD$_{\text{-valine}}$ medium (Figure 7B, No. 3 and 4). For the Ilv2Δ54 expressing transformants, only a few colonies grew on solid SCD$_{\text{-valine}}$ medium, after five days of incubation (Figure 7B, No. 5). Most likely, a prolonged incubation time would have been required to observe the growth of Ilv2Δ54 expressing transformants, as it is known that Ilv2Δ54 complements *ilv2*-deletion in *S. cerevisiae* (compare with Figure 6A, Line 2).

Cytosolic expression of Ilv2Δ54 has been shown to cause a deficient growth phenotype, but is also essential for cytosolic isobutanol production (Brat *et al.* 2012).

Consequently, growth assay using a Δ*ilv2* mutant in solid medium without valine was not sufficient to assess the capability of cytosolic ALS (e.g., Ilv2Δ54 or *ilvB*) in terms of cytosolic isobutanol production. To assess the capability of *ilvB* with respect to cytosolic isobutanol production, *ILV2Δ54* was replaced by *ilvB* in IsoV100$_K$, bearing the cyt-ILV enzymes (hereafter referred to as MBV099$_K$, or cyt-ILV_*ilvB*). MBV099$_K$ was then transformed in combination with the vector, *ilvN* (MBV083$_H$) or *ilvN*^{M13} (MBV084$_H$) into MBY25 (CEN.PK113-7D *Δilv2*). Transformation of MBY25 with IsoV100$_K$, in combination with the vector or the cytosolic small regulatory subunit Ilv6Δ61 (MBV076$_H$), served as a control. The SCD$_{-valine}$ medium was then fermented by the transformants in aerobic shake flask cultivation. Yields of ethanol as main fermentative product, acetoin and DIV as well as the isobutanol yield, are summarised in Figure 7.

Acetoin, unlike ALAC or DIV, is no intermediate of cytosolic isobutanol synthesis, but is used as a representative by-product to estimate the accumulation of ALAC. The latter is not detectable, since ALAC oxidises spontaneously to diacetyl under elimination of CO_2, which is catalysed by various electron acceptors. Diacetyl is then further reduced to acetoin and 2,3-butanediol by the cytosolic enzymes Bdh1 and Bdh2. Therefore, either acetoin or 2,3-butanediol yields were used in the following to estimate the ALAC yield in the isobutanol fermentations.

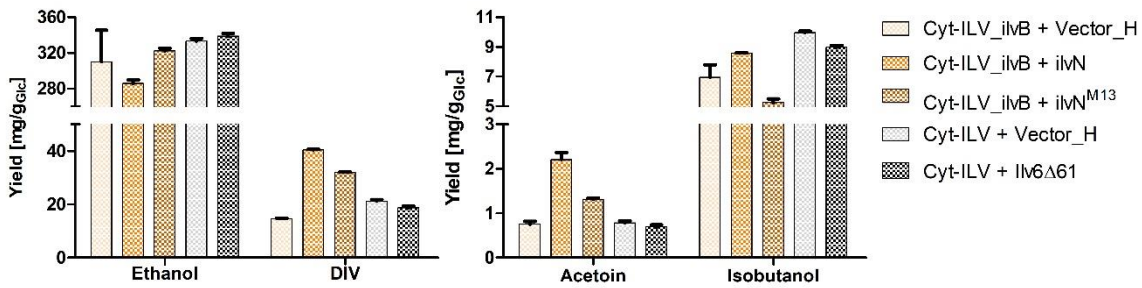

Figure 8 Yields of ethanol, DIV, acetoin and isobutanol after aerobic fermentation of SCD$_{-valine}$ by MBY25 expressing the cyt-ILV genes, varying ALS with respective regulatory subunits. MBY25 (CEN.PK113-7D *Δilv2*) was transformed with a plasmid constitutively expressing the cytosolic ILV genes with *ilvB* from *C. glutamicum* replacing Ilv2Δ54 (cyt-ILV_*ilvB*, MBV099$_K$) combined with vector, regulatory subunit *ilvN* (MBV083$_H$) or feedback insensitive *ilvN*^{M13} (MBV084), respectively. Additionally, MBY25 was transformed with a plasmid constitutively expressing the cytosolic ILV genes (cyt-ILV, IsoV100$_K$) and vector or cytosolic regulatory subunit Ilv6Δ61 (MBV076$_H$), respectively. SCD$_{-valine}$ was fermented in aerobic shake flask cultivation at 30 C (OD$_{600}$ of 8) by the transformants in duplicates with Geneticin and Hygromycin B added as selection marker. The yields were calculated after 24 h when glucose was fully consumed.

Figure 8 shows that ethanol remained the major fermentative product in all transformants tested, even though cyt-ILV enzymes were expressed. The ethanol yield varied from 286 mg/g$_{Glc}$ for cyt-ILV_*ilvB* + *ilvN* to 339 mg/g$_{Glc}$ for

cyt-ILV + Ilv6Δ61. The lowest acetoin yield of 0.7 mg/g_{Glc} was obtained by expression of cyt-ILV_*ilvB* + vector, and was highest at 2.1 mg/g_{Glc}, when cyt-ILV_*ilvB* + *ilvN* was expressed, demonstrating a significant improvement of catalytic activity due to co-expression of *ilvN*. The same tendency was observed for DIV. The lowest yield of 15 mg/g_{Glc} was observed by expression of cyt-ILV_*ilvB* + vector, but the highest yield of 40 mg/g_{Glc} was obtained by expression of cyt-ILV_*ilvB* + *ilvN*.

The isobutanol yields in ascending order were, 5.2 mg/g_{Glc} for cyt-ILV_*ilvB* + *ilvN*^{M13}, 7.0 mg/g_{Glc} for cyt-ILV_*ilvB* + vector, 8.6 mg/g_{Glc} for cyt-ILV_*ilvB* + *ilvN*, 9.0 mg/g_{Glc} for cyt-ILV + vector and 10 mg/g_{Glc} for cyt-ILV + Ilv6Δ61 expressing transformants. Consequently, the isobutanol yield was highest in the transformant expressing Ilv2Δ54, regardless of whether the cytosolic regulatory subunit Ilv6Δ61 was expressed.

The results show that *ilvB*^{ilvN} expressing transformants produced more acetoin and DIV and less ethanol than Ilv2Δ54 expressing transformants (Figure 8). This indicates good catalytic *in vivo* activity of *ilvB*^{ilvN}, without causing a deficient growth phenotype in solid YEPD medium (Figure 7). Therefore, *ilvB*^{ilvN} was considered a promising alternative for Ilv2Δ54 in cytosolic isobutanol production, according to Brat *et al.* (2012), even though isobutanol yields were slightly lower.

4.1.1.2. Cytosolic Isobutanol Production in Medium Supplemented With and Without Valine by Expression of Ilv2Δ54 and Ilv6 Variants

As already described above, like Ilv2, ALS is commonly feedback regulated by a small regulatory subunit (in case of Ilv2, the corresponding subunit is Ilv6), where the regulation is dependent on the intra cellular BCAA concentration. In the absence of BCAA, such as valine, Ilv2 activity is enhanced by Ilv6, but is also reduced when valine is available (Kakar and Wagner 1964; Xiao and Rank 1988; Pang and Duggleby 1999; Duggleby 1997). However, it is unknown whether immature apo-Ilv6, which has not yet been imported into the mitochondrion, is able to enhance or weaken the activity of cytosolically expressed Ilv2Δ54. If so, this would considerably impact cytosolic isobutanol production when valine is available in the fermentation broth. It is not yet known why valine has to be excluded from the fermentation media for efficient cytosolic isobutanol biosynthesis (Brat *et al.* 2012; Generoso *et al.* 2015). Thus, the impact of Ilv6, as well as cytosolic and feedback insensitive isoforms, was assessed with respect to cytosolic isobutanol production. Native *ILV6* (MBV075$_H$), cytosolic *ILV6Δ61* (MBV076$_H$), as well as feedback

insensitive isoforms *ILV6*^{N86A} (MBV077$_H$) and *ILV6*Δ*61*^{N86A} (MBV078$_H$), were cloned in pRS62$_H$ for constitutive gene expression (Takpho *et al.* 2018). To avoid endogenous *ILV6* expression, the latter was deleted in MBY25, resulting in CEN.PK113-7D Δ*ilv2* Δ*ilv6* (MBY51).

MBY25 was transformed with a plasmid expressing the cyt-ILV enzymes (IsoV100$_K$) combined with a vector control, or Ilv6Δ61 expressing plasmid (MBV076$_H$). MBY51 was transformed with IsoV100$_K$ and vector control, or one of the plasmids expressing the Ilv6 isoforms (MBV075-78$_H$), respectively. Aerobic shake flask cultivation was conducted in SCD, with and without valine supplement, at 30°C and 180 rpm, respectively (Figure 9).

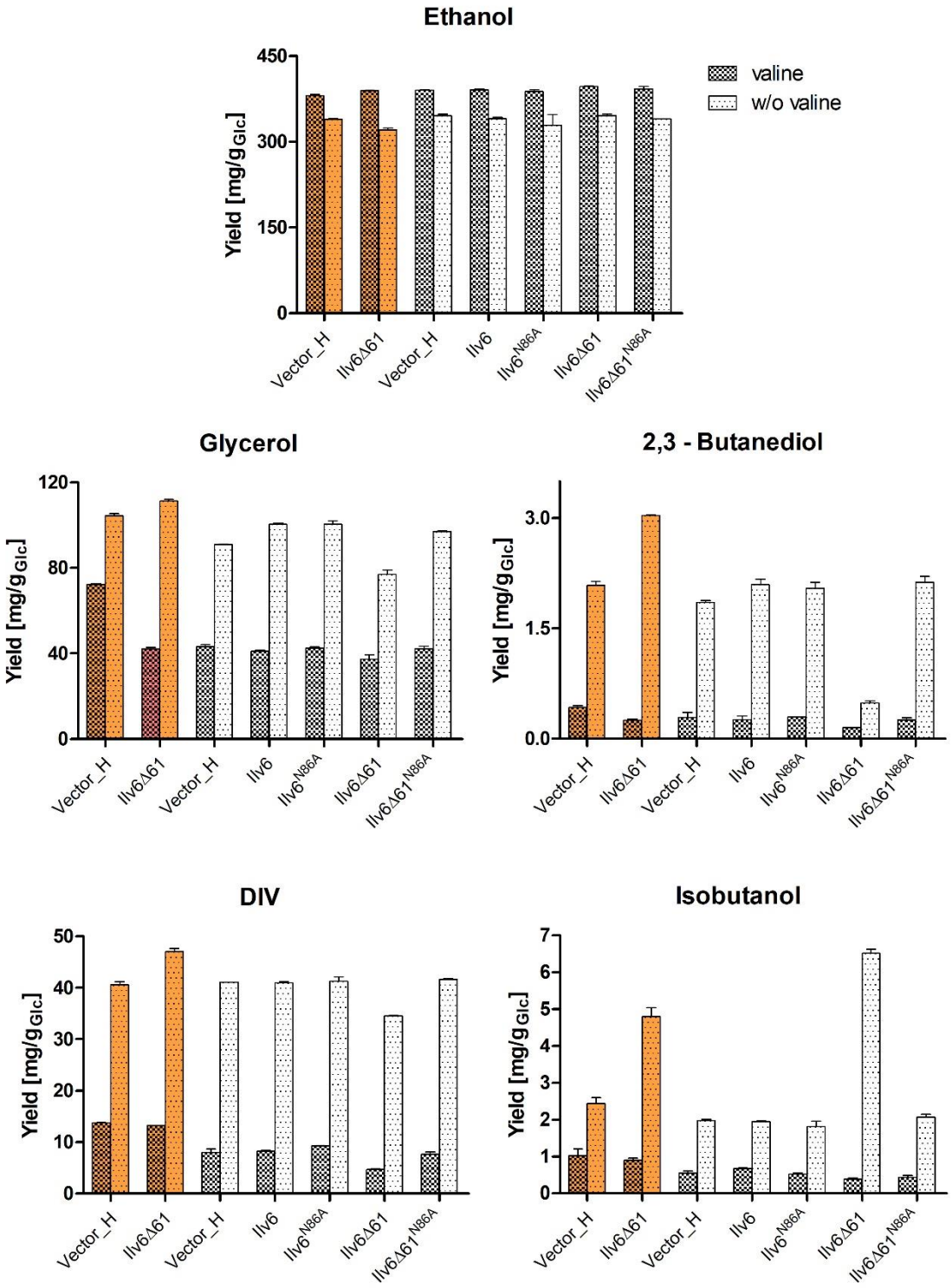

Figure 9 Yields of ethanol, glycerol, 2,3-butanediol, DIV and isobutanol after aerobic fermentation of SCD with and without valine by MBY25 (orange) and MBY51 (white) constitutively expressing the cytosolic ILV genes, varying small ALS regulatory subunits. MBY25 (CEN.PK113-7D *Δilv2*) was transformed with IsoV100 and vector or truncated cytosolic regulatory subunit Ilv6Δ61 (MBV076$_H$), respectively. MBY51 (CEN.PK113-7D *Δilv2, Δilv6*) was transformed with IsoV100 and vector, regulatory subunit Ilv6 (MBV075$_H$), feedback insensitive Ilv6^{N86A} (MBV078$_H$), cytosolic Ilv6Δ61 (MBV076$_H$) and cytosolic feedback insensitive Ilv6Δ61^{N86A} (MBV077$_H$), respectively. SCD and SCD$_{-valine}$ was fermented in aerobic shake flask cultivation (OD$_{600}$ of 8) at 30°C by the transformants in duplicates with Geneticin and Hygromycin B added as selection marker. The yields were calculated after 8 h when at least 85% of the glucose was consumed.

As shown in Figure 9, ethanol yields were increased for all fermentations in SCD (381-397 mg/g_{Glc}), compared to fermentations in $SCD_{-valine}$ (321-345 mg/g_{Glc}). However, the opposite was observed for glycerol, 2,3-butanediol and DIV, which were increased when valine was omitted. The same was observed for isobutanol yields, which were increased from 0.38-1.0 mg/g_{Glc} in SCD to 2.0-6.5 mg/g_{Glc} in $SCD_{-valine}$. This was observed for all transformants, regardless of whether *ilv6* was deleted. Expression of feedback-resistant $Ilv6^{N86A}$ and $Ilv6\Delta61^{N86A}$ did increase yields of intermediates and isobutanol slightly, compared to feedback-sensitive Ilv6 or Ilv6Δ61 when fermented in SCD. However, even with feedback-resistant isoforms, addition of valine decreased yields significantly. Furthermore, it was observed that expression of Ilv6Δ61 improved isobutanol biosynthesis in $SCD_{-valine}$ but not in SCD, regardless of whether *ilv6* was deleted. Isobutanol yields increased from 2.4 mg/g_{Glc} in MBY25 control (lane 1), to 4.7 mg/g_{Glc} in MBY25 expressing Ilv6Δ61 (lane 2). The same was observed in MBY51 where isobutanol yields increased from 2.1 mg/g_{Glc} in the control (lane 3) to 6.5 mg/g_{Glc} (lane 6) by expression of Ilv6Δ61.

The results demonstrated that feedback resistant $Ilv6^{N86A}$ isoforms were not able to prevent the isobutanol yields from decreasing when valine was added to the fermentation broth. By comparing the isobutanol yields of control MBY25 (Figure 9 lane 1) and *ilv6* deletion mutant MBY51 (Figure 9 lane 3 and 4), the hypothesis that apo-Ilv6 did considerably impact isobutanol production was not proven. However, expression of cytosolic Ilv6Δ61 significantly increased isobutanol yield, and therefore was considered a beneficial approach for isobutanol production.

4.1.2. Cytosolic Expression of Ketol-Acid Reductoisomerase

During isobutanol biosynthesis, two molecules of NAD^+ are utilised in glycolysis, whereas only one molecule of NAD^+ is recovered in the Ehrlich pathway by the alcohol dehydrogenase reaction of Adh2. The KARI (Ilv5) reaction during valine *de novo* synthesis requires NADPH. Thus, isobutanol biosynthesis is not co-factor balanced, making it impossible to establish the latter as a main fermentative pathway in *S. cerevisiae*. Whether the co-factor imbalance was already limiting during cytosolic isobutanol production in the aerobic shake flask cultivation has been investigated in the following sections.

4.1.2.1. EXPRESSION OF ILV5Δ48 OR *ILVC^{6E6}* WITH CYT-ILV AND EP-ENZYMES

For constitutive expression of all enzymes necessary during isobutanol biosynthesis, the EP-genes *ADH2* and *ARO10* were incorporated into the cyt-ILV genes expressing plasmid IsoV100$_K$ (hereafter referred to as MBV100$_K$, cyt-ILV+EP). It is known from the literature that NADH utilising KARI *ilvC^{6E6}* from *E. coli* is catalytically active in the yeast's cytosol (Bastian *et al.* 2011; Generoso *et al.* 2017). Thus, the gene *ILV5Δ54* in MBV100$_K$ was replaced by *ilvC*^{6E6}, making the isobutanol biosynthesis obtained from this plasmid co-factor balanced (hereafter referred to as MBV057$_K$, cyt-ILV+EP_*ilvC*^{6E6}). Both plasmids (MBV057$_K$ and MBV100$_K$) were designed also as destructive integrative vectors for the *ILV2* locus in *S. cerevisiae* after *PmeI* digestion of the plasmid, allowing for the integration of the respective cytosolic isobutanol pathway and simultaneous genomic *ilv2* deletion.

Plasmids MBV057$_K$ and MBV100$_K$ were transformed into MBY25 to express cyt-ILV+EP with *ilvC*^{6E6} or *ILV5Δ48,* respectively. IsoV100$_K$ (cyt-ILV) was transformed into MBY25 as a control, and SCD$_{-valine}$ was then fermented in an aerobic shake flask cultivation by the transformants at 30°C and 180 rpm. The results are summarised in Figure 10.

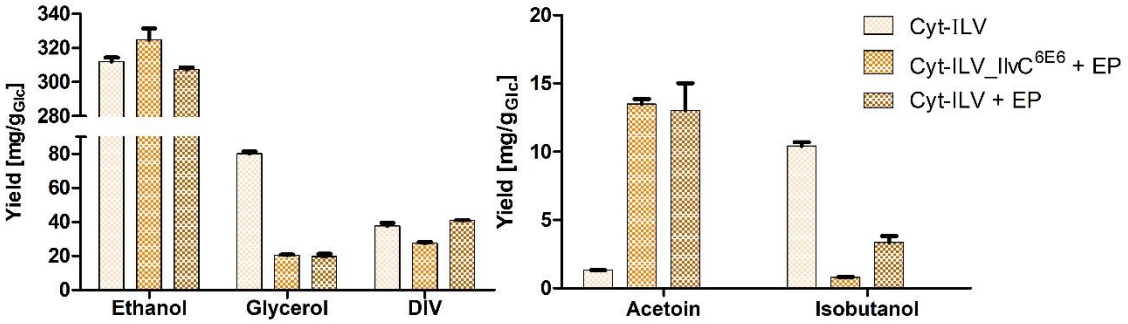

Figure 10 Yields of ethanol, glycerol, DIV, acetoin and isobutanol after aerobic fermentation of SCD$_{-valine}$ by MBY25 constitutive overexpressing cyt-ILV, cyt-ILV_*ilvC*^{6E6}+EP and cyt-ILV+EP genes. MBY25 (CEN.PK113-7D *Δilv2*) was transformed with a plasmid bearing cyt-ILV (IsoV100$_K$), cyt-ILV+EP (MBV100$_K$) and cyt-ILV_*ilvC*^{6E6}+EP genes with Ilv5Δ48 being replaced by *ilvC*^{6E6} from *E.* coli (MBV057$_K$), respectively. SCD$_{-valine}$ was fermented in aerobic shake flask cultivation at 30°C (OD$_{600}$ of 8) by the transformants in duplicates with Geneticin added as selection marker. The yields were calculated after 24 h when complete glucose was consumed.

Figure 10 shows that ethanol remained the major fermentative product in all transformants tested. The mean ethanol yield varied from 307 mg/g$_{Glc}$ for the transformant expressing cyt-ILV+EP to 325 mg/g$_{Glc}$ for the transformant expressing cyt-ILV_*ilvC*^{6E6}+EP. The transformant expressing cyt-ILV enyzmes was in between, with 312 mg/g$_{Glc}$ ethanol production. Glycerol yield of 80 mg/g$_{Glc}$ was highest for the

transformants that did not express the EP, compared to those that did. Once EP was expressed, the glycerol yield decreased to 20 mg/g_{Glc} and 21 mg/g_{Glc} for cyt-ILV_*ilvC*^{6E6} and cyt-ILV enzymes expressing transformants, respectively. The DIV yields were not affected by expression of the EP; only a small difference of 38 mg/g_{Glc} compared to 41 mg/g_{Glc} was observed for cyt-ILV enzymes with and without EP, respectively. Decreased DIV yield of 28 mg/g_{Glc} was observed for the transformant expressing cyt-ILV_*ilvC*^{6E6}+EP. However, the opposite tendency was observed for by-product acetoin, where the yield increased tenfold by expression of EP. The transformant expressing cyt-ILV enzymes achieved a yield of 1.3 mg/g_{Glc}. By additional expression of EP, the acetoin yield increased to 13 mg/g_{Glc} for both KARIs tested. Isobutanol yield was highest at 10 mg/g_{Glc} when cyt-ILV enzymes were expressed. With additional expression of EP, isobutanol yield decreased to 3.3 mg/g_{Glc}, and was lowest for cyt-ILV_*ilvC*^{6E6}+EP (0.8 mg/g_{Glc}).

The results showed that expression of EP enzymes significantly decreased isobutanol yields but increased acetoin yield. This was unexpected, as it is described in the literature that EP enzymes enhance the biosynthesis of isobutanol. However, by expression of EP enzymes, glycerol biosynthesis decreased significantly, indicating that the NAD^+ recovery was already limiting during the isobutanol biosynthesis, and was mitigated by the expression of Adh2. Substitution of *ILV5Δ48* by *ilvC*^{6E6} did neither improve NAD^+ recovery nor isobutanol production, which can most likely be attributed to a low *in vivo* activity of *ilvC*^{6E6}.

4.1.3. Cytosolic Expression of Dihydroxyacid Dehydratase

The cytosolic conversion of DIV to KIV is considered a limiting step during isobutanol production as the most secreted metabolite is DIV (Generoso *et al.* 2017). A reason might be a decreased enzyme activity of cytosolic Ilv3Δ19 due to insufficient ISC apo-protein maturation in the yeast's cytosol. *S. cerevisiae* exclusively assembles [4Fe-4S] ISC in the cytosol (only Grx3 and Grx4 assemble [2Fe-2S] in a non-canonical way). However, Ilv3 is known to be a [2Fe-2S] ISC enzyme (Mühlenhoff *et al.* 2011; Lill *et al.* 2015). Thus, native cytosolic ISC assembling machinery of *S. cerevisiae* might not be capable of efficiently maturing [2Fe-2S] ISC Ilv3Δ19 apo-protein. To enhance cytosolic DIV to KIV conversion, improvement of the cytosolic DHAD activity was attempted by improving cytosolic [2Fe-2S] ISC assembly for endogenous Ilv3Δ19 apo-protein maturation. Alternatively, it was

screened for heterologous [4Fe-4S] ISC containing DHAD. The results are summarised in the following section.

4.1.3.1. Altering the C-terminus of DHAD to Increase Affinity towards the Adapter Complex of the Cytosolic Iron-Sulphur Assembling Machinery

Cytosolic Ilv3Δ19 apo-protein might be insufficiently supplied with [2Fe-2S] ISC by cytosolic iron-sulphur-assembling (CIA) machinery, since in *S. cerevisiae,* only [4Fe-4S] ISC are assembled in cytosol by the CIA machinery (Mühlenhoff *et al.* 2011; Lill *et al.* 2015). A possible solution to overcome this issue is the heterologous expression of [4Fe-4S] ISC containing DHAD in *S. cerevisiae*. DHAD from 73 different organisms were compared by Mühlenhoff *et al.* (2011), who used a web-based algorithm (Dereeper *et al.* 2008, www.phylogeny.fr) to create an evolutionary tree in which the protein sequences were aligned with the sequence of [4Fe-4S] ISC containing *ilvD* from *E. coli* str. K-12, and [2Fe-2S] ISC containing *ilvD* from *Arabidopsis thaliana* (Mühlenhoff *et al.* 2011). From the data published by Mühlenhoff *et al.* (2011), a global protein alignment was performed using the BLOSUM62 scoring matrix (Henikoff and Henikoff 1992) to evaluate sequence variation of [4Fe-4S] ISC containing DHAD, compared to *ilvD* from *E. coli* str. K-12. The highest variation of sequence identity among the tested [4Fe-4S] DHAD was found to be only 87%, compared with *ilvD* reference from *E. coli*. Based on the results of the BLOSUM62 scoring matrix, the following DHAD were selected for heterologous expression in *S. cerevisiae*: *ilvD* from *E. coli* str. K-12 (reference containing [4Fe-4S] ISC (Flint *et al.* 1993)), *ilvD* from *Citrobacter sp*. 30_2 (96% identity), *ilvD* from *Pectobacterium carotovorum* subsp. WPP14 (90% identity), and *ilvD* from *Xenorhabdus nematophila* ATCC 19061 (87% identity). Also, *ilvD* from *Bacillus subtilis* NRRL B-14911, which showed 47% identity was selected as reference for [2Fe-2S] ISC containing DHAD. Furthermore, Ilv3 from *S. cerevisiae* was predicted to contain [2Fe-2S] ISC with an identity of 36% compared to *ilvD* from *E. coli*. Then, the codon optimised synthetic genes from the above-mentioned bacteria were cloned into the $pRS62_N$ vector for constitutive expression in *S. cerevisiae* (Table 28).

As demonstrated in Figure 3, the targeting-complex of the CIA machinery composed of Met18, Cia1, and Cia2 is responsible for the transfer of cytosolic [4Fe-4S] ISC into apo-proteins, e.g., Leu1. For some apo-proteins, an adapter-complex (e.g., Lto1-Yea1) is necessary to link the targeting-complex with the

apo-protein (e.g., Ril1). In this case, Yea1 recruits Ril1 apo-protein for ISC insertion, while Lto1 is essential to bind the Cia2 protein of the targeting complex. It was shown that a C-terminal tryptophan of the Lto1 protein is mandatory to bind Cia2 (Lill *et al.* 2015). Thus, a tryptophan was fused to the C-terminus of the selected DHADs, to investigate whether the affinity towards the CIA targeting-complex was increased, like in the case for Lto1. Additionally, the C-terminal amino acids (KVHQDW) of isopropylmalate isomerase (Leu1) were also fused to the C-terminus of the selected DHAD. Leu1 is the most abundant cytosolic ISC protein of *S. cerevisiae* and is involved in the biosynthesis of leucine (Ihrig *et al.* 2010). Leu1 is known to interact with the CIA targeting-complex (Srinivasan *et al.* 2007) and contains a C-terminal tryptophan (W). The above selected DHAD from bacteria were cloned as isoforms with a C-terminal tryptophane (W) or KVHQDW into $pRS62_N$ for constitutive expression. Additionally, IlvD2 from *Neurospora crassa* and *ilvD* from *Corynebacterium glutamicum* were included in the studies because both enzymes are known to be active in *S. cerevisiae (Altmiller and Wagner 1970; Dundon et al. 2009).* An overview of constructed plasmids expressing DHAD isoforms from selected organism is given in Table 28.

Table 28 This table summarises the different DHAD and C-terminal isoforms expressed from pRS62$_N$ vector. The table shows the vectors name and the organisms from which the DHAD sequence was isolated, the gene name (ISC if known), respective abbreviation as well as the C-terminal modification. Results of the vectors being expressed in IsoY10 on SCD and SCD$_{-valine}$ are summarised in Figure 11.

Vector Name	Organism	Abbreviation	Gene (ISC)	C-terminus
pWG046$_N$	*Neurospora crassa*	*Ncr_IlvD2*	*ILVD2^{co}*	Wilde type (wt)
MBV007$_N$				Tryptophane (W)
MBV008$_N$				KVHQDW (Leu1)
pWG044$_N$	*Corynebacterium glutamicum*	*Cglu_IlvD*	*ilvD*	Wilde type (wt)
MBV009$_N$				Tryptophane (W)
MBV010$_N$				KVHQDW (Leu1)
pWG017$_N$	*S. cerevisiae*	*ILV3Δ19*	*ILV3Δ19^{co}* ([2Fe-2S])	Wilde type (wt)
MBV011$_N$				Tryptophane (W)
MBV012$_N$				KVHQDW (Leu1)
MBV030$_N$	*Bacillus subtilis sp NRRL B-14911*	*Bsub_IlvD*	*ilvD^{co}* ([2Fe-2S])	Wilde type (wt)
MBV031$_N$				Tryptophane (W)
MBV032$_N$				KVHQDW (Leu1)
MBV033$_N$	*Citrobacter sp. 30_2*	*Cspe_IlvD*	*ilvD^{co}* ([4Fe-4S])	Wilde type (wt)
MBV034$_N$				Tryptophane (W)
MBV035$_N$				KVHQDW (Leu1)
MBV036$_N$	*Pectobacterium carotovorum subsp. WPP14*	*Pcar_IlvD*	*ilvD^{co}* ([4Fe-4S])	Wilde type (wt)
MBV037$_N$				Tryptophane (W)
MBV038$_N$				KVHQDW (Leu1)
MBV039$_N$	*Xenorhabdus nematophila ATCC 19061*	*Xnem_IlvD*	*ilvD^{co}* ([4Fe-4S])	Wilde type (wt)
MBV040$_N$				Tryptophane (W)
MBV041$_N$				KVHQDW (Leu1)
MBV024$_N$	*E. coli str. K-12*	*Ecol_IlvD*	*ilvD^{co}* ([4Fe-4S])	Wilde type (wt)
MBV042$_N$				Tryptophane (W)
MBV043$_N$				KVHQDW (Leu1)

All plasmids listed in Table 28 as well as vector control and pWG015 bearing an *ILV3* gene, were transformed into IsoY10 (CEN.PK2-1C Δ*ilv3*). Growth assays were conducted on solid SCD and SCD$_{-valine}$ mediums to assess *ilv3* complementation by the DHAD isoforms. The results are summarised in Figure 11.

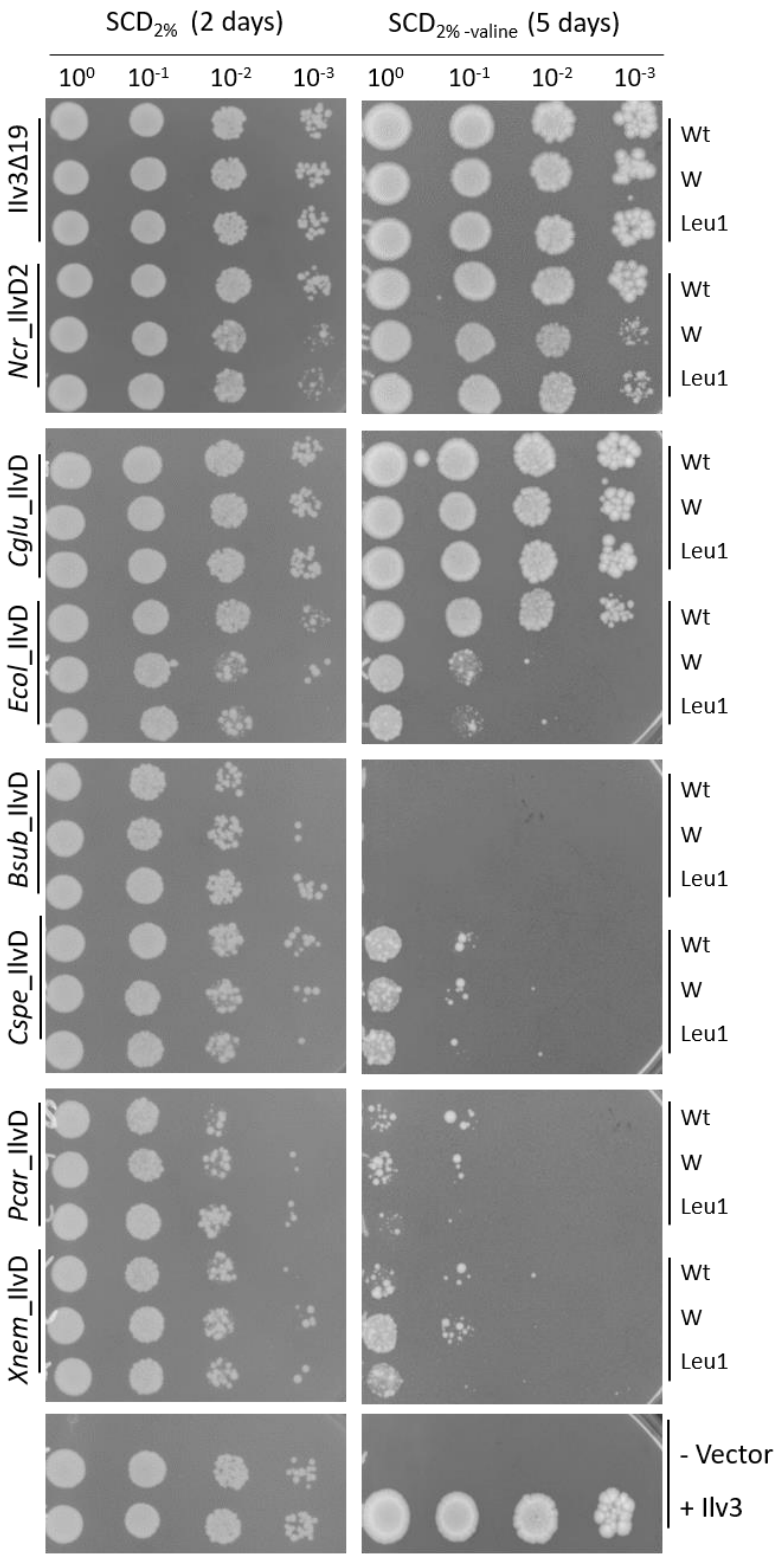

Figure 11 Growth assay to assess complementation of valine auxotrophy in IsoY10 by DHAD and isoforms from various organisms. IsoY10 (CEN.PK2-1C Δ*ilv3*) was transformed with plasmids expressing DHAD as wildtype (Wt), fused with C-terminal tryptophane (W) or KVHQDW (Leu1) from the following organisms: *S. cerevisiae* (Ilv3Δ19), *Neurospora crassa* (*Ncr_IlvD2*), *Corynebacterium glutamicum* (*Cglu_IlvD*), *E. coli str.* K-12 (*Ecol_IlvD*), *Bacillus subtilis sp* NRRL B-14911 (*Bsub_IlvD*), *Citrobacter sp*. 30_2 (*Cspe_IlvD*), *Pectobacterium carotovorum subsp.* WPP14 (*Pcar_IlvD*), and *Xenorhabdus nematophila ATCC 19061* (*Xnem_IlvD*). Additionally, IsoY10 was transformed with a plasmid expressing Ilv3 ($pWG015_N$) and vector as control. For an overview of respective plasmid see Table 28. The transformants were plated on solid SCD and $SCD_{-valine}$ mediums containing ClonNAT as section marker. 10^0 represents OD_{600} of 1 and was used for further serial dilution of 10^{-1}, 10^{-2} and 10^{-3}. The image was recorded after two days of incubation at 30°C for SCD and after five days for $SCD_{-valine}$.

Figure 11 shows that heterologous expression of DHADs (Table 28) did not cause negative growth phenotype in IsoY10 on the solid SCD medium. All transformants tested grew comparably to the control. However, difference in growth phenotype was observed on the selection medium. After five days of incubation on $SCD_{-valine}$, comparable growth with the Ilv3 control was observed through the expression of *Ncr*_IlvD2, *Cglu_ilvD* and Ilv3Δ19. However, no difference between the C-terminal isoforms was observed. A similar growth phenotype was also mediated by the expression of *Ecol_IlvD* (wt), but it was heterogeneous and deficient in the C-terminal isoforms (W and Leu1). Expression of *Cspe_IlvD*, *Pcar_IlvD*, and *Xnem_IlvD* did complement *ilv3* deletion in IsoY10, but were not as good as expressions of Ilv3Δ19. No effect was observed by the expression of the C-terminal isoforms (W and Leu1) of *Cspe_IlvD*, *Pcar_IlvD*, and *Xnem_IlvD.* Expression of all three [2Fe-2S] ISC containing DHAD isoforms from *Bsub_IlvD* did not complement *ilv3* deletion of IsoY10, even after five days of incubation on $SCD_{-valine}$.

The results showed that none of the tested DHAD enabled IsoY10 for better growth on $SCD_{-valine}$ than Ilv3Δ19, independent of the C-terminal isoforms or the ISC composition. However, DHAD from *N. crassa* and *C. glutamicum* showed similar *in vivo* activity as Ilv3Δ19, making them interesting candidates for cytosolic isobutanol production.

4.1.3.2. Establishing of a Cytosolic CIA Independent ISC Assembly Mechanism by Expression of Grx Proteins

Instead of replacing Ilv3Δ19 by a [4Fe-4S] ISC enzyme, it is also possible to achieve sufficient [2Fe-2S] ISC apo-protein maturation in a CIA independent manner. Natively, Grx5 facilitates [2Fe-2S] ISC integration into mitochondrial apo-proteins, for e.g., Ilv3 (Uzarska *et al.* 2013; Lill *et al.* 2015). Hence, truncated cytosolic isoform Grx5Δ29 was expressed in *S. cerevisiae* to assess if [2Fe-2S] ISC incorporation in Ilv3Δ19 apo-protein by a CIA machinery independent manner is possible (Rodríguez-Manzaneque *et al.* 2002). Furthermore, it has been shown that a *grx5* deletion can be complemented by mitochondrial expression of cytosolic Grx3 or Grx4 (Molina *et al.* 2004; Molina-Navarro *et al.* 2006).This indicates that Grx3 and Grx4 are also able to assemble a [2Fe-2S] ISC, independent of the CIA machinery, in a non-canonical way (Mühlenhoff *et al.* 2010). Therefore, Grx3 or Grx4 were also constitutively expressed in *S. cerevisiae* to assess if [2Fe-2S] ISC incorporation in Ilv3Δ19 apo-protein by a CIA machinery independent manner is possible.

Thus, *GRX3*, *GRX4*, *GRX5* and *GRX5Δ29* were cloned into pRS62$_N$ (further referred to as MBV044$_N$, MBV045$_N$, MBV046$_N$ and MBV048$_N$, respectively). Each of the plasmids and vectors were then transformed in combination with a plasmid bearing the cyt-ILV genes (IsoV100$_K$) into IsoY08 (CEN.PK2-1C Δ*ilv2*). SCD$_{-valine}$ was then fermented in an aerobic shake flask cultivation by the transformants at 30°C and 180 rpm. The results are summarised in Figure 12.

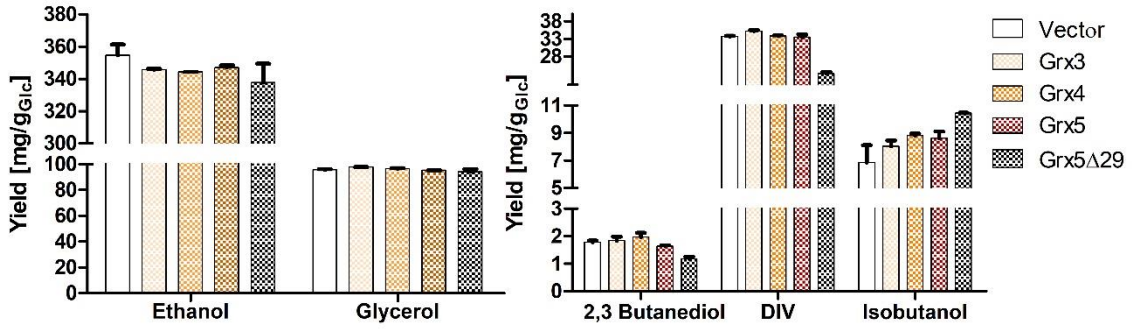

Figure 12 Yields of ethanol, glycerol, 2,3-butanediol, DIV and isobutanol after aerobic fermentation of SCD$_{-valine}$ by IsoY08 constitutive expressing the cyt-ILV genes, varying Grx proteins. IsoY08 (CEN.PK2-1C *Δilv2*) was transformed with a plasmid bearing cyt-ILV genes (IsoV100$_K$) and a plasmid expressing Grx3 (MBV044$_N$), Grx4 (MBV045$_N$), Grx5 (MBV046$_N$) and Grx5Δ29 (MBV048$_N$), respectively. SCD$_{-valine}$ was fermented in aerobic shake flask cultivation at 30°C (OD_{600} of 8) by the transformants in duplicates with ClonNat and Geneticin added as selection marker. Yields were calculated after 24 h, when glucose was fully consumed.

As shown in Figure 12, the expression of *Grx3-5* resulted in a lower ethanol yield which decreased from 355 mg/g$_{Glc}$ in the control to 338-347 mg/g$_{Glc}$ for Grx3-5 expressing transformants. However, glycerol yield was almost unaffected by Grx-protein expression. Glycerol yields ranged from 94-98 mg/g$_{Glc}$ for all transformants tested, including the control. By the expression of Grx5Δ29, the yields of 2,3-butanediol and DIV decreased. Control fermentation yielded 1.8 mg/g$_{Glc}$ of 2,3-butanediol and 34 mg/g$_{Glc}$ of DIV. Expression of Grx5Δ29 reduced the yields to 1.2 mg/g$_{Glc}$ and 23 mg/g$_{Glc}$, respectively. However, expression of the Grx3-5 resulted in an increase of isobutanol yields. The control's isobutanol yield was 6.9 mg/g$_{Glc}$, and increased to 8.0 mg/g$_{Glc}$ by expression of Grx3, to 8.8 mg/g$_{Glc}$ by Grx4, to 8.6 mg/g$_{Glc}$ by Grx5 and to 11 mg/g$_{Glc}$ by Grx5Δ29, corresponding to an increase of isobutanol of up to 52%.

4.1.3.3. Improved Cytosolic X-S Availability by Deletion of Protease Pim1

Mitochondrial ISC assembly is initiated by the scaffold protein Isu1, which is in complex with for e.g., Nfs1, as sulphur donor, and Jac1 as the Hsp70 chaperone that mediates cluster transfer from Isu1 to Grx5. However, this initial complex is post

translationally regulated by degradation of Isu1 through the Lon-type protease Pim1. If Isu1 is in complex with the chaperones, Isu1 is protected from degradation by Pim1, resulting in an increase of mitochondrial and cytosolic ISC assembly. It was seen that constitutive expression of Nfs1 and Jac1 increased ISC availability in *S. cerevisiae* by protecting Isu1 from degradation (Ciesielski *et al.* 2016). In the following, instead of expressing the chaperons Nfs1 and Jac1, the *pim1* gene was deleted in CEN.PK113-7D *ilv2* to prevent Isu1 degradation (further referred to as MBY19). This was done with the aim to increase the availability of the X-S substrate, which is necessary for cytosolic ISC assembly *via* the CIA machinery (Lill *et al.* 2014). To assess the impact of *pim1* deletion with respect to cytosolic isobutanol biosynthesis, MBY19 (CEN.PK113-7D Δ*ilv2* Δ*pim1)* and MBY25 (CEN.PK113 7D Δ*ilv2*) were transformed with a plasmid bearing the cyt-ILV genes (IsoV100$_K$). The Aerobic shake flask cultivation was performed with transformants in SCD$_{-valine}$. The results are summarised in Figure 13.

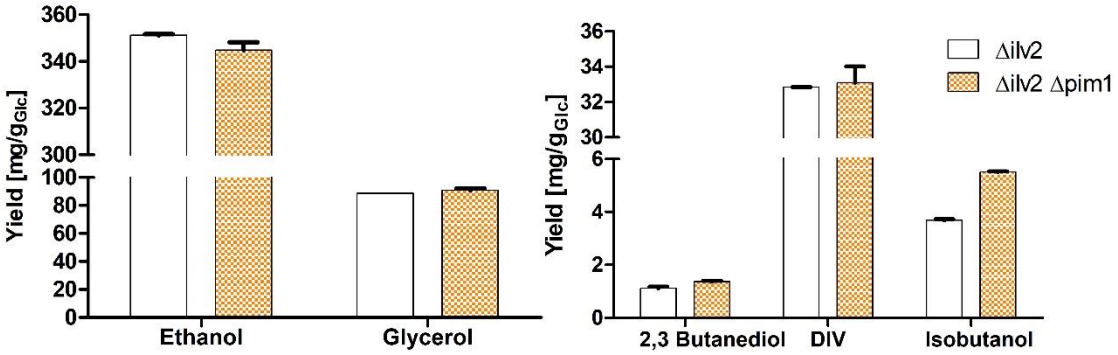

Figure 13 Yields of ethanol, glycerol, 2,3-butanediol, DIV and isobutanol after aerobic fermentation of SCD$_{-valine}$ by MBY25 and MBY19 constitutive expressing the cytosolic ILV genes. MBY25 (CEN.PK113-7D *Δilv2)* and MBY19 (CEN.PK113-7D *Δilv2, Δpim1)* were transformed with a plasmid bearing cyt-ILV genes (IsoV100$_K$). SCD$_{-valine}$ was fermented in aerobic shake flask cultivation at 30°C (OD$_{600}$ of8) by the transformants in duplicates with Geneticin added as selection marker. Yields were calculated after 48 h, when glucose was fully consumed.

As shown in Figure 13, deletion of Δ*pim1* in MBY19 affected ethanol yield only slightly, reducing the yield from 351 mg/g$_{Glc}$ in Δ*ilv2* control (MBY25) to 345 mg/g$_{Glc}$. Glycerol yield remained almost unchanged at 89 mg/g$_{Glc}$ in the control fermentation, and 91 mg/g$_{Glc}$ in Δ*pim1*. The intermediates of valine synthesis, namely 2,3-butanediol and DIV, also increased slightly. The 2,3-butanediol yield only slightly increased from 1.1 mg/g$_{Glc}$ in Δ*ilv2* control to 1.4 mg/g$_{Glc}$ by additional Δ*pim1* deletion. Almost no difference in DIV yield was observed for control and additional Δ*pim1* deletion at 33 mg/g$_{Glc}$ each. In contrast, the increase in isobutanol yield was evident,

which increased from 3.7 mg/g_{Glc} in control to 5.5 mg/g_{Glc} by additional Δ*pim1* deletion, which corresponded to an increase of 49%.

4.1.3.4. Improved Cytosolic Iron Availability by Deletion of the Regulatory Protein Fra2

Iron homeostasis in *S. cerevisiae* is regulated by the iron sensing proteins Fra1 and Fra2, as well as Grx3 and Grx4. The Fra- and Grx-proteins conjugate either in an ISC-independent or ISC-dependent manner. The Fra-Grx complex which binds in an ISC-independent manner is unable to enter the nucleus and thus cannot repress the genes responsible for iron-uptake. The [2Fe-2S] ISC-dependent Fra-Grx cluster, on the contrary, is translocated to the nucleus where the Fra proteins then bind to transcriptional factors Aft1 and Aft2 (which are bound to target DNA). The [2Fe–2S] ISC is then transferred from the Fra-complex to the Aft-complex, which releases Aft from the target DNA. Consequently, transcription of the Aft-regulated genes, including iron-uptake regulon, is repressed, causing a reduced iron uptake of *S. cerevisiae*. By the deletion of Grx3/4 or Fra2, iron accumulates within the microorganism (Kumánovics *et al.* 2008; Outten and Albetel 2013; Martínez-Pastor *et al.* 2017; Chi *et al.* 2018). However, the Grx proteins that transiently bind glutathione have an anti-oxidative effect, and protect the cells from reactive oxygen species (Pujol-Carrion *et al.* 2006). Furthermore, it is found in the literature that glutathione is essential for cytosolic ISC biogenesis, and therefore for cytosolic ISC apo-protein maturation (Sipos *et al.* 2002). Thus, Fra2 was the preferable genetic target for deletion to increased cytosolic Fe-content. Salusjärvi *et al.* (2017) were able to enhance the activity of ISC containing *xylD* by the deletion of *fra2* in *S. cerevisiae*. To assess the impact of *fra2* deletion with respect to cytosolic isobutanol biosynthesis in *S. cerevisiae*, *fra2* was deleted in combination with *ilv2* in CEN.PK113-7D (further to referred as MBY52). MBY52 and control MBY25 (CEN.PK113-7D Δ*ilv2*) were then transformed with a plasmid bearing the cyt-ILV genes ($IsoV100_K$). The aerobic shake flask cultivation was performed with transformants in $SCD_{-valine}$. The results are summarised in Figure 14.

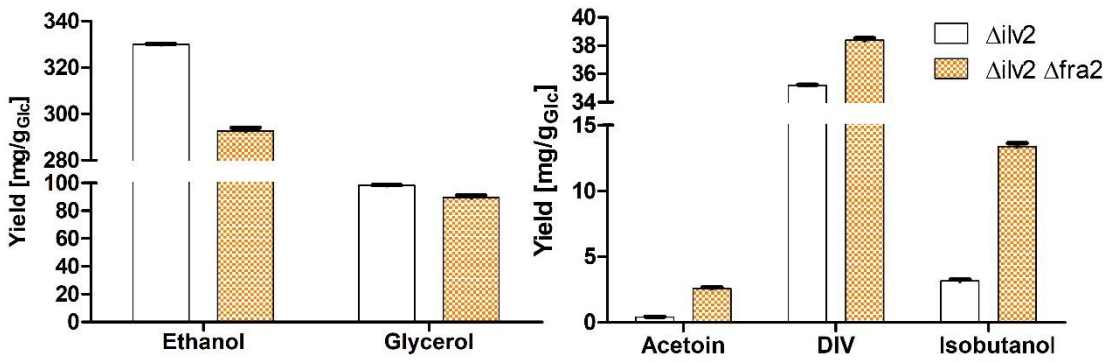

Figure 14 Yields of ethanol, glycerol, acetoin, DIV and isobutanol after aerobic fermentation of SCD$_{\text{-valine}}$ by MBY25 and MBY52 constitutive expressing the cyt-ILV genes. MBY25 (CEN.PK113-7D *Δilv2*) and MBY52 (CEN.PK113-7D *Δilv2, Δfra2*) were transformed with a plasmid bearing cyt-LV genes (IsoV100$_K$). SCD$_{\text{-valine}}$ was fermented in aerobic shake flask cultivation at 30 C (OD$_{600}$ of 8) by the transformants in duplicates with Geneticin added as selection marker. Yields were calculated after 24 h, when at glucose was fully consumed.

As shown in Figure 14, deletion of Δ*fra2* (MBY52) decreased ethanol yield from 330 mg/g$_{Glc}$ in Δ*ilv2* control (MBY25) to 293 mg/g$_{Glc}$. Glycerol yield also decreased from 98 mg/g$_{Glc}$ in the control to 90 mg/g$_{Glc}$, by additional Δ*fra2* deletion. The intermediates acetoin and DIV were increased due to the Δ*fra2* deletion. The acetoin yield increased from 0.4 mg/g$_{Glc}$ in control to 2.6 mg/g$_{Glc}$. Only a slight increase was observed for DIV yield, with 35 mg/g$_{Glc}$ in control to 38 mg/g$_{Glc}$, by additional Δ*fra2* deletion. The isobutanol yield increased from 3.2 mg/g$_{Glc}$ in control to 13.3 mg/g$_{Glc}$ in Δ*fra2*, which corresponded to an increase of 316%.

4.2. Evolutionary Engineering of *S. cerevisiae* to Increase Valine Production by Applying Selection Pressure with Norvaline

Besides rational metabolic engineering, which requires detailed knowledge about genes, proteins and enzymes involved in the metabolic pathway, evolutionary engineering can also be used to overcome existing bottlenecks. During evolutionary engineering, microbial evolution is simulated by applying a selection pressure to the organisms. Thus, only limited knowledge about the metabolic pathway is necessary, since random mutations manifest in the genome autonomously, if beneficial for the organism's fitness. The organisms that are fit to evolve beneficially can outperform competing mutants, and therefore accumulate in the fermentation broth. The challenge is then to isolate and identify the desirable mutation(s) from the evolved organisms (referred to as reverse engineering) to implement those mutation(s) into a production strain, through rational metabolic engineering. Several evolutionary engineering experiments have already been conducted successfully in various organisms (Shepelin *et al.* 2018). Evolutionary engineering was conducted by

applying selection pressure, like insufficient redox balance in the metabolic pathway (with this strategy L-lactic acid production in *E. coli* was improved (Fong *et al.* 2005)). Another approach was to apply oxidative stress, which led to increased antioxidant carotenoid production in yeast (Reyes *et al.* 2014).

One more example of successful evolutionary engineering is the increased isobutanol production in *E. coli* by supplementing norvaline in the fermentation broth (Liao 2011). Norvaline is an amino acid analogue of valine and is loaded to the tRNA by corresponding aminoacyl-tRNA synthetases, like valine, and thus is incorporated into the protein during translation. Due to the different structure of norvaline, incorporation may lead to non-functional enzymes and proteins, which can affect the viability of the organism. Thus, addition of norvaline to the fermentation broth creates a selection pressure that evolves *E. coli* towards improved valine production. In the evolved *E. coli*, the ratio of valine to norvaline shifted towards valine, and therefore increased the viability of the organism. Since KIV is a joint precursor of valine and isobutanol, increased valine production may also result in increased isobutanol synthesis. However, evolutionary engineering by using norvaline to improve valine production requires norvaline to be toxic for *S. cerevisiae*. Therefore, prototrophic CEN.PK113-7D was inoculated in duplicates to a concentration of 0.05 OD_{600} in $SCD_{-valine}$ containing 0 g/l, 5 g/l and 10 g/l DL-norvaline. Cells were then incubated at 30°C at 180 rpm for 24 h (Figure 15, grey bars).

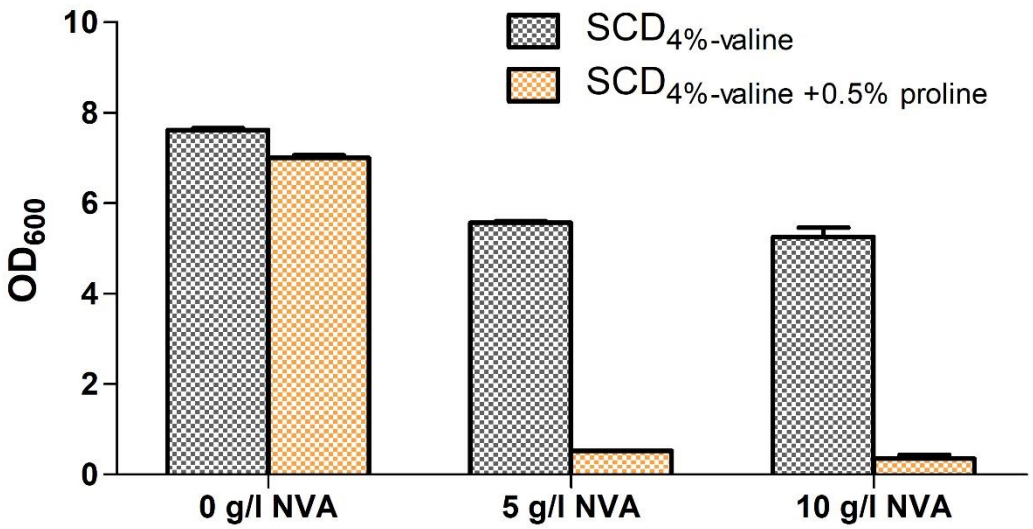

Figure 15 Growth test of CEN.PK113-7D in $SCD_{-valine}$ (grey) and $SCD_{-valine+0.5\%\ proline}$ (orange) with DL-norvaline (NVA) being added in different concentrations. Cultivation medium was inoculated with CEN.PK113-7D to an OD_{600} of 0.05 and incubated at 30°C with 180 rpm for 24 h, before OD_{600} was determined. Cultivation medium was $SCD_{-valine}$ or $SCD_{-valine}$ with 0.5% ammonium sulphate being replaced by 0.5% proline at pH of 5.3 ($SCD_{-valine+0.5\%\ proline}$). Both cultivation media were supplemented with 0 g/l, 5 g/l and 10 g/l DL-norvaline, respectively.

As shown in Figure 15, growth of *S. cerevisiae* was only slightly inhibited by the addition of 5 g/l or 10 g/l DL-norvaline. After 24 h, the control without norvaline grew to an OD_{600} of 7.62, whereas growth was inhibited by the addition of 5 g/l and 10 g/l DL-norvaline to an OD_{600} of 5.57 and 5.25, respectively. To investigate whether the poor toxicity of DL-norvaline was caused by poor uptake, the cultivation medium composition was adapted. It is known from the literature that yeast growing on a poor nitrogen source like proline, induce the general amino acid permease gene (*GAP1)* which allows *S cerevisiae* to take up a broad range of amino acids and related compounds (Magasanik and Kaiser 2002; Kingsbury *et al.* 2004). Therefore, the nitrogen source (0.5% ammonium sulphate) used in $SCD_{-valine}$ was substituted by L-proline, and pH was adapted from pH 6.3 to pH 5.3. This was done, because the isoelectric point of L-proline is 6.3, which leads to a poor solubility of the latter at pH 6.3. Prototrophic CEN.PK113-7D was inoculated to a concentration of 0.05 OD_{600} in $SCD_{-valine + 0.5\% proline}$ with 0 g/l, 5 g/l and 10 g/l DL-norvaline being added. Cells were then incubated at 30°C at 180 rpm for 24 h (Figure 15, orange bars). The growth of *S. cerevisiae* was significantly inhibited by the addition of DL-norvaline to $SCD_{-valine + 0.5\% proline}$. After 24 h, the control without DL-norvaline grew to an OD_{600} of 7.00, whereas growth was inhibited by the addition of 5 g/l and 10 g/l DL-norvaline to an OD_{600} of 0.52 and 0.35, respectively. Since toxicity of DL-norvaline towards *S. cerevisiae* was given under these conditions, the evolutionary engineering was conducted, as described, in the following. The integrative MBV057 vector was digested with *PmeI* restriction endonuclease and used as donor DNA to integrate the isobutanol cassette into *ILV2* of CEN.PK113-7D, by using CRISPR/Cas9. The resulting CEN.PK113-7D *ilv2*Δ::cyt-ILV_*ilvC*^{6E6}+EP strain (further to referred as MBY29) was then used for evolutionary engineering after the correct integration was verified. CEN.PK113-7D control and MBY29 were inoculated to an OD_{600} of 0.2 in $SCD_{-valine}$ preculture, and grown in an aerobic shake flask cultivation in duplicates. The precultures were continuously measured by the cell growth quantifier (Bruder *et al.* 2016) at 30°C and 180 rpm (Figure 16).

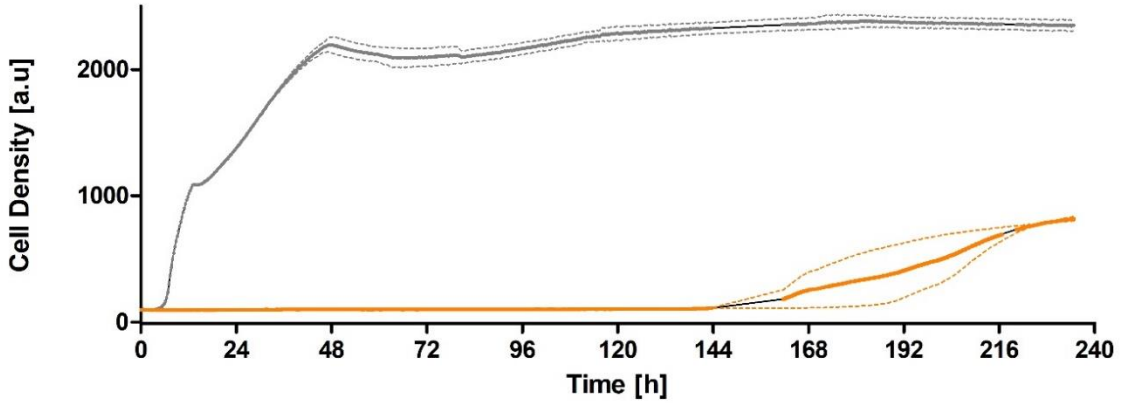

Figure 16 Growth test of precultures´(duplicates) for evolutionary engineering of CEN.PK113-7D (grey) and MBY29 (orange) in SCD$_{-valine}$ continuously measured by the Cell Growth Quantifier. Cultivation was started with OD_{600} of 0.2 at 30°C with 180 rpm in aerobic shake flasks.

As it can be seen from Figure 16, MBY29 demonstrated a reduced growth phenotype in SCD$_{-valine}$ compared to CEN.PK113-7D control. Log-phase of MBY29 was about 140 h, while it was only 12 h for control. After reaching the stationary growth phase, the cell density of MBY29 was lower at about 810 a.u. (corresponding to an OD_{600} of 4.2) compared to 2350 a.u. (corresponding to an OD_{600} of 8.1) for control. The MBY29 duplicate precultures were then pooled and used for evolutionary engineering in a DL-norvaline selection medium. SCD$_{-valine\ +0.5\%\ proline}$ medium was supplemented with 10 g/l DL-norvaline (further referred to as SCD$_{norvaline}$) and 0 g/l DL-norvaline for control cultivation. Both media were inoculated in triplicates with pooled MBY29 culture to an OD_{600} of 0.2, and grown at 30°C and 180 rpm in an aerobic shake flask cultivation. The OD_{600} was measured every 24 h and, if needed, freshly prepared SCD$_{norvaline}$ was re-inoculated to an OD_{600} of 0.1 with the evolved culture. The re-inoculation procedure ensured continuous evolutionary engineering cultivation by preventing MBY29 from reaching the stationary growth phase. The results of the evolutionary engineering are summarised in Figure 17.

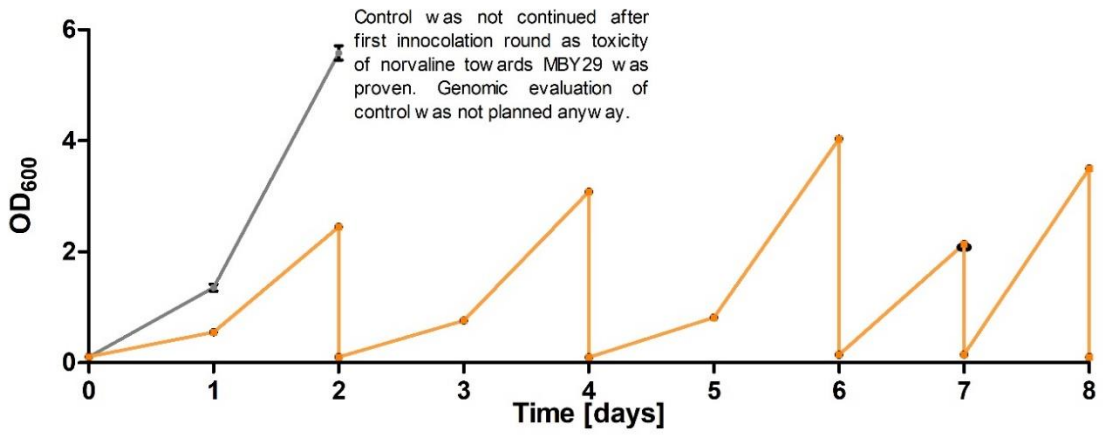

Figure 17 Evolutionary engineering of MBY29 in SCD$_{\text{-valine + 0.5\% proline}}$ with 0 g/l (grey) and 10 g/l (orange) DL-norvaline added. Both media were inoculated in triplicates with pooled MBY29 culture to an OD_{600} of 0.2 and grown at 30°C and 180 rpm in aerobic shake flask cultivation. OD_{600} was measured every 24 h and if needed freshly prepared SCD$_{\text{-valine+0.5\% proline}}$ with 10 g/l norvaline was re-inoculated to an OD_{600} of 0.2 again with the evolved culture. Control fermentation with 0 g/l norvaline was stopped after two days when reaching the stationary phase.

Figure 17 shows that the growth of MBY29 in the medium without DL-norvaline exceeded the growth of MBY29 in SCD$_{\text{norvaline}}$. However, the log-phase of MBY29 grown in SCD$_{\text{-valine + 0.5\% proline}}$ (about 24 h) was already shorter, such as during pre-cultivation in SCD$_{\text{-valine}}$ (Figure 16 about 140 h). After two days, the MBY29 triplicates grew to an OD_{600} of 2.5 in SCD$_{\text{norvaline}}$ and were re-inoculated to an OD_{600} of 0.1. Since the growth of the triplicates was very comparable, only mean OD_{600} values are discussed in the following sections. Again, two days later, at day four, the MBY29 triplicates grew to an OD_{600} of 3.1 and were re-inoculated. At day six, MBY29 triplicates already had grown to an OD_{600} of 4.0, which already demonstrated improved growth of MBY29 in SCD$_{\text{norvaline}}$ selection medium. From day six on, the triplicates were re-inoculated on a daily basis. Re-inoculation at day seven was performed on the triplicates having an OD_{600} of 2.1. The evolutionary engineering experiment was stopped after eight days at OD_{600} of 3.5, since the evolved cells now already showed better growth performance in SCD$_{\text{norvaline}}$ as the MBY29 control did in SCD$_{\text{-valine+0.5\% proline}}$ with 0 g/l DL-norvaline, in the first two days (compare Figure 17, grey line). The evolved triplicates (MBY29.NVA-1 to 3) were then inoculated in SCD$_{\text{-valine}}$ to assess whether improved growth performance was permitted by increased valine production or rather by improved DL-norvaline resistance through DL-norvaline degradation. Growth of MBY29.NVA-1 to 3 and unevolved MBY29 were continuously measured by using the cell growth quantifier (Bruder *et al.* 2016).

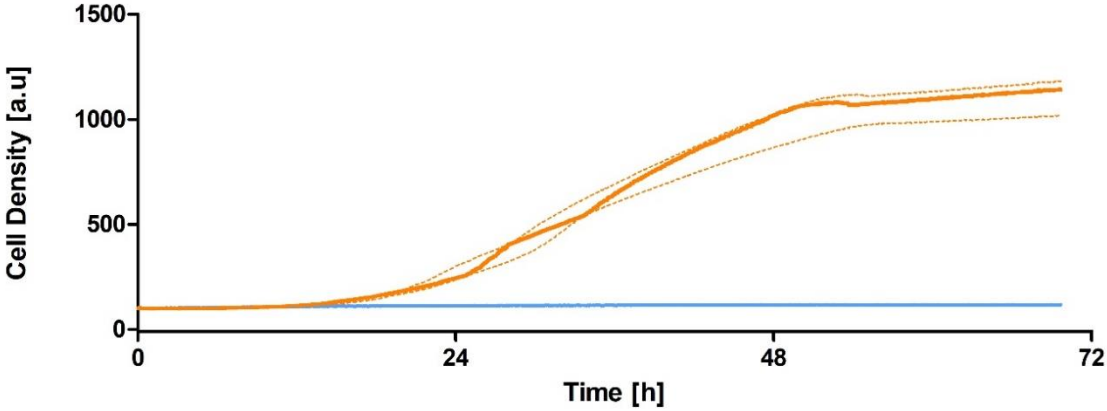

Figure 18 Growth test of evolved triplicates MBY29.NVA-1 to -3 (orange) and MBY29 (blue) in SCD$_{\text{-valine}}$ continuously measured by the Cell Growth Quantifier. Cultivation was started with OD_{600} of 0.2 at 30°C with 180 rpm in aerobic shake flasks.

Figure 18 demonstrates that the evolved MBY29.NVA-1 to 3 cultures grew after a log-phase of about 12 h, and reached stationary phase at about 48 h, while unevolved MY29 did not grow even after 72 h (also compare Figure 16). This result indicates that beneficial growth of evolved MBY29 strains result from increased valine production. To confirm that the beneficial growth phenotype was rather stable and no effect of medium adaptation was seen, three single colonies were isolated from each evolved culture (MBY29.NVA-1-3.1-3, nine in total), respectively. These isolated single colonies were then grown in a YEPD liquid medium and prepared as glycerol stock for permanent storage at -80°C. After storage of more than one week, stocks of the isolated single colonies were then plated exemplarily on solid SCD$_{\text{-valine}}$ and YEPD mediums; the prototrophic CEN.PK113-7D and unevolved MBY29 served as control (Figure 19 shows growth of MBY29.NVA-1.1-3 exemplarily).

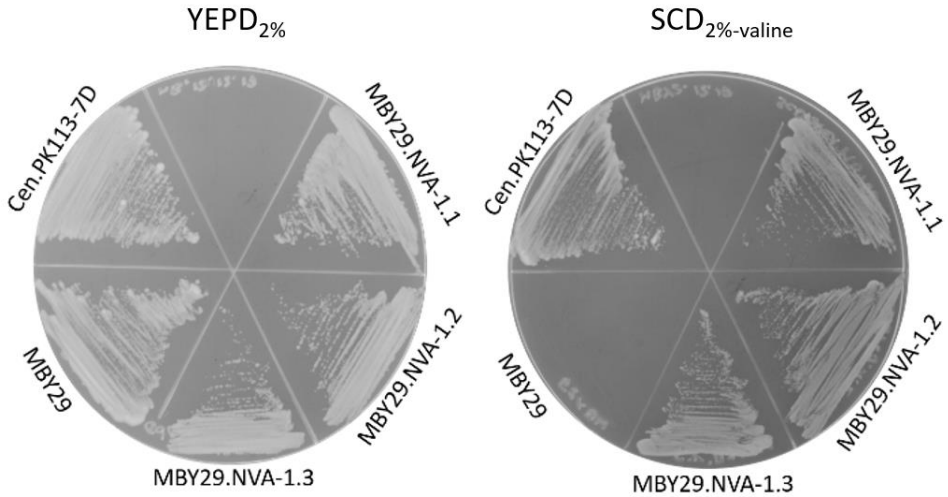

Figure 19 Growth test to assess if evolved and isolated colonies kept beneficial growth phenotypes on SCD$_{\text{-valine}}$. Evolved and isolated MBY29.NVA-1.1, MBY29.NVA-1.2, MBY29.NVA-1.3, unevolved MBY29 and prototrophic CEN.PK113-7D were plated from glycerol stock on solid YEPD and SCD$_{\text{-valine}}$ mediums. The image was recorded after two days of incubation at 30°C.

Figure 19 shows that all strains were able to grow on YEPD, compared to CEN.PK113-7D, without any growth phenotype being observed. However, evolved and isolated colonies MBY29.NVA-1.1-3 sustained the ability to grow compared to CEN.PK113-7D on $SCD_{-valine}$, while MBY29 did not grow after incubation for two days. The nine evolved and isolated colonies MBY29.NVA-1-3.1-3 (further to referred as MBY36-44, respectively) and unevolved MBY29 control were then grown in $SCD_{-valine}$ liquid medium, and continuously measured using the cell growth quantifier (Figure 20).

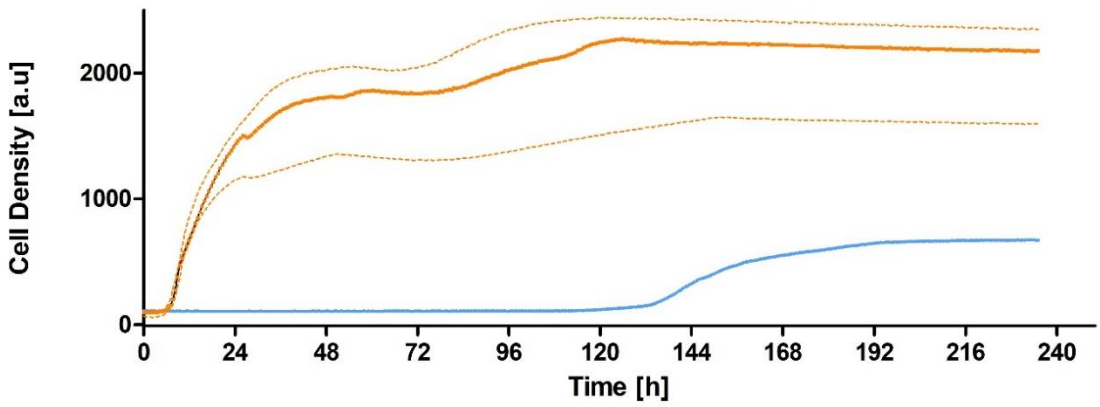

Figure 20 Growth of evolved and isolated colonies MBY36-44 (orange) and MBY29 (blue) in $SCD_{-valine}$ continuously measured by the Cell Growth Quantifier. Cultivation was started with OD_{600} of 0.2 at 30°C with 180 rpm in aerobic shake flasks.

As it can be seen in Figure 20, evolved and isolated strains kept the improved growth phenotype in $SCD_{-valine}$ liquid medium, too. Only a short log-phase of less than 12 h was observed. For the MBY29 control, the log-phase was about 130 h, which is comparable to the log-phase that was observed during the initial pre-culture experiment (compare Figure 16). However, the stationary phase for evolved cells was reached between 24 h and 48 h, depending on the individual strain. This reflects broader growth phenotype variations of the individual colonies, as compared to the evolved culture (compare Figure 18). To evaluate the isobutanol production, fermentation of $SCD_{-valine}$ was performed with MBY36, MBY39, MBY41 and MBY42 exemplarily. These strains were selected to cover the full range of the growth variation, observed in Figure 20. The results are summarised in Figure 21.

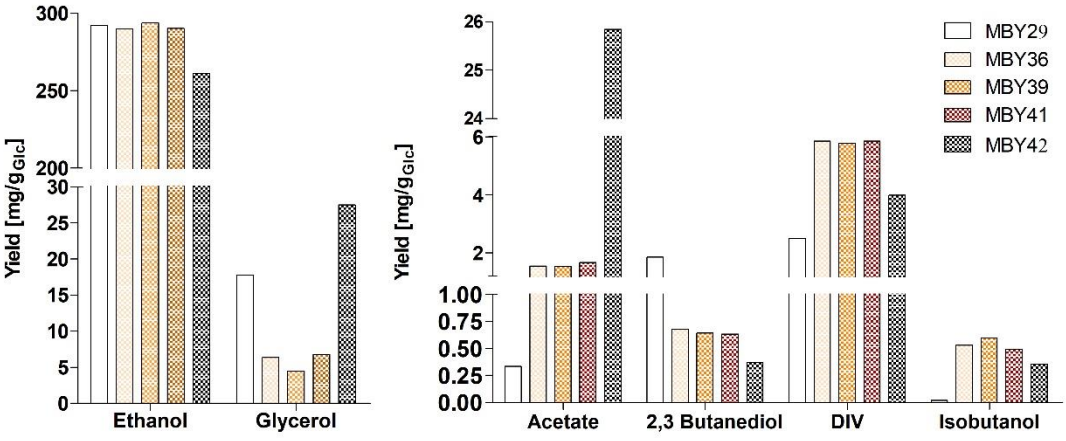

Figure 21 Yields of ethanol, glycerol, acetate, 2,3-butanediol, DIV and isobutanol after aerobic fermentation of $SCD_{-valine}$ by unevolved MBY29 and evolved and isolated MBY36, MBY39, MBY41 and MBY42. $SCD_{-valine}$ was fermented in aerobic shake flask cultivation at 30°C (OD_{600} of 8) by the above-mentioned strains. Yields were calculated after 72 h, when glucose was fully consumed (except for MBY29, for which only 30% of glucose was consumed).

As shown in Figure 21, ethanol yield of 292 mg/g_{Glc} in MBY29 decreased for evolved strain MBY42 to 261 mg/g_{Glc}, but remained at a comparable yield for MBY36, MBY39 and MBY41. In general, it was observed that monitored metabolites were similar for MBY36-41, but not for MBY42. Glycerol yield decreased from 18 mg/g_{Glc} for MBY29 to 4.0-7.2 mg/g_{Glc} for MBY36-41, and increased to 28 mg/g_{Glc} for MBY42. Acetate production was lowest for MBY29 at 0.3 mg/g_{Glc}, and increased to 1.5-1.7 mg/g_{Glc} for MBY36-41, and further increased to 26 mg/g_{Glc} for MBY42. The competing metabolite 2,3-butanediol decreased from 20 mg/g_{Glc} for MBY29 to 0.6-0.7 mg/g_{Glc} for MBY36-41, and was lowest at 0.4 mg/g_{Glc} for MBY42. The DIV yield increased from 2.5 mg/g_{Glc} for MBY29 to 5.8-5.9 mg/g_{Glc} for MBY36-41, and to 4.0 mg/g_{Glc} for MBY42. The isobutanol yield increased from 0.02 mg/g_{Glc} for MBY29 to 0.5-0.6 mg/g_{Glc} for MBY36-41, and 0.4 mg/g_{Glc} for MBY42.

Summarising, the evolutionary engineering of MBY29 was performed successfully with respect to the growth phenotype and isobutanol production. However, overall isobutanol yield in evolved strains expressing cyt-ILV genes genomically remained lower (0.6 mg/g_{Glc}) than when expressing cyt-ILV genes from a multicopy vector, such as $IsoV100_K$ (e.g., 3.2 mg/g_{Glc} in Figure 14).

4.2.1. Reverse Engineering of Evolved and Isolated MBY36, MBY39 and MBY42

To identify beneficial mutations, genomes of unevolved MBY29 and evolved strains of MBY36, MBY39, MBY42 were sequenced and evaluated for differences (Section 3.8.3). The differences were expressed as single nucleotide polymorphisms (SNPs) or alterations of the DNA by, for instance, deletions, insertions (InDels), etc. Due to the high number of mutations found in MBY36, MBY39 or MBY42, rules were defined to identify the most promising candidates. The mutations were selected according to the criteria described as follows. Only mutations which were detected on gene fragments that passed the parameter of “quality-control” were considered, indicating that computational alignment results can be considered as effective (sequencing procedure was not validated). In addition, the mutation had to be within an ORF and was not allowed to be a silent mutation. Since the initial growth phenotype of all isolated yeast strains was very comparable (compare Figure 20, first 24 h), it was assumed that beneficial mutations were fixed early in the evolutionary experiment, possibly already in the pre-culture (compare Figure 16, e.g., 144 h). Therefore, only mutations that were found in MBY36, MBY39 and MBY42, but not in MBY29, were considered. Filtering the sequencing data by the criteria described above, eight InDels in six genes (Table 29) and 39 SNps in 31 genes (Table 30) were found.

Table 29 List of altered genome regions (InDels) that were identified in evolved strains MBY36, MBY39 and MBY42. Altered genome regions were identified by filtering the genomic data according to the following criteria. I) Only altered regions that were found in all three evolved strains MBY36, MBY39 or MBY42, but not in MBY29, were selected. II) The fragment of interest met the parameter "passed quality-control", indicating that alignment results can be considered as valid. III) The mutation had to be within an ORF and was not allowed to be a silent mutation. Mutations highlighted in bold were selected for reverse engineering experiments.

Chrom. No.	Position of Mutation	Change	Systematic Gene name	Standard gene name	Plasmid name
I	224711	Codon change + deletion	YAR070C.1	-	-
I	224768				-
I	224772	Frame Shift			-
VII	**449281**	**Frame Shift**	**YGL025C.1**	**PGD1**	**MBV093**
VIII	66850	Frame Shift	YHL020C.1	OPI1	-
VIII	556908	Frame Shift	YHR217C.1	TEL08R	-
X	**531111**	**Frame Shift**	**YJR051W.1**	**OSM1**	**MBV092**
XIII	279147	Frame Shift	YMR006C.1	PLB2	-

Table 30 List of SNPs that were identified in evolved strains MBY36, MBY39 and MBY42. SNPs were identified by filtering the genomic data according to the following criteria. I) Only SNPs that were found in all three evolved strains MBY36, MBY39 or MBY42, but not in MBY29, were selected. II) The fragment of interest met the parameter "quality-control", indicating that alignment results can be considered valid. III) The mutation had to be within an ORF and was not allowed to be a silent mutation. Mutations highlighted in bold were selected for reverse engineering experiments.

Chrom. No.	Position of Mutation	Amino acid change	Systematic Gene name	Standard gene name	Plasmid name
I	24659	V1104I	YAL063C.1	*FLO9*	-
I	24814	A1052V			-
I	24826	T1048I			-
I	25070	G967S			-
I	27188	P261S			-
II	148349	S381G	YBL037W.1	*APL3*	-
III	316100	T30I	YCR108C.1	*TEL03R*	-
IV	1523586	V113D	YDR542W.1	*PAU10*	-
IV	1524740	R65H	YDR543C.1	*TEL04R*	-
V	571862	T128I	YER190W.1	*YRF1-2/ TEL05R*	-
VI	130421	G30S	YFL005W.1	*SEC4*	-
VI	178096	G883E	YFR016C.1	*YFR016C*	-
VII	346630	C64R	YGL087C.2	*MMS2*	-
VII	**893155**	**Y329S**	**YGR197C.1**	***SNG1***	**MBV094**
VIII	**20899**	**L25M**	**YHL040C.1**	***ARN1***	**MBV085**
VIII	432234	G1572D	YHR165C.1	*PRP8*	-
VIII	540668	M40I	YHR213W-A.1	-	-
VIII	541011	R71H	YHR213W-B.1	-	-
XI	264229	T294R	YKL094W.1	*YJU3*	
XI	**507478**	**S194L**	**YKR034W.1**	***DAL80***	**MBV088**
XI	541868	K2020E	YKR054C.1	*DYN1*	-
XII	**89634**	**I338F**	**YLL026W.1**	***HSP104***	**MBV091**
XIII	688288	S258N	YMR210W.1	*MGL2*	-
XIII	**792936**	**R145I**	**YMR261C.1**	***TPS3***	**MBV095**
XIII	908174	V271L	YMR317W.1	-	-
XIII	908175	V271A			-
XIII	908177	I272V			-
XIII	908179	I272M			-
XIII	908196	W278S			-
XIV	**629768**	**T432A**	**YNR001C.1**	***CIT1***	**MBV087**
XV	**165773**	**K20N**	**YOL083W.1**	***ATG34***	**MBV086**
XV	300865	L59S	YOL013W-B.1	*Ty1 LTR*	-
XV	**403134**	**R752K**	**YOR038C.1**	***HIR2***	**MBV090**
XV	**410939**	**Q24***	**YOR043W.1**	***WHI2***	**MBV096**
XV	794798	R179C	YOR245C.1	*DGA1*	-
XV	**924487**	**N185T**	**YOR324C.1**	***FRT1***	**MBV089**
XVI	13304	G351A	YPL279C.1	*FEX2*	-
XVI	83486	M237I	YPL247C.1	-	-
XVI	256277	I164K	YPL156C.1	*PRM4*	-

Due to the still high number of genes, only some were selected for the reverse engineering (indicated in bold in Table 29 and Table 30). Genes were PCR amplified from the evolved strain MBY36. However, here it was noticed during sequencing that both, mutations and wild type sequence of the respective genes, were observed. Thus, it was assumed that gene duplication occurred during evolutionary engineering. As a consequence, if the beneficial growth is attributed to one of the selected mutations, the mutation had to be dominant, since the wild type allele was still present. Therefore, the MBY36 amplified mutations were cloned into the low copy vector $pRS41_H$ (MBV085-96), instead of genomically integrating the mutation in MBY29. The vector $pRS41_H$ is controlled by an autonomously replicating sequence (ARS) in combination with a yeast centromere (CEN). Due to the low copy number of $pRS41_H$, protein expression from low copy vector $pRS41_H$ mimics genomic integration better than expression from a $pRS62_N$ multi copy vector. The respective ORFs of the plasmids MBV085-96 were sequenced to verify correct amplification.

The transformants were then incubated at 30°C on solid YEPD and $SCD_{-valine}$ mediums as well as liquid mediums with Hygromycin B as a selection marker, for several days. None of the transformants, except the MBY36 control, were capable of growing on the selection medium. Growth on the YEPD medium was unaffected in all transformants (data not shown). Consequently, no mutation responsible for improved growth phenotype of MBY36 on $SCD_{-valine}$ was identified using the reverse engineering approach, as described above.

4.3. Rational Engineering of *S. cerevisiae* to Avoid Intermediate Leakage into Competing Pathways during Isobutanol Production

During biosynthesis of isobutanol from glucose, various intermediates such as dihydroxyacetonphosphat (DHAP), pyruvate, ALAC, KIV or isobutyraldehyde serve as substrates for competing metabolic pathways. It is known that ethanol is the main fermentative product of *S. cerevisiae* under anaerobic conditions, or when glucose is available in high concentrations (Crabtree effect). Therefore, it is crucial to prevent ethanol formation from pyruvate since it is a joint precursor of isobutanol. Thus, genes for enzymes that link competing pathways with the abovementioned intermediates of the isobutanol biosynthesis were deleted sequentially in CEN.PK113-7D (summarised in Figure 22 and Table 31). The results of this chapter were achieved in collaboration with Dr Joahnnes Wess and have been published by Wess *et al.*

2019. The main achievement of the strain engineering work is briefly summarised in the following.

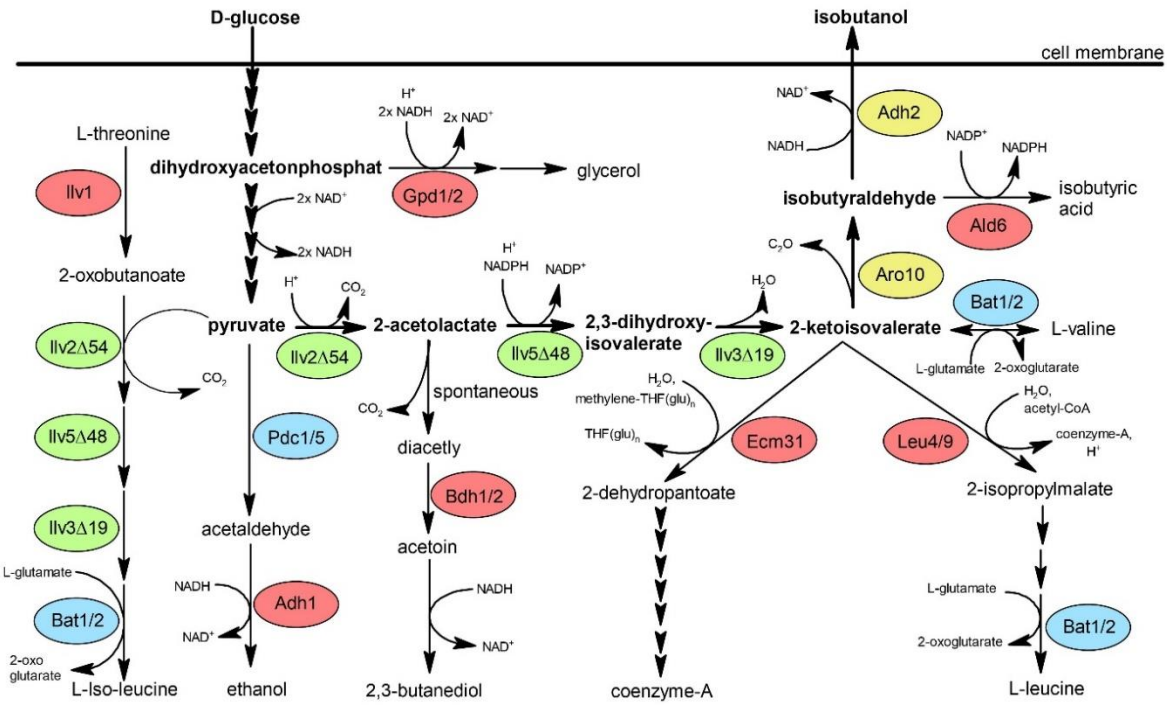

Figure 22 Schematic illustration of the cytosolic isobutanol pathway from glucose to isobutanol. The cyt-ILV enzymes involved in the *de novo* biosynthesis of valine are highlighted in green. Enzymes involved in the Ehrlich pathway are highlighted in yellow. Enzymes linking intermediates (highlighted with bold letters) of isobutanol biosynthesis to competing metabolic pathways are highlighted in red and blue. Red indicates that a deletion of this gene further improved isobutanol production, blue indicates that a deletion of this gene did not improve isobutanol production. For more information see Wess *et al.* (2019).

Table 31 summarises the constructed deletion mutants with improved isobutanol biosynthesis performance (for a full list of strains constructed in the framework of this project, see Wess *et al.* 2019).

Table 31 Deletion mutants, originating from CEN.PK113-7D, which were created to improve isobutanol production by disturbing metabolic flux of intermediates towards competing pathways. This table only contains deletion mutants with improved isobutanol biosynthesis performance. For a full list of all strains constructed in the framework of this project, see Wess *et al.* (2019).

Strain	Genetic Modifications
JWY00	*Δilv2*
JWY01	*Δilv2; Δbdh1; Δbdh2*
JWY02	*Δilv2; Δbdh1; Δbdh2; Δleu4; Δleu9*
JWY03	*Δilv2; Δbdh1; Δbdh2; Δleu4; Δleu9; Δecm31*
JWY04	*Δilv2; Δbdh1; Δbdh2; Δleu4; Δleu9; Δecm31; Δilv1*
JWY16	*Δilv2; Δbdh1; Δbdh2; Δleu4; Δleu9; Δecm31; Δilv1; adh1*
JWY19	*Δilv2; Δbdh1; Δbdh2; Δleu4; Δleu9; Δecm31; Δilv1; adh1; Δgpd1; Δgpd2*
JWY23	*Δilv2; Δbdh1; Δbdh2; Δleu4; Δleu9; Δecm31; Δilv1; adh1; Δgpd1; Δgpd2; Δald6*

Deletion mutants shown in Table 31 were transformed with plasmid expressing cyt-ILV genes ($IsoV100_K$). Subsequently, aerobic shake flask fermentation of $SCD_{-valine}$ was performed at 30°C and 180 rpm until glucose was fully consumed, or

remained at a stable concentration. Obtained isobutanol yields are summarised in Figure 23.

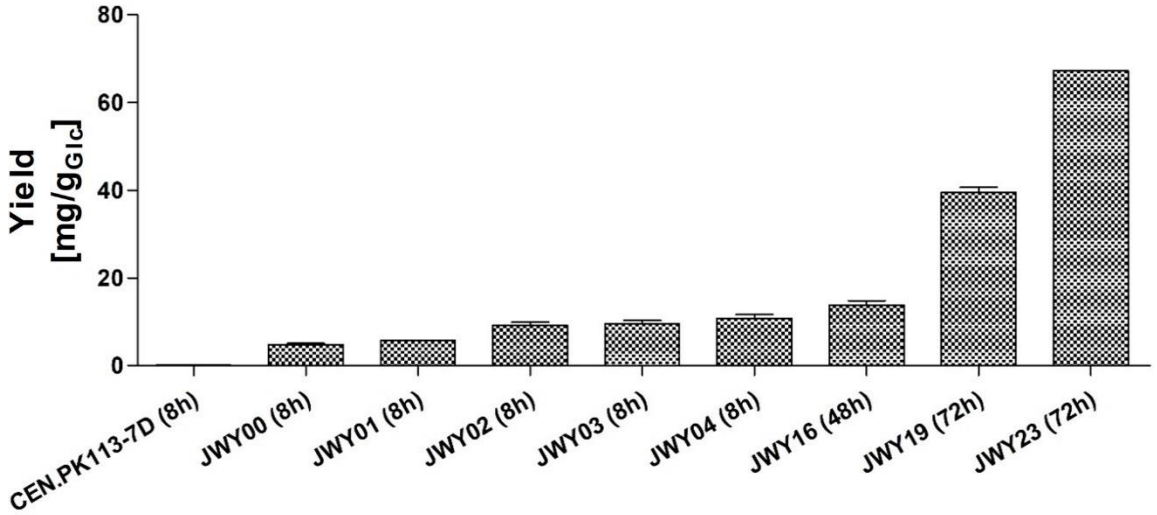

Figure 23 Isobutanol Yields after aerobic shake flask fermentation of SCD$_{-valine}$ by CEN.PK113-7D deletion mutants constitutive expressing the cyt-ILV genes (IsoV100$_K$). All deletion strains (for details about genomic modifications see Table 31) were transformed with a plasmid expressing cyt-ILV genes (IsoV100$_K$). SCD$_{-valine}$ was fermented in aerobic shake flask cultivation at 30°C (OD_{600} of 8) by the transformants in (at least) duplicates with Geneticin added as selection marker. Yields were calculated after the duration of fermentation that is indicated in the brackets. Calculation was based on fermentation data published in Wess *et al.* (2019).

As shown in Figure 23, a successive improvement of isobutanol yield was achieved by cumulative deletion of the genes summarised in Table 31 and Figure 23. CEN.PK113-7D produced 0.1 mg/g_{Glc} isobutanol. Deletion of *ilv2* (JWY00) increased the yield to 4.8 mg/g_{Glc}. The importance of *ilv2* deletion for cytosolic isobutanol production has been already discussed and published by Brat *et al.* (2012). In the following, the improvement of isobutanol production will be reported in average yields but also expressed in terms of relative improvement (in %), compared to the isobutanol yield of JWY00. Further deletion of *bdh1* and *bdh2* in JWY00 (resulting in JWY01) which connect 2,3-butanediol biosynthesis with ALAC increased the isobutanol yield by 20% to 5.7 mg/g_{Glc}. Further deletion of *leu4* and *leu9* (JWY02), which connect leucine biosynthesis to KIV, and additional deletion of *ecm31* (JWY03) that connects coenzyme-A biosynthesis with KIV, increased the yield by 94% (9.3 mg/g_{Glc}) and 101% (9.6 mg/g_{Glc}), respectively. Further deletion of *ilv1* (JWY04), which initiates pyruvate consuming isoleucine biosynthesis, increased the yield by 127% (10.8 mg/g_{Glc}). By additional deletion of *adh1* (JWY16) that converts acetaldehyde to ethanol, the isobutanol yield was increased by 190% (13.8 mg/g_{Glc}). Further deletions of *gpd1* and *gdp2* (JWY19), which connect glycerol biosynthesis on the level of DHAP with glycolysis, increased isobutanol yield by 729% (39.5 mg/g_{Glc}).

The last beneficial deletion was *ald6* (JWY23), which connects isobutyric acid biosynthesis with the joint precursor isobutyraldehyde. Fermentation with JWY23 increased isobutanol yield to 67.3 mg/g_{Glc} after 72 h of fermentation, correlating to an increase of 1312% compared to JWY00.

4.3.1. Additional Expression of Each Enzyme Involved in Isobutanol Production to Identify Existing Bottlenecks

To identify existing bottlenecks in a metabolic pathway, individual expression of the enzymes involved in this pathway can be performed to assess the impact on production of certain metabolites. This allows to evaluate which enzyme of a metabolic pathway lacks sufficient activity in the tested strain background. For this purpose, JWY16, the best isobutanol producer at the time, was transformed with a cyt-ILV genes expressing plasmid ($IsoV100_K$) and a plasmid bearing the gene for expression of Ilv2Δ54 ($MBV058_N$), *ilvC*^{6E6} ($MBV059_N$), Ilv3Δ19 ($MBV060_N$), Aro10 ($MBV061_N$) or Adh2 ($MBV062_N$). Enzymes of the glycolysis were not investigated as it was not expected to identify an existing bottleneck in the main fermentative pathway of *S. cerevisiae.* Since it was shown previously (Section 4.1.1) that high isobutanol production did not correlate with good growth phenotypes, the effect of enzyme expression was investigated with respect to both, growth and fermentative properties (Figure 24 and Figure 25). Aerobic shake flask fermentation of $SCD_{-valine}$ was performed at 30°C and 180 rpm until glucose was fully consumed or remained at a stable concentration. The results are summarised in Figure 24.

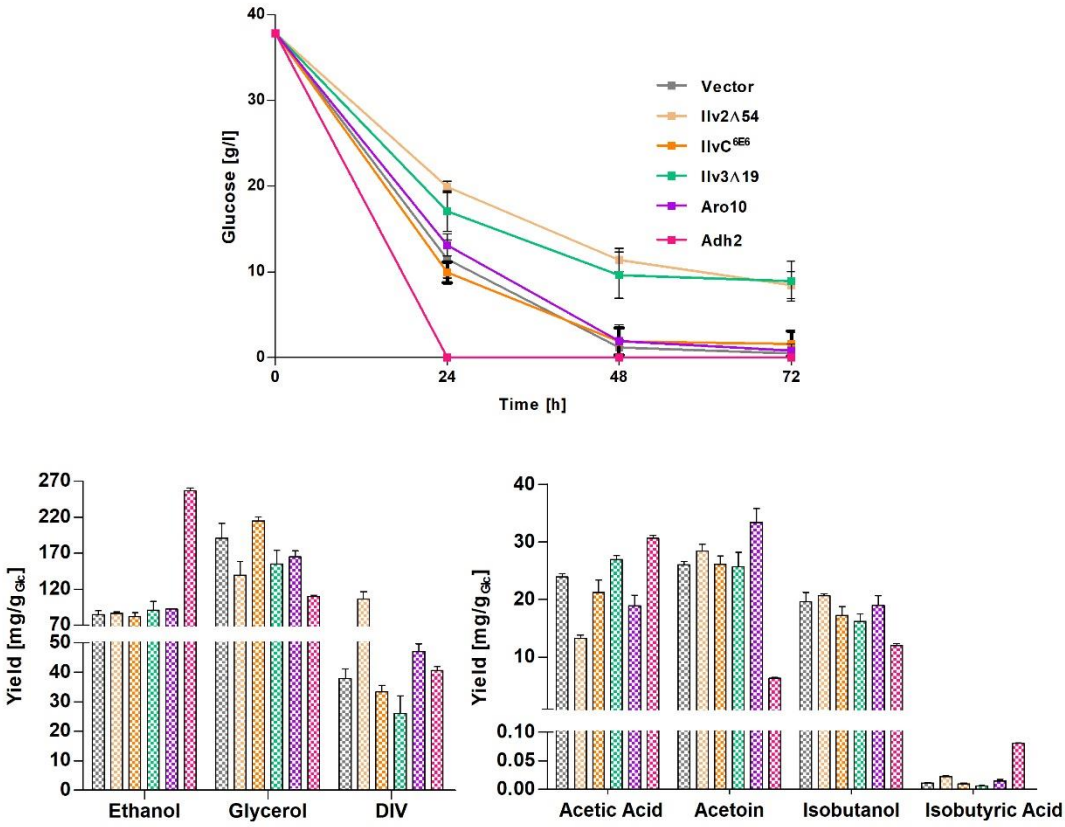

Figure 24 Glucose consumption and yields of ethanol, glycerol, acetoin, DIV and isobutanol after aerobic fermentation of SCD$_{\text{-valine}}$ by JWY16 constitutive expressing the cyt-ILV genes, varying genes of the isobutanol synthesis pathway downstream of pyruvate. JWY16 (*Δilv2; Δbdh1; Δbdh2; Δleu4; Δleu9; Δecm31; Δilv1; Δadh1*) was transformed with a plasmid bearing cyt-ILV genes (IsoV100$_K$) and a plasmid expressing Ilv2Δ54 (MBV058$_N$), *ilvC*^{6E6} (MBV059$_N$), Ilv3Δ19 (MBV060$_N$), Aro10 (MBV061$_N$), Adh2 (MBV062$_N$), or vector, respectively. SCD$_{\text{-valine}}$ was fermented in aerobic shake flask cultivation at 30°C (OD$_{600}$ of 8) by the transformants in duplicates with ClonNat and Geneticin added as selection marker. Yields were calculated after 24 h, when glucose was fully consumed or remained at a constant concentration.

As shown in Figure 24, supplemented glucose (40 g/l) was completely consumed after 24 h by the Adh2 expressing transformant only. Almost full glucose consumption was observed after 48 h for the control, *ilvC*^{6E6}, and Aro10 expressing transformants. Ilv2Δ54 and Ilv3Δ19 expressing transformants did not fully consume the glucose after 72 h but rather stagnated at 8.4 g/l and 8.9 g/l, respectively.

In the following, the most remarkable differences in yields that are shown in Figure 24 are summarised. Ethanol production was observed between 82 mg/g$_{Glc}$ and 93 mg/g$_{Glc}$ for Ilv2Δ54, *ilvC*^{6E6}, Ilv3Δ19 and Aro10 expressing transformants, comparable to the yields of the control (85 mg/g$_{Glc}$). However, ethanol formation was increased to 257 mg/g$_{Glc}$ by expression of Adh2, indicating the complementation of the *adh1* deletion by Adh2 expression. Acetic acid yield of the control was 24 mg/g$_{Glc}$ and was reduced to 13 mg/g$_{Glc}$ in the Ilv2Δ54 expressing transformant and increased to 31 mg/g$_{Glc}$ in the Adh2 expressing transformant. Glycerol formation of the control

was 191 mg/g_{Glc} and was only exceeded to 215 mg/g_{Glc} by the *ilvC*^{6E6} expressing transformant. For other transformants tested, lower glycerol yields were observed, ranging from 110 mg/g_{Glc} to 166 mg/g_{Glc}. Almost no difference was observed when comparing the acetoin yield of the control (26 mg/g_{Glc}) with transformants expressing the cyt-ILV enzymes, in which acetoin yields ranged from 26 mg/g_{Glc} to 28 mg/g_{Glc}. However, by expression of the EP enzymes, acetoin yield was increased to 33 mg/g_{Glc} in Aro10 and reduced in Adh2 expressing transformants (6.3 mg/g_{Glc}). When comparing the DIV yields of control (38 mg/g_{Glc}) with Ilv2Δ54 expressing transformants, a threefold increase to 107 mg/g_{Glc} was observed. Expression of the enzymes *ilvC*^{6E6} and Ilv3Δ19 decreased the yield to 33 mg/g_{Glc} and 26 mg/g_{Glc}, respectively. However, expression of EP enzymes Aro10 and Adh2 increased DIV yields in both transformants to 47 mg/g_{Glc} and 41 mg/g_{Glc}, respectively. The isobutanol yield of the control (20 mg/g_{Glc}) was slightly exceeded by the Ilv2Δ54 expressing transformant at 21 mg/g_{Glc}. Expression of all other enzymes tested did not increase the isobutanol production. The corresponding isobutyric acid was produced only in low amounts of 0.01 mg/g_{Glc} in the control. This was comparable with the isobutyric acid yields of 0.01-0.02 mg/g_{Glc} observed by the expression of Ilv2Δ54, *ilvC*^{6E6}, Ilv3Δ16, and Aro10. However, in the Adh2 expressing transformation, the yield increased eightfold to 0.08 mg/g_{Glc}.

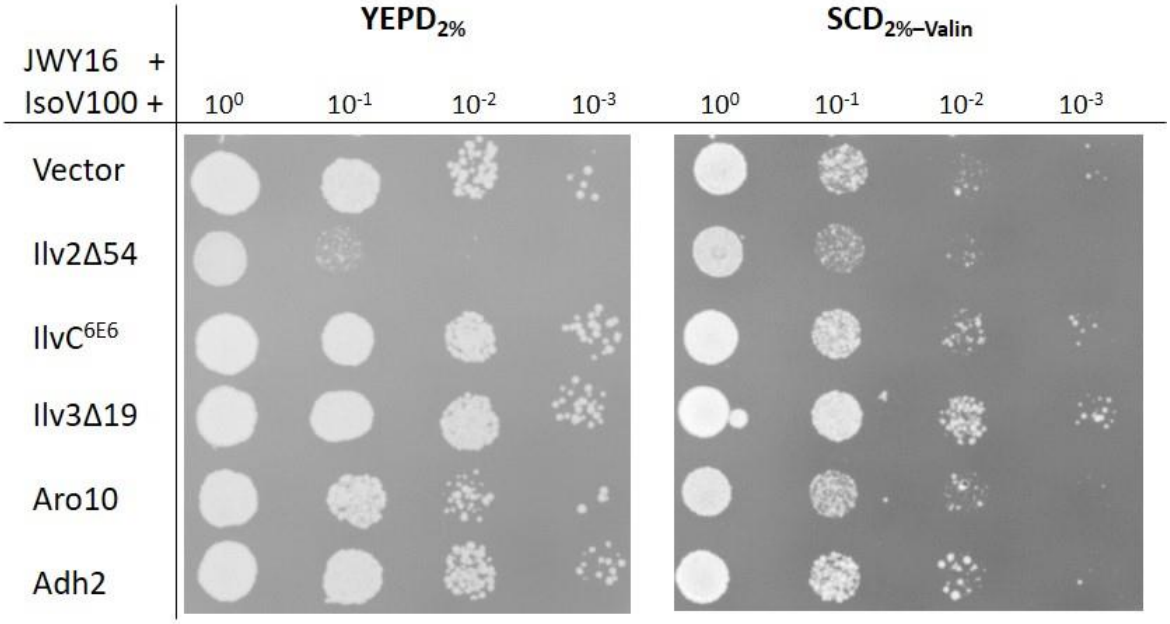

Figure 25 Growth assay of JWY16 expressing cyt-ILV genes, varying genes of the isobutanol synthesis pathway downstream of pyruvate. The serial dilution test was performed with JWY16 (Δ*ilv2; Δbdh1/2; Δleu4/9; Δecm31; Δilv1; Δadh1)* transformed with a plasmid bearing cyt-ILV genes ($IsoV100_K$) and a plasmid expressing Ilv2Δ54 ($MBV058_N$), *ilvC*^{6E6} ($MBV059_N$), Ilv3Δ19 ($MBV060_N$), Aro10 ($MBV061_N$), Adh2 ($MBV062_N$), or vector, respectively. The transformants were plated on YEPD and $SCD_{-valine}$ mediums containing ClonNAT as section marker, respectively. 10^0 represents OD_{600} of 1 and was used for further serial dilution of 10^{-1}, 10^{-2} and 10^{-3}. The image was recorded after four days of incubation at 30°C.

As shown in Figure 25, only the additional expression of Ilv2Δ54 resulted in a deficient growth phenotype on solid YEPD medium. For all other transformants tested, growth on solid YEPD medium was comparable to that of the control. On solid $SCD_{-valine}$ medium, heterogeneous growth was observed in all transformants tested, including control. The best growth phenotype was observed in transformants additionally expressing Adh2 or Ilv3Δ19.

The increased DIV secretion showed that Ilv2Δ54 activity on the one hand was still limiting isobutanol biosynthesis by insufficient competition about pyruvate, but on the other hand also caused the deficient growth phenotype. Furthermore, redox or co-factor imbalance did become increasingly limiting in JWY16, which was seen by the fact that the transformants were no longer able to fully consume glucose when no Adh2 was expressed. Enzymes of the EP still did not increase isobutanol production, indicating the catalytic bottlenecks to be with the *de novo* synthesis of valine.

4.4. Production of Isobutyric Acid in *S. cerevisiae*

As it is shown in Figure 22, isobutyric acid is an undesired side product during isobutanol production. However, isobutyric acid is also considered as a platform chemical which is utilised in many applications. It is, for example, used as a precursor for methyl methacrylic acid which is needed for the transparent thermoplastics, with an annual market size of up to 2.7 million tonnes. Another application in which isobutyric is utilised is the synthesis of sucrose acetic acid, a largely used emulsifier with an annual market volume of 100,000 tonnes (Petrognani *et al.* 2020; Zhang *et al.* 2011). Like isobutanol, also isobutyric acid is at present mainly derived from fossil resources, and therefore its replacement by a sustainable approach could contribute to solving the issues which are caused by the fossil industry.

In. *S. cerevisiae i*sobutyric acid is oxidised from isobutyric aldehyde by Ald6, which utilises $NADP^+$ that was previously oxidised by Ilv5Δ48. Regarding the NADP(H) co-factor, the isobutyric acid metabolic pathway is balanced. However, to establish isobutyric acid as a main fermentation pathway, two NADH molecules, which are reduced during glycolysis, must be recovered as well. To achieve NAD(H) co-factor balance during isobutyric acid production, a NADH oxidase (NOX) from *Streptococcus pneumoniae* found heterologous expression in *S. cerevisiae* (Shi *et al.* 2016). To identify an appropriate expression level, NOX was expressed

under the control of different promoters during isobutyric acid biosynthesis. In one transformant, NOX was expressed under the control of the strong *TPI1* promoter ($SBV85_H$ further to be referred as NOX_{high}) and in the other transformant, NOX was expressed under the control of the weaker *UBR2* promoter ($SBV89_H$ further referred to as NOX_{low}).

For this, JWY16 was transformed with plasmid expressing cyt-ILV genes ($IsoV100_K$), Ald6 ($MBV109_N$) and NOX expression plasmids $SBV85_H$ or $SBV89_H$. As control, JWY16 was transformed with $IsoV100_K$ and $MBV109_N$, $SBV85_H$ or $SBV89_H$ in combination with the corresponding vector. Aerobic shake flask fermentation of $SCD_{\text{-valine}}$ was performed at 30°C and 180 rpm until glucose was fully consumed or remained at a stable concentration. The results are summarised in Figure 26.

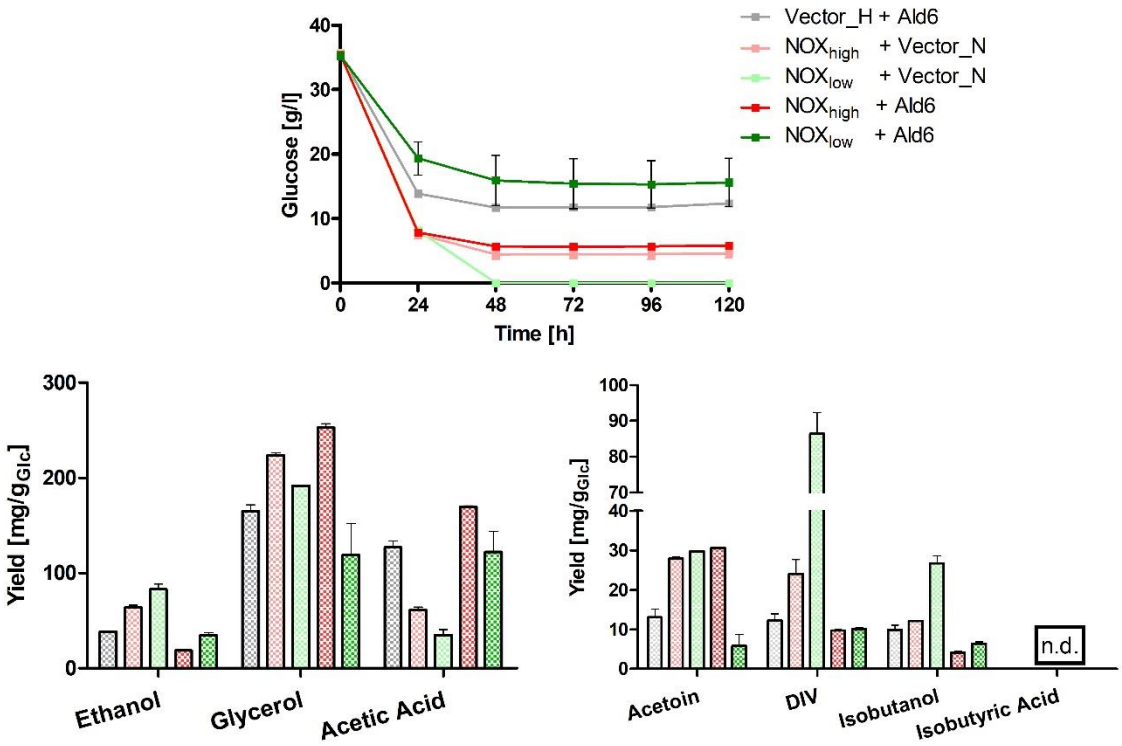

Figure 26 Glucose consumption as well as yields of ethanol, glycerol, acetic acid, acetoin, DIV, isobutanol and isobutyric acid after aerobic fermentation of $SCD_{\text{-valine}}$ by JWY16 constitutive expressing the cyt-ILV genes with varying Ald6 and NOX expression. JWY16 (*Δilv2; Δbdh1; Δbdh2; Δleu4; Δleu9; Δecm31; Δilv1; Δadh1*) was transformed with a plasmid expressing cyt-ILV genes ($IsoV100_K$) together with Ald6 ($MBV109_N$) and NOX expressed under the control of *TPI1* promotor ($SBV89_H$, red) or *UBR2* promotor ($SBV85_H$, dark green). As control JWY16 was transformed with $IsoV100_K$ together with vector and NOX expressed under the control of *TPI1* promotor ($SBV89_H$, orange) or *UBR2* promotor ($SBV85_H$, light green). Furthermore, JWY16 was transformed with $IsoV100_K$ together with vector and Ald6 ($MBV109_N$, grey). $SCD_{\text{-valine}}$ was fermented in aerobic shake flask cultivation at 30°C (OD_{600} of 8) by the transformants in duplicates with Geneticin, ClonNat and Hygromycin added as selection marker. Yields were calculated after 48 h, when glucose was fully consumed or remained at a stable concentration.

As shown in Figure 26, glucose was either fully consumed or remained at a constant concentration in all fermentations after 48 h. The transformant which solely expressed NOX_{low} was the only one able to fully utilise the complete 40 g/l of glucose. In fermentation with NOX_{high} expressing transformants, the glucose consumption stagnated at approximately 5 g/l, whether Ald6 was additionally expressed or not. When solely expressing Ald6, glucose consumption stagnated at approximately 12 g/l. The least glucose was consumed by a combined expression of Ald6 and NOX_{low}. In this fermentation, glucose consumption stagnated at approximately 16 g/l.

By comparing the ethanol yield, it was observed that the yield was higher when NOX was expressed solely (promoter-independent), rather than being expressed in combination with Ald6. Yields of transformants expressing NOX solely were between 64 mg/g_{Glc} and 83 mg/g_{Glc} for NOX_{high} and NOX_{low} expression, respectively. For transformants expressing Ald6 solely or in combination, ethanol yields were between 19-35 mg/g_{Glc}. Glycerol yields were higher in transformants expressing NOX_{high} than in those expressing NOX_{low}. This was observed regardless of whether NOX was expressed in combination with vector or Ald6. As it can be seen from Figure 26, expression of Ald6 was beneficial for the formation of acetic acid. Transformants solely expressing Ald6 achieved a yield of 127 mg/g_{Glc}. When NOX_{high} or NOX_{low} was co-expressed, acetic acid yields of 169 mg/g_{Glc} and 122 mg/g_{Glc} were observed, respectively. However, when solely NOX_{high} or NOX_{low} was expressed, the acetic acid yields decreased to 61 mg/g_{Glc} and 35 mg/g_{Glc}, respectively. While acetic acid production was observed, no isobutyric acid was detected in any of the fermentations. It is very unlikely that this was caused by an insufficient supply of the precursor isobutyraldehyde, since the competing product isobutanol (which originates from isobutyraldehyde), was observed in all transformants tested. The DIV yield was increased in transformants that only expressed NOX_{high} (24 mg/g_{Glc}) and NOX_{low} (86 mg/g_{Glc}) compared to the 10-12 mg/g_{Glc} observed in transformants additionally expressing Ald6. The same tendency was observed for isobutanol yield, which was increased for transformants solely expressing NOX_{high} (12 mg/g_{Glc}) and NOX_{low} (27 mg/g_{Glc}) compared to the 4-10 mg/g_{Glc} observed in transformants additionally expressing Ald6. Thus, it was seen that expression of NOX_{low} had a beneficial effect on isobutanol, but not on isobutyric acid production. Additional expression of Ald6 decreased isobutanol production, but also did not increase isobutyric acid production.

In Figure 24, isobutyric acid production was increased in JWY16 (Cen.PK113-7D *ilv2Δ; bdh1Δ; bdh2Δ; leu4Δ; leu9Δ; ecm31Δ; ilv1Δ; adh1Δ*) when Adh2, which complemented the *adh1* deletion, was expressed. This observation indicated that alcoholdehydrogenase activity is necessary for isobutyric acid production to occur. Therefore, the fermentation described in this chapter was repeated in the JWY04 strain background (Cen.PK113-7D *Δilv2; Δbdh1; Δbdh2; Δleu4; Δleu9; Δecm31; Δilv1)*. However, only NOX_{low} expression was investigated in this experiment, as results in Figure 26 indicate that the latter is more beneficial to pull the metabolic flux from acetic acid and glycerol towards DIV, which is required for isobutyric acid production.

JWY04 was transformed with the cyt-ILV genes expressing plasmid $IsoV100_K$ and NOX_{low} ($SBV89_H$) as well as Ald6 ($MBV109_N$) expressing plasmids. As a control, JWY04 was transformed with both vectors, and Ald6 ($MBV109_N$) or NOX_{low} ($SBV89_H$) expressing plasmid in combination with the respective vector. Aerobic shake flask fermentation of $SCD_{-valine}$ was performed at 30°C and 180 rpm until glucose was fully consumed or remained at a stable concentration. The results are summarised in Figure 27.

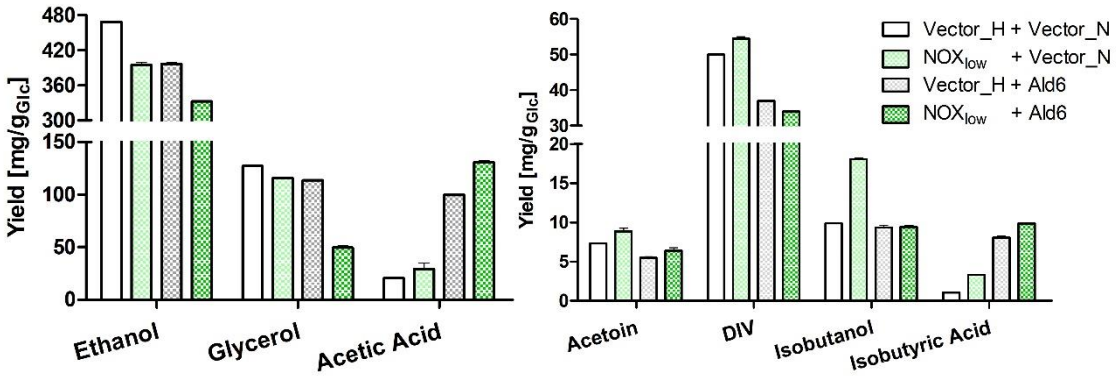

Figure 27 Yields of ethanol, glycerol, acetic acid, acetoin, DIV, isobutanol and isobutyric acid after aerobic fermentation of $SCD_{-valine}$ by JWY04 constitutive expressing the cyt-ILV genes with varying Ald6 and NOX expression. JWY04 (*Δilv2; Δbdh1; Δbdh2; Δleu4; Δleu9; Δecm31; Δilv1*) was transformed with a plasmid expressing the cyt-ILV genes ($IsoV100_K$) together with plasmids expressing Ald6 ($MBV109_N$) and NOX_{low} under the control of *UBR2* promotor ($SBV85_H$). As control JWY04 was transformed with $IsoV100_K$, together with both vectors, with Ald6 ($MBV109_N$) or NOX_{low} ($SBV85_H$) expressing plasmid. $SCD_{-valine}$ was fermented in aerobic shake flask cultivation at 30°C (OD_{600} of 8) by the transformants in duplicates with Geneticin, ClonNat and Hygromycin added as selection marker. Yields were calculated after 48 h, when about 70% of glucose was consumed.

As shown in Figure 27, a considerably higher ethanol yield was obtained in JWY04 transformants compared to the experiments with JWY16 (compare Figure 26). Ethanol yield was highest in the vector control with 469 mg/g_{Glc} and decreased to the

lowest yield of 333 mg/g_{Glc} by the combined expression of Ald6 and NOX_{low}. The same tendency was observed for glycerol yields. The highest yield was obtained in vector control with 127 mg/g_{Glc} and decreased to the lowest value of 49 mg/g_{Glc} by the combined expression of Ald6 and NOX_{low}. An opposite tendency was observed for acetic acid production. Yield was lowest in the vector control with 20 mg/g_{Glc} and was increased to 29 mg/g_{Glc} by expression of Nox_{low}, and further increased to 100 mg/g_{Glc} by expression of Ald6 only. The maximum yield of 130 mg/g_{Glc} was obtained by the combined expression of Ald6 and Nox_{low}. Unlike in the experiment with JWY16, this tendency was also observed for isobutyric acid production (compare Figure 26). Isobutyric acid yield was lowest in the vector control with 1.1 mg/g_{Glc}, and was increased to 3.3 mg/g_{Glc} (200% increase) by expression of NOX_{low}, and to 8.1 mg/g_{Glc} (636% increase) by expression of Ald6 only. The maximum isobutyric acid yield of 9.8 mg/g_{Glc} (791% increase) was obtained by the combined expression of Ald6 and NOX_{low}. Beneficial effect of NOX_{low} expression regarding isobutanol yield was also observed in JWY04. Yields nearly doubled from 9.9 mg/g_{Glc} in vector control to 18.0 mg/g_{Glc} by expression of NOX_{low}. In conclusion, isobutanol production was increased by NOX_{low} expression.

It can be summarised that alcoholdehydrogenase activity is important for the isobutyric acid production. Therefore, the highest isobutyric acid yield of 9.8 mg/g_{Glc} was obtained by the co-expression of NOX_{low} and Ald6 in JWY04, which corresponds to a 791% increase compared to the vector control.

4.5. Confirmation of Beneficial Approaches for Isobutanol Production Using the Best Isobutanol Producer at Time

The most promising approaches in terms of isobutanol production investigated in this work were tested in the genetic background of the best isobutanol producer currently available at time: JWY23 (Cen.PK113-7D *Δilv2; Δbdh1; Δbdh2; Δleu4; Δleu9; Δecm31; Δilv1; Δadh1; Δald6*). The approaches listed in the following were introduced into the JWY23 strain: i) Deletion of the *FRA2* gene, ii) Expression of Grx5Δ29, iii) Expression of Ilv6Δ61, iv) Expression of NOX_{low}.

The *fra2* gene was deleted in JWY23 (further referred to as MBY63), and transformed with the cyt-ILV enzyme expressing plasmid $IsoV100_K$. Furthermore, JWY23 was transformed with $IsoV100_K$, and each of the plasmids expressing Grx5Δ29 ($MBV048_N$), Ilv6Δ61 ($MBV076_H$), or NOX_{low} ($SBV089_H$). As control, JWY23

was transformed with IsoV100$_K$ and a vector. Aerobic shake flask fermentation of SCD$_{-valine}$ was performed at 30°C and 180 rpm until glucose was fully consumed or remained at a stable concentration. The results are summarised in Figure 28.

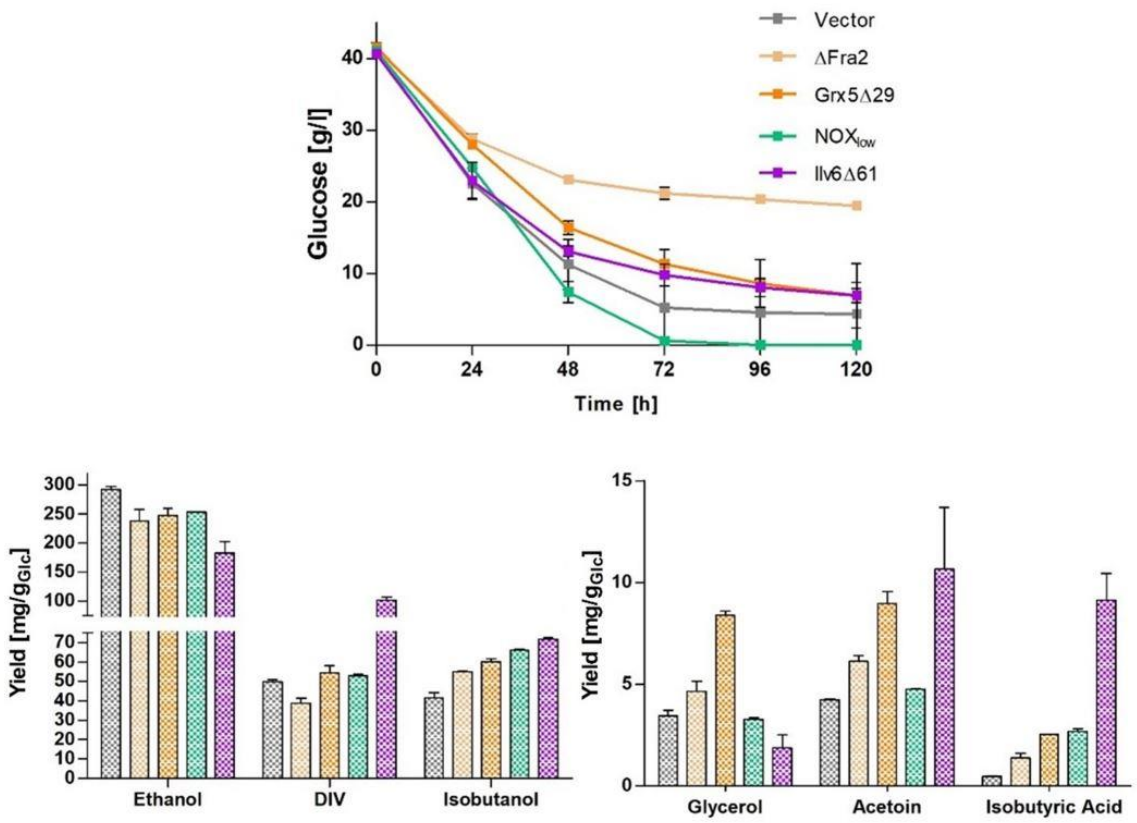

Figure 28 Glucose consumption as well as yields of ethanol, glycerol, acetoin, DIV, isobutanol and isobutyric acid after aerobic fermentation of SCD$_{-valine}$ by JWY23 constitutive expressing the cyt-ILV genes with varying beneficial approaches which were investigated in the frame of this work. *fra2* was deleted in JWY23 (CEN.PK113-7D *Δilv2; Δbdh1; Δbdh2; Δleu4; Δleu9; Δecm31; Δilv1; Δadh1; Δgpd1; Δgpd2; Δald6*) (further to referred as MBY063) and transformed with a plasmid expressing cyt-ILV genes (IsoV100$_K$). Additionally, JWY23 was transformed with IsoV100$_K$ together with Grx5Δ (MBV048$_N$), NOX$_{low}$ (SBV089$_H$), Ilv6Δ61 (MBV076$_H$) expressing plasmid or vector as control. SCD$_{-valine}$ was fermented in aerobic shake flask cultivation at 30°C (OD$_{600}$ of 8) by the transformants in duplicates with Geneticin, ClonNat and Hygromycin added in the required combination as selection marker. Yields were calculated after 24 h.

As shown in Figure 28, ethanol yield was decreased in all fermentations compared with the vector control (292 mg/g$_{Glc}$). The lowest ethanol yield was observed at 182 mg/g$_{Glc}$ for the transformant expressing Ilv6Δ61. The formation of the competitive product glycerol was reduced due to the *gdp1* and *gdp2* deletions in JWY23. Therefore, only a low yield of 4 mg/g$_{Glc}$ was observed for the control, and ranged from 2 mg/g$_{Glc}$ for the Ilv6Δ61 expressing transformant to 8 mg/g$_{Glc}$ in the Grx5Δ29 expressing transformant. While yields of ethanol and glycerol were observed to be lowest in the Ilv6Δ61 expressing transformant, the highest yields of the DIV, acetoin, isobutyric acid and isobutanol were observed in fermentations with this transformant. DIV yield of 50 mg/g$_{Glc}$ was observed in the control and was reduced to 39 mg/g$_{Glc}$ by

deletion of *fra2*. In NOX_{low} and Grx5Δ29 expressing transformants, the yield increased to 53 mg/g_{Glc} and 55 mg/g_{Glc}, respectively. As mentioned before, the highest DIV production was observed in the Ilv6Δ61 expressing transformant, with the yield doubling to 102 mg/g_{Glc}. The acetoin yield of the control was lowest at 4 mg/g_{Glc}. The highest acetoin production, on contrary, was also observed for the Ilv6Δ61 expressing transformant at 11 mg/g_{Glc}. Although *ald6* was deleted in JWY23 and MBY63, isobutyric acid was observed in the fermentation. The lowest yield of 0.5 mg/g_{Glc} was observed in the control and increased for each of the approaches tested. In the *fra2* deletion mutant MBY63, an acetic acid yield of 1.4 mg/g_{Glc} was observed, and 2.5 mg/g_{Glc} and 2.7 mg/g_{Glc} were observed by the expression of NOX_{low} and Grx5Δ29, respectively. The highest isobutyric acid production was observed for the Ilv6Δ61 expressing transformant at 9.1 mg/g_{Glc}. The same yield tendency was observed for isobutanol production. The control showed the lowest yield of 41 mg/g_{Glc} which increased to 55 mg/g_{Glc} (34% increase) by the deletion of *fra2* in MBY63. This yield was followed by the Grx5Δ29 expressing transformant to 60 mg/g_{Glc}, corresponding to a 46% increase. Additional expression of NOX_{low} further increased the yield to 66 mg/g_{Glc} which represents a 61% increase. The highest isobutanol yield was observed at 72 mg/g_{Glc} in the Ilv6Δ61 expressing transformant, corresponding to a 76% increase compared to the JWY23 control.

5. DISCUSSION

Brat *et al.* (2012) demonstrated that by expression of the cyt-ILV and EP enzymes, combined with deletion of *ilv2*, the isobutanol yield in *S. cerevisiae* increases up to 15 mg/g_{Glc}. However, this is still far from the theoretical maximum yield of 410 mg/g_{Glc}. Thus, limitations of cytosolic isobutanol biosynthesis in *S. cerevisiae* were investigated to improve the isobutanol yield, with respect to its industrial applications.

5.1. OPTIMISATION OF THE CYTOSOLIC ISOBUTANOL BIOSYNTHESIS METABOLIC PATHWAY IN *S. CEREVISIAE*

The approaches that were investigated in this work to overcome existing limitations of the cytosolic isobutanol pathway are discussed as follows.

5.1.1. CYTOSOLIC EXPRESSION OF ACETOLACTATE SYNTHASES AND THEIR IMPACT ON CELL GROWTH AND MEDIUM COMPOSITION

In *S. cerevisiae* the isobutanol biosynthesis is associated with glycolysis, the major metabolic pathway, by the enzymatic reaction of the ALS Ilv2. In the Ilv2 catalysed reaction, two molecules of pyruvate are condensed to form one molecule of ALAC. Therefore, a strong ALS activity is required for isobutanol biosynthesis (Ishii *et al.* 2018). However, Brat *et al.* (2012) showed that only a strong expression of cyt-ILV enzymes is not sufficient to improve isobutanol biosynthesis. For so far unknown reasons, native *ilv2* needs to be deleted in the producer strain and the fermentation medium must not contain valine. This makes it challenging to use this cytosolic isobutanol biosynthesis strategy for industrial applications, since the lignocellulosic feedstock is often not well-defined and may contain proteins, and thus valine. Proteins are usually considered waste and are not metabolised by the producer in fermentation processes based on lignocellulosic feedstocks (Upadhyay and Mishra 2019; Li *et al.* 2018) However, during cytosolic isobutanol biosynthesis, as described by Brat *et al.* (2012), valine would have an inhibitory effect.

To investigate why deletion of *ilv2* together with the valine omission is mandatory for cytosolic isobutanol biosynthesis, Ilv2Δ54 and Ilv2 were expressed in prototrophic CEN.PK113-7D and grown on solid YEPD medium, respectively (Figure 4). Heterogeneous, and significantly deficient growth was observed for the transformant expressing Ilv2Δ54. No growth phenotype was observed for the transformant expressing Ilv2. The growth deficient caused by Ilv2Δ54 expression was not

attributable to insufficient valine production, as prototrophic transformants were grown on solid valine containing YEPD medium. All plasmids that were re-isolated from the suppressor mutants (T^{1-3}), encoded only fragments of the *ILV2Δ54* ORF without catalytic activity. Such plasmids that were isolated from the growth-deficient cells (T^{4-6}), encoded an error-free *ILV2Δ54* ORF (Figure 5). From this finding, it was concluded that transformants expressing catalytically inactive *ILV2Δ54* isoforms lost the deficient growth phenotype. Because the *ILV2Δ54* ORFs expressed by the plasmids isolated from suppressor mutants were strongly truncated or entirely lost, it was not possible to evaluate whether the cytosolic Ilv2Δ54 enzyme itself or the cytosolically produced ALAC (or downstream products of the latter) caused the growth deficit.

In case an enzyme possesses additional functions beyond catalytic activity, this is referred to as a “moonlight effect”. Moonlight proteins can use their protein structure to cause non-catalytic effects. Often, the different functions of moonlighting proteins are observed at different times, or in different compartments (Jeffery 1999; Copley 2012). Due to the translocation of the Ilv2 protein from mitochondria to the cytosol, it cannot be excluded that non-catalytic effects occur from the protein Ilv2Δ54, which would not occur from Ilv2 in the mitochondria. Espinosa-Cantú *et al.* (2017) described that the loss of catalytic function of Ilv2 does not only reflect the loss of the corresponding enzyme, suggesting a moonlighting behaviour of Ilv2. However, the *ILV2Δ54* ORFs of the plasmids isolated from the suppressor colonies were significantly truncated or completely missing, so that the potentially responsible region for a moonlighting function may also have been lost. Therefore, the Ilv2Δ54^{E138A} non-catalytic mutant that comprises the full cytosolic protein length (described by Espinosa-Cantú *et al.* (2017)]), was expressed in an *ilv2* deletion background (Figure 6). In contrast to Ilv2Δ54, the non-catalytic mutant Ilv2Δ54^{E138A} was unable to complement the *ilv2* deletion but also caused no deficient growth phenotype. This indicated that cytosolic catalytic activity of Ilv2Δ54 rather than Ilv2Δ54 protein caused the deficient growth phenotype. Park and Hahn (2019) also described a deficient growth phenotype in the presence of strong ALS activity and attributed the deficiency to the accumulation of ALAC. In their study it was shown that additional expression of Ilv5Δ48, Ilv3Δ19 or α-acetolactate decarboxylase (*alsD*) from *B. subtilis*, that converts ALAC to acetoin, mitigated the deficient growth phenotype. From this, it was concluded that an efficient conversion of ALAC is mitigating the

deficient growth phenotype. This hypothesis was not confirmed in the experiments of this work, in which *IlvC*^{6E6} or Ilv3Δ19 was individually expressed, in addition to cyt-ILV enzymes in a JWY16 background (Figure 25). In JWY16, enzymes from competing metabolic pathways downstream of ALAC are deleted. Thus, the conversion of ALAC into downstream metabolites is limited, and the expected growth deficit, if caused by ALAC accumulation, should have been evident. In addition, the conclusion of Park and Hahn (2019) is in contrast to the results shown in Figure 7 and Figure 8, which show that the expression of the ALS *ilvB* (together with *ilvN*) from *C. glutamicum* did not result in a deficient growth phenotype. Both, growth on valine-free medium (Figure 7) and yield of DIV and acetoin (Figure 8) were increased compared to the Ilv2Δ54 control, indicating strong ALS activity without deficient growth phenotype. Comparison of the protein sequences from Ilv2Δ54 and *ilvB,* using the “Blast 2 sequences” algorithm, revealed only 44% identity (Altschul *et al.* 2005). Due to the different protein structure, if the deficient growth phenotype was caused by a moonlight function of Ilv2Δ54, the moonlighting effect would be unlikely for the *ilvB* protein. But as demonstrated by the experiments with Ilv2Δ54^{E138A}, it is more likely that catalytic activity caused the deficient growth phenotype. However, the deficient growth phenotype is probably not only caused by the accumulation of ALAC, as hypothesised by Park and Hahn (2019), because strong ALS activity without growth phenotype was also observed for *ilvB* expression. An alternative explanation for the deficient growth phenotype could be the enzyme specificity toward cytosolic keto-acids and their downstream products. For example, Ilv2Δ54 could condense keto-acids of the cytosol more non-specifically than *ilvB*, causing the deficient growth phenotype.

Even though the growth deficit inducing mechanism has not been finally elucidated, it can be seen that the expression of Ilv2Δ54 was the reason. This is most likely the explanation of the phenomenon that *ilv2* must be deleted in isobutanol producers and valine must be excluded from the fermentation medium for efficient isobutanol production. A valine auxotrophy selection seems necessary to prevent *S. cerevisiae* from recombining *ILV2Δ54* to mitigate the deficient growth phenotype. Selection of the cyt-ILV enzymes expression plasmid IsoV100$_K$ is permitted by an antibiotic resistance gene *kanMX* (permits resistance towards antibiotic G418). Due to the high combinatorial activity of *S. cerevisiae*, the *ILV2Δ54* gene on the plasmid could be lost and mutants would still be viable, if *ilv2* is not deleted in the host and

valine not omitted. Since slow growth is observed for cyt-ILV enzymes expressing *ilv2* deletion transformants in valine-free medium, the pre-cultures of isobutanol producers were cultivated in a YEPD liquid medium. The selection pressure in the pre-cultures was mediated by the antibiotic G418, rather than valine auxotrophy. This resulted in the chance of valine auxotroph mutant accumulation without functional Ilv2Δ54 expression. In the subsequent fermentation that was conducted in $SCD_{-valine}$, isobutanol was no longer produced by the valine auxotroph mutants. The hypothesis that mutants with catalytical inactive Ilv2Δ54 did accumulate in the pre-cultures is supported by comparing the growth of Ilv2Δ54 expressing transformants, derived from the YEPD liquid culture and those obtained from the solid YEPD transformation medium (Figure 6). Strong Ilv2Δ54 activity in the producer is a fundamental requirement for cytosolic valine, and thus isobutanol production (Ishii *et al.* 2018). The results from Figure 24 confirm that transformants that additionally expressed Ilv2Δ54, together with cyt-ILV ($IsoV100_K$), obtained highest DIV yields. Since recombination of *S. cerevisiae* is a spontaneous process, the ratio of accumulated valine auxotroph mutants (poor isobutanol producer) and Ilv2Δ54 expressing transformants (good isobutanol producer) vary, depending on the cultivation period of the pre-culture. This might explain the high isobutanol yields variation between fermentations, observed during this work. The variation in isobutanol yields obtained with the same producer strain (*ilv2* deletion strain, expressing cyt-ILV enzymes) from different fermentations are summarised in Table 32.

Table 32 Presentation of isobutanol yields obtained from high-OD (OD_{600} of 8) fermentation of $SCD_{-valine}$ liquid medium by *ilv2*Δ strains expression cyt-ILV enzymes ($IsoV100_K$).

No.	Genotype	Isobutanol Yield [mg/g_{Glc}]	Relative to reference	Data from
1	*ilv2 null*	9.0	Reference (100%)	Figure 8
2		2.4	27 %	Figure 9
3		10.0	111 %	Figure 10
4		6.9	77 %	Figure 12
5		3.7	41 %	Figure 13
6		3.2	36 %	Figure 14
7		4.8	53 %	Figure 23

As shown in Figure 6, deficient growth was noticed when *ilv2* deletion was complemented by cytosolic Ilv2Δ54 from $SCD_{-valine}$ solid medium. Furthermore, valine auxotrophy caused by *ilv2* deletion was only complemented when *ILV2Δ54* was expressed from a *2µ* high copy vector (such as $IsoV100_K$). Genomic integration of *ILV2Δ54* into an *ilv2* deletion strain did not enable MBY29 to grow on solid $SCD_{-valine}$

medium (Figure 19) and in $SCD_{-valine}$ liquid medium, only after a lag-phase of approximately 144 h (Figure 16). However, the time required for cell cultivation and fermentation is one of the most significant cost drivers, and thus a key parameter for the successful commercialisation of a fermentation process (Banat *et al.* 2014). The fact that efficient cultivation of an *ilv2* deletion strain is only feasible in a complete medium, which then results in significant variations of isobutanol yield during biosynthesis, remains a challenge for industrial isobutanol biosynthesis. Park and Hahn (2019) described the expression of ALS under the control of a cupper inducible promoter. This approach would allow producer strains to be grown in a complete medium without any harmful effects caused by *ILV2Δ54* expression. Thus, no selection pressure would apply on the *ILV2Δ54* ORF, and consequently no accumulation of non-catalytic mutants would be observed during cultivation. For the subsequent fermentation, isobutanol biosynthesis would be initiated by inducing the promoter of *ILV2Δ54*.

It is known that Ilv2 activity is inhibited by the small regulatory subunit Ilv6 in the presence of valine (Cullin *et al.* 1996; Duggleby 1997; Pang and Duggleby 1999). Therefore, it was investigated whether feedback inhibition of Ilv2Δ54 by native Ilv6 may also be a reason for the required valine exclusion from the fermentation medium. As shown in Figure 9, neither the *ilv6* deletion in strain MBY51 nor the expression of a feedback insensitive $Ilv6\Delta61^{N86A}$ prevented the isobutanol yield decrease in the presence of valine. However, if feedback inhibition by Ilv6 was the reason for decreased isobutanol biosynthesis in the presence of valine, no reduced isobutanol yield should have been observed in the presence of valine. Furthermore, increased isobutanol yield was observed by expression of cytosolic Ilv6Δ61 in a valine-free medium, which is attributed to the ALS activity enhancing impact of Ilv6Δ61 in the absence of BCAAs (Pang and Duggleby 1999).

In summary, it has been shown for the first time that *ILV2Δ54* expression in *S. cerevisiae* can cause a deficient growth phenotype, resulting in a negative selection of the *ILV2Δ54* gene. Because of this, the *ilv2* gene must be deleted in the producer strain and valine must be omitted from the fermentation medium. By this valine auxotrophy selection, *ILV2Δ54* expression is assured. Therefore, cytosolic isobutanol production using undefined valine-containing media (also on an industrial scale) will not become efficient until the harmful effect of *ILV2Δ54* expression is

eliminated. Otherwise, if valine is present, the beneficial approaches that are discussed below will not contribute to an increase in isobutanol yield.

5.1.2. Approaches to Overcome the Co-Factor and Redox Imbalances of the Isobutanol Pathway

Another limitation of implementing the isobutanol biosynthesis as the main fermentative metabolic pathway in *S. cerevisiae* is the redox imbalance. During glycolysis, two NADH are generated for each glucose, whereas only one NAD^+ is recovered by the Adh2 catalysed reduction of isobutyraldehyde to isobutanol. The Ilv5 catalysed reaction, on the contrary, requires NADPH (Figure 1), which is not recovered within the isobutanol biosynthesis. Therefore, isobutanol biosynthesis is neither NADH nor NADPH neutral. In the literature, approaches are discussed to overcome the issue of the redox imbalanced isobutanol biosynthesis. For example, the expression of a transhydrogenase-like shunt (Figure 2) to convert excess NADH to NADPH is described (Matsuda *et al.* 2013; Suga *et al.* 2013). Substitution of NADPH dependent Ilv5 with engineered bacterial NADH dependent KARIs is another widely used approach for isobutanol biosynthesis (Bastian *et al.* 2011; Brinkmann-Chen *et al.* 2013; Generoso *et al.* 2017).

However, it was still unclear whether NADH or NADPH already limited the cytosolic isobutanol biosynthesis in *S. cerevisiae* during the aerobic shake flask fermentation. Therefore, NADPH dependent Ilv5Δ48 of cyt-ILV enzymes was replaced by the NADH dependent *ilvC*^{6E6}, and expressed with and without enzymes of the EP (Figure 10). In the control fermentation, without enzymes of the EP, a glycerol yield of 80 mg/g_{Glc} was observed. Glycerol is a by-product of the redox neutral ethanol biosynthesis, and it is assumed that the major function of NADH dependent glycerol formation is the maintenance of cytosolic redox balance by compensation of cellular NAD^+ dependent reactions, like isobutanol biosynthesis (Dijken and Scheffers 1986; Nevoigt and Stahl 1997; Smidt *et al.* 2012). Once the EP enzymes, Aro10 and Adh2, were expressed, the glycerol yield decreased independently of the expressed KARI to approximately 20 mg/g_{Glc} (Figure 10). This was explained by the expression of NADH dependent Adh2, resulting in an enhanced reduction of aldehydes available, which caused a more NADH balanced metabolism. However, a tenfold acetoin yield increase, again KARI independent, was observed when EP enzymes were expressed. No acetolactate decarboxylase is known for *S. cerevisiae*, and thus ALAC must oxidise spontaneously to diacetyl before the latter

is reduced by NADH dependent Bdh1 and Bdh2 to acetoin and 2,3-butanediol, respectively. Due to the expression of the EP enzymes, no increase in oxidative cytosolic environment was expected, which would cause an increased diacetyl or acetoin concentration. It is more likely that acetoin is formed by the pyruvate decarboxylase activity of constitutively expressed Aro10. It is known that acetoin can be formed from pyruvate and acetaldehydes by the PDC isoenzymes in an NADH independent manner (Chen and Jordan 1984). Expression of Adh2 furthermore supports the accumulation of acetaldehyde, which is required for the acetoin synthesis by pyruvate decarboxylases (Maestre *et al.* 2008). Furthermore, acetoin is known to be an NADH oxidising reagent, and therefore might contribute to compensate the NADH excess, which may also explain the reduced glycerol formation (Bakker *et al.* 2001). Thus, the expression of Adh2 and Aro10 can improves the NADH co-factor balance of the metabolism, but creates competition for the joint substrate pyruvate between Aro10 and Ilv2Δ54. This competition is the reason for reduced isobutanol yield, which was observed when the EP enzymes were expressed (Figure 10). Competition of Aro10 and Ilv2Δ54 for pyruvate could be relieved by substrate channelling between Ilv2Δ54 and Pyk2 to improve valine biosynthesis, as described by Kim *et al.* (2016). This would allow simultaneous expression of cyt-ILV and EP enzymes without reducing the isobutanol yield.

Based on the results discussed above, it was assumed that NADH excess already limited isobutanol biosynthesis in aerobic shake flask fermentation. This hypothesis was also supported by the results shown in Figure 26 and Figure 27. Here, it was shown that heterologous expression of NADH-oxidase (NOX) from *Streptococcus pneumoniae,* in combination with cyt-ILV enzymes, resulted in increased isobutanol yield. NOX catalyses the oxidation of NADH by using O_2 to form water (Shi *et al.* 2016). Thus, the NADH excess was reduced during aerobic shake flask fermentation, resulting in increased isobutanol biosynthesis.

While NADH excess limited isobutanol biosynthesis already at low yields, this was not observed for NADP. Substitution of Ilv5Δ48 by the NADH dependent *ilvC*^{6E6} (cyt-ILV_*ilvC*^{6E6}) makes isobutanol biosynthesis both NADPH independent and NADH neutral (Bastian *et al.* 2011; Milne *et al.* 2016). However, it is shown in Figure 10 that by expression of *ilvC*^{6E6} instead of Ilv5Δ48, no difference in glycerol biosynthesis was observed. This suggests that the expression of *ilvC*^{6E6} did not improve NADH balance. Furthermore, it was observed that the expression of *ilvC*^{6E6}

rather than Ilv5Δ48 led to reduced yields of DIV and isobutanol, suggesting a reduced *in vivo* activity of *ilvC*^{6E6}. Most likely, the catalytic activity of native mitochondrially Ilv5 was sufficient to metabolise most of the cytosolically produced ALAC. That the intermediates of valine, e.g. ALAC, are able to pass through the mitochondrial membrane has been described in the literature (Brat *et al.* 2012). This assumption was supported by the results shown in Figure 24, which demonstrate that the additional expression of *ilvC*^{6E6} together with cyt-ILV enzymes had no effect on glucose consumption and metabolite formation. Experiments with the mutant *IlvC*$^{P2\text{-}D1A1}$, described by Brinkmann-Chen *et al.* (2013), which has a K_m of 26 µM for NADH (*ilvC*^{6E6} 30 µM) and a K_m of >1,400 µM for NADPH (*ilvC*^{6E6} 650 µM), also showed no improved *in vivo* activity compared to Ilv5Δ48 (data not shown, experiments were performed with plasmids MBV113 and MBV114). An alternative enzyme that makes isobutanol biosynthesis NADPH independent and NADH neutral could be the recently described KARI from *Sulfolobus acidocaldarius*, which is both NADH and NADPH dependent (Chen *et al.* 2018).

While NADH accumulation was proven to be limiting for cytosolic isobutanol biosynthesis, this was not observed for NADPH accumulation. The pentose phosphate pathway is the major source of NADPH in *S. cerevisiae*. Deletion of *pgi1* prevents the conversion of glucose-6-phosphate to fructose-6-phosphate, thus making it impossible for *S. cerevisiae* to metabolise glucose in glycolysis. As a result, glucose-6-phosphate is metabolised by the pentose phosphate pathway, resulting in the formation of two molecules of NADPH per molecule of glucose. Due to the accumulation of NADPH, *pgi*Δ mutants are not tolerant of high glucose concentrations (Maitra 1971; Heux *et al.* 2008). Introduction of a strong NADPH consuming reaction, such as the Ilv5Δ48 catalysed reductoisomerase, increases glucose tolerance of *pgi1*Δ mutants by consuming the accumulated NADPH of the pentose phosphate pathway. However, growth experiments with MBY59 (JWY18 *pgi1*Δ) and MBY60 (JWY19 *pgi1*Δ) on solid YEP medium containing fructose with increasing glucose concentration did not reveal increased glucose tolerance for transformants expressing cyt-ILV enzymes (data not shown). This showed that demand for NADPH in isobutanol production is low and can still be covered by the metabolism of *S. cerevisiae*.

5.1.3. Approaches to harmonise Iron-Sulphur-Cluster Biogenesis and DHAD activity in the Cytosol of *S. cerevisiae*

Moreover, cytosolic conversion of DIV to KIV is considered to be a limitation of isobutanol biosynthesis in *S. cerevisiae* (Milne *et al.* 2016; Generoso *et al.* 2017). DIV is secreted during cytosolic isobutanol biosynthesis and is not further metabolised. During cytosolic isobutanol biosynthesis, the secreted DIV yield often exceeds that of the product isobutanol (see e.g., Figure 12 to Figure 14). Attempts to identify responsible transporters to prevent DIV secretion or to allow DIV re-import were not successful (experiments were conducted in collaboration with Dr Wesley Cardoso Generoso). Therefore, the results will not be discussed in the context of this work. For a detailed description of the experiments, see Generoso *et al.* (2017).

Another approach was to increase the cytosolic DHAD activity (e.g., Ilv3Δ19) to ensure more efficient catalysis of DIV to KIV, in order to prevent DIV secretion. The downstream product KIV may still be secreted, but can be taken up again by *S. cerevisiae* (Generoso *et al.* 2017). Secreted valine could also be taken up again by the amino acid permease Gap1 (Garrett 2008). The poor cytosolic Ilv3Δ19 activity is attributed to the insufficient loading of [2Fe-2S] ISC during apo-protein maturation (Generoso *et al.* 2015). In the cytosol of *S. cerevisiae,* mainly [4Fe-4S] ISC are assembled and involved in cytosolic ISC dependent reactions. Thus, [4Fe-4S] ISC dependent DHADs were also screened for *in vivo* activity in *S. cerevisiae* (Figure 11). Furthermore, cytosolic ISC availability and DHAD apo-protein maturation were optimised by different approaches, like Grx protein expression or deletion of *pim1* or *fra2,* which are involved in the ISC maturation (Figure 12 to Figure 14).

As can be seen in Figure 11, no enhanced *in vivo* activity of DHAD was observed by a fusion of a C-terminal tryptophan. The activity of DHAD with modified C-terminus either remained unchanged or became even worse in the case of the [4Fe-4S] ISC dependent *ilvD* from *E. coli*. Therefore, it was concluded that the altered C-terminus did not improve ISC dependent apo-protein maturation due to an increased affinity toward the CIA complex. The necessity of the C-terminal tryptophan for high affinity of Lto1 toward the CIA machinery seemed to be a Lto1 specific characteristic, which cannot be applied to other cytosolic ISC dependent proteins (Lill *et al.* 2015). Nevertheless, all the bacterial [4Fe-4S] ISC containing DHADs demonstrated *in vivo* activity and complemented the *ilv3* deletion on solid $SCD_{-valine}$ medium. The *in vivo* activity of *ilvD* from *E. coli* and *C. glutamicum* was higher compared to the other

bacterial [4Fe-4S] ISC containing DHADs. However, all bacterial [4Fe-4S] ISC containing DHADs tested have the identical ISC binding pattern Cys-X_2-Cys-X_2-Cys, namely CPTCGSC (Watanabe *et al.* 2006). Thus, different *in vivo* activities of the bacterial [4Fe-4S] ISC DHADs could not be explained by a different coordination of the [4-Fe-4S] ISC. It is more likely that affinity toward yeast CIA machinery (despite high sequence identity of the DHAD tested) was the reason for the observed variation of *in vivo* activities.

Apo-protein maturation of ISC proteins in prokaryotes occurs through three distinct ISC assembly pathways. These are the ISC-system, which occurs in eukaryotes and prokaryotes, as well as the SUF- and the NIF-systems, which are primarily observed in prokaryotes and archaea, respectively (Braymer *et al.* 2021). It is known that apo-protein maturation of *ilvD* from *E. coli* occurs through the SUF- or ISC-system (Tan *et al.* 2009). The ISC assembly system is highly conserved across all domains of life (Mühlenhoff *et al.* 2011). Due to this, it is likely that the ISC machinery of *S. cerevisiae* will show good compatibility with the *ilvD* from *E. coli,* resulting in good *in vivo* activity (Figure 11). Apo-protein maturation of other DHADs tested has not been described in the literature to date. Therefore, it cannot be excluded that apo-protein maturation of the tested DHADs, may not have a good compatibility with the ISC system of *S. cerevisiae*, since these DHADs might be matured in their originating organisms *via* the NIF- or SUF-systems. Thus, when choosing heterologous ISC enzymes (e.g., DHADs) for expression in *S. cerevisiae,* it might be helpful to focus on ISC enzymes that originate from organisms in which the apo-protein maturation occurs through the ISC system.

The [2Fe-2S] ISC-containing *ilvD* from *B. subtilis* (47% sequence identity with *ilvD* from *E. coli*) was unable to complement the *ilv3* deletion in *S. cerevisiae* on solid $SCD_{\text{-valine}}$ medium (Figure 11). The *ilvD* from *B. subtilis* has evolved towards the proteins of the SUF-system, since *B. subtilis* possesses only this assembly system for ISC apo-protein maturation (Albrecht *et al.* 2010). Therefore, it was very unlikely that *ilvD* from *B. subtilis* showed good compatibility with the ISC- and CIA-system of *S. cerevisiae.* The observation that Ilv3Δ19 was able to complement the *ilv3* deletion, despite the requirement for [2Fe-2S] ISC, might also be attributed to the good affinity of Ilv3Δ19 toward the endogenous ISC-system.

Also, a CIA-independent apo-protein maturation of Ilv3Δ19 by cytosolic Grx proteins might be the reason for good *in vivo* activity. Natively, Grx5 facilitates [2Fe-2S] ISC incorporation into mitochondrial Ilv3 apo-protein (Uzarska *et al.* 2013; Lill *et al.* 2015). Furthermore, it has been shown that a *grx5* deletion is complemented by mitochondrial expression of Grx3 or Grx4, indicating a common function of the Grx proteins (Molina *et al.* 2004; Molina-Navarro *et al.* 2006). The results of Figure 12 show that expression of cytosolic Grx5Δ29 together with cyt-ILV enzymes decreased DIV secretion from 34 mg/g_{Glc} to 23 mg/g_{Glc}. In contrast, isobutanol yield increased from 6.9 mg/g_{Glc} to 10.5 mg/g_{Glc} (52% increase). This indicates an optimised metabolic flux with reduced secretion of DIV, due to the improved Ilv3Δ19 apo-protein maturation caused by Grx5Δ29. The assumption that cytosolic Ilv3Δ19 is matured by cytosolic Grx proteins in a CIA independent manner is not discussed in the literature to date. However, the results from Figure 12 and Figure 28 provide a first indication for this assumption, although further research is needed for confirmation.

In contrast to the directed Ilv3Δ19 apo-protein maturation by Grx5Δ29, deletion of *pim1* and *fra2* are aimed to increase the overall ISC availability in *S. cerevisiae,* and thereby increased apo-protein maturation (Ciesielski *et al.* 2016; Salusjärvi *et al.* 2017). Unlike in fermentations with Grx5Δ29 expressing transformants (Figure 12), no decreased DIV secretion was observed in fermentations of *pim1* (Figure 13) and *fra2* (Figure 14) deletion mutants, although increased isobutanol yields were observed. Since the assembly of cytosolic available ISC starts in the mitochondria, it is likely that increased mitochondrial ISC availability mainly contributed to the mitochondrial Ilv3 apo-protein maturation (Lill *et al.* 2015). As a result, mitochondrially available DIV was increasingly converted to KIV. The mitochondrially derived KIV (or valine) was then subsequently converted to isobutyraldehyde and isobutanol, respectively. By increasing the overall availability of ISC, competition was created between mitochondrial and cytosolic isobutanol biosynthesis. On the one hand, this resulted in an increase in isobutanol but, on the other, the DIV secretion was not decreased because maturation of cytosolic Ilv3Δ19 apo-protein was discriminated, as compared to mitochondrial Ilv3 due to compartmentalisation.

5.1.4. Combination of Approaches for Improves Cytosolic Isobutanol Biosynthesis in *S. cerevisiae*

Finally, the approaches that enhanced isobutanol biosynthesis were investigated in the background of the best isobutanol producer to date, namely cyt-ILV enzymes expressing JWY23. Enhanced isobutanol yields were confirmed for NOX_{low}, Grx5Δ29 or Ilv6Δ61 expression as well as for additional *fra2* deletion in JWY23 (Figure 28). Additional expression of the cytosolic small regulatory subunit Ilv6Δ61 resulted in an isobutanol yield of 72 mg/g_{Glc}, which is, to our best knowledge, the highest isobutanol yield ever obtained with *S. cerevisiae,* in shake flask cultivation. However, it was observed that vector control and Grx5Δ29 and Ilv6Δ61 expressing JWY23 transformants, consumed glucose only up to a concentration of approximately 5 g/l. Glucose consumption of transformants bearing the additional *fra2* deletion, stagnated already at a concentration of about 24 g/l. Stagnation in glucose consumption was not observed for the fermentation of the said approaches, implemented to an *ilv2* deletion background only (Ilv6Δ61: Figure 9, Grx5Δ29: Figure 12; *fra2*Δ: Figure 14). Only JWY23 transformants expressing NOX_{low} were able to metabolise the complete glucose added. This observation indicated that the isobutanol pathway in JWY23 was optimised to the extent where NADH excess increasingly limited isobutanol biosynthesis. By *adh1, gpd1, gpd2, bdh1* and *bdh2* deletion in JWY23, important enzymes for the oxidation of NADH were removed (Wess *et al.* 2019). Although *adh1* was deleted in JWY23, high ethanol yields were observed. Ethanol was most likely produced by suppressor mutants with upregulated alcohol dehydrogenase activity of Adh2 to Adh5 or Sfa1, which are known for *S. cerevisiae* (Dickinson *et al.* 2003). It is likely that this suppressor mutant originated due to the accumulation of NADH in engineered JWY23. Based on the results of this work, the NADH imbalance in JWY23 was best solved by the expression of NOX_{low}, because NADH dependent $ilvC^{6E6}$ isoform lacked high *in vivo* activity (Figure 10). However, it remains unclear whether the expression of NOX_{low} can be used for NADH recovery in commercial isobutanol biosynthesis, since the oxidative reaction requires oxygen. The industrial application of pathways that require an aerobic environment presents a major challenge for the commercial production of low-cost fuels. This is due to the additional operating costs which are required for the supply of oxygen to the culture as well as the lower scalability of aerobic, compared to anaerobic, processes (McMillan and Beckham 2017). Furthermore, it is notable that expression of cytosolic Ilv6Δ61, together with cyt-ILV enzymes, nearly doubled the DIV yield in JWY23. This was not observed

when Ilv6Δ61 was expressed together with cyt-ILV enzymes in an *ilv2* deletion background (Figure 9). Due to the deletion of *ilv1* and *adh1*, it was likely that more pyruvate was available in JWY23 to form ALAC by the Ilv2Δ54$^{Ilv6\Delta61}$ catalysed condensation. Consequently, an enhanced ALAC to DIV conversion occurred, and the latter was increasingly secreted due to the insufficient Ilv3Δ19 activity. However, this would imply that the Ilv5Δ48-catalysed ALAC to DIV conversion was still not limited in the improved isobutanol producer JWY23. Thus, it was concluded that the NADPH availability in *S. cerevisiae* was still not limited in the presence of a strong isobutanol biosynthesis pathway, since sufficient NADPH is produced by the pentose phosphate pathway (Maitra 1971). Based on this result, it was concluded that by co-expression of NOX_{low}, Ilv6Δ61 and cyt-ILV enzymes in JWY23, full glucose consumption could be achieved together with the high isobutanol yields caused by Ilv2Δ54$^{Ilv6\Delta61}$ activity, resulting in high isobutanol titres. The expected DIV secretion could be mitigated by selectively improving Ilv3Δ19 activity. As mentioned above, expression of Grx5Δ29 is the preferred approach over *fra2* deletion to improve Ilv3Δ19 activity, because Grx5Δ29 did not create competition between the mitochondrial and cytosolic isobutanol biosynthetic pathways, unlike *fra2* deletion. Therefore, it is assumed that co-expression of Ilv6Δ61, NOX_{low}, Grx5Δ29, cyt-ILV enzymes in JWY23 could further reduce the existing limitations, and the highest achieved isobutanol yield of 72 mg/g_{Glc} can be even further increased by this approach.

5.2. Optimisation of *S. cerevisiae* for efficient isobutanol production

In this work, not only the pathway was engineered for efficient isobutanol biosynthesis but also the producer *S. cerevisiae* was optimised. For this purpose, rational and evolutionary strain engineering was applied. In both approaches, improved isobutanol yields were observed (Figure 21 and Figure 23).

Evolutionary engineering of MBY29 in $SCD_{norvaline}$ resulted in clearly improved growth of evolved cultures (Figure 18) and isolated mutants (Figure 19 and Figure 20) on $SCD_{-valine}$. No responsible mutations were identified during the reverse engineering approach, as described in Section 4.2.1. However, when the selected genes were amplified from evolved MBY36, both wild-type and mutant alleles were found. In the raw data of the sequencing chromatograms, it was evident that a clear peak was observed for both nucleobases, the wildtype and the mutated nucleobase.

This observation makes sequencing errors very unlikely, and supports the theory that both alleles were indeed present in the evolved strain MBY36. Therefore, it was assumed that gene duplications occurred during the evolutionary engineering experiment. The genes listed in Table 29 and Table 30 are located on different chromosomes, so that even a full genome duplication was conceivable. Gene or genome duplications can occur in *S. cerevisiae* within few generations, in both nature and in laboratory experiments (Barrick and Lenski 2013; Naseeb *et al.* 2017). Genome duplication confers an evolutionary advantage to the organism, because the new and redundant genetic material is not restricted to any metabolic functions and is able to mutate without obligations. Thus, new (neofunctionalisation) or optimised and specialised functions (subfunctionalisation) can evolve for the redundant genes (Ohno 1970; Voordeckers and Verstrepen 2015). Although no responsible mutation was identified during reverse engineering, it could not be excluded that neofunctionalisation or subfunctionalisation was responsible for the improved growth of evolved *S. cerevisiae* in $SCD_{-valine}$. However, it was more likely that the improved growth in $SCD_{-valine}$ was caused by gene dosage, which is described as third option for genes raised from a duplication event (Ohno 1970). Both copies of the duplication may retain the function of the ancestor, introducing redundancy and/or increased activity of the gene (Kondrashov *et al.* 2002). A well-known example for successful gene dosage by genome duplication in *S. cerevisiae* is the dose increase of glycolytic genes, which provided an immediate growth advantage by improved glucose fermentation (Conant and Wolfe 2007). Therefore, it was considered that gene dosage was the reason for the improved growth of MBY36 on $SCD_{-valine}$. First, at least two copies of *ILV2Δ54* were present in MBY36 due to duplication, which seems to be necessary to complement the *ilv2* deletion. Second, the duplication also allowed gene dosages for the *ILV5Δ48* and *ILV3Δ19* genes to permit efficient conversion of the toxic product, derived from Ilv2Δ54 activity, to DIV or other less toxic intermediates. This suggestion was supported by results of the bachelor thesis of Marcel Mayer, which was supervised in the frame of this thesis (Mayer 2018). In his work, the genes *ILV2Δ54*, $ilvC^{6E6}$ and *ILV3Δ19* were randomly assembled with promoters and terminators that modulated different expression levels by using a modified GoldenGate cloning approach (Engler *et al.* 2009; Lee *et al.* 2015). This so constructed plasmid library was then transformed intoo IsoY16, (CEN.PK2-1C Δ*ilv2,* Δ*ilv5,* Δ*ilv3*). The transformants were then screened for growth on solid $SCD_{-valine}$

medium. The plasmids of the best growing transformants were then isolated and sequenced. Here, it was observed that *ILV2Δ54* was under control of a medium-strong *pRET2* promoter and a *tADH1* terminator. In contrast, *ILV3Δ19* and *ilvC*^{6E6} were expressed by the strongest *pTDH3* promoter used in the work, and a *tSSA1* terminator (Mayer 2018). This shows that growth on solid SCD$_{\text{-valine}}$ medium was improved by gene dosage of *ILV2Δ54*, *ilvC*^{6E6} and *ILV3Δ19.* Also, Park and Hahn (2019) demonstrated that the toxic effect of four ALS genes (*alsS* from *Bacillus subtilis*) promoted the multicopy integration of *ILV5Δ48* and *ILV3Δ19* into the rDNA of *S. cerevisiae* via the Kozak sequence. Four copies of *alsS* in *S. cerevisiae* were sufficient to cause the integration of three gene copies of *ILV5Δ48* and *ILV3Δ19*, which mitigated the toxic effect of ALS by gene dosage (Park and Hahn 2019). These results support the assumption that improved growth on SCD$_{\text{-valine}}$ of evolved *S. cerevisiae* was rather caused by the gene dosage effect, than by neofunctionalisation or subfunctionalisation due to specific mutation.

Not only growth but also metabolite analysis of the fermentation broth from evolved strains MBY36, MBY39, MBY41, MBY42 and the unevolved MBY29 revealed differences (Figure 21). Glucose consumption of the evolved strains was significantly increased. In fermentations with evolved strains, glucose was completely consumed after 72 h, whereas MBY29 only metabolised about 30% of the glucose. Due to the variation in glucose consumption, the evolved strains started to degrade the previously formed ethanol after 72 h, unlike MBY29. This explained the increased acetate yields that were observed for the evolved cells (especially for MBY42). In the literature, this effect is described for *S. cerevisiae* as “make-accumulate-consume”, and is also attributed to the whole-genome duplication (Piskur *et al.* 2006; Voordeckers and Verstrepen 2015). Not only the glucose consumption was improved by the evolutionary engineering, but also improved valine biosynthesis was concluded from the metabolite analysis of the evolved strains (Figure 21). Increased DIV secretion was indicative of enhanced valine biosynthesis in evolved strains, whereas reduced 2,3-butanediol yield suggested improved conversion of ALAC to DIV (e.g., by gene dosage). Additionally, increased isobutanol yields were observed in evolved strains. The selection pressure, applied by the addition of norvaline, directed the evolution toward increased valine rather than isobutanol production. Therefore, the observed increase in isobutanol yield, which was caused by the evolutionary engineering, appeared to be unexpected at first. However, the Bat2

catalysed transamination of valine is reversible. The resulting α-keto acid (e.g., KIV), on the contrary, is irreversibly directed into the EP by the Aro10 catalysed decarboxylation (Ehrlich 1907; Pires *et al.* 2014). Since valine and the joint precursor KIV are in a reversible balance, the yield of the irreversibly produced by-product isobutanol is also affected by increased valine production.

Despite the successful evolutionary engineering of MBY29 towards growth on $SCD_{-valine}$ and improved glucose consumption, the overall yields remained comparatively low with a maximum of 6 mg/g_{Glc} of DIV and 0.75 mg/g_{Glc} of isobutanol (Figure 21). On the contrary, an isobutanol yield of 41 mg/g_{Glc} was obtained with JWY23 expressing the cyt-ILV enzymes from a *2µ*-multi-copy vector (Figure 28). However, JWY23 consumed glucose only partially and slowly over a period of 120 h (Wess *et al.* 2019). Although isobutanol yield was increased in JWY23 by deletion of competing metabolic pathways, biosynthesis was time-consuming, and due to non-exhaustive consumption of glucose, the highest possible titre was not achieved. A combinatorial approach of rational strain engineering and evolutionary engineering could result in an isobutanol producer combining the beneficial properties of both engineering approaches. Therefore, multiple integration of the cyt-ILV genes in JWY23 with subsequent evolutionary engineering on $SCD_{norvaline}$ could improve glucose consumption (high titre) and isobutanol production (high yield).

To our best knowledge, it has so far not been possible to grow *pdc* deletion mutants anaerobically on high glucose concentrations, by expression of an isobutanol pathway (Milne *et al.* 2016). Also, in this work (data not shown), it was impossible to evolve MBY32 (TAM Ilv2Δ::cyt-ILV_*ilvC*^{6E6}+EP) anaerobically towards efficient isobutanol production, to mitigate insufficient redox balance (van Maris *et al.* 2004; Oud *et al.* 2012). Among others, insufficient valine biosynthesis prevents isobutanol biosynthesis from being established as the main fermentative pathway. Thus, the norvaline evolution engineering approach of *S. cerevisiae* could enable a two-step evolutionary engineering to improve not only valine but also isobutanol biosynthesis. The second evolutionary engineering would then be based on the insufficient NADH oxidising capacity of the isobutanol pathway, compared to the NAD^+ reducing glycolysis. First, the cyt-ILV enzymes expressing JWY23 (with NADH dependent KARI and other beneficial approaches, such as expression of Ilv6Δ61 and Grx5Δ48) must be evolved in $SCDn_{orvaline}$ as described. Then *pdc* deletion and *MTH1-ΔT* integration must be conducted (Oud *et al.* 2012; van Maris *et al.* 2004).

This strain could then possibly be further evolved under anaerobic conditions, with respect to isobutanol biosynthesis.

5.3. Production of Isobutyric Acid in *S. cerevisiae*

Like isobutanol, isobutyric acid (IBA) is considered a platform chemical which is utilised in many applications, like for the production of transparent thermoplastics or sucrose acetic acid, a largely used emulsifier (Petrognani *et al.* 2020; Zhang *et al.* 2011). Isobutanol and IBA share the Aro10 derived precursor isobutyraldehyde. Therefore, optimisation of the isobutanol pathway also raises the possibility of increasing IBA yields. Microbial host have been engineered for IBA production, like *E. coli* (Zhang *et al.* 2011) or *Pseudomonas sp* (Lang *et al.* 2014). However, to the best of our knowledge, only one approach for *S. cerevisiae* is recorded in the literature (Yu *et al.* 2016).

The isobutanol producer JWY16, with *adh1* among others being deleted, was used for IBA production (Figure 26). However, despite expression of cyt-ILV enzymes in various combinations with Ald6 and NOX, no IBA was produced. Comparatively, low ethanol yields were observed because of the *adh1* deletion (up to 83 mg/g_{Glc} ethanol). Therefore, the metabolism of JWY16 was probably not NAD^+ neutral, since NADH was not oxidised in sufficient amounts during ethanol biosynthesis, resulting in the formation of glycerol as the main fermentative product. However, it is also described in literature that not only glycerol production is increased when *adh1* is deleted, but also a significant amount of acetaldehyde is produced (Smidt *et al.* 2012). This is consistent with the high acetic acid yields observed for the Ald6 expressing transformants. Intracellular acetaldehyde is toxic for *S. cerevisiae*, causing a defence reaction of the yeasts. This involves, e.g., acetaldehyde being metabolised to acetic acid by Ald6 (Maestre *et al.* 2008). Therefore, acetaldehyde was a competitive inhibitor for isobutyraldehyde, which could explain the lack of IBA production in JWY16. Moreover, two NADPH are consumed per glucose to form acetic acid by Ald6, whereas only one $NADP^+$ is generated per glucose in the Ilv5 catalysed reaction. Thus, the toxic intracellular acetaldehyde was not only a competitive inhibitor but also may have caused an accumulation of NADPH. This further inhibited the $NADP^+$ dependent formation of IBA, whereas the NADH dependent formation of isobutanol from the common precursor isobutyraldehyde was favoured by the NADH accumulation. Since *S. cerevisiae* possesses up to five Adh, and the enzyme Sfa1, a basal alcohol dehydrogenase activity can be assumed for

JWY16, notwithstanding the *adh1* deletion (Smidt *et al.* 2012). Because of this, together with the NADH accumulation, isobutanol rather than IBA was produced in JWY16, despite *adh1* deletion and Ald6 expression. By using strain JWY04, in which *adh1* was not deleted, the limitations described above were circumvented. A yield of 9.8 mg/g_{Glc} corresponding to a titre of 295.4 mg/l, was achieved in cyt-ILV enzymes, NOX_{low} and Ald6 expressing JWY04 transformants in an aerobic shake flask cultivation with $SCD_{-valine}$. In the work of Yu *et al.* (2016), the maximum IBA titre of 56.8 mg/l in $YEPD_{2\%}$ is reported for *S. cerevisiae*, which is constitutively expressing the four enzymes Bat1, Aro10, Ald2 and Ald5. Assuming full glucose consumption, this corresponds to a yield of about 2.8 mg/g_{Glc}. Therefore, an IBA yield of 9.8 mg/g_{Glc} is, to our best knowledge, the highest yield that has been reported in *S. cerevisiae* so far.

6. ZUSAMMENFASSUNG

Die Endlichkeit fossiler Rohstoffe sowie die durch deren Nutzung verursachten Umweltprobleme machen alternative Technologien notwendig. Die Transformation von einer auf fossilen Rohstoffen basierenden Wirtschaft hin zu einer auf erneuerbarer Biomasse basierenden Wirtschaft nennt man "Bioökonomie". Gegenwärtig werden für die industrielle Großproduktion von biobasierten Chemikalien hauptsächlich primäre Kohlenstoffquellen wie bspw. Zuckerrohr, Maisstärke und Pflanzenöl verwendet. Daher besteht eine Herausforderung der Bioökonomie darin, das Spektrum der Kohlenstoffquellen zu erweitern, um auch lignozellulosehaltige Kohlenstoffquellen wie bspw. Ernteabfälle, forstwirtschaftliche Rückstände oder den kommunalen Bioabfall zu verwenden. So ließe sich die Konkurrenz zwischen landwirtschaftlicher Nahrungsmittelproduktion und Bioökonomie vermeiden. Doch nicht nur die Bereitstellung alternativer Kohlenstoffquellen, sondern auch die Entwicklung neuer Mikroorganismen, welche werthaltige Chemikalien produzieren, ist eine zentrale Herausforderung der Bioökonomie. Mikroorganismen sind oft keine natürlichen Produzenten eines gewünschten Produkts oder produzieren dieses nicht in kommerziell rentablen Ausbeuten. Durch Methoden der Systembiologie und synthetischen Biologie oder dem evolutionären und metabolischen Engineering wurden unterschiedlichste Mikroorganismen jedoch zur industriellen Biosynthese gewünschter Chemikalien befähigt. Die bekanntesten Mikroorganismen für die industrielle Biosynthese verschiedenster Produkte sind die Hefe *Saccharomyces cerevisiae* sowie die Bakterien *Corynebacterium glutamicum* und *Escherichia coli*.

S. cerevisiae wird vom Menschen seit Jahrtausenden für die mikrobielle Brot-, Bier- und Weinherstellung genutzt. Anders als die meisten Bakterien ist *S. cerevisiae* robust gegenüber Prozessen mit hoher Zuckerkonzentration, hohem osmotischem Druck oder niedrigem pH-Wert. Außerdem kann *S. cerevisiae* unter anaeroben Bedingungen kultiviert werden und ist resistent gegenüber unterschiedlichsten toxischen Produkten oder Inhibitoren aus Biomassen. Aufgrund des frühen Interesses und der robusten Eigenschaften ist *S. cerevisiae* ein gut untersuchter, eukaryotischer Modellorganismus geworden. Heute ist *S. cerevisiae* von der FDA als "Generally Recognized As Safe" (GRAS) Organismus anerkannt und kann ohne weitere Zulassung für die Lebensmittel- und Medikamentenproduktion verwendet werden. Daher werden mittlerweile komplexe Produkte wie bspw. Impfstoffe gegen

Hepatitis A und B, Aromastoffe, Insektenschutzmittel oder Feinchemikalien in *S. cerevisiae* produziert. Die größte industrielle Anwendung ist jedoch die Biosynthese von Bioethanol, welches als erster kommerzieller Benzinersatz verwendet wurde. Aufgrund seiner geringen Energiedichte und hohen Hygroskopizität ist Ethanol jedoch nicht optimal zur Kraftstoffbeimischung geeignet. *S. cerevisiae* bildet neben dem Hauptprodukt Ethanol auch langkettige Fuselalkohole, wie bspw. Butanole oder Amylalkohole, welche als Nicht-Ethanol Alternativen für die Biokraftstoffproduktion relevant sind. Unter den von *S. cerevisiae* produzierten Butanolisomeren ist Isobutanol der geeignetste Biokraftstoff um fossile Kraftstoffe zu ersetzen. Es besitzt einen höheren Flammpunkt, eine höhere Oktanzahl und Energiedichte sowie einen geringen Dampfdruck und ist weniger hygroskopisch als Ethanol. Daher kann Isobutanol besser als Ethanol mit der für die fossilen Kraftstoffe bestehenden Infrastruktur (bspw. Pipelines und Verbrennungsmotoren) verwendet werden.

S. cerevisiae ist ein natürlicher Produzent von Isobutanol, welches durch die Kombination der Valin Biosynthese und dessen Abbau durch den Ehrlichstoffwechselweg entsteht. Die Valin Biosynthese von *S. cerevisiae* ist in den Mitochondrien lokalisiert und wird mit der durch die Acetolactat Synthase (Ilv2) katalysierten Kondensation von zwei Pyruvatmolekülen zu 2-Acetolactat (ALAC) eingeleitet. Anschließend wird ALAC durch Acetohydroxysäure Reductoisomerase (Ilv5) durch Verbrauch von NADPH zu 2,3-Dihydroxyisovalerat (DIV) umgewandelt. Die Dihydroxysäure Dehydratase (Ilv3) dehydratisiert DIV anschließend zu 2-Ketoisovalerat (KIV). Durch die reversible Reaktion der Aminotransferasen Bat1 oder Bat2 wird KIV in einem letzten Schritt zu Valin umgewandelt. In *S. cerevisiae* werden Aminosäuren cytosolisch über den Ehrlichstoffwechselweg vergoren, wodurch unterschiedliche Fuselalkohole entstehen. Das Abbauprodukt der verzweigtkettigen Aminosäure Valin ist Isobutanol. Zuerst wird Valin erneut durch Bat1 oder Bat2 zu KIV desaminiert, welches anschließend zu Isobutyraldehyd decarboxyliert wird. Für die Decarboxylierung von Ketosäuren sind in *S. cerevisiae* viele Enzyme bekannt. Die Umwandlung von KIV zu Isobutyraldehyd wird jedoch vorrangig durch Pdc1, Pdc5 und Aro10 katalysiert. Anschließend wird Isobutyraldehyd von den vorhandenen Alkoholdehydrogenasen der Hefe unter NADH Verbrauch zu Isobutanol reduziert.

Die Kompartimentierung der mitochondriellen Valin Biosynthese und des cytosolischen Ehrlichstoffwechselwegs limitiert die Isobutanol Biosynthese in *S. cerevisiae*. Brat *et al.* (2012) zeigten, dass durch die cytosolische Relokalisierung von Ilv2Δ54, Ilv5Δ48 und Ilv3Δ19 durch N-terminale Verkürzung (zusammen bezeichnet als cyt-ILV), bei gleichzeitiger Deletion von *ilv2,* die Isobutanol Ausbeute in *S. cerevisiae* gesteigert wird. Trotz der gemeinsamen cytosolischen Lokalisierung der Valin Biosynthese und des Ehrlichstoffwechselwegs wurde nur eine maximale Isobutanol Ausbeute von 15 mg/g_{Glc} erreicht, was 3,7% der theoretischen Maximalausbeute von 410 mg/g_{Glc} entspricht. Dies deutet auf weiterhin existierende Limitationen bei der Isobutanol Biosynthese in *S. cerevisiae* hin, welche im Rahmen der vorliegenden Arbeit untersucht wurden.

Bei der von Brat *et al.* (2012) beschriebenen Isobutanol Biosynthese wurde Isobutanol aus bisher ungeklärten Gründen nur in Fermentationsmedien ohne Valin gebildet. Im Rahmen dieser Arbeit durchgeführte Wachstumstests auf Vollmedium zeigten, dass die Expression von Ilv2Δ54 ein defizitäres Wachstum verursachte, welches bei der Expression einer katalytisch inaktiven Ilv2Δ54^{E139A} nicht beobachtet wurde. Daher wurde die wachstumshemmende Wirkung von Ilv2Δ54 auf die katalytische Aktivität und nicht auf das cytosolische Protein zurückgeführt. Allerdings wurde in Wachstumstests auf Vollmedium für funktionell exprimiertes *ilvB* aus *C. glutamicum* kein defizitäres Wachstum beobachtet. Der unterschiedliche Wachstumsphänotyp beider ALS könnte auf die Substrat Spezifität von Ilv2Δ54 und *ilvB* zurückgeführt werden. Möglicherweise kondensierte Ilv2Δ54 andere cytosolische Ketosäuren effizienter als *ilvB*, sodass die Akkumulation anderer Folgeprodukte das Wachstumsdefizit verursachte. Unabhängig von der Ursache des defizitären Wachstumsphänotyps erzeugte die toxische Wirkung von Ilv2Δ54 jedoch eine negative Selektion auf das *ILV2Δ54* Gen. Die funktionelle Expression des *ILV2Δ54* Gens wurde daher nur durch die *ilv2* Deletion bei gleichzeitigem Ausschluss von Valin sichergestellt. Die bisher angenommene Ursache, dass Valin durch die Ilv6 Regulation eine inhibierende Wirkung auf die Aktivität von Ilv2Δ54 verursacht, konnte nicht bestätigt werden. Auch in Fermentationen mit der rückkopplungsunempfindlichen Ilv6Δ61^{N86A} oder mit *ilv6*Δ Mutanten verringerte sich durch Zugabe von Valin die Isobutanol Ausbeute deutlich. Allerdings wurde eine erhöhte Isobutanol Ausbeute bei zusätzlicher Expression von zytosolischem Ilv6Δ61 in valinfreiem Fermentationsmedium beobachtet, was auf die positive Regulation von

Ilv2Δ54 bei Abwesenheit von verzweigtkettigen Aminosäuren (BCAAs) durch Ilv6Δ61 zurückgeführt wird.

Eine weitere Einschränkung bei der Implementierung der Isobutanol Biosynthese als fermentativer Hauptstoffwechselweg ist das Co-Faktor Ungleichgewicht. In der Glykolyse werden pro Glukose zwei NADH generiert, während die Reduktion von Isobutyraldehyd zu Isobutanol nur ein NADH verbraucht. Die Ilv5Δ54 katalysierte Reaktion hingegen benötigt NADPH, welches in der Isobutanol Biosynthese nicht mehr zurückgewonnen wird. Die Isobutanol Biosynthese ist daher weder NADH noch NADPH neutral.

In dieser Arbeit wurde NADPH abhängiges Ilv5Δ48 durch bspw. eine NADH abhängige *ilvC*^{6E6} aus *E. coli* ersetzt und zusammen mit den Enzymen des Ehrlichstoffwechselwegs exprimiert, um Isobutanol NADH neutral und NADPH unabhängig zu produzieren. Jedoch reduzierte *ilvC*^{6E6} die DIV- und Isobutanol Ausbeute, was auf eine geringe *in vivo* Aktivität von *ilvC*^{6E6} schließen lässt. Folglich verbesserte die Expression von *ilvC*^{6E6} die NADH Balance nicht. Durch die Expression des Ehrlichstoffwechselwegs kam es jedoch zu einer geringeren Isobutanol- und Glycerin Ausbeute sowie einer verzehnfachten Acetoin Ausbeute. Die verringerte Glycerin Ausbeute konnte durch die NADH abhängige Adh2 Expression erklärt werden, wodurch mehr NADH für unterschiedliche Reduktionen verbraucht wurde. Dass die Enzyme des Ehrlichstoffwechselwegs trotz verbesserter NADH Balance eine geringere Isobutanol Ausbeute verursachten, lässt sich durch die Aro10 Expression erklären. Acetoin wurde durch Aro10 ausgehend von Pyruvat und Acetaldehyd auf eine NADH unabhängige Weise gebildet. Die Expression von Adh2 und Aro10 verbesserte somit die limitierende NADH Balance, erzeugte gleichzeitig aber eine Konkurrenz zwischen Ilv2Δ54 und Aro10 um das Substrat Pyruvat, was eine geringere Isobutanol Ausbeute verursachte.

Die alternative Strategie, den limitierenden NADH Überschuss in aeroben Schüttelkolbenfermentationen durch Expression einer NADH-Oxidase (NOX) abzubauen, wurde erfolgreich implementiert. Heterolog exprimierte NOX aus *S. pneumoniae,* welche die Oxidation von NADH unter Verwendung von O_2 katalysiert, erhöhte in verschiedenen Produzenten die Isobutanol Ausbeute. Die Isobutanol Ausbeute wurde so durch Reduzierung des NADH Überschusses gesteigert. Eine Limitierung der Isobutanol Biosynthese durch mangelnde

Verfügbarkeit von NADPH konnte in Experimenten mit *pgi1*Δ-Mutanten nicht nachgewiesen werden.

Während der zytosolischen Isobutanol Biosynthese wird DIV sekretiert, welches nicht mehr aufgenommen werden kann und somit für die weitere Isobutanol Biosynthese nicht mehr zur Verfügung steht. Die Sekretion von DIV wird auf eine geringe zytosolische Ilv3Δ19 Aktivität durch unzureichende Apo-Proteinbeladung mit [2Fe-2S] Eisen-Schwefel-Clustern (ISC) zurückgeführt, da im Zytosol von *S. cerevisiae* fast ausschließlich [4Fe-4S] ISC durch die zytosolische Eisen-Schwefel-Cluster (CIA) Maschinerie assembliert werden. In Zusammenarbeit mit Dr. Wesley Generoso wurde erfolglos versucht, die Sekretion von DIV durch kumulative Deletion verschiedener Transporter zu verhindern. Auch Versuche, die Wiederaufnahme von DIV zu ermöglichen, blieben erfolglos (Generoso *et al.* 2017).

In Wachstumstests auf festem SCD_{-Valin} Medium mit *ilv3*Δ Mutanten, welche unterschiedliche Dihydroxysäure Dehydratasen (DHAD) exprimierten, wurden mehrere *ilv3*Δ komplementierende DHADs identifiziert. Diese stammten aus den Organismen *Xenorhabdus nematophila, Neurospora crassa*, *Citrobacter sp.* 30_2, *Corynebacterium glutamicum*, *Pectobacterium carotovorum* und *E. coli*. Allerdings besaß keine der heterologen DHAD eine deutlich bessere *in vivo* Aktivität als Ilv3Δ19. Daher wurde im Rahmen dieser Arbeit vorrangig versucht, die Ilv3Δ19 Apo-Proteinbeladung mit [2Fe-2S] ISC zu optimieren. Durch die Deletion von *fra2* oder *pim1* wurde die in den Mitochondrien beginnende ISC Assemblierung optimiert, um die ISC Verfügbarkeit im Produzenten zu erhöhen. Bei der zytosolischen Isobutanol Biosynthese nach Brat *et al.* (2012) exprimierten die Produzenten jedoch auch natives Ilv3, weshalb durch die *fra2* oder *pim1* Deletion vorrangig die Ilv3 Apo-Protein Reifung verbessert wurde. Dies führte zwar zu höheren Isobutanol Ausbeuten, aber verhinderte die Sekretion von zytosolischen DIV nicht.

Eine andere Strategie, um die DIV Sekretion zu minimieren, war die gezielte Beladung von Ilv3Δ19 mit [2Fe-2S] ISC durch die Expression von Grx5Δ29. In *S. cerevisiae* wird das Ilv3 Apo-Protein natürlicherweise in den Mitochondrien von Grx5 mit [2Fe-2S] ISC beladen, wodurch das funktionelle Holo-Enzym entsteht. Durch die zytosolische Expression von Grx5Δ29 konnte Ilv3Δ19 gezielt auf eine CIA-unabhängige Weise mit [2Fe-2S] ISC beladen werden, was zu einer verringerten DIV Sekretion bei gleichzeitig gesteigerter Isobutanol Biosynthese führte.

Jedoch wurden nicht nur Limitierungen des cytosolischen Isobutanol Stoffwechselwegs untersucht, sondern auch der Produzent *S. cerevisiae* für die zytosolische Isobutanol Biosynthese optimiert. In Zusammenarbeit mit Dr. Johannes Wess wurden Gene von konkurrierenden Enzymen kumulativ deletiert, welche Stoffwechselwege mit den Intermediaten der Isobutanol Biosynthese verbanden. Der daraus resultierende Produzent JWY23 (Cen.PK113-7D *Δilv2; Δbdh1; Δbdh2; Δleu4; Δleu9; Δecm31; Δilv1; Δadh1; Δgpd1; Δgpd2; Δald6)* erzielte durch Expression der cyt-ILV Enzyme eine Isobutanol Ausbeute von 67,3 mg/g_{Glc}.

Des Weiteren wurden für evolutionäres Engineering die cyt-ILV Gene in den *ilv2* Locus von CEN.PK113-7D integriert (MBY29), statt diese mittels eines *2µ* multi-copy Vektors zu exprimieren. MBY29 wurde anschließend in $SCD_{4\%\text{-Valin}+0.5\%\text{ Prolin}+10\text{ g/l Norvalin}}$ ($SCD_{Norvalin}$) Flüssigmedium evolviert. Norvalin ist ein Aminosäureanalogon von Valin und wird gleichermaßen durch die Aminoacyl-tRNA-Synthetasen an die tRNA gebunden, was den anschließenden Proteineinbau während der Translation ermöglicht. Aufgrund der unterschiedlichen Struktur von Norvalin und Valin kommt es dadurch zu nicht funktionellen Proteinen; dies beeinträchtigt die Lebensfähigkeit des Organismus. Durch die Zugabe von Norvalin zum Fermentationsmedium wird ein Selektionsdruck erzeugt, der bspw. durch erhöhte Valin Produktion abgeschwächt werden kann. Da KIV die gemeinsame Vorstufe von Valin und Isobutanol ist, kann die erhöhte Valin Produktion auch zu einer erhöhten Isobutanol Biosynthese führen.

Nach mehrtägiger Evolution von MBY29 in $SCD_{Norvalin}$ wurden erfolgreich Einzelklone isoliert, die gegenüber MBY29 ein verbessertes Wachstum in valinfreiem Medium besaßen. Ebenso zeigten die isolierten Einzelklone erhöhte DIV und Isobutanol Ausbeuten, welche mit maximal 0,59 mg/g_{Glc} dennoch geringer waren als bei der Expression der cyt-ILV Enzyme von einem *2µ* multi-copy Vektor. Durch Genomsequenzierung der erfolgreich evolvierten und isolierten Einzelklone konnten jedoch keine Gene identifiziert werden, die für die verbesserte Valin Biosynthese verantwortlich waren. Stattdessen kam es während der Evolution auf $SCD_{Norvalin}$ zu Gendosierungseffekten, welche die verbesserte Valin Biosynthese verursachten.

Die vielversprechendsten Ansätze in Bezug auf die Isobutanol Produktion wurden abschließend im besten verfügbaren Isobutanol Produzenten JWY23 bestätigt. Alle getesteten Ansätze, nämlich die Deletion von *fra2* sowie die Expression von

Grx5Δ29, Ilv6Δ61 und NOX, führten zu einer Steigerung der Isobutanol Ausbeute. Die höchste Isobutanol Ausbeute dieser Arbeit wurde mit 72 mg/g_{Glc} für Ilv6Δ61 exprimierende JWY23 Transformanten beobachtet, was 17,6% der theoretisch maximalen Ausbeute entspricht.

Isobuttersäure Produktion

Isobuttersäure (IBA) ist ein bei der Isobutanol Biosynthese unerwünschtes Nebenprodukt, das von der Industrie jedoch auch als werthaltige Plattformchemikalie betrachtet wird. Wie Isobutanol, wird auch IBA derzeit hauptsächlich aus fossilen Ressourcen gewonnen. Daher wurden die für die Isobutanol Biosynthese förderlichen Erkenntnisse aus dieser Arbeit auch für die Biosynthese von IBA verwendet. Im Zytosol von *S. cerevisiae* wird Isobutyraldehyd von Ald6 unter NADPH Verbrauch zu IBA oxidiert. Da die Ilv5Δ48 Reaktion zuvor NADPH erzeugt, ist der IBA Stoffwechselweg NADPH neutral. Um IBA als fermentativen Hauptstoffwechselweg zu etablieren, muss das NADH Ungleichgewicht der Glykolyse analog zur Isobutanol Biosynthese beseitigt werden. Unter allen getesteten Ansätzen wurde die höchste IBA Ausbeute in einer $SCD_{4\%\text{-Valin}}$ Schüttelkolbenfermentation mit einer cyt-ILV Enzyme, NOX und Ald6 exprimierenden JWY04 Transformante (Cen.PK113-7D *Δilv2; Δbdh1; Δbdh2; Δleu4; Δleu9; Δecm31; Δilv1*) beobachtet. Die IBA Ausbeute von 9,8 mg/g_{Glc} (Titer von 295,4 mg/l) entsprach einer 791%igen Steigerung gegenüber der Kontrolle und ist nach unserem Kenntnisstand die höchste IBA Ausbeute, die bisher für *S. cerevisiae* berichtet wurde.

7. REFERENCES

Agmon, N; Mitchell, LA; Cai, Y; Ikushima, S; Chuang, J; Zheng, A; Choi, W-J; Martin, JA; Caravelli, K; Stracquadanio, G; Boeke, JD (2015): Yeast Golden Gate (yGG) for the Efficient Assembly of *S. cerevisiae* Transcription Units. In *ACS synthetic biology* 4 (7), pp. 853–859. DOI: 10.1021/sb500372z.

Albrecht, AG; Netz, DJA; Miethke, M; Pierik, AJ; Burghaus, O; Peuckert, F; Lill, R; Marahiel, MA (2010): SufU is an essential iron-sulfur cluster scaffold protein in *Bacillus subtilis*. In *Journal of bacteriology* 192 (6), pp. 1643–1651. DOI: 10.1128/JB.01536-09.

Altmiller, DH; Wagner, RP (1970): Purification and properties of dihydroxy acid dehydratase from soluble and mitochondrial fractions of *Neurospora crassa*. In *Archives of biochemistry and biophysics* 138 (1), pp. 160–170. DOI: 10.1016/0003-9861(70)90295-x.

Altschul, SF; Wootton, JC; Gertz, EM; Agarwala, R; Morgulis, A; Schäffer, AA; Yu, Y-K (2005): Protein database searches using compositionally adjusted substitution matrices. In *The FEBS journal* 272 (20), pp. 5101–5109. DOI: 10.1111/j.1742-4658.2005.04945.x.

Arfin, SM; Ratzkin, B; Umbarger, HE (1969): The metabolism of valine and isoleucine in *Escherichia coli* XVII the role of induction in the depression of acetohydroxy acid isomeroreductase. In *Biochemical and Biophysical Research Communications* 37 (6), pp. 902–908. DOI: 10.1016/0006-291X(69)90216-2.

Atsumi, S; Hanai, T; Liao, JC (2008): Non-fermentative pathways for synthesis of branched-chain higher alcohols as biofuels. In *Nature* 451 (7174), pp. 86–89. DOI: 10.1038/nature06450.

Atsumi, S; Wu, T-Y; Eckl, E-M; Hawkins, SD; Buelter, T; Liao, JC (2010): Engineering the isobutanol biosynthetic pathway in *Escherichia coli* by comparison of three aldehyde reductase/alcohol dehydrogenase genes. In *Applied microbiology and biotechnology* 85 (3), pp. 651–657. DOI: 10.1007/s00253-009-2085-6.

Avalos, JL; Fink, GR; Stephanopoulos, G (2013): Compartmentalization of metabolic pathways in yeast mitochondria improves production of branched chain alcohols. In *Nature biotechnology* 31 (4), pp. 335–341. DOI: 10.1038/nbt.2509.

Avendaño, A; DeLuna, A; Olivera, H; Valenzuela, L; Gonzalez, A (1997): *GDH3* encodes a glutamate dehydrogenase isozyme, a previously unrecognized route for glutamate biosynthesis in *Saccharomyces cerevisiae*. In *Journal of bacteriology* 179 (17), pp. 5594–5597. DOI: 10.1128/jb.179.17.5594-5597.1997.

Baeshen, NA; Baeshen, MN; Sheikh, A; Bora, RS; Ahmed, MMM; Ramadan, HAI; Saini, KS; Redwan, EM (2014): Cell factories for insulin production. In *Microb Cell Fact* 13 (1), p. 141. DOI: 10.1186/s12934-014-0141-0.

Bai, W; Geng, W; Wang, S; Zhang, F (2019): Biosynthesis, regulation, and engineering of microbially produced branched biofuels. In *Biotechnology for Biofuels* 12, p. 84. DOI: 10.1186/s13068-019-1424-9.

Bakker, BM; Overkamp, KM; van Maris, AJ; Kötter, P; Luttik, MA; van Dijken, JP; Pronk, JT (2001): Stoichiometry and compartmentation of NADH metabolism in *Saccharomyces cerevisiae*. In *FEMS microbiology reviews* 25 (1), pp. 15–37. DOI: 10.1111/j.1574-6976.2001.tb00570.x.

Banat, IM; Satpute, SK; Cameotra, SS; Patil, R; Nyayanit, NV (2014): Cost effective technologies and renewable substrates for biosurfactants' production. In *Frontiers in microbiology* 5, p. 697. DOI: 10.3389/fmicb.2014.00697.

Barrick, JE; Lenski, RE (2013): Genome dynamics during experimental evolution. In *Nature reviews. Genetics* 14 (12), pp. 827–839. DOI: 10.1038/nrg3564.

Bastian, S; Liu, X; Meyerowitz, JT; Snow, CD; Chen, MMY; Arnold, FH (2011): Engineered ketol-acid reductoisomerase and alcohol dehydrogenase enable anaerobic 2-methylpropan-1-ol production at theoretical yield in *Escherichia coli*. In *Metabolic engineering* 13 (3), pp. 345–352. DOI: 10.1016/j.ymben.2011.02.004.

Benisch, F; Boles, E (2014): The bacterial Entner-Doudoroff pathway does not replace glycolysis in *Saccharomyces cerevisiae* due to the lack of activity of ironsulfur cluster enzyme 6-phosphogluconate dehydratase. In *Journal of Biotechnology* 171, pp. 45–55. DOI: 10.1016/j.jbiotec.2013.11.025.

Borodina, I; Nielsen, J (2014): Advances in metabolic engineering of yeast *Saccharomyces cerevisiae* for production of chemicals. In *Biotechnology journal* 9 (5), pp. 609–620. DOI: 10.1002/biot.201300445.

Brat, D; Weber, C; Lorenzen, W; Bode, HB; Boles, E (2012): Cytosolic re-localization and optimization of valine synthesis and catabolism enables increased isobutanol production with the yeast *Saccharomyces cerevisiae*. In *Biotechnology for Biofuels* 5 (1), p. 65. DOI: 10.1186/1754-6834-5-65.

Braymer, JJ; Freibert, SA; Rakwalska-Bange, M; Lill, R (2021): Mechanistic concepts of iron-sulfur protein biogenesis in Biology. In *Biochimica et biophysica acta. Molecular cell research* 1868 (1), p. 118863. DOI: 10.1016/j.bbamcr.2020.118863.

Braymer, JJ; Lill, R (2017): Iron-sulfur cluster biogenesis and trafficking in mitochondria. In *The Journal of biological chemistry* 292 (31), pp. 12754–12763. DOI: 10.1074/jbc.R117.787101.

Brinkmann-Chen, S; Flock, T; Cahn, JKB; Snow, CD; Brustad, EM; McIntosh, JA; Meinhold, P; Zhang, L; Arnold, FH (2013): General approach to reversing ketol-acid reductoisomerase cofactor dependence from NADPH to NADH. In *Proceedings of the National Academy of Sciences of the United States of America* 110 (27), pp. 10946–10951. DOI: 10.1073/pnas.1306073110.

Bruder, S; Reifenrath, M; Thomik, T; Boles, E; Herzog, K (2016): Parallelised online biomass monitoring in shake flasks enables efficient strain and carbon source dependent growth characterisation of *Saccharomyces cerevisiae*. In *Microbial cell factories* 15 (1), p. 127. DOI: 10.1186/s12934-016-0526-3.

Buijs, NA; Siewers, V; Nielsen, J (2013): Advanced biofuel production by the yeast *Saccharomyces cerevisiae*. In *Current opinion in chemical biology* 17 (3), pp. 480–488. DOI: 10.1016/j.cbpa.2013.03.036.

Bussey, H; Umbarger, HE (1969): Biosynthesis of branched chain amino acids in yeast: regulation of synthesis of the enzymes of isoleucine and valine biosynthesis. In *Journal of bacteriology* 98 (2), pp. 623–628. DOI: 10.1128/JB.98.2.623-628.1969.

Carlsen, S; Ajikumar, PK; Formenti, LR; Zhou, K; Phon, TH; Nielsen, ML; Lantz, AE; Kielland-Brandt, MC; Stephanopoulos, G (2013): Heterologous expression and characterization of bacterial 2-C-methyl-D-erythritol-4-phosphate pathway in *Saccharomyces cerevisiae*. In *Applied microbiology and biotechnology* 97 (13), pp. 5753–5769. DOI: 10.1007/s00253-013-4877-y.

Chae, TU; Choi, SY; Kim, JW; Ko, Y-S; Lee, SY (2017): Recent advances in systems metabolic engineering tools and strategies. In *Current opinion in biotechnology* 47, pp. 67–82. DOI: 10.1016/j.copbio.2017.06.007.

Chen, C-Y; Ko, T-P; Lin, K-F; Lin, B-L; Huang, C-H; Chiang, C-H; Horng, J-C (2018): NADH/NADPH bi-cofactor-utilizing and thermoactive ketol-acid reductoisomerase from *Sulfolobus acidocaldarius*. In *Scientific reports* 8 (1), p. 7176. DOI: 10.1038/s41598-018-25361-4.

Chen, GC; Jordan, F (1984): Brewers' yeast pyruvate decarboxylase produces acetoin from acetaldehyde: a novel tool to study the mechanism of steps subsequent to carbon dioxide loss. In *Biochemistry* 23 (16), pp. 3576–3582. DOI: 10.1021/bi00311a002.

Chen, X; Nielsen, KF; Borodina, I; Kielland-Brandt, MC; Karhumaa, K (2011): Increased isobutanol production in *Saccharomyces cerevisiae* by overexpression of genes in valine metabolism. In *Biotechnology for Biofuels* 4, p. 21. DOI: 10.1186/1754-6834-4-21.

Chi, C-B; Tang, Y; Zhang, J; Dai, Y-N; Abdalla, M; Chen, Y; Zhou, C-Z (2018): Structural and biochemical insights into the multiple functions of yeast Grx3. In *Journal of molecular biology* 430 (8), pp. 1235–1248. DOI: 10.1016/j.jmb.2018.02.024.

Choi, KR; Jang, WD; Yang, D; Cho, JS; Park, D; Lee, SY (2019): Systems metabolic engineering strategies: integrating systems and synthetic biology with metabolic engineering. In *Trends in Biotechnology* 37 (8), pp. 817–837. DOI: 10.1016/j.tibtech.2019.01.003.

Chunduru, SK; Mrachko, GT; Calvo, KC (1989): Mechanism of ketol acid reductoisomerase-steady-state analysis and metal ion requirement. In *Biochemistry* 28 (2), pp. 486–493. DOI: 10.1021/bi00428a012.

Ciesielski, SJ; Schilke, B; Marszalek, J; Craig, EA (2016): Protection of scaffold protein Isu from degradation by the Lon protease Pim1 as a component of Fe-S cluster biogenesis regulation. In *Molecular biology of the cell* 27 (7), pp. 1060–1068. DOI: 10.1091/mbc.E15-12-0815.

Colón, M; Hernández, F; López, K; Quezada, H; González, J; López, G; Aranda, C; González, A (2011): *Saccharomyces cerevisiae* Bat1 and Bat2 aminotransferases have functionally diverged from the ancestral-like *Kluyveromyces lactis* orthologous enzyme. In *PLOS ONE* 6 (1), e16099. DOI: 10.1371/journal.pone.0016099.

Conant, GC; Wolfe, KH (2007): Increased glycolytic flux as an outcome of whole-genome duplication in yeast. In *Molecular systems biology* 3, p. 129. DOI: 10.1038/msb4100170.

Copley, SD (2012): Moonlighting is mainstream: paradigm adjustment required. In *BioEssays : news and reviews in molecular, cellular and developmental biology* 34 (7), pp. 578–588. DOI: 10.1002/bies.201100191.

Cordes, C; Möckel, B; Eggeling, L; Sahm, H (1992): Cloning, organization and functional analysis of *ilvA, ilvB* and *ilvC* genes from *Corynebacterium glutamicum*. In *Gene* 112 (1), pp. 113–116. DOI: 10.1016/0378-1119(92)90311-C.

Courel, M; Lallet, S; Camadro, J-M; Blaiseau, P-L (2005): Direct activation of genes involved in intracellular iron use by the yeast iron-responsive transcription factor Aft2 without its paralog Aft1. In *Molecular and Cellular Biology* 25 (15), pp. 6760–6771. DOI: 10.1128/MCB.25.15.6760-6771.2005.

Crippa, M; Guizzardi, D; Muntean, M; Schaaf, E; Solazzo, E; Monforti-Ferrario, F; Olivier, J; Vignati, E (2020): Fossil CO_2 and GHG emissions of all world countries - 2020 report. In *Publications Office of the European Union,* Luxembourg 2020. DOI: 10.2760/56420.

Cullin, C; Baudin-Baillieu, A; Guillemet, E; Ozier-Kalogeropoulos, O (1996): Functional analysis of *YCL09C*: Evidence for a role as the regulatory subunit of acetolactate synthase. In *Yeast* 12 (15), pp. 1511–1518. DOI: 10.1002/(SICI)1097-0061(199612)12:15<1511::AID-YEA41>3.0.CO;2-B.

Dasari, S; Kölling, R (2011): Cytosolic localization of acetohydroxyacid synthase Ilv2 and its impact on diacetyl formation during beer fermentation. In *Applied and environmental microbiology* 77 (3), pp. 727–731. DOI: 10.1128/AEM.01579-10.

DeLuna, A; Avendano, A; Riego, L; Gonzalez, A (2001): NADP-glutamate dehydrogenase isoenzymes of *Saccharomyces cerevisiae*. Purification, kinetic properties, and physiological roles. In *The Journal of biological chemistry* 276 (47), pp. 43775–43783. DOI: 10.1074/jbc.M107986200.

Dereeper, A; Guignon, V; Blanc, G; Audic, S; Buffet, S; Chevenet, F; Dufayard, J-F; Guindon, S; Lefort, V; Lescot, M; Claverie, J-M; Gascuel, O (2008): Phylogeny.fr: robust phylogenetic analysis for the non-specialist. In *Nucleic acids research* 36 (Web Server issue), W465-9. DOI: 10.1093/nar/gkn180.

Dickinson, JR; Harrison, SJ; Hewlins, MJ (1998): An investigation of the metabolism of valine to isobutyl alcohol in *Saccharomyces cerevisiae*. In *The Journal of biological chemistry* 273 (40), pp. 25751–25756. DOI: 10.1074/jbc.273.40.25751.

Dickinson, JR; Lanterman, MM; Danner, DJ; Pearson, BM; Sanz, P; Harrison, SJ; Hewlins, MJ (1997): A ^{13}C nuclear magnetic resonance investigation of the metabolism of leucine to isoamyl alcohol in *Saccharomyces cerevisiae*. In *The Journal of biological chemistry* 272 (43), pp. 26871–26878. DOI: 10.1074/jbc.272.43.26871.

Dickinson, JR; Salgado, LEJ; Hewlins, MJE (2003): The catabolism of amino acids to long chain and complex alcohols in *Saccharomyces cerevisiae*. In *The Journal of biological chemistry* 278 (10), pp. 8028–8034. DOI: 10.1074/jbc.M211914200.

Dijken, JP; Scheffers, AW (1986): Redox balances in the metabolism of sugars by yeasts. In *FEMS Microbiology Letters* 32 (3-4), pp. 199–224. DOI: 10.1111/j.1574-6968.1986.tb01194.x.

Dower, WJ; Miller, JF; Ragsdale, CW (1988): High efficiency transformation of *E. coli* by high voltage electroporation. In *Nucleic acids research* 16 (13), pp. 6127–6145. DOI: 10.1093/nar/16.13.6127.

Duggleby, RG (1997): Identification of an acetolactate synthase small subunit gene in two eukaryotes. In *Gene* 190 (2), pp. 245–249. DOI: 10.1016/S0378-1119(97)00002-4.

Dundon, CA; Aristidou, A; Hawkins, A; Lies, D; Albert, L (2009): Methods of increasing dihydroxy acid dehydratase activity to improve production of fuels, chemicals, and amino acids. Gevo Inc. (US8273565B2).

Eden, A; Simchen, G; Benvenisty, N (1996): Two yeast homologs of *ECA39*, a target for c-Myc regulation, code for cytosolic and mitochondrial branched-chain amino acid aminotransferases. In *The Journal of biological chemistry* 271 (34), pp. 20242–20245. DOI: 10.1074/jbc.271.34.20242.

Eden, A; van Nedervelde, L; Drukker, M; Benvenisty, N; Debourg, A (2001): Involvement of branched-chain amino acid aminotransferases in the production of fusel alcohols during fermentation in yeast. In *Applied microbiology and biotechnology* 55 (3), pp. 296–300. DOI: 10.1007/s002530000506.

Eggeling, I; Cordes, C; Eggeling, L; Sahm, H (1987): Regulation of acetohydroxy acid synthase in *Corynebacterium glutamicum* during fermentation of *α*-ketobutyrate to l-isoleucine. In *Appl Microbiol Biotechnol* 25 (4). DOI: 10.1007/BF00252545.

Ehrlich, F (1907): Über die Bedingungen der Fuselölbildung und über ihren Zusammenhang mit dem Eiweißaufbau der Hefe. In *Berichte der deutschen chemischen Gesellschaft* 40 (1), pp. 1027–1047. DOI: 10.1002/cber.190704001156.

Elisakova, V; Patek, M; Holatko, J; Nesvera, J; Leyval, D; Goergen, J-L; Delaunay, S (2005): Feedback-resistant acetohydroxy acid synthase increases valine production in *Corynebacterium glutamicum*. In *Applied and environmental microbiology* 71 (1), pp. 207–213. DOI: 10.1128/AEM.71.1.207-213.2005.

Engler, C; Gruetzner, R; Kandzia, R; Marillonnet, S (2009): Golden gate shuffling: a one-pot DNA shuffling method based on type IIs restriction enzymes. In *PLOS ONE* 4 (5), e5553. DOI: 10.1371/journal.pone.0005553.

Espinosa-Cantú, A; Ascencio, D; Herrera-Basurto, S; Xu, J; Roguev, A; Krogan, NJ; DeLuna, A (2017): Protein moonlighting revealed by noncatalytic phenotypes of yeast enzymes. In *Genetics* 208 (1), pp. 419–431. DOI: 10.1534/genetics.117.300377.

Flint, DH; Emptage, MH; Finnegan, MG; Fu, W; Johnson, MK (1993): The role and properties of the iron-sulfur cluster in *Escherichia coli* dihydroxyacid dehydratase. In *The Journal of biological chemistry* 268 (20), pp. 14732–14742. DOI: 10.1016/S0021-9258(18)82394-8.

Fong, SS; Burgard, AP; Herring, CD; Knight, EM; Blattner, FR; Maranas, CD; Palsson, BO (2005): In silico design and adaptive evolution of *Escherichia coli* for production of lactic acid. In *Biotechnology and bioengineering* 91 (5), pp. 643–648. DOI: 10.1002/bit.20542.

Furuya, T; Arai, Y; Kino, K (2012): Biotechnological production of caffeic acid by bacterial cytochrome P450 CYP199A2. In *Applied and environmental microbiology* 78 (17), pp. 6087–6094. DOI: 10.1128/AEM.01103-12.

Garrett, JM (2008): Amino acid transport through the *Saccharomyces cerevisiae* Gap1 permease is controlled by the Ras/cAMP pathway. In *The international journal of biochemistry & cell biology* 40 (3), pp. 496–502. DOI: 10.1016/j.biocel.2007.08.012.

Generoso, WC; Brinek, M; Dietz, H; Oreb, M; Boles, E (2017): Secretion of 2,3-dihydroxyisovalerate as a limiting factor for isobutanol production in *Saccharomyces cerevisiae*. In *FEMS yeast research* 17 (3). DOI: 10.1093/femsyr/fox029.

Generoso, WC; Gottardi, M; Oreb, M; Boles, E (2016): Simplified CRISPR-Cas genome editing for *Saccharomyces cerevisiae*. In *Journal of microbiological methods* 127, pp. 203–205. DOI: 10.1016/j.mimet.2016.06.020.

Generoso, WC; Schadeweg, V; Oreb, M; Boles, E (2015): Metabolic engineering of *Saccharomyces cerevisiae* for production of butanol isomers. In *Current opinion in biotechnology* 33, pp. 1–7. DOI: 10.1016/j.copbio.2014.09.004.

Gibson, DG; Young, L; Chuang, R-Y; Venter, JC; Hutchison, CA; Smith, HO (2009): Enzymatic assembly of DNA molecules up to several hundred kilobases. In *Nature methods* 6 (5), pp. 343–345. DOI: 10.1038/nmeth.1318.

Gietz, RD; Schiestl, RH (2007): High-efficiency yeast transformation using the LiAc/SS carrier DNA/PEG method. In *Nature protocols* 2 (1), pp. 31–34. DOI: 10.1038/nprot.2007.13.

Grote, A; Hiller, K; Scheer, M; Münch, R; Nörtemann, B; Hempel, DC; Jahn, D (2005): JCat: a novel tool to adapt codon usage of a target gene to its potential expression host. In *Nucleic acids research* 33 (Web Server issue), W526-31. DOI: 10.1093/nar/gki376.

Guo, M; Song, W (2019): The growing U.S. bioeconomy: Drivers, development and constraints. In *New biotechnology* 49, pp. 48–57. DOI: 10.1016/j.nbt.2018.08.005.

Hammer, SK; Avalos, JL (2017): Harnessing yeast organelles for metabolic engineering. In *Nat Chem Biol* 13 (8), pp. 823–832. DOI: 10.1038/nchembio.2429.

Hazelwood, LA; Daran, J-M; van Maris, AJA; Pronk, JT; Dickinson, JR (2008): The Ehrlich pathway for fusel alcohol production: a century of research on *Saccharomyces cerevisiae* metabolism. In *Applied and environmental microbiology* 74 (8), pp. 2259–2266. DOI: 10.1128/AEM.02625-07.

Heijne, G von (1986): Mitochondrial targeting sequences may form amphiphilic helices. In *The EMBO Journal* 5 (6), pp. 1335–1342.

Henikoff, S; Henikoff, JG (1992): Amino acid substitution matrices from protein blocks. In *Proceedings of the National Academy of Sciences of the United States of America* 89 (22), pp. 10915–10919. DOI: 10.1073/pnas.89.22.10915.

Henritzi, S; Fischer, M; Grininger, M; Oreb, M; Boles, E (2018): An engineered fatty acid synthase combined with a carboxylic acid reductase enables de novo production of 1-octanol in *Saccharomyces cerevisiae*. In *Biotechnol Biofuels* 11 (1), pp. 1–12. DOI: 10.1186/s13068-018-1149-1.

Heux, S; Cadiere, A; Dequin, S (2008): Glucose utilization of strains lacking *PGI1* and expressing a transhydrogenase suggests differences in the pentose phosphate capacity among *Saccharomyces cerevisiae* strains. In *FEMS Yeast Res* 8 (2), pp. 217–224. DOI: 10.1111/j.1567-1364.2007.00330.x.

Ida, K; Ishii, J; Matsuda, F; Kondo, T; Kondo, A (2015): Eliminating the isoleucine biosynthetic pathway to reduce competitive carbon outflow during isobutanol production by *Saccharomyces cerevisiae*. In *Microbial cell factories* 14, p. 62. DOI: 10.1186/s12934-015-0240-6.

Ihrig, J; Hausmann, A; Hain, A; Richter, N; Hamza, I; Lill, R; Mühlenhoff, U (2010): Iron regulation through the back door: iron-dependent metabolite levels contribute to transcriptional adaptation to iron deprivation in *Saccharomyces cerevisiae*. In *Eukaryotic cell* 9 (3), pp. 460–471. DOI: 10.1128/EC.00213-09.

Ishii, J; Morita, K; Ida, K; Kato, H; Kinoshita, S; Hataya, S; Shimizu, H; Kondo, A; Matsuda, F (2018): A pyruvate carbon flux tugging strategy for increasing 2,3-butanediol production and reducing ethanol subgeneration in the yeast *Saccharomyces cerevisiae*. In *Biotechnology for Biofuels* 11, p. 180. DOI: 10.1186/s13068-018-1176-y.

Jansen, MLA; Bracher, JM; Papapetridis, I; Verhoeven, MD; Bruijn, H de; Waal, PP de; van Maris, AJA; Klaassen, P; Pronk, JT (2017): *Saccharomyces cerevisiae* strains for second-generation ethanol production: from academic exploration to industrial implementation. In *FEMS yeast research* 17 (5). DOI: 10.1093/femsyr/fox044.

Jeffery, CJ (1999): Moonlighting proteins. In *Trends in Biochemical Sciences* 24 (1), pp. 8–11. DOI: 10.1016/S0968-0004(98)01335-8.

Johnson, CW; Salvachúa, D; Khanna, P; Smith, H; Peterson, DJ; Beckham, GT (2016): Enhancing muconic acid production from glucose and lignin-derived aromatic compounds *via* increased protocatechuate decarboxylase activity. In *Metabolic engineering communications* 3, pp. 111–119. DOI: 10.1016/j.meteno.2016.04.002.

Kakar, SN; Wagner, RP (1964): Genetic and biochemical Analysis of isoleucine-valine mutants of yeast. In *Genetics* 49 (2), pp. 213–222.

Kallscheuer, N; Vogt, M; Stenzel, A; Gätgens, J; Bott, M; Marienhagen, J (2016): Construction of a *Corynebacterium glutamicum* platform strain for the production of stilbenes and (2S)-flavanones. In *Metabolic engineering* 38, pp. 47–55. DOI: 10.1016/j.ymben.2016.06.003.

Kaplan, CD; Kaplan, J (2009): Iron acquisition and transcriptional regulation. In *Chemical reviews* 109 (10), pp. 4536–4552. DOI: 10.1021/cr9001676.

Kim, S; Bae, S-J; Hahn, J-S (2016): Redirection of pyruvate flux toward desired metabolic pathways through substrate channeling between pyruvate kinase and pyruvate-converting enzymes in *Saccharomyces cerevisiae*. In *Scientific reports* 6, p. 24145. DOI: 10.1038/srep24145.

Kingsbury, JM; Yang, Z; Ganous, TM; Cox, GM; McCusker, JH (2004): *Cryptococcus neoformans* Ilv2p confers resistance to sulfometuron methyl and is required for survival at 37 °C and *in vivo*. In *Microbiology (Reading, England)* 150 (Pt 5), pp. 1547–1558. DOI: 10.1099/mic.0.26928-0.

Kircher, M (2015): Sustainability of biofuels and renewable chemicals production from biomass. In *Current opinion in chemical biology* 29, pp. 26–31. DOI: 10.1016/j.cbpa.2015.07.010.

Kondo, T; Tezuka, H; Ishii, J; Matsuda, F; Ogino, C; Kondo, A (2012): Genetic engineering to enhance the Ehrlich pathway and alter carbon flux for increased isobutanol production from glucose by *Saccharomyces cerevisiae*. In *Journal of Biotechnology* 159 (1-2), pp. 32–37. DOI: 10.1016/j.jbiotec.2012.01.022.

Kondrashov, FA; Rogozin, IB; Wolf, YI; Koonin, EV (2002): Selection in the evolution of gene duplications. In *Genome biology* 3 (2), RESEARCH0008. DOI: 10.1186/gb-2002-3-2-research0008.

Kulawiak, B; Höpker, J; Gebert, M; Guiard, B; Wiedemann, N; Gebert, N (2013): The mitochondrial protein import machinery has multiple connections to the respiratory chain. In *Biochimica et Biophysica Acta (BBA) - Bioenergetics* 1827 (5), pp. 612–626. DOI: 10.1016/j.bbabio.2012.12.004.

Kumánovics, A; Chen, OS; Li, L; Bagley, D; Adkins, EM; Lin, H; Dingra, NN; Outten, CE; Keller, G; Winge, D; Ward, DM; Kaplan, J (2008): Identification of *FRA1* and *FRA2* as genes involved in regulating the yeast iron regulon in response to decreased mitochondrial ironsulfur cluster synthesis. In *The Journal of biological chemistry* 283 (16), pp. 10276–10286. DOI: 10.1074/jbc.M801160200.

Lang, K; Zierow, J; Buehler, K; Schmid, A (2014): Metabolic engineering of *Pseudomonas sp.* strain VLB120 as platform biocatalyst for the production of isobutyric acid and other secondary metabolites. In *Microb Cell Fact* 13 (1), p. 2. DOI: 10.1186/1475-2859-13-2.

Larroy, C; Parés, X; Biosca, JA (2002): Characterization of a Saccharomyces cerevisiae NADP(H)-dependent alcohol dehydrogenase (ADHVII), a member of the cinnamyl alcohol dehydrogenase family. In *European journal of biochemistry* 269 (22), pp. 5738–5745. DOI: 10.1046/j.1432-1033.2002.03296.x.

Lee, JW; Na, D; Park, JM; Lee, J; Choi, S; Lee, SY (2012a): Systems metabolic engineering of microorganisms for natural and non-natural chemicals. In *Nat Chem Biol* 8 (6), pp. 536–546. DOI: 10.1038/nchembio.970.

Lee, K-M; Kim, S-K; Lee, Y-G; Park, K-H; Seo, J-H (2018): Elimination of biosynthetic pathways for L-valine and L-isoleucine in mitochondria enhances isobutanol production in engineered *Saccharomyces cerevisiae*. In *Bioresource technology* 268, pp. 271–277. DOI: 10.1016/j.biortech.2018.07.150.

Lee, ME; DeLoache, WC; Cervantes, B; Dueber, JE (2015): A highly characterized yeast toolkit for modular, multipart assembly. In *ACS synthetic biology* 4 (9), pp. 975–986. DOI: 10.1021/sb500366v.

Lee, W-H; Seo, S-O; Bae, Y-H; Nan, H; Jin, Y-S; Seo, J-H (2012b): Isobutanol production in engineered *Saccharomyces cerevisiae* by overexpression of 2-ketoisovalerate decarboxylase and valine biosynthetic enzymes. In *Bioprocess and biosystems engineering* 35 (9), pp. 1467–1475. DOI: 10.1007/s00449-012-0736-y.

Li, H; Outten, CE (2012): Monothiol CGFS glutaredoxins and BolA-like proteins: [2Fe-2S] binding partners in iron homeostasis. In *Biochemistry* 51 (22), pp. 4377–4389. DOI: 10.1021/bi300393z.

Li, L; Bagley, D; Ward, DM; Kaplan, J (2008): Yap5 is an iron-responsive transcriptional activator that regulates vacuolar iron storage in yeast. In *Molecular and Cellular Biology* 28 (4), pp. 1326–1337. DOI: 10.1128/MCB.01219-07.

Li, L; Miao, R; Bertram, S; Jia, X; Ward, DM; Kaplan, J (2012): A role for iron-sulfur clusters in the regulation of transcription factor Yap5-dependent high iron transcriptional responses in yeast. In *J. Biol. Chem.* 287 (42), pp. 35709–35721. DOI: 10.1074/jbc.M112.395533.

Li, M; Kildegaard, KR; Chen, Y; Rodriguez, A; Borodina, I; Nielsen, J (2015): *De novo* production of resveratrol from glucose or ethanol by engineered *Saccharomyces cerevisiae*. In *Metabolic engineering* 32, pp. 1–11. DOI: 10.1016/j.ymben.2015.08.007.

Li, S-Y; Ng, I-S; Chen, PT; Chiang, C-J; Chao, Y-P (2018): Biorefining of protein waste for production of sustainable fuels and chemicals. In *Biotechnology for Biofuels* 11, p. 256. DOI: 10.1186/s13068-018-1234-5.

Liang, S; Chen, H; Liu, J; Wen, J (2018): Rational design of a synthetic Entner-Doudoroff pathway for enhancing glucose transformation to isobutanol in *Escherichia coli*. In *Journal of industrial microbiology & biotechnology* 45 (3), pp. 187–199. DOI: 10.1007/s10295-018-2017-5.

Liao, JC (2011): An evolutionary strategy for isobutanol production strain development in *Escherichia coli*. In *Metabolic engineering* 13 (6), pp. 674–681. DOI: 10.1016/j.ymben.2011.08.004.

Lill, R (2020): From the discovery to molecular understanding of cellular iron-sulfur protein biogenesis. In *Biological chemistry* 401 (6-7), pp. 855–876. DOI: 10.1515/hsz-2020-0117.

Lill, R; Dutkiewicz, R; Freibert, SA; Heidenreich, T; Mascarenhas, J; Netz, DJ; Paul, VD; Pierik, AJ; Richter, N; Stümpfig, M; Srinivasan, V; Stehling, O; Mühlenhoff, U (2015): The role of mitochondria and the CIA machinery in the maturation of cytosolic and nuclear iron-sulfur proteins. In *European journal of cell biology* 94 (7-9), pp. 280–291. DOI: 10.1016/j.ejcb.2015.05.002.

Lill, R; Srinivasan, V; Mühlenhoff, U (2014): The role of mitochondria in cytosolic-nuclear iron–sulfur protein biogenesis and in cellular iron regulation. In *Current opinion in microbiology* 22, pp. 111–119. DOI: 10.1016/j.mib.2014.09.015.

Lilly, M; Bauer, FF; Styger, G; Lambrechts, MG; Pretorius, IS (2006): The effect of increased branched-chain amino acid transaminase activity in yeast on the production of higher alcohols and on the flavour profiles of wine and distillates. In *FEMS Yeast Res* 6 (5), pp. 726–743. DOI: 10.1111/j.1567-1364.2006.00057.x.

Liu, S; Qureshi, N (2009): How microbes tolerate ethanol and butanol. In *New biotechnology* 26 (3-4), pp. 117–121. DOI: 10.1016/j.nbt.2009.06.984.

Lukins, HB; Tham, SH; Wallace, PG; Linnane, AW (1966): Correlation of membrane bound succinate dehydrogenase with the occurrence of mitochondrial profiles in *Saccharomyces cerevisiae*. In *Biochemical and Biophysical Research Communications* 23 (4), pp. 363–367. DOI: 10.1016/0006-291X(66)90734-0.

Maarse, AC; van Loon, AP; Riezman, H; Gregor, I; Schatz, G; Grivell, LA (1984): Subunit IV of yeast cytochrome c oxidase: cloning and nucleotide sequencing of the gene and partial amino acid sequencing of the mature protein. In *The EMBO Journal* 3 (12), pp. 2831–2837.

MacLean, HL; Lave, LB (2003): Evaluating automobile fuel/propulsion system technologies. In *Progress in Energy and Combustion Science* 29 (1), pp. 1–69. DOI: 10.1016/S0360-1285(02)00032-1.

Maestre, O; García-Martínez, T; Peinado, RA; Mauricio, JC (2008): Effects of *ADH2* overexpression in *Saccharomyces bayanus* during alcoholic fermentation. In *Applied and environmental microbiology* 74 (3), pp. 702–707. DOI: 10.1128/AEM.01805-07.

Magasanik, B; Kaiser, CA (2002): Nitrogen regulation in *Saccharomyces cerevisiae*. In *Gene* 290 (1-2), pp. 1–18. DOI: 10.1016/s0378-1119(02)00558-9.

Maitra, PK (1971): Glucose and fructose metabolism in a phosphoglucoisomeraseless mutant of *Saccharomyces cerevisiae*. In *Journal of bacteriology* 107 (3), pp. 759–769. DOI: 10.1128/JB.107.3.759-769.1971.

Martínez-Pastor, MT; Perea-García, A; Puig, S (2017): Mechanisms of iron sensing and regulation in the yeast *Saccharomyces cerevisiae*. In *World Journal of Microbiology and Biotechnology* 33 (4), p. 75. DOI: 10.1007/s11274-017-2215-8.

Matsuda, F; Ishii, J; Kondo, T; Ida, K; Tezuka, H; Kondo, A (2013): Increased isobutanol production in *Saccharomyces cerevisiae* by eliminating competing pathways and resolving cofactor imbalance. In *Microbial cell factories* 12, p. 119. DOI: 10.1186/1475-2859-12-119.

Mayer, M (2018): Promoter and terminator shuffling of genes encoding valine synthesis enzymes with Golden Gate Cloning for enhanced isobutanol production in *Saccharomyces cerevisiae*. Bachelorarbeit. Goethe Universität Frankfurt am Main, Frankfurt am Main. Physiology and Genetics of Lower Eukaryotes, checked on 7/20/2021.

McMillan, JD; Beckham, GT (2017): Thinking big: towards ideal strains and processes for large-scale aerobic biofuels production. In *Microbial biotechnology* 10 (1), pp. 40–42. DOI: 10.1111/1751-7915.12471.

Meadows, AL; Hawkins, KM; Tsegaye, Y; Antipov, E; Kim, Y; Raetz, L; Dahl, RH; Tai, A; Mahatdejkul-Meadows, T; Xu, L; Zhao, L; Dasika, MS; Murarka, A; Lenihan, J; Eng, D; Leng, JS; Liu, C-L; Wenger, JW; Jiang, H; Chao, L; Westfall, P; Lai, J; Ganesan, S; Jackson, P; Mans, R; Platt, D; Reeves, CD; Saija, PR; Wichmann, G; Holmes, VF; Benjamin, K; Hill, PW; Gardner, TS; Tsong, AE (2016): Rewriting yeast central carbon metabolism for industrial isoprenoid production. In *Nature* 537 (7622), pp. 694–697. DOI: 10.1038/nature19769.

Meadows, CW; Kang, A; Lee, TS (2018): Metabolic engineering for advanced biofuels production and recent advances toward commercialization. In *Biotechnology journal* 13 (1). DOI: 10.1002/biot.201600433.

Miller, SM; Magasanik, B (1990): Role of NAD-linked glutamate dehydrogenase in nitrogen metabolism in *Saccharomyces cerevisiae*. In *Journal of bacteriology* 172 (9), pp. 4927–4935. DOI: 10.1128/jb.172.9.4927-4935.1990.

Milne, N; van Maris, AJA; Pronk, JT; Daran, JM (2015): Comparative assessment of native and heterologous 2-oxo acid decarboxylases for application in isobutanol production by *Saccharomyces cerevisiae*. In *Biotechnology for Biofuels* 8, p. 204. DOI: 10.1186/s13068-015-0374-0.

Milne, N; Wahl, SA; van Maris, AJA; Pronk, JT; Daran, JM (2016): Excessive by-product formation: A key contributor to low isobutanol yields of engineered *Saccharomyces cerevisiae* strains. In *Metabolic engineering communications* 3, pp. 39–51. DOI: 10.1016/j.meteno.2016.01.002.

Mohd Azhar, SH; Abdulla, R; Jambo, SA; Marbawi, H; Gansau, JA; Mohd Faik, AA; Rodrigues, KF (2017): Yeasts in sustainable bioethanol production: A review. In *Biochemistry and biophysics reports* 10, pp. 52–61. DOI: 10.1016/j.bbrep.2017.03.003.

Molina, MM; Bellí, G; La Torre, MA de; Rodríguez-Manzaneque, MT; Herrero, E (2004): Nuclear monothiol glutaredoxins of *Saccharomyces cerevisiae* can function as mitochondrial glutaredoxins. In *The Journal of biological chemistry* 279 (50), pp. 51923–51930. DOI: 10.1074/jbc.M410219200.

Molina-Navarro, MM; Casas, C; Piedrafita, L; Bellí, G; Herrero, E (2006): Prokaryotic and eukaryotic monothiol glutaredoxins are able to perform the functions of Grx5 in the biogenesis of Fe/S clusters in yeast mitochondria. In *FEBS letters* 580 (9), pp. 2273–2280. DOI: 10.1016/j.febslet.2006.03.037.

Moye, WS; Amuro, N; Rao, JK; Zalkin, H (1985): Nucleotide sequence of yeast *GDH1* encoding nicotinamide adenine dinucleotide phosphate-dependent glutamate dehydrogenase. In *The Journal of biological chemistry* 260 (14), pp. 8502–8508. DOI: 10.1016/S0021-9258(17)39500-5.

Mühlenhoff, U; Molik, S; Godoy, JR; Uzarska, MA; Richter, N; Seubert, A; Zhang, Y; Stubbe, J; Pierrel, F; Herrero, E; Lillig, CH; Lill, R (2010): Cytosolic monothiol glutaredoxins function in intracellular iron sensing and trafficking *via* their bound ironsulfur cluster. In *Cell metabolism* 12 (4), pp. 373–385. DOI: 10.1016/j.cmet.2010.08.001.

Mühlenhoff, U; Richter, N; Pines, O; Pierik, AJ; Lill, R (2011): Specialized function of yeast Isa1 and Isa2 proteins in the maturation of mitochondrial [4Fe-4S] proteins. In *The Journal of biological chemistry* 286 (48), pp. 41205–41216. DOI: 10.1074/jbc.M111.296152.

Naseeb, S; Ames, RM; Delneri, D; Lovell, SC (2017): Rapid functional and evolutionary changes follow gene duplication in yeast. In *Proceedings. Biological sciences* 284 (1861). DOI: 10.1098/rspb.2017.1393.

Nevoigt, E; Stahl, U (1997): Osmoregulation and glycerol metabolism in the yeast *Saccharomyces cerevisiae*. In *FEMS microbiology reviews* 21 (3), pp. 231–241. DOI: 10.1111/j.1574-6976.1997.tb00352.x.

Noda, S; Mori, Y; Oyama, S; Kondo, A; Araki, M; Shirai, T (2019): Reconstruction of metabolic pathway for isobutanol production in *Escherichia coli*. In *Microbial cell factories* 18 (1), p. 124. DOI: 10.1186/s12934-019-1171-4.

Noda, S; Shirai, T; Oyama, S; Kondo, A (2016): Metabolic design of a platform *Escherichia coli* strain producing various chorismate derivatives. In *Metabolic engineering* 33, pp. 119–129. DOI: 10.1016/j.ymben.2015.11.007.

Ohno, S (1970): Evolution by gene duplication. In *Springer-Verlag Berlin Heidelberg* 1970 (1). DOI: 10.1007/978-3-642-86659-3.

Oud, B; Flores, C-L; Gancedo, C; Zhang, X; Trueheart, J; Daran, J-M; Pronk, JT; van Maris, AJA (2012): An internal deletion in *MTH1* enables growth on glucose of pyruvate-decarboxylase negative, non-fermentative *Saccharomyces cerevisiae*. In *Microb Cell Fact* 11, p. 131. DOI: 10.1186/1475-2859-11-131.

Outten, CE; Albetel, A-N (2013): Iron sensing and regulation in *Saccharomyces cerevisiae*: ironing out the mechanistic details. In *Current opinion in microbiology* 16 (6), pp. 662–668. DOI: 10.1016/j.mib.2013.07.020.

Pang, SS; Duggleby, RG (1999): Expression, purification, characterization, and reconstitution of the large and small subunits of yeast acetohydroxyacid synthase. In *Biochemistry* 38 (16), pp. 5222–5231. DOI: 10.1021/bi983013m.

Pang, SS; Duggleby, RG; Guddat, LW (2002): Crystal structure of yeast acetohydroxyacid synthase: a target for herbicidal inhibitors. In *Journal of molecular biology* 317 (2), pp. 249–262. DOI: 10.1006/jmbi.2001.5419.

Park, JH; Lee, SY (2010): Fermentative production of branched chain amino acids: a focus on metabolic engineering. In *Appl Microbiol Biotechnol* 85 (3), pp. 491–506. DOI: 10.1007/s00253-009-2307-y.

Park, S-H; Hahn, J-S (2019): Development of an efficient cytosolic isobutanol production pathway in *Saccharomyces cerevisiae* by optimizing copy numbers and expression of the pathway genes based on the toxic effect of α-acetolactate. In *Scientific reports* 9 (1), p. 3996. DOI: 10.1038/s41598-019-40631-5.

Park, S-H; Kim, S; Hahn, J-S (2014): Metabolic engineering of *Saccharomyces cerevisiae* for the production of isobutanol and 3-methyl-1-butanol. In *Appl Microbiol Biotechnol* 98 (21), pp. 9139–9147. DOI: 10.1007/s00253-014-6081-0.

Park, S-H; Kim, S; Hahn, J-S (2016): Improvement of isobutanol production in *Saccharomyces cerevisiae* by increasing mitochondrial import of pyruvate through mitochondrial pyruvate carrier. In *Applied microbiology and biotechnology* 100 (17), pp. 7591–7598. DOI: 10.1007/s00253-016-7636-z.

Partow, S; Siewers, V; Daviet, L; Schalk, M; Nielsen, J (2012): Reconstruction and evaluation of the synthetic bacterial MEP pathway in *Saccharomyces cerevisiae*. In *PloS one* 7 (12), e52498. DOI: 10.1371/journal.pone.0052498.

Petrognani, C; Boon, N; Ganigué, R (2020): Production of isobutyric acid from methanol by *Clostridium luticellarii*. In *Green Chem.* 22 (23), pp. 8389–8402. DOI: 10.1039/D0GC02700F.

Pires, EJ; Teixeira, JA; Brányik, T; Vicente, AA (2014): Yeast: the soul of beer's aroma-a review of flavour-active esters and higher alcohols produced by the brewing yeast. In *Appl Microbiol Biotechnol* 98 (5), pp. 1937–1949. DOI: 10.1007/s00253-013-5470-0.

Pirrung, MC; Holmes, CP; Horowitz, DM; Nunn, DS (1991): Mechanism and stereochemistry of α,β-dihydroxyacid dehydratase. In *J. Am. Chem. Soc.* 113 (3), pp. 1020–1025. DOI: 10.1021/ja00003a042.

Piskur, J; Rozpedowska, E; Polakova, S; Merico, A; Compagno, C (2006): How did *Saccharomyces* evolve to become a good brewer? In *Trends in genetics : TIG* 22 (4), pp. 183–186. DOI: 10.1016/j.tig.2006.02.002.

Plaza, M; FernÃ¡ndez de Palencia, P; PelÃ¡ez, C; Requena, T (2004): Biochemical and molecular characterization of α-ketoisovalerate decarboxylase, an enzyme involved in the formation of aldehydes from amino acids by *Lactococcus lactis*. In *FEMS Microbiology Letters* 238 (2), pp. 367–374. DOI: 10.1111/j.1574-6968.2004.tb09778.x.

Polakis, ES; Bartley, W; Meek, GA (1964): Changes in the structure and enzyme activity of *Saccharomyces cerevisiae* in response to changes in the environment. In *The Biochemical journal* 90 (2), pp. 369–374. DOI: 10.1042/bj0900369.

Pujol-Carrion, N; Belli, G; Herrero, E; Nogues, A; La Torre-Ruiz, MA de (2006): Glutaredoxins Grx3 and Grx4 regulate nuclear localisation of Aft1 and the oxidative stress response in *Saccharomyces cerevisiae*. In *Journal of cell science* 119 (Pt 21), pp. 4554–4564. DOI: 10.1242/jcs.03229.

Reifenrath, M; Boles, E (2018): Engineering of hydroxymandelate synthases and the aromatic amino acid pathway enables *de novo* biosynthesis of mandelic and 4-hydroxymandelic acid with *Saccharomyces cerevisiae*. In *Metabolic engineering* 45, pp. 246–254. DOI: 10.1016/j.ymben.2018.01.001.

Reyes, LH; Gomez, JM; Kao, KC (2014): Improving carotenoids production in yeast via adaptive laboratory evolution. In *Metabolic engineering* 21, pp. 26–33. DOI: 10.1016/j.ymben.2013.11.002.

Rodríguez-Manzaneque, MT; Tamarit, J; Bellí, G; Ros, J; Herrero, E (2002): Grx5 Is a mitochondrial glutaredoxin required for the activity of iron/sulfur enzymes. In *Molecular biology of the cell* 13 (4), pp. 1109–1121. DOI: 10.1091/mbc.01-10-0517.

Roise, D; Horvath, SJ; Tomich, JM; Richards, JH; Schatz, G (1986): A chemically synthesized pre-sequence of an imported mitochondrial protein can form an amphiphilic helix and perturb natural and artificial phospholipid bilayers. In *The EMBO Journal* 5 (6), pp. 1327–1334.

Romagnoli, G; Luttik, MAH; Kötter, P; Pronk, JT; Daran, J-M (2012): Substrate specificity of thiamine pyrophosphate-dependent 2-oxo-acid decarboxylases in *Saccharomyces cerevisiae*. In *Applied and environmental microbiology* 78 (21), pp. 7538–7548. DOI: 10.1128/AEM.01675-12.

Runguphan, W; Keasling, JD (2014): Metabolic engineering of *Saccharomyces cerevisiae* for production of fatty acid-derived biofuels and chemicals. In *Metabolic engineering* 21, pp. 103–113. DOI: 10.1016/j.ymben.2013.07.003.

Salusjärvi, L; Toivari, M; Vehkomäki, M-L; Koivistoinen, O; Mojzita, D; Niemelä, K; Penttilä, M; Ruohonen, L (2017): Production of ethylene glycol or glycolic acid from D-xylose in *Saccharomyces cerevisiae*. In *Applied microbiology and biotechnology* 101 (22), pp. 8151–8163. DOI: 10.1007/s00253-017-8547-3.

Sambrook, J; Russell, DW (2001): Molecular cloning. A laboratory manual. 3rd edition, Cold Spring Harbor Laboratory Press.

Satyanarayana, T; Umbarger, HE (1968): Biosynthesis of branched-chain amino acids in yeast: correlation of biochemical blocks and genetic lesions in leucine auxotrophs. In *Journal of bacteriology* 96 (6), pp. 2012–2017.

Schadeweg, V; Boles, E (2016): Increasing n-butanol production with *Saccharomyces cerevisiae* by optimizing acetyl-CoA synthesis, NADH levels and trans-2-enoyl-CoA reductase expression. In *Biotechnology for Biofuels* 9 (1), p. 257. DOI: 10.1186/s13068-016-0673-0.

Schure, EG ter; Flikweert, MT; van Dijken, JP; Pronk, JT; Verrips, CT (1998): Pyruvate decarboxylase catalyzes decarboxylation of branched-chain 2-oxo acids but is not essential for fusel alcohol production by *Saccharomyces cerevisiae*. In *Applied and environmental microbiology* 64 (4), pp. 1303–1307. DOI: 10.1128/AEM.64.4.1303-1307.1998.

Shepelin, D; Hansen, ASL; Lennen, R; Luo, H; Herrgård, MJ (2018): Selecting the best: evolutionary engineering of chemical production in microbes. In *Genes* 9 (5). DOI: 10.3390/genes9050249.

Shi, X; Zou, Y; Chen, Y; Zheng, C; Ying, H (2016): Overexpression of a water-forming NADH oxidase improves the metabolism and stress tolerance of *Saccharomyces cerevisiae* in aerobic fermentation. In *Frontiers in microbiology* 7, p. 1427. DOI: 10.3389/fmicb.2016.01427.

Si, T; Luo, Y; Xiao, H; Zhao, H (2014): Utilizing an endogenous pathway for 1-butanol production in *Saccharomyces cerevisiae*. In *Metabolic engineering* 22, pp. 60–68. DOI: 10.1016/j.ymben.2014.01.002.

Sipos, K; Lange, H; Fekete, Z; Ullmann, P; Lill, R; Kispal, G (2002): Maturation of cytosolic iron-sulfur proteins requires glutathione. In *The Journal of biological chemistry* 277 (30), pp. 26944–26949. DOI: 10.1074/jbc.M200677200.

Smidt, O de; Du Preez, JC; Albertyn, J (2012): Molecular and physiological aspects of alcohol dehydrogenases in the ethanol metabolism of *Saccharomyces cerevisiae*. In *FEMS yeast research* 12 (1), pp. 33–47. DOI: 10.1111/j.1567-1364.2011.00760.x.

Srinivasan, V; Netz, DJA; Webert, H; Mascarenhas, J; Pierik, AJ; Michel, H; Lill, R (2007): Structure of the yeast WD40 domain protein Cia1, a component acting late in iron-sulfur protein biogenesis. In *Structure (London, England : 1993)* 15 (10), pp. 1246–1257. DOI: 10.1016/j.str.2007.08.009.

Srivastava, RK (2018): A review on sustainable yeast biotechnological processes and applications. In *Microbiological Research* 207, pp. 83–90. DOI: 10.1016/j.micres.2017.11.013.

Suga, H; Matsuda, F; Hasunuma, T; Ishii, J; Kondo, A (2013): Implementation of a transhydrogenase-like shunt to counter redox imbalance during xylose fermentation in *Saccharomyces cerevisiae*. In *Appl Microbiol Biotechnol* 97 (4), pp. 1669–1678. DOI: 10.1007/s00253-012-4298-3.

Takpho, N; Watanabe, D; Takagi, H (2018): High-level production of valine by expression of the feedback inhibition-insensitive acetohydroxyacid synthase in *Saccharomyces cerevisiae*. In *Metabolic engineering* 46, pp. 60–67. DOI: 10.1016/j.ymben.2018.02.011.

Tan, G; Lu, J; Bitoun, JP; Huang, H; Ding, H (2009): IscA/SufA paralogues are required for the [4Fe-4S] cluster assembly in enzymes of multiple physiological pathways in *Escherichia coli* under aerobic growth conditions. In *The Biochemical journal* 420 (3), pp. 463–472. DOI: 10.1042/BJ20090206.

Thomik, T; Wittig, I; Choe, J-Y; Boles, E; Oreb, M (2017): An artificial transport metabolon facilitates improved substrate utilization in yeast. In *Nature chemical biology* 13 (11), pp. 1158–1163. DOI: 10.1038/nchembio.2457.

Upadhyay, SN; Mishra, PK (2019): Biofuels from protein-rich lignocellulosic biomass: new approach. In P. K. Mishra, S. N. Upadhyay (Eds.): Sustainable Approaches for Biofuels Production Technologies. From Current Status to Practical Implementation, vol. 7. Cham: Springer International Publishing (Biofuel and Biorefinery Technologies, 7), pp. 83–92.

Urano, J; Dundon, CA; Meinhold, P (2009): Cytosolic isobutanol pathway localization for the production of isobutanol. In *US20140308721A1*.

Uzarska, MA; Dutkiewicz, R; Freibert, S-A; Lill, R; Mühlenhoff, U (2013): The mitochondrial Hsp70 chaperone Ssq1 facilitates Fe/S cluster transfer from Isu1 to Grx5 by complex formation. In *Molecular biology of the cell* 24 (12), pp. 1830–1841. DOI: 10.1091/mbc.E12-09-0644.

van Maris, AJA; Geertman, J-MA; Vermeulen, A; Groothuizen, MK; Winkler, AA; Piper, MDW; van Dijken, JP; Pronk, JT (2004): Directed evolution of pyruvate decarboxylase-negative Saccharomyces cerevisiae, yielding a C2-independent, glucose-tolerant, and pyruvate-hyperproducing yeast. In *Applied and environmental microbiology* 70 (1), pp. 159–166. DOI: 10.1128/AEM.70.1.159-166.2004.

Verhoef, S; Wierckx, N; Westerhof, RGM; Winde, JH de; Ruijssenaars, HJ (2009): Bioproduction of p-hydroxystyrene from glucose by the solvent-tolerant bacterium *Pseudomonas putida* S12 in a two-phase water-decanol fermentation. In *Applied and environmental microbiology* 75 (4), pp. 931–936. DOI: 10.1128/AEM.02186-08.

Voordeckers, K; Verstrepen, KJ (2015): Experimental evolution of the model eukaryote *Saccharomyces cerevisiae* yields insight into the molecular mechanisms underlying adaptation. In *Current opinion in microbiology* 28, pp. 1–9. DOI: 10.1016/j.mib.2015.06.018.

Vuralhan, Z; Luttik, MAH; Tai, SL; Boer, VM; Morais, MA; Schipper, D; Almering, MJH; Kötter, P; Dickinson, JR; Daran, J-M; Pronk, JT (2005): Physiological characterization of the *ARO10*-dependent, broad-substrate-specificity 2-oxo acid decarboxylase activity of *Saccharomyces cerevisiae*. In *Applied and environmental microbiology* 71 (6), pp. 3276–3284. DOI: 10.1128/AEM.71.6.3276-3284.2005.

Wallace, PG; Huang, M; Linnane, AW (1968): The biogenesis of mitochondria. II. The influence of medium composition on the cytology of anaerobically grown Saccharomyces cerevisiae. In *The Journal of cell biology* 37 (2), pp. 207–220. DOI: 10.1083/jcb.37.2.207.

Watanabe, S; Shimada, N; Tajima, K; Kodaki, T; Makino, K (2006): Identification and characterization of L-arabonate dehydratase, L-2-keto-3-deoxyarabonate dehydratase, and L-arabinolactonase involved in an alternative pathway of L-arabinose metabolism. In *The Journal of biological chemistry* 281 (44), pp. 33521–33536. DOI: 10.1074/jbc.M606727200.

Weber, C; Farwick, A; Benisch, F; Brat, D; Dietz, H; Subtil, T; Boles, E (2010): Trends and challenges in the microbial production of lignocellulosic bioalcohol fuels. In *Applied microbiology and biotechnology* 87 (4), pp. 1303–1315. DOI: 10.1007/s00253-010-2707-z.

Wess, J; Brinek, M; Boles, E (2019): Improving isobutanol production with the yeast *Saccharomyces cerevisiae* by successively blocking competing metabolic pathways as well as ethanol and glycerol formation. In *Biotechnol Biofuels* 12 (1), pp. 1–15. DOI: 10.1186/s13068-019-1486-8.

Wixom, RL; Shatton, JB; Strassman, M (1960): Studies on a dehydrase in valine biosynthesis in yeast. In *The Journal of biological chemistry* 235 (1), pp. 128–131. DOI: 10.1016/S0021-9258(18)69597-3.

Xiao, W; Rank, GH (1988): The yeast *ILV2* gene is under general amino acid control. In *Genome* 30 (6), pp. 984–986. DOI: 10.1139/g88-156.

Yim, H; Haselbeck, R; Niu, W; Pujol-Baxley, C; Burgard, A; Boldt, J; Khandurina, J; Trawick, JD; Osterhout, RE; Stephen, R; Estadilla, J; Teisan, S; Schreyer, HB; Andrae, S; Yang, TH; Lee, SY; Burk, MJ; van Dien, S (2011): Metabolic engineering of *Escherichia coli* for direct production of 1,4-butanediol. In *Nat Chem Biol* 7 (7), pp. 445–452. DOI: 10.1038/nchembio.580.

Yoshimoto, H; Fukushige, T; Yonezawa, T; Sone, H (2002): Genetic and physiological analysis of branched-chain alcohols and isoamyl acetate production in *Saccharomyces cerevisiae*. In *Applied microbiology and biotechnology* 59 (4-5), pp. 501–508. DOI: 10.1007/s00253-002-1041-5.

Yu, A-Q; Pratomo Juwono, NK; Foo, JL; Leong, SSJ; Chang, MW (2016): Metabolic engineering of *Saccharomyces cerevisiae* for the overproduction of short branched-chain fatty acids. In *Metabolic engineering* 34, pp. 36–43. DOI: 10.1016/j.ymben.2015.12.005.

Yuan, J; Ching, CB (2015): Combinatorial assembly of large biochemical pathways into yeast chromosomes for improved production of value-added compounds. In *ACS synthetic biology* 4 (1), pp. 23–31. DOI: 10.1021/sb500079f.

Zelenaya-Troitskaya, O; Perlman, PS; Butow, RA (1995): An enzyme in yeast mitochondria that catalyzes a step in branched-chain amino acid biosynthesis also functions in mitochondrial DNA stability. In *The EMBO Journal* 14 (13), pp. 3268–3276.

Zhang, K; Woodruff, AP; Xiong, M; Zhou, J; Dhande, YK (2011): A synthetic metabolic pathway for production of the platform chemical isobutyric acid. In *ChemSusChem* 4 (8), pp. 1068–1070. DOI: 10.1002/cssc.201100045.

Zhao, EM; Zhang, Y; Mehl, J; Park, H; Lalwani, MA; Toettcher, JE; Avalos, JL (2018): Optogenetic regulation of engineered cellular metabolism for microbial chemical production. In *Nature* 555 (7698), pp. 683–687. DOI: 10.1038/nature26141.

Zimmermann, FK (1975): Procedures used in the induction of mitotic recombination and mutation in the yeast *Saccharomyces cerevisiae*. In *Mutation Research/Environmental Mutagenesis and Related Subjects* 31 (2), pp. 71–86. DOI: 10.1016/0165-1161(75)90069-2.

APPENDIX

I. ABBREVIATION

General Abbreviation	
[2Fe-2S]	iron-sulphur-cluster composed of 2 iron and 2 sulphur ions
[4Fe-4S]	iron-sulphur-cluster composed of 4 iron and 4 sulphur ions
°C	degree Celsius
µF	microfarad -nit of capacitance
µg	microgram
µl	microliter
µM	micromolar
a.u.	artificial units
A_{260}	absorbance at 260 nm
A_{280}	absorbance at 280 nm
AA-mix	amino acid mix
AAA	aromatic amino acids
AHBA	2-aceto-2-hydroxybutanoic acid
ALAC	2-acetolactate
ALS	acetolactate synthase
ARS	autonomously replicating sequence
BCAA	Branched chain amino acids
bp	base pairs
CEN	yeast centromere
CGQ	Cell Growth Quantifier
CIA machinery	cytosolic ISC assembly machinery
ClonNAT	Nourseothricin
cm	centimetre
^{Co}	^{Co} indicated a codon optimised gene
CO_2	carbon dioxide
CRISPR	clustered regularly interspaced short palindromic repeats
C-terminal	carboxyl-terminus of a peptide
cyt-ILV	N-terminal truncated Ilv2Δ54^{Co}, Ilv5Δ48^{Co}, and Ilv3Δ19^{Co} enzymes
cyt-ILV+EP	N-terminal truncated Ilv2Δ54^{Co}, Ilv5Δ48^{Co}, Ilv3Δ19^{Co}, Aro10^{Co}, and Adh2
D	glucose
ddH_2O	double-distilled water
DHAD	dihydroxy acid dehydratase
DHAP	dihydroxyacetonphosphat
DIV	2-dihydroxyisovalerate
DMSO	dimethyl sulfoxide
DMV	2,3-dihydroxy-methylvalerate
DNA	deoxyribonucleic acid
dNTP	deoxynucleoside triphosphate
DTT	1,4-Dithiothreitol
EDP	Entner–Doudoroff pathway
EDTA	ethylenediaminetetraacetic acid
EP	Ehrlich pathway
F	fructose
FAD	flavin-adenine-dinucleotide
FCC	frozen competent cell
FDA	United States Food and Drug Administration
g	gram
G418	Geneticin
GAAC	General Amino Acid Control
GAP	D-glyceraldehyde-3-phosphate
GRAS	generally recognized as safe
gRNA	guide-RNA
H	Hygromycin B
h	hours
HPLC	high performance liquid chromatography
IBA	isobutyric acid
ILV	Ilv2, Ilv5 and Ilv3 enzymes
InDels	genomic integration or deletions
ISC	iron-sulphur-cluster
K	Geneticin
KARI	ketol-acid reductoisomerase
kb	kilobases
k_{cat}	turnover number.
KDPG	2-dehydro-3-deoxy-D-gluconate-6-phosphate from *E. coli*
KIV	2-Ketoisovalerat
K_m	Michaelis constant
KMV	2-keto-3-methylvalerate
kV	kilovolt
l	litre
LB	Luria-Bertani

M	molar concentration
min	minutes
ml	millilitre
mM	millimolar concentration
mm	millimetre
mtDNA	mitochondrial DNA
MTS	mitochondrial-targeting-sequence
N	Nourseothricin
NADH	nicotinamide adenine dinucleotide
NADPH	Nicotinamide adenine dinucleotide phosphate
ng	nanogram
nm	nanometre
nt	nucleotide
N-terminal	amino terminus of a peptide
NVA	DL-norvaline
O_2	dioxygen
OD_{600}	optical density at 600 nm
ORF	open reading frame
PAM	protospacer adjacent motif
PCR	polymerase chain reaction
Pdc	pyruvate dehydrogenase
PEG	polyethylene glycol
pH	potential of hydrogen
pmol	picomole
P^{ZXXXY}	amino acid Z at position XXX in protein P was substituted by amino acid Y
RNA	ribonucleic acid
S.O.C	Super Optimal broth with Catabolite repression
SC	synthetic complete
SDS	sodium dodecyl sulphate
sec	second
SNP	single nucleotide polymorphisms
TAE	Tris-acetate-EDTA
TPP	thiamine-pyrophosphate
U	enzyme unit
V	volt
v/v	volume per volume
w/v	weight per volume
YEP	yeast extract peptone
Ω	ohm -unit of electrical resistance

Organisms	
B. subtilis	*Bacillus subtilis*
C. glutamicum	*Corynebacterium glutamicum*
Citrobacter sp	*Citrobacter species*
E. coli	*Escherichia coli*
L. lactis	*Lactococcus lactis*
L. plantarum	*Lactobacillus plantarum*
N. crassa	*Neuraspora crassa*
P. carotovorum	*Pectobacterium carotovorum*
P. putida	*Pseudomonas putida*
S. pyogenes	*Streptococcus pyogenes*
S. acidocaldarius	*Sulfolobus acidocaldarius*
S. cerevisiae	*Saccharomyces cerevisiae*
S. pneuminiae	*Streptococcus pneuminiae*
X. nematophila	*Xenorhabdus nematophila*

Proteins and Genes*	
Adh1	NAD(H) dependent alcohol dehydrogenase
Adh2	NAD(H) dependent, glucose-repressible alcohol dehydrogenase
Adh3	NAD(H) dependent, mitochondrial alcohol dehydrogenase
Adh4	NAD(H) dependent alcohol dehydrogenase
Adh5	NAD(H) dependent alcohol dehydrogenase
Adh6	cinnamyl alcohol dehydrogenase
Adh7	cinnamyl alcohol dehydrogenase
adhA	NAD(H) dependent alcohol dehydrogenase from *L. lactis*
adhA^{RE1}	modified NADH dependent alcohol dehydrogenase from *L. lactis*
Ald1	NADP(H) dependent cytosolic aldehyde dehydrogenases
Ald2	NAD(H) dependent cytosolic aldehyde dehydrogenases
Ald3	NAD(H) dependent mitochondrial dehydrogenases
Ald4	NAD(P)(H) dependent mitochondrial dehydrogenases
Ald5	NADP(H) dependent mitochondrial dehydrogenases
Ald6	NADP(H) dependent cytosolic aldehyde dehydrogenases

alsD	acetolactate decarboxylase from *B. subtilis*,
alsLP	acetohydroxy acid synthase from *L. plantarum*
alsS	acetohydroxy acid synthase from B. subtilis
Aro8	aromatic aminotransferase I
Aro9	aromatic aminotransferase II
Aro10	phenylpyruvate decarboxylase
Bat1	branched-chain amino acid aminotransferase
Bat2	branched-chain amino acid aminotransferase
Bdh1	NAD(H) dependent (R,R)-butanediol dehydrogenase
Bdh2	putative NAD(H) dependent medium-chain alcohol dehydrogenase
Cas9	CRISPR associated protein 9
Cox4	subunit IV of cytochrome C oxidase
Ecm31	ketopantoate hydroxymethyltransferase
Fra2	cytosolic protein involved in repression of iron regulon transcription
Gap1	general amino acid permease
Gdh1	NADP(H) dependent glutamate dehydrogenase
Gdh2	NAD(H) dependent glutamate dehydrogenase
Gdh3	NADP(H) dependent glutamate dehydrogenase
Gpd1	NAD(H) dependent glycerol-3-phosphate dehydrogenase
Gpd2	NAD(H) dependent glycerol 3-phosphate dehydrogenase
Grx3	glutathione-dependent oxidoreductase
Grx4	glutathione-dependent oxidoreductase and glutathione S-transferase
Grx5	mitochondrial glutathione-dependent oxidoreductase
Grx5Δ29	N-terminal truncated cytosolic glutathione-dependent oxidoreductase
Ilv1	threonine deaminase
Ilv2	acetolactate synthase
Ilv2Δ54	N-terminal truncated cytosolic acetolactate synthase
Ilv3	dihydroxyacid dehydratase
Ilv3Δ19	N-terminal truncated cytosolic dihydroxyacid dehydratase
Ilv5	ketol-acid reductoisomerase
Ilv5Δ48	N-terminal truncated cytosolic ketol-acid reductoisomerase
Ilv6	regulatory subunit of acetolactate synthase
Ilv6Δ61	N-terminal truncated cytosolic regulatory subunit of acetolactate synthase
ilvB	acetohydroxy acid synthase from *C. glutamicum*
ilvB^{ilvN}	acetohydroxy acid synthase complex AHAS I from *E. coli*
ilvC	NADP(H) dependent ketol-acid reductoisomerase from *E. coli* and *C. glutamicum*
ilvC^{6E6}	modified NAD(H) dependent ketol-acid reductoisomerase from *E. coli*
ilvD	dihydroxyacid dehydratase from various organisms
ilvG^{ilvM}	acetohydroxy acid synthase complex AHAS II from *E. coli*
ilvI^{ilvH}	acetohydroxy acid synthase complex AHAS III from *E. coli*
ilvN	small regulatory unit for *ilvB* from *C. glutamicum*
ilvN^{M13}	modified feedback insensitive small regulatory unit for *ilvB* from *C. glutamicum*
ispG	1-hydroxy-2-methyl-2-(E)-butenyl-4-phosphate synthase from *E. coli*
ispH	1-hydroxy-2-methyl-2-(E)-butenyl-4-phosphate reductase from *E. coli*
kdcA	Branched-chain alpha-ketoacid decarboxylase *L. lactis*
Leu1	isopropylmalate isomerase

Leu3	transcription factor, repressor and activator; regulates genes involved in branched chain amino acid biosynthesis
Leu3Δ601	modified constitutively active form of Leu3 transcriptional activator
Leu4	alpha-isopropylmalate synthase I
Leu9	alpha-isopropylmalate synthase II
leuC	3-isopropylmalate dehydratase large subunit from *E. coli*
leuD	3-isopropylmalate dehydratase small subunit from *E. coli*
Lpd1	dihydrolipoamide dehydrogenase
Mae1	mitochondrial malic enzyme; catalyses the oxidative decarboxylation of malate
Mdh2	malate dehydrogenase
Mth1	negative regulator of the glucose-sensing signal transduction pathway
NOX	NADH Oxidase from *S. pneuminiae*
NOX_{high}	NADH Oxidase from *S. pneuminiae* under control of the *UBR2* promotor
NOX_{low}	NADH Oxidase from *S. pneuminiae* under control of the *TPI1* promotor
Pdc1	Major of three pyruvate decarboxylase isozymes
Pdc5	Minor isoform of pyruvate decarboxylase
Pdc6	Minor isoform of pyruvate decarboxylase
pflB	Formate acetyltransferase 1 from *E. coli*
PGDH	6-phospho-D-gluconatedehydratase from *E. coli*
Pim1	ATP-dependent Lon type protease
Pyc2	pyruvate carboxylase
Sfa1	formaldehyde dehydrogenase
sMae1	N-terminal truncated cytosolic malic enzyme
Thi3	Regulatory protein that binds Pdc2

*Nomenclature for genes is not separately listed in this table. If an endogenous gene of *S. cerevisiae* is mentioned in this work, it is written in italic capital letters. If a heterologous gene is mentioned, it is written with in italic small letters with an italic capital letter in the end.

Nucleobase	
A	adenosine
C	cytidine
G	guanosine
T	thymidine

Amino Acids		
1-letter-	**3-letter-**	**amino acid**
A	**Ala**	alanine
C	**Cys**	cysteine
D	**Asp**	aspartic acid
E	**Glu**	glutamic acid
F	**Phe**	phenylalanine
G	**Gly**	glycine
H	**His**	histidine
I	**Ile**	isoleucine
K	**Lys**	lysine
L	**Leu**	leucine
M	**Met**	methionine
N	**Asn**	asparagine
P	**Pro**	proline
Q	**Gln**	glutamine
R	**Arg**	arginine
S	**Ser**	serine
T	**Thr**	threonine
V	**Val**	valine
W	**Trp**	tryptophan
Y	**Tyr**	tyrosine

II. OLIGONUCLEOTIDES / PRIMERS

Table 33 Oligonucleotides and primers used in this work, provided by Boles Group. Homologous regions of the amplified fragment with used promotors (p) or terminators (t) are underlined. Start codon *ATG* and Stop codon *TAA/TAG* of ORF are highlighted in *italic*. Non-binding modification for e.g., insertion of an amino acid change is highlighted in **bold**.

Number	Name	Sequence	Description
WGP036	T-c.op-ILV3_Fw	AACAAAGAATAAACACAAAAACAAAAAGTTTTTTTAATTTTAATCAAAAA*ATG*GCTAAGAAGTTGAACAAGTAC	amplification of *ILV3Δ19^{Co}* from *S. cerevisiae,* overhang homologous to the 3' end of the truncated *HXT7p*
WGP100	IlvCE6E_Fw	AACAAAGAATAAACACAAAAACAAAAAGTTTTTTTAATTTTAATCAAAAA*ATG*GCTAACTACTTCAACACCTTG	amplification *ilvD* from *E. coli,* overhang homologous to the 3' end of the truncated *HXT7p*
WGP105	Cgl_IlvD_Fw	AGAATAAACACAAAAACAAAAAGTTTTTTTAATTTTAATCAAAAA*ATG*ATCCCACTTCGTTCAAAAG	amplification of *ilvD* from *C. glutamicum,* overhang homologous to the 3' end of the truncated *HXT7p*
WGP113	CoNcrILVD2_Fw	AGAATAAACACAAAAACAAAAAGTTTTTTTAATTTTAATCAAAAA*ATG*GCTTCCAACCAAGATAAC	amplification of *ILVD2* from *N. crassa,* overhang homologous to the 3' end of the truncated *HXT7p*
ISOP69	-	AACACAAAAACAAAAAGTTTTTTTAATTTTAATCAAAAA*ATG*TCCATCATTTACGAAAC	amplification of *ILV6Δ61,* overhang homologous to the 3' end of the truncated *HXT7p*
WGP310	S5-pCenIlv_Fw	GATGGACAGATTGTCTAACCC	sequencing of pWG109
MOP289	-	CAAGAACAAACAAGCTCAAC	sequencing of genes under the control of the truncated *HXT7*p
MOP290	-	ACCTAGACTTCAGGTTGTC	sequencing of genes under the control of the truncated *CYC1t*
HDP470	I-ILV3_F	ACACCTGGCATGTTCTTGTCAC	primer for construction and/or sequencing of MBV057
ISOP131		AGCTTTTATATAAAAAATCTGAAACAAAATCATATCAAAGATGGCTAAGAAGTTGAACAA	primer for construction and/or sequencing of MBV057
ISOP132		AATACTCATTAAAAAACTATATCAATTAATTTGAATTAACTTAAGCGTCCAAAACACAAC	primer for construction and/or sequencing of MBV057

Table 34 Oligonucleotides and Primers used in this work. Homologous regions of the amplified fragment with used promotors (p) or terminators (t) are underlined. Start codon *ATG* and Stop codon *TAA/TAG* of ORF are highlighted in *italic*. Non-binding modification for e.g., insertion of an amino acid change is highlighted in **bold**.

MBP	Name	Sequence	Description
001	NC_IlvD2 w_co-R	CATAACTAATTACATGACTCGA GGCGGCCGC*TTA***CCA**GTAAGC ATCACCACCCAAATC	amplification of *ILVD2* from *N. crassa* with C-terminal **W** and overhang homologous to the 5' end of the *CYC1*t
002	Cgl_IlvDw -R	CATAACTAATTACATGACTCGA GGCGGCCGC*TTA***CCA**GTCGAC CTGACGGACTG	amplification of *ilvD* from *C. glutamicum* with C-terminal **W** and overhang homologous to the 5' end of the *CYC1*t
003	Ilv3D19w _co-R	CATAACTAATTACATGACTCGA GGCGGCCGC*TTA***CCA**AGCGTC CAAAACACAACC	amplification of *ILV3Δ19^{CO}* from *S. cerevisiae* with C-terminal **W** and overhang homologous to the 5' end of the *CYC1*t
004	NC_IlvD2 +6aa_co-R	CATAACTAATTACATGACTCGA GGCGGCCGC*TTA***CCAGTCTTG GTGAACCTT**GTAAGCATCACC ACCCAAATC	amplification of *ILVD2* from *N. crassa* with C-terminal **KVHQDW** and overhang homologous to the 5' end of the *CYC1*t
005	Cgl_IlvD+ 6aa-R	CATAACTAATTACATGACTCGA GGCGGCCGC*TTA***CCAGTCTTG GTGAACCTT**GTCGACCTGACG GACTG	amplification of *ilvD* from *C. glutamicum* with C-terminal **KVHQDW** and overhang homologous to the 5' end of the *CYC1*t
006	Ilv3D19+6 aa_co-R	CATAACTAATTACATGACTCGA GGCGGCCGC*TTA***CCAGTCTTG GTGAACCTT**AGCGTCCAAAAC ACAACC	amplification of *ILV3Δ19^{CO}* from *S. cerevisiae* with C-terminal **KVHQDW** and overhang homologous to the 5' end of the *CYC1*t
011	Eco_IlvD w-cyc1t-R	CATAACTAATTACATGACTCGA GGCGGCCGC*TTA***CCA**ACCCCC CAGTTTCGATTTATC	amplification of *ilvD^{CO}* from *E. coli* with C-terminal **W** and overhang homologous to the 5' end of the *CYC1*t
012	Eco_IlvD+ 6aa-cyc1t -R	CATAACTAATTACATGACTCGA GGCGGCCGC*TTA***CCAGTCTTG GTGAACCTT**ACCCCCCAGTTT CGATTTATC	amplification of *ilvD^{CO}* from *E. coli* with C-terminal **KVHQDW** and overhang homologous to the 5' end of the *CYC1*t
094	Hxt7-Eco _IlvD-co-F	AAAGAATAAACACAAAAACAAA AAGTTTTTTTAATTTTAATCAAA AA*ATG*CCAAAGTACAGATCTGC TAC	amplification of *ilvD^{CO}* from *E. coli*, overhang homologous to the 3' end of the truncated *HXT7p*
095	Eco_IlvD- co-CYC1t -R	GGAGGGCGTGAATGTAAGCGT GACATAACTAATTACATGACTC GAG*TTA*ACCACCCAACTTAGAC TTGTC	amplification of *ilvD^{CO}* from *E. coli* and overhang homologous to the 5' end of the *CYC1*t
105	HXT7p-B acsub_Ilv D-co_F	AAACACAAAAACAAAAAGTTTT TTTAATTTTAATCAAAAAGCGG CCGCATGGCTGAATTGAGATC TAACATG	amplification of *ilvD^{CO}* from *B. subtilis*, overhang homologous to the 3' end of the truncated *HXT7p*
106	Bacsub_Il vD-W-co_ CYC1t_R	CGTGAATGTAAGCGTGACATA ACTAATTACATGACTCGAGGC GGCCGC*TTA***CCA**GATCTTCAT GATACCACCAGTG	amplification of *ilvD^{CO}* from *B. subtilis* with C-terminal **W** and overhang homologous to the 5' end of the *CYC1*t
107	Bacsub_Il vD-Leu1- co_CYC1t _R	CGTGAATGTAAGCGTGACATAACT AATTACATGACTCGAGGCGGCCG C*TTA***CCAGTCTTGGTGAACCTT**GA TCTTCATGATACCACCAGTG	amplification of *ilvD^{CO}* from *B. subtilis* with C-terminal **KVHQDW** and overhang homologous to the 5' end of the *CYC1*t

MBP	Name	Sequence	Description
108	HXT7p-Citsp_IlvD-co_F	AAACACAAAAACAAAAAGTTTTTTTAATTTTAATCAAAAAGCGGCCGC*ATG*CCAAAGTACAGATCTGC	amplification of *ilvD*^{CO} from *Citrobacter sp*, overhang homologous to the 3' end of the truncated *HXT7p*
109	Citsp_IlvD-W-co_CYC1t_R	CGTGAATGTAAGCGTGACATAACTAATTACATGACTCGAGGCGGCCGC*TTA***CCA**ACCACCCAACTTAGACTTG	amplification of *ilvD*^{CO} from *Citrobacter sp or P. carotovorum* with C-terminal **W** and overhang homologous to the 5' end of the *CYC1*t
110	Citsp_IlvD-Leu1-co_CYC1t_R	CGTGAATGTAAGCGTGACATAACTAATTACATGACTCGAGGCGGCCGC*TTA***CCAGTCTTGGTGAACCTT**ACCACCCAACTTAGACTTG	amplification of *ilvD*^{CO} from *Citrobacter sp or P. carotovorum* with C-terminal **KVHQDW** and overhang homologous to the 5' end of the *CYC1*t
111	Xennem_IlvD-W-co_CYC1t_R	CGTGAATGTAAGCGTGACATAACTAATTACATGACTCGAGGCGGCCGC*TTA***CCA**ACAACCCAACTTAGTCTTGTC	amplification of *ilvD*^{CO} from *X. nematophila* with C-terminal **W** and overhang homologous to the 5' end of the *CYC1*t
112	Xennem_IlvD-Leu1-co_CYC1t_R	CGTGAATGTAAGCGTGACATAACTAATTACATGACTCGAGGCGGCCGC*TTA***CCAGTCTTGGTGAACCTT**ACAACCCAACTTAGTCTTGTC	amplification of *ilvD*^{CO} from *X. nematophila* with C-terminal **KVHQDW** and overhang homologous to the 5' end of the *CYC1*t
113	HXT7p-Grx5_F	TAAACACAAAAACAAAAAGTTTTTTTAATTTTAATCAAAAAATGTTTCTCCCAAAATTCAATCC	amplification of *GRX5*, overhang *homologous to the 3' end of the truncated HXT7p*
114	Grx5-FBA1t_R	AATACTCATTAAAAAACTATATCAATTAATTTGAATTAACTCAACGATCTTTGGTTTCTTC	amplification of *GRX5,* overhang homologous to the 5' end of the *FBA1*t
116	HXT7p-Grx5D29_F	AAACACAAAAACAAAAAGTTTTTTTAATTTTAATCAAAAAATGTTGAGCACAGAGATAAG	amplification of *GRX5*Δ29, overhang *homologous to the 3' end of the truncated HXT7p*
117	HXT7p-Grx3_F	AAACACAAAAACAAAAAGTTTTTTTAATTTTAATCAAAAAATGCCTGTTATTGAAATTAACGATC	amplification of *GRX3*, overhang *homologous to the 3' end of the truncated HXT7p*
118	Grx3-FBA1t_R	AATACTCATTAAAAAACTATATCAATTAATTTGAATTAACTTAAGATTGGAGAGCATGCTG	amplification of *GRX3,* overhang homologous to the 5' end of the *FBA1*t
119	HXT7p-Grx4_F	AAACACAAAAACAAAAAGTTTTTTTAATTTTAATCAAAAAATGACTGTGGTTGAAATAAAAAGC	amplification of *GRX4*, overhang *homologous to the 3' end of the truncated HXT7p*
120	Grx4-FBA1t_R	AATACTCATTAAAAAACTATATCAATTAATTTGAATTAACTTACTGTAGAGCATGTTGGAAATATTC	amplification of *GRX4,* overhang homologous to the 5' end of the *FBA1*t
121	FMO1-Ilv2p-F	CGTAAAAAGGAATGTACTTGTATAG	primer for construction and/or sequencing of MBV057
122	FMO1-Ilv2p-R	CTGTGCGGATTTTCCAG	primer for construction and/or sequencing of MBV057
123	Ilv2p-PFK1p-F	GAAAACTTTCTTTTTGAATCTGGAAAATCCGCACAGGTTTAAACTCCGGATTGAAAATTGATTCTGTTGTATTTATCTCC	primer for construction and/or sequencing of MBV057

MBP	Name	Sequence	Description
124	Ilv2p-PFK1p-R	AAAAAAAAACCGATTTCACTTTCTCATCCTTATATTTTTCTCCGGAATGAAAGGTGACAAACGCC	primer for construction and/or sequencing of MBV057
125	FBA1p-F	TGGGTCATTACGTAAATAATGATAG	primer for construction and/or sequencing of MBV057
126	FBA1p-R	CCCGGGTTTGAATATGTATTACTTGGTTATG	primer for construction and/or sequencing of MBV057
127	PFK1p-IlvCE6E-F	ATATATAACCATAACCAAGTAATACATATTCAAACCCGGGATGGCTAACTACTTCAACAC	primer for construction and/or sequencing of MBV057
128	IlvCE6E-PGK1t-R	AAAAATTGATCTATCGATTTCAATTCAATTCAATCCCGGGTTAACCAGCAACAGCAATTC	primer for construction and/or sequencing of MBV057
129	IlvCE6E-PGK1t-F	GACCGACATGAAGAGAATTGCTGTTGCTGGTTAACCCGGGATTGAATTGAATTGAAATCGATAG	primer for construction and/or sequencing of MBV057
130	PGK1t-ADH1p-R	CGGAGGGGTGTTACCCCCCTTCTCTACTAGCATTGGACTTAAATAATATCCTTCTCGAAAGC	primer for construction and/or sequencing of MBV057
131	PGK1t-ADH1p-F	AAATTCTGCGTTCGTTAAAGCTTTCGAGAAGGATATTATTTAAGTCCAATGCTAGTAGAG	primer for construction and/or sequencing of MBV057
132	ADH1p-Aro10-co-R	TTCTTGGTTAACGAACTTTTCGATAGTAACTGGAGCCATGGATCCTGTATATGAGATAGTTGATTGTATG	primer for construction and/or sequencing of MBV057
133	ADH1p-Aro10-co-F	TCAAGCTATACCAAGCATACAATCAACTATCTCATATACAGGATCCATGGCTCCAGTTACTATCG	primer for construction and/or sequencing of MBV057
134	GUS1t-PGK1p-R	AGCGTGTCTGGGTTTTTTCAGTTTTGTTCTTTTTGCAAACATATCCTTCAAGTACCTTTTGTAAC	primer for construction and/or sequencing of MBV057
135	GUS1t-PGK1p-F	AAGGAAAATATTCAAAGTTACAAAAGGTACTTGAAGGATATGTTTGCAAAAAGAACAAAAC	primer for construction and/or sequencing of MBV057
136	PGK1p-Adh2-F	TAGAAGATAATGGCTTTTTGAGTTTCTGGAATAGACATCCGCGGTGTTTTATATTTGTTGTAAAAAGTAG	primer for construction and/or sequencing of MBV057
137	PGK1p-Adh2-F	AGGAAGTAATTATCTACTTTTTACAACAAATATAAAACACCGCGGATGTCTATTCCAGAAACTCAAAAAG	primer for construction and/or sequencing of MBV057
144	FMO1-R	GAGGGAAACGAAATATTAAGCGGCAC	primer for construction and sequencing of MBV057
145	PFKp-F	GAAAAATATAAGGATGAGAAAGTGAAATC	primer for construction and sequencing of MBV057
158	CC-PIM1_F	CATACACGGCGATCCGTCCGGTTTTAGAGCTAGAAATAGCAAGTTAAAATAAGG	amplification of *PIM1* targeting sequence for CrisprCas according to Generoso *et al.* (2016)

MBP	Name	Sequence	Description
159	CC-PIM1_R	CCGGACGGATCGCCGTGTATGGATCATTTATCTTTCACTGCGGAG	amplification of *PIM1* targeting sequence for CrisprCas according to Generoso *et al.* (2016)
160	A1-PIM1_F	CCTGCTGGTCGTTGGTTCTC	sequencing primer to confirm *pim1* deletion
161	A4-PIM1_R	CGCGATTCCGCCATCTTG	sequencing primer to confirm *pim1* deletion
162	DR-PIM1	GTTTTCGAGGTGCTTGAACGAAAAGATTTGCAAATAGAGCCTTTTCATCTAAATGGATTAAATACCTGTTTAAACATTCT	donor DNA for CisprCas deletion of *PIM1* according to Generoso *et al.* (2016)
225	DR-Ilv2_F	TGAGCTAAGAGGAGATAAATACAACAGAATCAATTTTCAAATTTCAAAAACATTTATTTCAAAAGCATTTTCAGTAAAAA	donor DNA for CrisprCas deletion of *ILV2* according to Generoso *et al.* (2016)
226	DR-Ilv2_R	TTTTTACTGAAAATGCTTTTGAAATAAATGTTTTTGAAATTTGAAAATTGATTCTGTTGTATTTATCTCCTCTTAGCTCA	donor DNA for CrisprCas deletion of *ILV2* according to Generoso *et al.* (2016)
227	tTEF-Ilv2p_F	CTGCTGTCGATTCGATACTAACGCCGCCATCCAGTGTCGAGTTTAAACTCCGGAATGAAAGGTGACAAACGC	primer for construction and/or sequencing of MBV057
228	Ilv2p-PFK1p	AAAAAAAAACCGATTTCACTTTCTCATCCTTATATTTTTCTCCGGATTGAAAATTGATTCTGTTGTATTTATCTC	primer for construction and/or sequencing of MBV057
229	TUB1t-ILV2t_F	CCCATTTCCATGATTATTTCACGGATTTCATTAGTAATTGGCGGCCGCATTTCAAAAACATTTATTTCAAAAGCATTTTC	primer for construction and/or sequencing of MBV057
230	ILV2t-pBR322-R	GTCAGGGGGGCGGAGCCTATGGAAAAACGCCAGCAACGCGGTTTAAACGCGGCCGCATGCTTTATTATAAACTATAACCTTTAAATACATAG	primer for construction and/or sequencing of MBV057
231	HXT7-Ilv2D48_F	AAACACAAAAACAAAAAGTTTTTTTAATTTTAATCAAAAA*ATG*CCAGAACCAGCTC	amplification of *ILV2Δ54*^{CO}, and overhang homologous to the 3' end of the truncated *HXT7p*
232	Ilv2D48-Cyc1_R	GGAGGGCGTGAATGTAAGCGTGACATAACTAATTACATGA*TTA*GTGCTTACCACCGG	amplification of *ILV2Δ54*^{CO}, and overhang homologous to the 5' end of the *CYC1*t
233	HXT7p-Ilv3D19_F	AAACACAAAAACAAAAAGTTTTTTTAATTTTAATCAAAAA*ATG*GCTAAGAAGTTGAACAAGTAC	amplification of *ILV3Δ19*^{CO}, and overhang homologous to the 3' end of the truncated *HXT7p*
234	Ilv3D19-CYC1t_R	GGAGGGCGTGAATGTAAGCGTGACATAACTAATTACATGA*TTA*AGCGTCCAAAACACAAC	amplification of *ILV3Δ19*^{CO}, and overhang homologous to the 5' end of the *CYC1*t
235	HXT7p-IlvC6E6_F	AAACACAAAAACAAAAAGTTTTTTTAATTTTAATCAAAAA*ATG*GCTAACTACTTCAACACC	amplification of *ilvC*$^{6E6-CO}$ from *E. coli*, overhang homologous to the 3' end of the truncated *HXT7p*

MBP	Name	Sequence	Description
236	IlvC6E6-CYC1t_R	GGAGGGCGTGAATGTAAGCGTGACATAACTAATTACATGA*TTA*ACCAGCAACAGCAATTC	amplification of *ilvC*$^{6E6\text{-}CO}$ from *E. coli* and overhang homologous to the 5' end of the *CYC1*t
237	HXT7p-Adh2_F	AAACACAAAAACAAAAAGTTTTTTTAATTTTAATCAAAAA*ATG*TCTATTCCAGAAACTCAAAAAGC	amplification of *ADH2*, and overhang homologous to the 3' end of the truncated *HXT7p*
238	Adh2-CYC1t_R	GGAGGGCGTGAATGTAAGCGTGACATAACTAATTACATGA*TTA*TTTAGAAGTGTCAACAACGTATCTAC	amplification of *ADH2*, and overhang homologous to the 5' end of the *CYC1*t
239	HXT7p-Aro10_F	AAACACAAAAACAAAAAGTTTTTTTAATTTTAATCAAAAA*ATG*GCTCCAGTTACTATCG	amplification of *ARO10*^{CO}, and overhang homologous to the 3' end of the truncated *HXT7p*
240	Aro10-CYC1t_R	GGAGGGCGTGAATGTAAGCGTGACATAACTAATTACATGA*TTA*CTTCTTGTTTCTCTTCAAAGC	amplification of *ARO10*^{CO}, and overhang homologous to the 5' end of the *CYC1*t
241	Seq-IlvC6E6_R	GCGTAAGCTCTCAACTTAG	internal reverse sequencing primer to confirm *ilvC*$^{6E6\text{-}CO}$ sequence
242	Seq-GUSt_F	CTTTTATAAGTGAATGGTTTGCTTTCTG	internal forward sequencing primer for MBV057
243	Ilv2E139A-F	CTTCGTTCTTCCAAAACACGCTCAAGGTGCCGGTCACATG	amplification of *ILV2* fragment with point mutation E139A
244	Ilv2E139A-R	CATGTGACCGGCACCTTGAGCGTGTTTTGGAAGAACGAAG	amplification of *ILV2* fragment with point mutation E139A
245	HXT7p-Ilv2_F	AAACACAAAAACAAAAAGTTTTTTTAATTTTAATCAAAAA*ATG*ATCAGACAATCTACGCTAAAAAACTTCG	amplification of *ILV2*, and overhang homologous to the 3' end of the truncated *HXT7p*
246	Ilv2-CYC1t_R	CGTGAATGTAAGCGTGACATAACTAATTACATGACTCGAG*TCA*GTGCTTACCGCCTGTAC	amplification of *ILV2*, and overhang homologous to the 5' end of the *CYC1*t
247	Ilv2D54_invers-R	GAAAGATGGAGCTGGTTCTG	internal reverse sequencing primer to confirm *ILV2*Δ*54* sequence
248	Ilv2D54_invers-F	GAGAACCGGTGGTAAGC	internal forward sequencing primer to confirm *ILV2*Δ*54* sequence
249	Ilv2E139A-Co_R	CCTTCAGCCATGTGACCAGCACCTTG**AGC**GTGCTTTGGC	amplification of *ILV2*^{CO} fragment with point mutation E139A
250	Ilv2E139A-co_F	GCCAAAGCAC**GCT**CAAGGTGCTGGTCACATGGCTGAAGG	amplification of *ILV2*^{CO} fragment with point mutation E139A
251	CC_Ilv6_Rv	CTCTACGCCGTCCTAGACTATGATCATTTATCTTTCACTGCGGAG	amplification of *ILV6* targeting sequence for CrisprCas according to Generoso *et al.* (2016)
252	CC-Ilv6_Fw	ATAGTCTAGGACGGCGTAGAGTTTTAGAGCTAGAAATAGCAAGTTAAAATAAGG	amplification of *ILV6* targeting sequence for CrisprCas according to Generoso *et al.* (2016)
253	DR-Ilv6	AATCTTTAGAACATCTGAGCTCACTAACCCAGTCTTTCTAAGGTCGTGTCGTCGACATCAGCGAAACAAGCTGTATTGTG	donor DNA for CrisprCas deletion of *ilv6* according to according to Generoso *et al.* (2016)
254	HXT7-Ilv6_Fw	AAACACAAAAACAAAAAGTTTTTTTAATTTTAATCAAAAA*ATG*CTGAGATCGTTATTG	amplification of *ILV6*, and overhang homologous to the 3' end of the truncated *HXT7p*

MBP	Name	Sequence	Description
255	Ilv6_FBA1t_Rv	ATACTCATTAAAAAACTATATCAATTAATTTGAATTAAC*CTA*ACCAGGTGGTAGT	amplification of *ILV6*, and overhang homologous to the 5' end of the *FBA1t*
256	Ilv6Asn86Ala_Rv	TCTGGACAAGACACCGGGTTC**AGC**TTGCACCAAACAGTTCAAGAC	amplification of *ILV6* fragment with point mutation N86A
257	Ilv6Asn86Ala_Fw	GTCTTGAACTGTTTGGTGCAA**GCT**GAACCCGGTGTCTTGTCCAGA	amplification of *ILV6* fragment with point mutation N86A
258	CC_Fra2_Rv	CCGAGAGGATAGAATCAGCCAGATCATTTATCTTTCACTGCGGAG	amplification of *FRA2* targeting sequence for CrisprCas according to Generoso *et al.* (2016)
259	CC_Fra2_Fw	TGGCTGATTCTATCCTCTCGGTTTTAGAGCTAGAAATAGCAAGTTAAAATAAGG	amplification of *FRA2* targeting sequence for CrisprCas according to Generoso *et al.* (2016)
260	DR-Fra2	TATTGGAATAAGTTTTTCGGTGTTATATATATACATATATAAAGGATGATATTGTTCTATTATTAAGTTTCGAAAGGAGA	donor DNA for CrisprCas deletion of *fra2* according to Generoso *et al.* (2016)
261	A1-Fra2_Fw	CAAGTCGTCAGTTTCGC	sequencing primer to confirm *fra2* deletion
262	A4-Fra2_Rv	AAAGCCATTCTACTGTTCCC	sequencing primer to confirm *fra2* deletion
263	A1-Ilv6_fw	TCGCCATCGACAAGAAC	sequencing primer to confirm *ilv6* deletion
264	A4-Ilv6_Rv	AAAGGGAATGACCTCGTTG	Internal reverse sequencing primer to confirm *ilv6* deletion
267	pHXT7-IlvN_Fw	AAACACAAAAACAAAAAGTTTTTTTAATTTTAATCAAAAA*ATG*GCTAACTCTGACGTTAC	amplification of *ilvN*$^{M13\text{-}CO}$ *from C. glutamicum*, overhang homologous to the 3' end of the truncated *HXT7p*
268	IlvN-tFBA1_Rv	AATACTCATTAAAAAACTATATCAATTAATTTGAAT*TAA*CTTAGATCTTAGCTGGAGCC	amplification of *ilvN*$^{M13\text{-}CO}$ *from C. glutamicum,* overhang homologous to the 5' end of the *FBA1*t
269	IlvN-DDF2GII_Rv	AGTTGAAAGCTCTTCTAGTGAACATACCAGAAACTCTAGA**GATGATACC**GTCAACGTCTTGAACCAAAAC	amplification of *ilvN*$^{\text{-}CO}$ *from ilvN*$^{M13\text{-}CO}$ by inserting mutations for a protein sequence change at position 20-21 from DDF to GII, with overhang *homologous to the 3' end of the truncated HXT7p*
270	IlvN-DDF2GII_Fw	TACTAGACACATCTTGTCTGTTTTGGTTCAAGACGTTGAC**GGTATCATC**TCTAGAGTTTCTGGTATGTTCAC	amplification of *ilvN*$^{\text{-}CO}$ *from C. glutamicum,* overhang homologous to the 5' end of the *FBA1*t
271	ARN1_Fw	CCAAGCAAATCGGAGTACAG	sequencing primer to confirm *ARN1* mutation in MBY36
272	ARN1_Rv	GTAGTGCCGCACTATAC	sequencing primer to confirm *ARN1* mutation in MBY36
273	ATG34_Fw	CAGGCATGAAACTCAGTC	sequencing primer to confirm *ATG34* mutation in MBY36
274	AGT34_Rv	GGATAATATCCTCAAAAAGTCGC	sequencing primer to confirm *ATG34* mutation in MBY36
275	CIT1_Fw	GGATTGCTAGTCTTAAGGGGG	sequencing primer to confirm *CIT1* mutation in MBY36

MBP	Name	Sequence	Description
276	CIT1_Rv	CATAACCGGTAGGCATAGGG	sequencing primer to confirm *CIT1* mutation in MBY36
277	DAL80_Fw	CAGCGTCAGCTTGAATTTGG	sequencing primer to confirm *DAL80* mutation in MBY36
278	DAL80_Rv	CAGTGCGATGTCTGACTTCC	sequencing primer to confirm *DAL80* mutation in MBY36
279	HIR2_Fw	TCGGCTAGCATCATGAAGTC	sequencing primer to confirm *HIR2* mutation in MBY36
280	HIR2_Rv	TCCAAAGAAGGCTGGAACTC	sequencing primer to confirm *HIR2* mutation in MBY36
281	HIR2_Seq_Fw	GGATGGGTTCACCTTGTTTG	sequencing primer to confirm *HIR2* mutation in MBY36
282	HSP104_Fw	GGGCGCAAACTTATGCAACC	sequencing primer to confirm *HSP104* mutation in MBY36
283	HSP104_Rv	TTTGCTCGGGTGTCAAGTTC	sequencing primer to confirm *HSP104* mutation in MBY36
284	HSP104_Seq_Fw	CGGTGCCACCACCAATAACG	sequencing primer to confirm *HSP104* mutation in MBY36
285	OSM1_Fw	TCCGAGCTGCAGATATGAAG	sequencing primer to confirm *OSM1* mutation in MBY36
286	OSM1_Rv	GGCAATGGTGACACTTCAAC	sequencing primer to confirm *OSM1* mutation in MBY36
287	PGD1_Fw	TTTGCGAGACAAGCGAAGAG	sequencing primer to confirm *PGD1* mutation in MBY36
288	PGD1_Rv	GTCTGTCGGTGTGCTATGTC	sequencing primer to confirm *PGD1* mutation in MBY36
289	SNG1_Fw	GACTGGCGTAGTCAATAAGC	sequencing primer to confirm *SNG1* mutation in MBY36
290	SNG1_Rv	AGCTACCCGGAATGAAACAC	sequencing primer to confirm *SNG1* mutation in MBY36
291	TPS3_Fw	CGTTGCTATTCCGCTTCATC	sequencing primer to confirm *TPS3* mutation in MBY36
292	TPS3_Rv	CCGTCAGAGTCGTTCTTACC	sequencing primer to confirm *TPS3* mutation in MBY36
293	TPS3_seq_Fw	GGGTAGGTACAATGGGAATC	sequencing primer to confirm *TPS3* mutation in MBY36
294	TPS3_seq_Fw	CCTTGTGGATGCGCTGAGAG	sequencing primer to confirm *TPS3* mutation in MBY36
295	WHI2_Fw	AAGCGCAAGAAGACAACTCC	sequencing primer to confirm *WHI2* mutation in MBY36
296	WHI2_Rv	GGATGGGAAGATACGAAGAG	sequencing primer to confirm *WHI2* mutation in MBY36
297	FRT1_Fw	ATCTGGGTCGGATAGTTCAC	sequencing primer to confirm *FRT1* mutation in MBY36
298	FRT1_Rv	ATGTCCATGCGCGTTGATTG	sequencing primer to confirm *FRT1* mutation in MBY36
299	IlvB_int_Rv	ATTCTTCGTGAGCGTCAGCCTTG	internal sequencing primer to confirm *ilvB*^{CO} sequence from *C. glutamicum*
300	IlvB_int_Fw	CAAGGCTGACGCTCACGAAGAATTG	Internal sequencing primer to confirm *ilvB*^{CO} sequence from *C. glutamicum*

MBP	Name	Sequence	Description
301	HXT7p_IlvB_Fw	CACAAAAACAAAAAGTTTTTTTAATTTTAATCAAAAAATGAACGTTGCTGCTTCTCAAC	amplification of *ilvB^{CO}* from *C. glutamicum,* overhang homologous to the 3' end of the truncated *HXT7p*
302	IlvB_CYC1t_Rv	AAGCGTGACATAACTAATTACATGACTCGAGTTAAGCTTCAGTAGATTCAACAGCAGCG	amplification of *ilvB^{CO}* from *C. glutamicum,* overhang homologous to the 5' end of the *CYC1t*
303	CYC1t_ARN1p_Fw	CATTATACTGAAAACCTTGCTTGAGAAGGTTTTGGGACGCATAGTCAACTCATCGCAGG	amplification of putative *ARN1p and ARN1*, overhang *homologous to the 3' end of the CYC1t*
304	ARN1t_pBR322_Rv	GGGGGGCGGAGCCTATGGAAAAACGCCAGCAACGCGGGTACATAATTATTCAACGCCTC	amplification of putative *ARN1t and ARN1*, overhang *homologous to the 5' end of the pBR322 origin*
305	CYC1t_ATG34p_Fw	ATACTGAAAACCTTGCTTGAGAAGGTTTTGGGACGCCAATACTTGGACAAGAAGAATTC	amplification of putative *ATG34p and ATG34*, overhang *homologous to the 3' end of the CYC1t*
306	ATG34t_pBR322_Rv	GGGGGCGGAGCCTATGGAAAAACGCCAGCAACGCGGTGTCAGCATCTTAATAGTATTGG	amplification of putative *ATG34t and ATG34*, overhang *homologous to the 5' end of the pBR322 origin*
307	CYC1t_CIT1p_Fw	TTATACTGAAAACCTTGCTTGAGAAGGTTTTGGGACGCTCATCTTATTGTTGTCAGCCC	amplification of putative *CIT1p and CIT1*, overhang *homologous to the 3' end of the CYC1t*
308	CIT1t_pBR322_Rv	AGGGGGGCGGAGCCTATGGAAAAACGCCAGCAACGCGCGTTAGTTACACCTTGACGTAG	amplification of putative *CIT1t and CIT1*, overhang *homologous to the 5' end of the pBR322 origin*
309	CYC1t_DAL80p_Fw	AACATTATACTGAAAACCTTGCTTGAGAAGGTTTTGGGACGAATGCATGCTTCCTCTCC	amplification of putative *DAL80p and DAL80*, overhang *homologous to the 3' end of the CYC1t*
310	DAL80t_pBR322_Rv	TCAGGGGGGCGGAGCCTATGGAAAAACGCCAGCAACGCGCATTAAGAGCACGTTTGAGC	amplification of putative *DAL80t and DAL80*, overhang *homologous to the 5' end of the pBR322 origin*
311	CYC1t_FRT1p_Fw	AAACCGACGCCCCAGCACTCGTCCGAGGGCAAAGGAATAATATGGGGATACCAGCATCG	amplification of putative *FRT1p and FRT1*, overhang *homologous to the 3' end of the CYC1t*
312	FRT1t_pBR322_Rv	TGAATGTAAGCGTGACATAACTAATTACATGACTCGAGAATATTGGTTGCCTGTGCTCC	amplification of putative *FRT1t and FRT1*, overhang *homologous to the 5' end of the pBR322 origin*
313	CYC1t_HIR2p_Fw	AACATTATACTGAAAACCTTGCTTGAGAAGGTTTTGGGACGGTAGCGTGCATGGATGAG	amplification of putative *HIR2p and HIR2*, overhang *homologous to the 3' end of the CYC1t*
314	HIR2t_pBR322_Rv	TCAGGGGGGCGGAGCCTATGGAAAAACGCCAGCAACGCGCCAGAAATCAATCACGAAGC	amplification of putative *HIR2t and HIR2*, overhang *homologous to the 5' end of the pBR322 origin*
315	CYC1t_HSP104_Fw	TATACTGAAAACCTTGCTTGAGAAGGTTTTGGGACGCAGCCGGAACCTAAATTGATTAG	amplification of putative *HSP104p and HSP104*, overhang *homologous to the 3' end of the CYC1t*
316	HSP104p_pBR322_Rv	CTCGTCAGGGGGGCGGAGCCTATGGAAAAACGCCAGCAACGCGAATGGACCAATCCGCG	amplification of putative *HSP104t and HSP104*, overhang *homologous to the 5' end of the pBR322 origin*
317	CYC1t_OSM1p_Fw	ACATTATACTGAAAACCTTGCTTGAGAAGGTTTTGGGACGAAGAATGGCTCAAGCAGTC	amplification of putative *OSM1p and OSM1*, overhang *homologous to the 3' end of the CYC1t*

MBP	Name	Sequence	Description
318	OSM1t_pBR322_Rv	GGGGCGGAGCCTATGGAAAAACGCCAGCAACGCGCATTCAGTTTGTTAGAAGAGGGAAC	amplification of putative *OSM1t and OSM1*, overhang *homologous to the 5' end of the pBR322 origin*
319	CYC1t_PGD1p_Fw	TAACATTATACTGAAAACCTTGCTTGAGAAGGTTTTGGGACGCCCACTAAGGACCACTG	amplification of putative *PGD1p and PGD1*, overhang *homologous to the 3' end of the CYC1t*
320	PGD1t_pBR322_Rv	CAGGGGGGCGGAGCCTATGGAAAAACGCCAGCAACGCGATATCTACACCACCATCCTGG	amplification of putative *PGD1t and PGD1*, overhang *homologous to the 5' end of the pBR322 origin*
321	CYC1t_SNG1p_Fw	TAACATTATACTGAAAACCTTGCTTGAGAAGGTTTTGGGACGGTTTTGCAGGCCCATTC	amplification of putative *SNG1p and SNG1*, overhang *homologous to the 3' end of the CYC1t*
322	SNG1t_pBR322_Rv	CAGGGGGGCGGAGCCTATGGAAAAACGCCAGCAACGCGCGATTTCTTTCTACCGACCTG	amplification of putative *SNG1t and SNG1*, overhang *homologous to the 5' end of the pBR322 origin*
323	CYC1t_TPS3p_Fw	TTATACTGAAAACCTTGCTTGAGAAGGTTTTGGGACGACCGATTTCTCCAATCACACTG	amplification of putative *TPS3p and TPS3*, overhang *homologous to the 3' end of the CYC1t*
324	TPS3t_pBR322_Rv	GCGGAGCCTATGGAAAAACGCCAGCAACGCGGCAAGTACACCTTCTACATAAGTAAAGG	amplification of putative *TPS3t and TPS3*, overhang *homologous to the 5' end of the pBR322 origin*
325	CYC1t_WHI2p_Fw	ACATTATACTGAAAACCTTGCTTGAGAAGGTTTTGGGACGCCAACCTGATGGGTGTATG	amplification of putative *WHI2p and WHI2*, overhang *homologous to the 3' end of the CYC1t*
326	WHI2t_pBR322_Rv	TCAGGGGGGCGGAGCCTATGGAAAAACGCCAGCAACGCGGAAATCCAGACGTGAGTCAG	amplification of putative *WHI2t and WHI2*, overhang homologous to the 5' end of the *pBR322* origin
332	DR-PGI1_Fw	TCTTGCAAAATCGATTTAGAATCAAGATACCAGCCTAAAAGGTCTTCTCAGGTAACAGACCAACTACCTCTATCTTGGCT	donor DNA for CrisprCas deletion of *PGI1* according to Generoso *et al.* (2016)
333	DR-PGI1_Rv	AGCCAAGATAGAGGTAGTTGGTCTGTTACCTGAGAAGACCTTTTAGGCTGGTATCTTGATTCTAAATCGATTTTGCAAGA	donor DNA for CrisprCas deletion of *PGI1* according to Generoso *et al.* (2016)
334	CC-PGI1_Rv	CGACAGACAACAAACCACCCAGATCATTTATCTTTCACTGCGGAG	amplification of *PGI1* targeting sequence for CrisprCas according to Generoso *et al.* (2016)
335	CC-PGI1_Fw	TGGGTGGTTTGTTGTCTGTCGTTTTAGAGCTAGAAATAGCAAGTTAAAATAAGG	amplification of *PGI1* targeting sequence for CrisprCas according to Generoso *et al.* (2016)
336	A1-PGI1-seq_Fw	ATCGGACATGCTACCTTACG	sequencing primer to confirm *pgi1* deletion
337	A4-PGI1-seq_Rv	CGCGCACTGATTCATCTTTG	sequencing primer to confirm *pgi1* deletion
338	FPA1p-Ilv5D48_Fw	TTCTTTTTCTTTTGTCATATATAACCATAACCAAGTAATACATATTCAAAATGAAGCAAATTAACTTCGGTGG	amplification to insert *ILV5Δ48*^{CO} into IsoV100 or MBV57 under the control of *FBA1*p and *PGK1*t

MBP	Name	Sequence	Description
339	Ilv5D48-PGK1t_Rv	AAAGAAAAAAATTGATCTATCGATTTCAATTCAATTCAATTTATTGGTTTTCTGGTCTCAACTTTCTAAC	amplification to insert *ILV5Δ48*^{CO} into IsoV100 or MBV57 under the control of *FBA1*p and *PGK1*t
350	HXT7p-ALD6_Fw	AAACACAAAAACAAAAAGTTTTTTTAATTTTAATCAAAAA*ATG*ACTAAGCTACACTTTGACAC	amplification of *ALD6,* overhang *homologous to the 3' end of the truncated HXT7p*
351	ALD6-CYC1t_Rv	CGTGAATGTAAGCGTGACATAACTAATTACATGACTCGAG*TTA*CAACTTAATTCTGACAGCTTTTAC	amplification of *ALD6,* overhang homologous to the 5' end of the *FBA1*t
352	CYC1t_FBA1t_F	TTGCTTGAGAAGGTTTTGGGACGCTCGAAGGCTTTAATTTTGGGTCATTACGTAAATAATGATAG	amplification to insert *ilvC*^{CO} variants from *E. coli* into IsoV100 or MBV57 under the control of *FBA1*p and *PGK1*t
353	FBA1p_IlvC6E6_R	ATTGTTGTCTCAAGTTCAAGGTGTTGAAGTAGTTAGCCATTTTGAATATGTATTACTTGGTTATGG	amplification to insert *ilvC*^{CO} variants from *E. coli* into IsoV100 or MBV57 under the control of *FBA1*p and *PGK1*t
354	FBA1t_IlvC6E6_F	TTTGTCATATATAACCATAACCAAGTAATACATATTCAAAATGGCTAACTACTTCAACAC	amplification to insert *ilvC*^{CO} variants from *E. coli* into IsoV100 or MBV57 under the control of *FBA1*p and *PGK1*t
355	IlvC6E6_PGK1t_R	AAAGAAAAAAATTGATCTATCGATTTCAATTCAATTCAATTTAACCAGCAACAGCAATTC	amplification to insert *ilvC*^{CO} variants from *E. coli* into IsoV100 or MBV57 under the control of *FBA1*p and *PGK1*t
356	IlvC6E6_PGK1t_F	TTACATGACCGACATGAAGAGAATTGCTGTTGCTGGTTAAATTGAATTGAATTGAAATCGATAGATC	amplification to insert *ilvC*^{CO} variants from *E. coli* into IsoV100 or MBV57 under the control of *FBA1*p and *PGK1*t
357	PFK1t_TEFp_R	AAGACTGTCAAGGAGGGTATTCTGGGCCTCCATGTCGCTGAAATAATATCCTTCTCGAAAGCTTTAAC	amplification to insert *ilvC*^{CO} variants from *E. coli* into IsoV100 or MBV57 under the control of *FBA1*p and *PGK1*t
358	IlvC_Asp146Gly_R	TGGAGCAACCATAACAACGGTAAT**ACC**CTTTCTAATTTGTTCACCAACTTC	amplification of *ilvC*^{CO} fragment from *E. coli* with point mutation N146G for construction of
359	IlvC_Asp146Gly_F	TGTTGAAGTTGGTGAACAAATTAGAAAG**GGT**ATTACCGTTGTTATGGTTGC	amplification of *ilvC*^{CO} fragment from *E. coli* with point mutation N146G
360	IlvC_Gly185Arg_R	AGCCCAAGCCTTAGCAATAGCCATACCTTC**TCT**CTTTGGGTCGTTTTCTGG	amplification of *ilvC*^{CO} fragment from *E. coli* with point mutation G185R
361	IlvC_Gly185Arg_F	GCTGTTCACCCAGAAAACGACCCAAAG**AGA**GAAGGTATGGCTATTGCTAAG	amplification of *ilvC*^{CO} fragment from *E. coli* with point mutation G185R
362	IlvC_Lys433Glu_R	GTCACCTGGTTGCAATTCAGCCATGAATGG**TTC**CAACAATGGAACACAAGC	amplification of *ilvC*^{CO} fragment from *E. coli* with point mutation K433Q
363	IlvC_Lys433Glu_F	TGTTCTCTTACGCTTGTGTTCCATTGTTG**GAA**CCATTCATGGCTGAATTGC	amplification of *ilvC*^{CO} fragment from *E. coli* with point mutation K433Q

III. SYNTHETIC GENES

Table 35 Sequence of synthetic codon optimized genes, used in this work. Homologous regions which do not belong to the ORF are underlined.

Synthetic gene sequence of *ilvD*^{CO} from *E. coli*

TCAAGCTATACCAAGCATACAATCAACTATCTCATATACAGCGGCCGCATGCCAAAGTACAGATCTGCTACTACTACTCA
CGGTAGAAACATGGCTGGTGCTAGAGCTTTGTGGAGAGCTACTGGTATGACTGACGCTGACTTCGGTAAGCCAATCATCG
CTGTTGTTAACTCTTTCACTCAATTCGTTCCAGGTCACGTTCACTTGAGAGACTTGGGTAAGTTGGTTGCTGAACAAATC
GAAGCTGCTGGTGGTGTTGCTAAGGAATTCAACACTATCGCTGTTGACGACGGTATCGCTATGGGTCACGGTGGTATGTT
GTACTCTTTGCCATCTAGAGAATTGATCGCTGACTCTGTTGAATACATGGTTAACGCTCACTGTGCTGACGCTATGGTTT
GTATCTCTAACTGTGACAAGATCACTCCAGGTATGTTGATGGCTTCTTTGAGATTGAACATCCCAGTTATCTTCGTTTCT
GGTGGTCCAATGGAAGCTGGTAAGACTAAGTTGTCTGACCAAATCATCAAGTTGGACTTGGTTGACGCTATGATCCAAGG
TGCTGACCCAAAGGTTTCTGACTCTCAATCTGACCAAGTTGAAAGATCTGCTTGTCCAACTTGTGGTTCTTGTTCTGGTA
TGTTCACTGCTAACTCTATGAACTGTTTGACTGAAGCTTTGGGTTTGTCTCAACCAGGTAACGGTTCTTTGTTGGCTACT
CACGCTGACAGAAAGCAATTGTTCTTGAACGCTGGTAAGAGAATCGTTGAATTGACTAAGAGATACTACGAACAAAACGA
CGAATCTGCTTTGCCAAGAAACATCGCTTCTAAGGCTGCTTTCGAAAACGCTATGACTTTGGACATCGCTATGGGTGGTT
CTACTAACACTGTTTTGCACTTGTTGGCTGCTGCTCAAGAAGCTGAAATCGACTTCACTATGTCTGACATCGACAAGTTG
TCTAGAAAGGTTCCACAATTGTGTAAGGTTGCTCCATCTACTCAAAAGTACCACATGGAAGACGTTCACAGAGCTGGTGG
TGTTATCGGTATCTTGGGTGAATTGGACAGAGCTGGTTTGTTGAACAGAGACGTTAAGAACGTTTTGGGTTTGACTTTGC
CACAAACTTTGGAACAATACGACGTTATGTTGACTCAAGACGACGCTGTTAAGAACATGTTCAGAGCTGGTCCAGCTGGT
ATCAGAACTACTCAAGCTTTCTCTCAAGACTGTAGATGGGACACTTTGGACGACGACAGAGCTAACGGTTGTATCAGATC
TTTGGAACACGCTTACTCTAAGGACGGTGGTTTGGCTGTTTTGTACGGTAACTTCGCTGAAAACGGTTGTATCGTTAAGA
CTGCTGGTGTTGACGACTCTATCTTGAAGTTCACTGGTCCAGCTAAGGTTTACGAATCTCAAGACGACGCTGTTGAAGCT
ATCTTGGGTGGTAAGGTTGTTGCTGGTGACGTTGTTGTTATCAGATACGAAGGTCCAAAGGGTGGTCCAGGTATGCAAGA
AATGTTGTACCCAACTTCTTTCTTGAAGTCTATGGGTTTGGGTAAGGCTTGTGCTTTGATCACTGACGGTAGATTCTCTG
GTGGTACTTCTGGTTTGTCTATCGGTCACGTTTCTCCAGAAGCTGCTTCTGGTGGTTCTATCGGTTTGATCGAAGACGGT
GACTTGATCGCTATCGACATCCCAAACAGAGGTATCCAATTGCAAGTTTCTGACGCTGAATTGGCTGCTAGAAGAGAAGC
TCAAGACGCTAGAGGTGACAAGGCTTGGACTCCAAAGAACAGAGAAAGACAAGTTTCTTTCGCTTTGAGAGCTTACGCTT
CTTTGGCTACTTCTGCTGACAAGGGTGCTGTTAGAGACAAGTCTAAGTTGGGTGGTTAAGCGGCCGCACACTCTCCCCCC
CCCTCCCCCTCTGATCTTTCCTGTTGC

Synthetic gene sequence of *ilvD*^{CO} from *Citrobacter sp. 30_2*

CTTTTCTAAGAACAAAGAATAAACACAAAAACAAAAAGTTTTTTTAATTTTAATCAAAAAGCGGCCGCATGCCAAAGTAC
AGATCTGCTACTACTACTCACGGTAGAAACATGGCTGGTGCTAGAGCTTTGTGGAGAGCTACTGGTATGACTGACGACGA
CTTCGGTAAGCCAATCATCGCTGTTGTTAACTCTTTCACTCAATTCGTTCCAGGTCACGTTCACTTGAGAGACTTGGGTA
AGTTGGTTGCTGAACAAATCGAAGCTTCTGGTGGTGTTGCTAAGGAATTCAACACTATCGCTGTTGACGACGGTATCGCT
ATGGGTCACGGTGGTATGTTGTACTCTTTGCCATCTAGAGAATTGATCGCTGACTCTGTTGAATACATGGTTAACGCTCA
CTGTGCTGACGCTATGGTTTGTATCTCTAACTGTGACAAGATCACTCCAGGTATGTTGATGGCTTCTTTGAGATTGAACA
TCCCAGTTATCTTCGTTTCTGGTGGTCCAATGGAAGCTGGTAAGACTAAGTTGTCTGACCAAATCATCAAGTTGGACTTG
GTTGACGCTATGATCCAAGGTGCTGACCCAAAGGTTTCTGACTCTCAATCTGAACAAGTTGAAAGATCTGCTTGTCCAAC
TTGTGGTTCTTGTTCTGGTATGTTCACTGCTAACTCTATGAACTGTTTGACTGAAGCTTTGGGTTTGTCTCAACCAGGTA
ACGGTTCTTTGTTGGCTACTCACGCTGACAGAAAGGAATTGTTCTTGACTGCTGGTCAAAGAATCGTTGAATTGACTAAG
AGATACTACGAACAAGACGACGCTTCTGCTTTGCCAAGAAACATCGCTTCTAAGGCTGCTTTCGAAAACGCTATGACTTT
GGACATCGCTATGGGTGGTTCTACTAACACTGTTTTGCACTTGTTGGCTGCTGCTCAAGAAGCTGAAATCGACTTCACTA
TGTCTGACATCGACAAGTTGTCTAGAAAGGTTCCACAATTGTGTAAGGTTGCTCCATCTACTCAAAAGTACCACATGGAA
GACGTTCACAGAGCTGGTGGTGTTTTGGGTATCTTGGGTGAATTGGACAGAGCTGGTTTGTTGAACAGAGACGTTAAGAA
CGTTTTGGGTTTGACTTTGCCACAAACTTTGGACAGATACGACGTTATGTTGACTAAGGACGACGCTGTTAAGAAGATGT
TCAGAGCTGGTCCAGCTGGTATCAGAACTACTCAAGCTTTCTCTCAAGACTGTAGATGGGACACTTTGGACGACGACAGA
GCTGAAGGTTGTATCAGATCTTTGGAACACGCTTACTCTAAGGACGGTGGTTTGGCTGTTTTGTACGGTAACTTCGCTGA
AAACGGTTGTATCGTTAAGACTGCTGGTGTTGACGACTCTATCTTGAAGTTCACTGGTCCAGCTAAGGTTTACGAATCTC
AAGACGACGCTGTTGAAGCTATCTTGGGTGGTAAGGTTGTTGCTGGTGACGTTGTTGTTATCAGATACGAAGGTCCAAAG
GGTGGTCCAGGTATGCAAGAAATGTTGTACCCAACTACTTTCTTGAAGTCTATGGGTTTGGGTAAGGCTTGTGCTTTGAT
CACTGACGGTAGATTCTCTGGTGGTACTTCTGGTTTGTCTATCGGTCACGTTTCTCCAGAAGCTGCTTCTGGTGGTAACA
TCGCTATCATCGAAGACGGTGACATGATCGCTATCGACATCCCAAACAGAGGTATCCAATTGCAATTGTCTGACGCTGAA
ATCGCTGCTAGAAGAGAAGCTCAAGAAGCTAGAGGTGACAAGGCTTGGACTCCAAAGGACAGACAAAGACAAGTTTCTTT
CGCTTTGAGAGCTTACGCTTCTTTGGCTACTTCTGCTGACAAGGGTGCTGTTAGAGACAAGTCTAAGTTGGGTGGTTAAA
TCCGCTGCGGCCGCCTCGAGTCATGTAATTAGTTATGTCACGCTTACATTCACGCCCTCCCCCCAC

Synthetic gene sequence of *ilvD*^{CO} from *Pectobacterium carotovorum subsp. WPP14*

CTTTTCTAAGAACAAAGAATAAACACAAAAACAAAAAGTTTTTTTAATTTTAATCAAAAAGCGGCCGCATGCCAAAGTAC
AGATCTGCTACTACTACTCACGGTAGAAACATGGCTGGTGCTAGAGCTTTGTGGAGAGCTACTGGTATGACTGACGACGA
CTTCGGTAAGCCAATCATCGCTGTTGTTAACTCTTTCACTCAATTCGTTCCAGGTCACGTTCACTTGAGAGACTTGGGTA
AGTTGGTTGCTGAACAAATCGAAGCTTCTGGTGGTGTTGCTAAGGAATTCAACACTATCGCTGTTGACGACGGTATCGCT
ATGGGTCACGGTGGTATGTTGTACTCTTTGCCATCTAGAGAATTGATCGCTGACTCTGTTGAATACATGGTTAACGCTCA
CTGTGCTGACGCTATGGTTTGTATCTCTAACTGTGACAAGATCACTCCAGGTATGTTGATGGCTTCTTTGAGATTGAACA
TCCCAGTTATCTTCGTTTCTGGTGGTCCAATGGAAGCTGGTAAGACTAAGTTGTCTGACCAAATCATCAAGTTGGACTTG
GTTGACGCTATGATCCAAGGTGCTGACCCAAAGGTTTCTGACGAACAATCTGAACAAGTTGAAAGATCTGCTTGTCCAAC

TTGTGGTTCTTGTTCTGGTATGTTCACTGCTAACTCTATGAACTGTTTGACTGAAGCTTTGGGTTTGTCTCAACCAGGTA
ACGGTTCTTTGTTGGCTACTCACGCTGACAGAAAGCAATTGTTCTTGAACGCTGGTAAGAGAATCGTTGGTTTGGCTAAG
AGATACTACGAACAAGACGACGCTTCTGTTTTGCCAAGAAACATCGCTAACAAGGCTGCTTTCGAAAACGCTATGGTTTT
GGACATCGCTATGGGTGGTTCTACTAACACTGTTTTGCACTTGTTGGCTGCTGCTCAAGAAGGTGAAGTTGACTTCACTA
TGACTGACATCGACAGATTGTCTAGACAAGTTCCACACTTGTGTAAGGTTGCTCCATCTACTCAAAAGTACCACATGGAA
GACGTTCACAGAGCTGGTGGTGTTATCGGTATCTTGGGTGAATTGGACAGAGCTGGTTTGTTGAACAGAGAAGTTAACAA
CGTTTTGGGTAAGACTTTGCCAGAAACTTTGGAAGCTTACGACGTTATGTTGACTCAAGACGACTCTGTTAAGTCTATGT
ACTCTGCTGGTCCAGCTGGTATCAGAACTACTAAGGCTTTCTCTCAAGACTGTAGATGGGACTCTTTGGACACTGACAGA
CAAGAAGGTTGTATCAGATCTAGAGAATACGCTTACTCTCAAGACGGTGGTTTGGCTGTTTTGTACGGTAACTTGGCTGA
AAACGGTTGTATCGTTAAGACTGCTGGTGTTGACGAAGGTTCTTTGGTTTTCAGAGGTCCAGCTAAGGTTTACGAATCTC
AAGACGACGCTGTTGAAGCTATCTTGGGTGGTAAGGTTGTTGCTGGTGACGTTGTTGTTATCAGATACGAAGGTCCAAAG
GGTGGTCCAGGTATGCAAGAAATGTTGTACCCAACTACTTACTTGAAGTCTATGGGTTTGGGTAAGTCTTGTGCTTTGAT
CACTGACGGTAGATTCTCTGGTGGTACTTCTGGTTTGTCTATCGGTCACGCTTCTCCAGAAGCTGCTTCTGGTGGTACTA
TCGCTTTGGTTCAAGACGGTGACACTATCGCTATCGACATCCCAAACAGATCTATCGCTTTGGTTTTGGACGACGCTGAA
TTGGCTTCTAGAAGAGAAGCTGAAGAAGCTAGAGGTGAACAAGCTTGGACTCCACACAACAGAGAAAGACAAGTTTCTTT
CGCTTTGAGAGCTTACGCTTCTTTGGCTACTTCTGCTGACAAGGGTGCTGTTAGAGACAAGTCTAAGTTGGGTGGTTAAG
CGGCCGCCTCGAGTCATGTAATTAGTTATGTCACGCTTACATTCACGCCCTCCCCCCACATCCGCT

Synthetic gene sequence of *ilvD*^{CO} from *Xenorhabdus nematophila ATCC 19061*

CTTTTCTAAGAACAAAGAATAAACACAAAAACAAAAAGTTTTTTTAATTTTAATCAAAAAGCGGCCGCATGCCAAAGTAC
AGATCTGCTACTACTACTCACGGTAGAAACATGGCTGGTGCTAGAGCTTTGTGGAGAGCTACTGGTATGACTGACGCTGA
CTTCGGTAAGCCAATCATCGCTGTTGTTAACTCTTTCACTCAATTCGTTCCAGGTCACGTTCACTTGAGAGACTTGGGTA
AGTTGGTTGCTGAACAAATCGAAGCTTCTGGTGGTGTTGCTAAGGAATTCAACACTATCGCTGTTGACGACGGTATCGCT
ATGGGTCACGGTGGTATGTTGTACTCTTTGCCATCTAGAGAATTGATCGCTGACTCTGTTGAATACATGGTTAACGCTCA
CTGTGCTGACGCTATGGTTTGTATCTCTAACTGTGACAAGATCACTCCAGGTATGTTGATGGCTTCTTTGAGATTGAACA
TCCCAGTTATCTTCGTTTCTGGTGGTCCAATGGAAGCTGGTAAGACTAGATTGTCTGACCAAATCATCAAGTTGGACTTG
GTTGACGCTATGATCCAAGGTGCTAACCCAAACGTTTCTGACGAACAATCTGACCAAATCGAAAGATCTGCTTGTCCAAC
TTGTGGTTCTTGTTCTGGTATGTTCACTGCTAACTCTATGAACTGTTTGACTGAAGCTTTGGGTTTGTCTCAACCAGGTA
ACGGTTCTTTGTTGGCTACTCACGCTGACAGAAAGACTTTGTTCATCAACGCTGGTAAGAGAATCGTTGCTTTGACTAAG
AGATACTACGAAAAGAACGACGACTCTGCTTTGCCAAGAAACATCGCTACTAAGGCTGCTTTCGAAAACGCTATGACTTT
GGACATCGCTATGGGTGGTTCTACTAACACTGTTTTGCACTTGTTGGCTGCTGCTCAAGAAGGTGAAGTTGACTTCACTA
TGGCTGACATCGACAGATTGTCTAGACAAGTTCCACACTTGTGTAAGGTTGCTCCATCTACTCAAAAGTACCACATGGAA
GACGTTCACAGAGCTGGTGGTGTTATGGGTATCTTGGGTGAATTGGACAGAGCTGGTTTGTTGAGAAGAGGTGTTAAGAA
CATCTTGGGTTTGGACTTGGCTCAAACTTTGGTTCAATACGACATCATGTTGACTGAAAACGAACACGTTAAGCACATGT
ACTCTGCTGGTCCAGCTGGTATCAGAACTACTCAAGCTTTCTCTCAAGACTGTAGATGGCCATCTTTGGACATCGACAGA
CAAGAAGGTTGTATCAGAGAAAGAGCTTACGCTTACTCTCAAGACGGTGGTTTGGCTGTTTTGTTCGGTAACGTTGCTGC
TAACGGTTGTATCGTTAAGACTGCTGGTGTTGACGAAGGTTCTTTGACTTTCAGAGGTCCAGCTAAGGTTTACGAATCTC
AAGACGACGCTGTTGACGCTATCTTGGGTGGTAAGGTTGTTGCTGGTGACGTTGTTATCATCAGATACGAAGGTCCAAAG
GGTGGTCCAGGTATGCAAGAAATGTTGTACCCAACTACTTACTTGAAGTCTATGGGTTTGGGTAAGTCTTGTGCTTTGAT
CACTGACGGTAGATTCTCTGGTGGTACTTCTGGTTTGTCTATCGGTCACGTTTCTCCAGAAGCTGCTAACGGTGGTTTGA
TCGGTTTGATCCAAGACGGTGACATCATCGAAATCGACATCCCAAACAGAAAGATCCAATTGGACGTTGCTGAAACTGAA
TTGGCTGAAAGAGCTCAAGCTGAATTGTCTAGAGGTGACAAGGCTTGGACTCCAAAGTCTAGAGAAAGACAAGTTTCTTT
CGCTTTGAGAGCTTACGCTTCTTTGGCTACTTCTGCTGACAAGGGTGCTGTTAGAGACAAGACTAAGTTGGGTTGTTAAG
CGGCCGCCTCGAGTCATGTAATTAGTTATGTCACGCTTACATTCACGCCCTCCCCCCACATCCGCT

Synthetic gene sequence of *ilvD*^{CO} from *Bacillus subtilis sp NRRL B-14911*

TAAAATAATAAAACATCAAGAACAAACAAGCTCAACTTGTCTTTTCTAAGAACAAAGAATAAACACAAAAACAAAAAGTT
TTTTTAATTTTAATCAAAAAGCGGCCGCATGGCTGAATTGAGATCTAACATGATCACTCAAGGTATCGACAGAGCTCCAC
ACAGATCTTTGTTGAGAGCTGCTGGTGTTAAGGAAGAAGACTTCGGTAAGCCATTCATCGCTGTTTGTAACTCTTACATC
GACATCGTTCCAGGTCACGTTCACTTGCAAGAATTCGGTAAGATCGTTAAGGAAGCTATCAGAGAAGCTGGTGGTGTTCC
ATTCGAATTCAACACTATCGGTGTTGACGACGGTATCGCTATGGGTCACATCGGTATGAGATACTCTTTGCCATCTAGAG
AAATCATCGCTGACTCTGTTGAAACTGTTGTTTCTGCTCACTGGTTCGACGGTATGGTTTGTATCCCAAACTGTGACAAG
ATCACTCCAGGTATGTTGATGGCTGCTATGAGAATCAACATCCCAACTATCTTCGTTTCTGGTGGTCCAATGGCTGCTGG
TAGAACTTCTGACGGTAGAAAGATCTCTTTGTCTTCTGTTTTCGAAGGTGTTGGTGCTTACCAAGCTGGTAAGATCAACG
AAAACGAATTGCAAGAATTGGAACAATTCGGTTGTCCAACTTGTGGTTCTTGTTCTGGTATGTTCACTGCTAACTCTATG
AACTGTTTGTCTGAAGCTTTGGGTTTGGCTTTGCCAGGTAACGGTACTATCTTGGCTACTTCTCCAGAAAGAAAGGAATT
CGTTAGAAAGTCTGCTGCTCAATTGATGGAAACTATCAGAAAGGACATCAAGCCAAGAGACATCGTTACTGTTAAGGCTA
TCGACAACGCTTTCGCTTTGGACATGGCTTTGGGTGGTTCTACTAACACTGTTTTGCACACTTTGGCTTTGGCTAACGAA
GCTGGTGTTGAATACTCTTTGGAAAGAATCAACGAAGTTGCTGAAAGAGTTCCACACTTGGCTAAGTTGGCTCCAGCTTC
TGACGTTTTCATCGAAGACTTGCACGAAGCTGGTGGTGTTTCTGCTGCTTTGAACGAATTGTCTAAGAAGGAAGGTGCTT
TGCACTTGGACGCTTTGACTGTTACTGGTAAGACTTTGGGTGAAACTATCGCTGGTCACGAAGTTAAGGACTACGACGTT
ATCCACCCATTGGACCAACCATTCACTGAAAAGGGTGGTTTGGCTGTTTTGTTCGGTAACTTGGCTCCAGACGGTGCTAT
CATCAAGACTGGTGGTGTTCAAAACGGTATCACTAGACACGAAGGTCCAGCTGTTGTTTTCGACTCTCAAGACGAAGCTT
TGGACGGTATCATCAACAGAAAGGTTAAGGAAGGTGACGTTGTTATCATCAGATACGAAGGTCCAAAGGGTGGTCCAGGT
ATGCCAGAAATGTTGGCTCCAACTTCTCAAATCGTTGGTATGGGTTTGGGTCCAAAGGTTGCTTTGATCACTGACGGTAG
ATTCTCTGGTGCTTCTAGAGGTTTGTCTATCGGTCACGTTTCTCCAGAAGCTGCTGAAGGTGGTCCATTGGCTTTCGTTG
AAAACGGTGACCACATCATCGTTGACATCGAAAAGAGAATCTTGGACGTTCAAGTTCCAGAAGAAGAATGGGAAAAGAGA
AAGGCTAACTGGAAGGGTTTCGAACCAAAGGTTAAGACTGGTTACTTGGCTAGATACTCTAAGTTGGTTACTTCTGCTAA

CACTGGTGGTATCATGAAGATCTAAGCGGCCGCCTCGAGTCATGTAATTAGTTATGTCACGCTTACATTCACGCCCTCCC
CCCACATCCGCTCTAACCGAAAAGGAAGGAGTTAGACAACCTGAAGTCTAGGT

Synthetic gene sequence of *ilvB*^{CO} from *Corynebacterium glutamicum*

ATGAACGTTGCTGCTTCTCAACAACCAACTCCAGCTACTGTTGCTTCTAGAGGTAGATCTGCTGCTCCAGAAAGAATGAC
TGGTGCTAAGGCTATCGTTAGATCTTTGGAAGAATTGAACGCTGACATCGTTTTCGGTATCCCAGGTGGTGCTGTTTTGC
CAGTTTACGACCCATTGTACTCTTCTACTAAGGTTAGACACGTTTTGGTTAGACACGAACAAGGTGCTGGTCACGCTGCT
ACTGGTTACGCTCAAGTTACTGGTAGAGTTGGTGTTTGTATCGCTACTTCTGGTCCAGGTGCTACTAACTTGGTTACTCC
AATCGCTGACGCTAACTTGGACTCTGTTCCAATGGTTGCTATCACTGGTCAAGTTGGTTCTGGTTTGTTGGGTACTGACG
CTTTCCAAGAAGCTGACATCAGAGGTATCACTATGCCAGTTACTAAGCACAACTTCATGGTTACTAACCCAAACGACATC
CCACAAGCTTTGGCTGAAGCTTTCCACTTGGCTATCACTGGTAGACCAGGTCCAGTTTTGGTTGACATCCCAAAGGACGT
TCAAAACGCTGAATTGGACTTCGTTTGGCCACCAAAGATCGACTTGCCAGGTTACAGACCAGTTTCTACTCCACACGCTA
GACAAATCGAACAAGCTGTTAAGTTGATCGGTGAAGCTAAGAAGCCAGTTTTGTACGTTGGTGGTGGTGTTATCAAGGCT
GACGCTCACGAAGAATTGAGAGCTTTCGCTGAATACACTGGTATCCCAGTTGTTACTACTTTGATGGCTTTGGGTACTTT
CCCAGAATCTCACGAATTGCACATGGGTATGCCAGGTATGCACGGTACTGTTTCTGCTGTTGGTGCTTTGCAAAGATCTG
ACTTGTTGATCGCTATCGGTTCTAGATTCGACGACAGAGTTACTGGTGACGTTGACACTTTCGCTCCAGACGCTAAGATC
ATCCACGCTGACATCGACCCAGCTGAAATCGGTAAGATCAAGCAAGTTGAAGTTCCAATCGTTGGTGACGCTAGAGAAGT
TTTGGCTAGATTGTTGGAAACTACTAAGGCTTCTAAGGCTGAAACTGAAGACATCTCTGAATGGGTTGACTACTTGAAGG
GTTTGAAGGCTAGATTCCCAAGAGGTTACGACGAACAACCAGGTGACTTGTTGGCTCCACAATTCGTTATCGAAACTTTG
TCTAAGGAAGTTGGTCCAGACGCTATCTACTGTGCTGGTGTTGGTCAACACCAAATGTGGGCTGCTCAATTCGTTGACTT
CGAAAAGCCAAGAACTTGGTTGAACTCTGGTGGTTTGGGTACTATGGGTTACGCTGTTCCAGCTGCTTTGGGTGCTAAGG
CTGGTGCTCCAGACAAGGAAGTTTGGGCTATCGACGGTGACGGTTGTTTCCAAATGACTAACCAAGAATTGACTACTGCT
GCTGTTGAAGGTTTCCCAATCAAGATCGCTTTGATCAACAACGGTAACTTGGGTATGGTTAGACAATGGCAAACTTTGTT
CTACGAAGGTAGATACTCTAACACTAAGTTGAGAAACCAAGGTGAATACATGCCAGACTTCGTTACTTTGTCTGAAGGTT
TGGGTTGTGTTGCTATCAGAGTTACTAAGGCTGAAGAAGTTTTGCCAGCTATCCAAAAGGCTAGAGAAATCAACGACAGA
CCAGTTGTTATCGACTTCATCGTTGGTGAAGACGCTCAAGTTTGGCCAATGGTTTCTGCTGGTTCTTCTAACTCTGACAT
CCAATACGCTTTGGGTTTGAGACCATTCTTCGACGGTGACGAATCTGCTGCTGAAGACCCAGCTGACATCCACGAAGCTG
TTTCTGACATCGACGCTGCTGTTGAATCTACTGAAGCTTAA

Synthetic gene sequence of *ilvN*$^{M13\text{-}Co}$ from *Corynebacterium glutamicum*

ATGGCTAACTCTGACGTTACTAGACACATCTTGTCTGTTTTGGTTCAAGACGTTGACGACGACTTCTCTAGAGTTTCTGG
TATGTTCACTAGAAGAGCTTTCAACTTGGTTTCTTTGGTTTCTGCTAAGACTGAAACTCACGGTATCAACAGAATCACTG
TTGTTGTTGACGCTGACGAATTGAACATCGAACAAATCACTAAGCAATTGAACAAGTTGATCCCAGTTTTGAAGGTTGTT
AGATTGGACGAAGAAACTACTATCGCTAGAGCTATCATGTTGGTTAAGGTTTCTGCTGACTCTACTAACAGACCACAAAT
CGTTGACGCTGCTAACATCTTCAGAGCTAGAGTTGTTGACGTTGCTCCAGACTCTGTTGTTATCGAATCTACTGGTACTC
CAGGTAAGTTGAGAGCTTTGTTGGACGTTATGGAACCATTCGGTATCAGAGAATTGATCCAATCTGGTCAAATCGCTTTG
AACAGAGGTCCAAAGACTATGGCTCCAGCTAAGATCTAA

Synthetic gene sequence of *alsLP*^{CO} from *Lactobacillus plantarum WCFS1*

ATGCCAGACAAGAAGTACTACGGTGCTGACGCTATCGTTGACTCTTTGGTTAACCACGACGTTAAGTACGTTTTCGGTAT
CCCAGGTGCTAAGATCGACAGAGTTTTCGAAAGATTGGAACACCCAGTTAACCCAAAGTCTCCAAGATTGATCGTTACTA
GACACGAACAAAACGCTGCTTTCATCGCTGCTGGTATCGGTAGAATCACTGGTAAGCCAGGTGTTGTTATGACTACTTCT
GGTCCAGGTGCTTCTAACTTGGCTACTGGTTTGGTTACTGCTACTGCTGAAGGTGACCCAGTTTTGGCTATCTCTGGTCA
AGTTCAAAGAGCTGACTTGTTGAGATTGACTCACCAATCTATGAACAACGCTGCTTTGTTCAAGCCAATCACTAAGTACT
CTGCTGAAGTTCAAGAACCAGAAAACATCTCTGAAGTTTTGGCTAACGCTTACCAAGAAGCTACTGCTGCTAAGCAAGGT
GCTTCTTTCGTTTCTGTTCCACAAGACGTTACTGACTCTATCGTTAGAACTCCAGTTATCACTCCAATCCAAGCTCCAAA
GTTGGGTCCAGCTTCTCCAGTTGAAGCTACTTTGTTGGCTCAAAAGATCAAGGCTGCTAAGTTGCCAGTTTTGTTGGTTG
GTATGAGAGCTTCTTCTCCAGAAGTTACTAAGGCTATCAGAAACTTGGTTGCTGCTGCTAACTTGCCAGTTGTTGAAACT
TTCCAAGCTGCTGGTGTTATCTCTAGAGACTTGGAAGCTAACCACTTCTTCGGTAGAGTTGGTTTGTTCAGAAACCAACC
AGGTGACATGTTGTTGAAGAAGTCTGACTTGGTTATCGCTGTTGGTTACGACCCAATCGAATACGAACCAAGAAACTGGA
ACGCTGAAGGTAAGTCTAGAATCGTTGTTATCGACGCTATGAGAGCTGAAATCGACCACAACTTCCAACCAGAAACTGAA
TTGATCGGTGACATCGCTCAAACTTTGGACTTCTTGTTGCCATACATGAAGGGTTACGACATCTCTGACTCTGCTAGAGC
TTACTTGGGTGAATTGCAAGAAAGATTGCAAACTAGAGACTTCGTTCCAAACATCGACAAGCAATCTAAGTTGAACCACC
CATTGTCTGTTATCGCTGCTTTGCAACAAAGAGTTTCTGACGACATGACTGTTACTGTTGACGTTGGTTCTCACTACATC
TGGATGGCTAGACACTTCAGATCTTACGAACCAAGACACTTGTTGTTCTCTAACGGTATGCAAACTTTGGGTGTTGCTTT
GCCATGGGCTATCGCTGCTGCTTTGGTTAGACCAGACACTCAAATCGTTTCTGTTTCTGGTGACGGTGGTTTCTTGTTCT
CTGCTCAAGAATTGGAAACTGCTGTTAGATTGAAGCAAAACATCGTTCACTTGATCTGGAACGACGGTACTTACGACATG
GTTAAGTTCCAAGAAGAAATGAAGTACGGTGAAGACGCTGCTGTTCACTTCGGTCCAGTTGACTTCGTTAAGTACGCTGA
ATCTTTCGGTGCTACTGGTTTGAGAGTTAACCAACCAGCTGACTTGGAAAAGGTTTTGGACCAAGCTTTCGCTACTGACG
GTCCAGTTGTTGTTGACATCCCAATCGACTACTCTGACAACAAGGCTTTGGGTAAGACTATGTTGCCAGACCAATTCTAC

IV. ZUSAMMENFASSUNG (KURZ)

Die Endlichkeit fossiler Rohstoffe sowie die durch deren Nutzung verursachten Umweltprobleme erfordern alternative Ansätze. Die Transformation der fossilen Wirtschaft zu einer auf erneuerbarer Biomasse basierenden Wirtschaft nennt man "Bioökonomie". Die Entwicklung neuer Mikroorganismen zur Biosynthese von Chemikalien aus Biomasse ist dabei eine zentrale Herausforderung. Es wurden bereits verschiedene Mikroorganismen für die Biosynthese gewünschter Chemikalien modifiziert. Der bekannteste Organismus für die industrielle Biosynthese ist die Hefe *Saccharomyces cerevisiae*, welche vor allem für die industrielle Produktion von Bioethanol als Benzinersatz bekannt ist. *S. cerevisiae* bildet allerdings in geringen Mengen auch Isobutanol; dieses wäre als Benzinersatz besser geeignet. Isobutanol wird durch Kombination der mitochondriellen Valin Biosynthese (katalysiert durch Ilv2, Ilv5, Ilv3 und Bat1/2) sowie dessen cytosolischen Abbau durch den Ehrlichstoffwechselweg (katalysiert durch bspw. Aro10 und Adh2) gebildet. Die unterschiedliche Kompartimentierung beider Stoffwechselwege limitierte die Isobutanol Biosynthese, weshalb Brat *et al.* (2012) durch cytosolische Relokalisierung der Enzyme Ilv2Δ54, Ilv5Δ48 und Ilv3Δ19 (abgekürzt als cyt-ILV) bei gleichzeitiger Deletion von *ilv2* die Isobutanol Ausbeute steigerte. Die so maximal erzielte Ausbeute entspricht etwa 3,7% der theoretischen Ausbeute von 410 mg/g_{Glc}, was auf bestehende Limitationen bei der Isobutanol Biosynthese hindeutet. Diese wurden im Rahmen der vorliegenden Arbeit untersucht.

Aus bisher ungeklärten Gründen wird Isobutanol gemäß Brat *et al.* (2012) effizient nur in valinfreiem Medium gebildet. Im Rahmen dieser Arbeit wurde gezeigt, dass dies auf die katalytische Aktivität von Ilv2Δ54 zurückzuführen ist, welche toxisch wirkt. Dadurch wird eine negative Selektion auf das *ILV2Δ54* Gen ausgeübt. Diese macht eine *ilv2* Deletion bei gleichzeitigem Valin Ausschluss notwendig, um das toxische Gen funktionell zu exprimieren. Der Valin Ausschluss ist daher nicht, wie bisher angenommen, auf die von Ilv6 erzeugte Endprodukt Hemmung zurückzuführen. Vielmehr wurde eine erhöhte Isobutanol Ausbeute bei Expression von zytosolischen Ilv6Δ61 in valinfreiem Medium beobachtet, was auf die positive Regulation von Ilv2Δ54 durch Ilv6Δ61 zurückgeführt wird. Weiterhin wurde gezeigt, dass das durch die NADPH abhängige Ilv5Δ54 verursachte Co-Faktor Ungleichgewicht der Isobutanol Biosynthese besser durch Expression einer NADH-Oxidase (NOX) als durch die Expression der NADH abhängigen $ilvC^{6E6}$ gelöst

werden konnte, da letzteres eine geringe *in vivo* Aktivität besaß. Untersuchungen der Co-Faktor Ungleichgewichte zeigten, dass das NAD(H) Ungleichgewicht bereits limitierend auf die Isobutanol Biosynthese wirkte, nicht aber das NADP(H) Ungleichgewicht. Eine weitere Limitierung bei der zytosolischen Isobutanol Biosynthese bildet sekretiertes DIV, welches von *S. cerevisiae* nicht mehr aufgenommen werden kann und somit zu geringeren Isobutanol Ausbeuten führt. Dies wird auf eine geringe Ilv3Δ19 Aktivität durch unzureichende Apo-Proteinbeladung mit Eisen-Schwefel-Clustern (ISC) zurückgeführt. Daher wurde versucht, Ilv3Δ19 durch heterologe DHAD zu ersetzen. Trotz funktioneller Expression einiger DHADs, besaß keine eine bessere *in vivo* Aktivität als Ilv3Δ19. Im anschließenden Versuch, die Ilv3Δ19 Apo-Proteinbeladung mit ISC zu optimieren, gelang dies sowohl durch die Deletion von *fra2* oder *pim1* wie auch durch die Expression von cytosolischem Grx5Δ29.

Neben dem Isobutanol Stoffwechselweg selbst wurde auch *S. cerevisiae* mittels evolutionärem Engineering für die Isobutanol Biosynthese optimiert. Dazu wurden die notwendigen Gene in den *ilv2* Locus integriert und die Mutante anschließend in norvalinhaltigem Medium evolviert. So evolvierte Einzelklone besaßen verbesserte Wachstumseigenschaften in valinfreiem Medium sowie eine erhöhte Isobutanol Ausbeute (0,59 mg/g_{Glc}) gegenüber dem Ausgangstamm, was auf einen Gendosierungseffekt zurückgeführt wird. Zusätzlich wurden in Zusammenarbeit mit Dr. J. Wess die Gene konkurrierender Stoffwechselwege kumulativ deletiert. Der daraus resultierende Stamm JWY23 erzielte durch Expression von cyt-ILV eine Isobutanol Ausbeute von 67,3 mg/g_{Glc}. Die vielversprechendsten Ansätze dieser Arbeit, nämlich die Deletion von *fra2* sowie die Expression von Grx5Δ29, Ilv6Δ61 und NOX, wurden im JWY23 Hintergrund bestätigt. Die höchste Isobutanol Ausbeute dieser Arbeit wurde mit 72 mg/g_{Glc} für den cyt-ILV und Ilv6Δ61 exprimierenden JWY23 Stamm beobachtet, was 17,6% der theoretischen Ausbeute entspricht.

Isobuttersäure (IBA) ist ein Nebenprodukt der Isobutanol Biosynthese, welches jedoch als werthaltige Plattformchemikalie gilt. Daher wurden die Erkenntnisse aus dieser Arbeit für die Biosynthese von IBA im Zytosol von *S. cerevisiae* verwendet. Die höchste IBA Ausbeute von 9,8 mg/g_{Glc} wurde in valinfreiem Medium durch Expression von cyt-ILV, NOX und Ald6 in JWY04 beobachtet. Dies entsprach einer 8,9-fachen Steigerung gegenüber der Kontrolle und ist nach unserem Kenntnisstand die höchste IBA Ausbeute, die bisher für *S. cerevisiae* berichtet wurde.